Measurement of nitric oxide metabolites and protein nitration in healthy and inflammatory human tissues and bio-fluids

Submitted by Annie Rose Knight, to the University of Exeter
as a thesis for the degree of
Doctor of Philosophy in Medical Studies
In August 2016.

I certify that all material in this thesis which is not my own work has been identified and that no material has previously been submitted and approved for the award of a degree by this or any other University.

DSTL/PUB09182

Abstract

The central thesis of this project is that damage caused by reactive nitrogen species, e.g. 3-nitrotyrosine (Tyr-NO_2), constitutes a marker of disease progression/severity. A new sensitive electrochemiluminescence ELISA was optimised and validated for Tyr-NO_2 measurement, giving a lower limit of quantification of 0.04 nM BSA-NO_2, intra- and inter-assay CVs of 6.5% and 11.3%, an average recovery of 106 ± 3% and average linearity 0.998 ± 0.001.

Nitrative stress, carbonyl stress and C-reactive protein (CRP) concentrations were measured before and after major elective surgery. CRP measurements confirmed the induction of an inflammatory response. Median serum Tyr-NO_2 levels increased post-surgery to a median (inter-quartile range) value of 0.97 (0 – 1.7) fmol nitrated BSA (BSA-NO_2) equivalents/mg protein compared with a pre-surgery level of 0.59 (0 – 1.3) fmol BSA-NO_2 equivalents/mg protein ($p<0.05$). Oxidative damage was confirmed by serum protein carbonyl levels ($p<0.05$).

In a second pre-/post- surgery study, patients who developed sepsis postoperatively had significantly higher serum Tyr-NO_2 levels one day prior to diagnosis (median (IQR) 4.5 (1.65 – 8.21) fmol BSA-NO_2 equivalents/mg protein) compared to patients without sepsis (1.2 (0.74 – 5.97) fmol BSA-NO_2 equivalents/mg protein; $p<0.05$). Tyr-NO_2 levels have not previously been measured before clinical diagnosis. However, Tyr-NO_2 did not improve upon CRP as a diagnostic marker (area under the curve: Tyr-NO_2 0.69 versus CRP 0.88).

Nitrate (NO_3^-) supplementation in healthy smokers was also studied. Plasma Tyr-NO_2 levels were unaltered by supplementation or smoking status. Salivary nitration was unaffected by smoking and decreased with NO_3^- supplementation: the median (IQR) pre-supplementation was 0.67 (0.31-1.14) and post-supplementation was 0.43 (0.12-0.61) pmol BSA-NO_2 equivalents/mg protein. Ozone-based chemiluminescence was utilised for nitrite (NO_2^-) and NO_3^- measurement as indicators of $^{\bullet}NO$ production. Plasma and salivary NO_2^- and NO_3^- concentrations increased significantly with NO_3^- supplementation ($p<0.05$).

In contrast to published studies, brain frontal lobe Tyr-NO_2 levels were not higher in dementia: the median (IQR) levels in dementia were 0.29 (0.19-0.57) and in non-dementia controls were 0.3 (0.22-0.55) pmol BSA-NO_2 equivalents/mg protein. However, the median brain tissue NO_2^- concentration was significantly higher in the Alzheimer's disease group ($p<0.05$). Western blotting revealed that nitration was predominantly in a few select proteins, with TOF-MS/MS analysis suggesting haemoglobin is one of these proteins.

Measurement of nitrative stress using ozone-based chemiluminescence and an electrochemiluminescence-based-ELISA overcomes earlier methodological flaws, such as low sensitivity. Detection of total Tyr-NO_2 in different inflammatory states indicates that its measurement could have potential as a marker of disease, but measurement of nitration in specific proteins may be more informative than total Tyr-NO_2.

Contents

Tables and Figures

Acknowledgments

First and foremost I would like to thank Paul, Emma and Roman for sharing their knowledge, encouraging me and for being patient with me. There are so many people who have helped me but special thanks must go to Miranda and Daniel, for being both wonderful colleagues and friends, and to Susan Westoby, for preventing the chaos that would ensue if we were left to our own devices.

Thank you to The Defence Science and Technology Laboratory (DSTL) and The University of Exeter Open Innovation Platform for funding my project.

Thank you to my collaborators within the University of Exeter, at Aston University and at The South West Dementia Brain Bank, it has been a pleasure working with you.

Finally, to my family and friends that do not understand what it is I do, I thank you for your blind belief that I could do whatever ‘it’ was.

Abbreviations

Ab	Antibody
AD	Alzheimer's disease
APP	Acute phase protein
APR	Acute phase response
APS	Ammonium persulfate
AUC	Area under the curve
BCA	Bicinchoninic acid
BSA	Bovine serum albumin
BSA-NO_2	Nitrated bovine serum albumin
CO_2	Carbon dioxide
$CO_3^{\bullet -}$	Carbonate radical
COPD	Chronic obstructive pulmonary disease
CRP	C-reactive protein
CV	Coefficient of variation
DAMPs	Danger-associated molecular patterns
DNP	Dinitrophenylhydrazine
DSTL	Defence Science and Technology Laboratories
DTT	Dithiothreitol
ECL	Electrochemiluminescence
EIA	Enzyme immunoassay
ELISA	Enzyme-linked immunosorbent assay
emPAI	Exponentially modified protein abundance index
eNOS	Endothelial nitric oxide synthase
FBS	Foetal bovine serum
GC	Gas chromatography
GSH	Glutathione
-GSSG	Oxidised glutathione
H_2O_2	Hydrogen peroxide
Hb	Haemoglobin
HCl	Hydrochloric acid
HG	High glucose
HPLC	High pressure liquid chromatography
IAA	Iodoacetamide
IHC	Immunohistochemistry

iNOS	Inducible nitric oxide synthase
IQR	Interquartile range
kDa	Kilo Dalton
LDL	Low density lipoprotein
LLOQ	Lower limit of quantification
LOD	Limit of detection
LPS	Lipopolysaccharide
MC	Monocytic cell
MCI	Mild cognitive impairment
MnO_2	Manganese oxide
MPO	Myeloperoxidase
MRM	Multiple reaction monitoring
MS/MS	Tandem mass spectrometry
MSD	Meso Scale Discovery
NADPH oxidase	Nicotinamide adenine dinucleotide phosphate oxidase
NaOH	Sodium hydroxide
NG	Normal glucose
NIR	Near infrared
nNOS	Neuronal nitric oxide synthase
NO_2^-	Nitrite
NO_3^-	Nitrate
$^{\bullet}NO_2$	Nitrogen dioxide
$^{-}NO_2$	Nitro groups
$^{\bullet}NO$	Nitric oxide
NOS	Nitric oxide synthase
NRI	Net reclassification indices
$O_2^{\bullet-}$	Superoxide anion radical
$^{\bullet}OH$	Hydroxyl radical
$ONOO^-$	Peroxynitrite
$ONOOCO_2^-$	Nitrosoperoxocarboxylate
PAMPs	Pathogen-associated molecular patterns
PBS	Phosphate buffered saline
PIRO	Predisposition, Infection, Response and Organ dysfunction
PMI	Post mortem interval
PMN	Polymorphonuclear cells

PRR	Pattern recognition receptor
PTM	Post-translational modification
RA	Rheumatoid arthritis
RBC	Red blood cell
R.L.U	Relative light units
RNS	Reactive nitrogen species
ROC	Receiver operating characteristic
ROS	Reactive oxygen species
SD	Standard deviation
SDS	Sodium dodecyl sulfate
SDS-PAGE	Sodium dodecyl sulfate polyacrylamide gel electrophoresis
-SH	Thiol group
SIRS	Systemic inflammatory response syndrome
SLE	Systemic lupus erythematosus
SOD	Superoxide dismutase
SWDBB	South West Dementia Brain Bank
TCA	Trichloroacetic acid
Tg	Transgenic
TLR	Toll-like receptor
TOF	Time of flight
Tyr	Tyrosine
Tyr-NO_2	3-Nitrotyrosine
VaD	Vascular dementia
WBC	White blood cell
WT	Wildtype
XIC	Extracted ion chromatograms
XO	Xanthine oxidase
$ZnSO_4$	Zinc sulfate

Chapter 1
Introduction

1.1. The Inflammatory Response

Inflammation is a physiological response to infection or injury and is non-specific in nature. In particular, acute inflammation acts to remove pathogens and repair damaged tissue. The cardinal signs of the inflammatory response are heat, redness, swelling, pain and loss of function (Punchard et al, 2004). Many non-infectious diseases involve an inflammatory response (e.g. autoimmunity, cardiovascular disease, and some neurodegenerative diseases); this pathological inflammation often causes tissue damage, exacerbating the disease state (e.g. plaque formation in atherosclerosis (Willerson and Ridker, 2004; Lalkhen and McCluskey, 2008)).

Inflammatory signals are activated when pattern recognition receptors (PRRs), such as Toll-like receptors, found on leukocytes resident in the tissue or circulating in the blood, bind either alarmins/danger associated molecular patterns (DAMPs) or pathogen-associated molecular patterns (PAMPs) (de Jong et al, 2010; Newton and Dixit, 2012). Alarmins and DAMPs are host molecules that are produced or exposed as the result of tissue or cell damage, e.g. heat shock proteins (Castellheim et al, 2009). PAMPs are molecules that are found on a variety of pathogens but not within the host, e.g. lipopolysaccharide (LPS). Recognised by the toll-like receptor 4, LPS is an endotoxin found only on the outside of gram-negative bacteria and can induce a lethal immune response in mammals (Salomao et al, 2012). Recognition of these molecules is non-specific, i.e. recognition is an innate immune response (Castellheim et al, 2009). Activation of PRRs leads to the release of cytokines and acute phase proteins (synthesised in the liver and released into the blood stream) along with the activation of cascade systems such as complement (**Figure 1.1**) (de Jong et al, 2010).

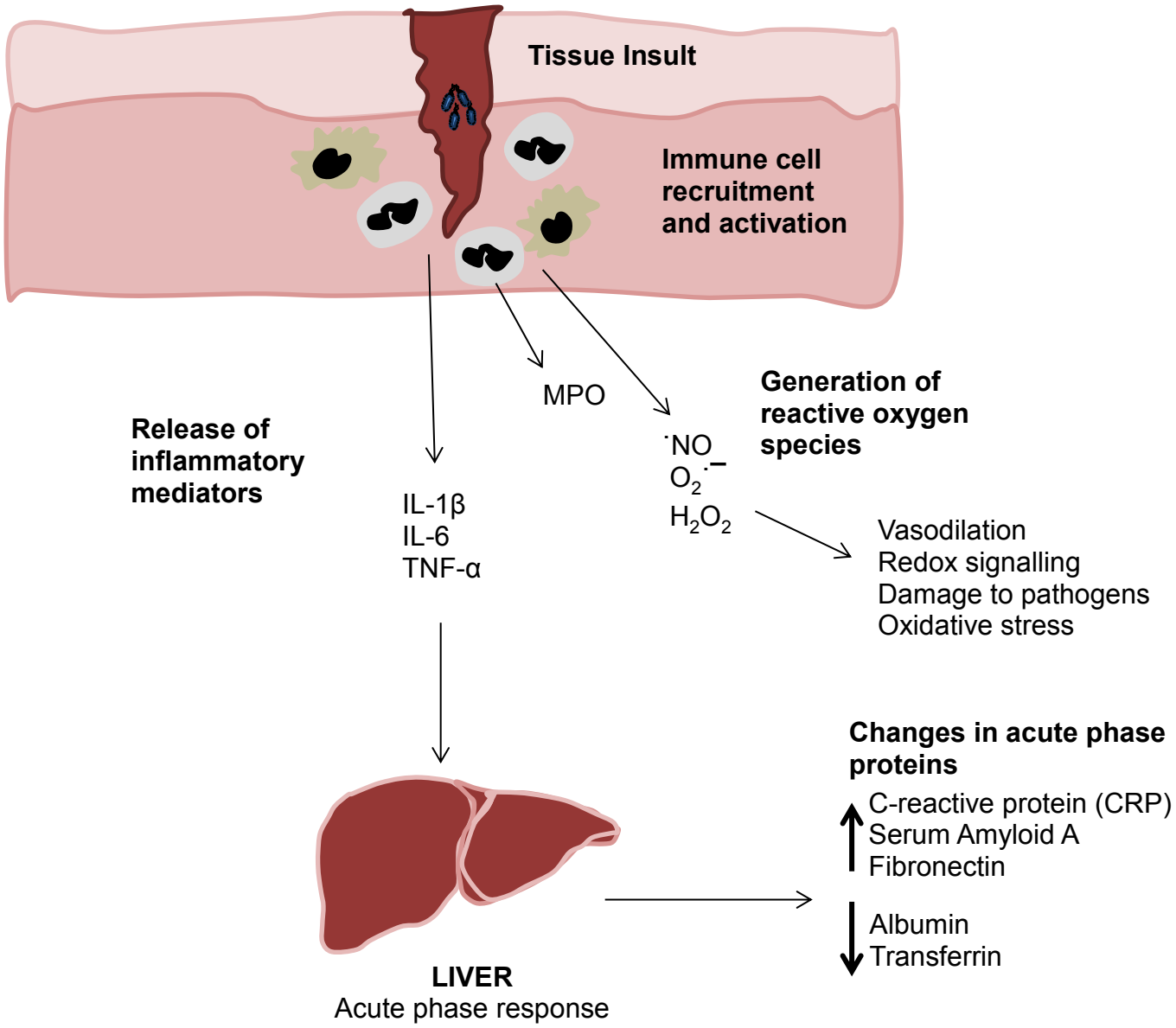

Figure 1.1: Basic overview of the inflammatory response

Briefly, inflammation is initiated by the presence of pathogens or damaged host tissue. The diagram above shows a wound that has penetrated the layers of skin and been infected with bacteria. Macrophages and neutrophils have been recruited to the area of injury/infection. These cells release pro-inflammatory cytokines (see section 1.2) and reactive oxygen species (see section 1.3). Pro-inflammatory cytokines and ROS will then act as signals for further response, such as IL-6 activating the acute phase response, and $^{\bullet}NO$ causing vasodilatation (Gabay and Kushner, 1999; Gruys et al, 2005; Lalkhen and McCluskey, 2008).

The innate immune response involves the recruitment of monocytes (e.g. macrophages) and polymorphonuclear cells (e.g. neutrophils) to sites of infection or damage (Newton and Dixit, 2012). These cells carry out many important functions to aid in the removal of pathogens, clearance of dead cells and tissue repair (Fujiwara and Kobayashi, 2005; Kolaczkowska and Kubes, 2013). During pathogen clearance, phagocytic cells (e.g. macrophages and neutrophils) undergo an oxidative burst (Slauch, 2011; Chen and Junger, 2012), which involves the assembly of the nicotinamide adenine dinucleotide phosphate (NADPH) oxidase complex in the cell membrane, catalysing the reduction of oxygen to the free radical superoxide anion ($O_2^{\bullet -}$) (**Figure 1.2A**) (Chen and Junger, 2012). $O_2^{\bullet -}$ dismutates to hydrogen peroxide (H_2O_2) by one of the three superoxide dismutase (SOD) isoforms (**Figure 1.2B**) which are expressed in different cellular locations; the mitochondria (SOD2), the cytoplasm (SOD1) and extracellularly (SOD3) (Fukai and Ushio-Fukai, 2011). H_2O_2 is able to pass through the cell membrane, whereas $O_2^{\bullet -}$ cannot, and H_2O_2 acts in a bacteriostatic manner in the surrounding tissue (Dunnill et al, 2015). H_2O_2 may also be utilised in reactions that produce further reactive oxygen species (ROS) (Costa et al, 2005). Inflammatory signals also lead to the activation of inducible nitric oxide synthase (iNOS), an enzyme that catalyses the production of the free radical nitric oxide ($^{\bullet}NO$) from the amino acid, L-arginine (**Figure 1.2C**) (Lirk et al, 2002). The production of these free radicals/ROS will aid the destruction of the engulfed pathogen (Roos et al, 2003) and act as secondary messengers, aiding wound healing (Dunnill et al, 2015). $^{\bullet}NO$ also acts as a vasodilator, increasing blood flow to the affected area (Salvemini and Marino, 1998) and contributing to the swelling associated with inflammation. The ROS and free radicals released during inflammation are discussed further in section 1.3.

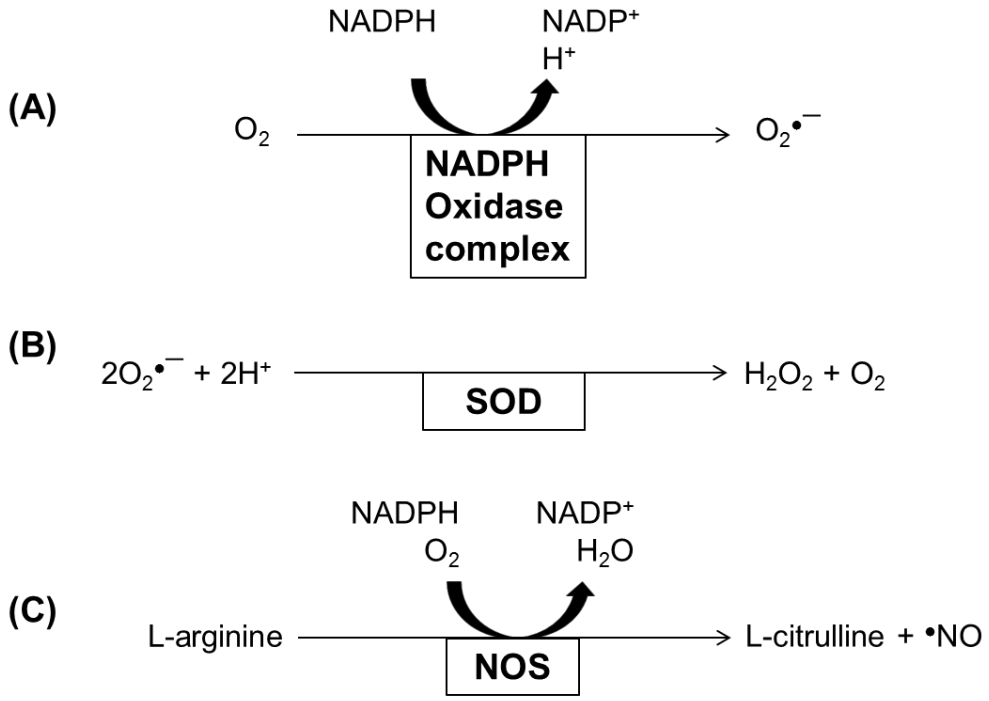

Figure 1.2: Enzymatic production of reactive oxygen species during inflammation

During inflammation concentrations of the following ROS are increased (A) superoxide anion production is catalysed by the NADPH oxidase, (B) hydrogen peroxide production catalysed by a SOD isoform and (C) nitric oxide production catalysed by inducible NOS.

1.2. Inflammatory mediators: cytokines, the acute phase response and complement

Cytokines

Cytokines are a vital part of inflammation and immunity with a diverse range of functions such as inducing fever, stimulating the acute phase response and migration of white blood cells (Borish and Steinke, 2003; Dinarello, 2007). Cytokines are not purely pro-inflammatory, as some induce the resolution of inflammation and promote tissue repair, e.g. IL-10 (Borish and Steinke, 2003). There are many families of cytokines, such as interleukins, interferons and tumour necrosis factors (Dinarello, 2007).

The levels of circulating cytokines can be affected by several factors, including the time of day and diet. Cytokines typically have a short lifetime and immune cells have been shown to continue secreting cytokines in whole blood samples.

Both of these factors can lead to over- or under-reporting the levels of circulating cytokines present in whole blood (Zhou et al, 2010).

Acute phase response

The acute phase response (APR) is a term to describe a systemic innate immune response to injury or infection (Gruys et al, 2005). The APR leads to increases in circulating pro-inflammatory cytokines and non-specific host defences, fever and changes in serum protein concentrations (Suffredini et al, 1999; Gruys et al, 2005). These proteins, which fluctuate in concentration during the course of the inflammatory response, are referred to as acute phase proteins (APPs) and are divided into two groups: the positive APPs, which are defined as proteins whose plasma concentration increases by at least 25% during inflammatory illnesses (**Table 1.1** for examples) and the negative APPs, which show a >25% decrease in plasma concentration, such as, albumin, transferrin, retinol binding protein and factor XII (Gabay and Kushner, 1999).

Table 1.1: Well-known positive acute phase proteins and their roles

The plasma concentration of the proteins detailed below increases during the acute phase response (Suankratay et al, 1998; Gruys et al, 2005; Eklund et al, 2012; Murakami et al, 2012).

Protein	Role/s
Fibrinogen	Coagulation
α1-Protease inhibitor	Anti-proteases
Caeruloplasmin	Transport protein
C-reactive protein (CRP)	Binds bacteria/activates complement
Serum amyloid A	Induces cytokine synthesis/chemotactic for neutrophils and mast cells
Procalcitonin	Stimulates release of pro-inflammatory cytokines from monocytes

These positive acute phase proteins are often used as biomarkers of inflammation, providing information on disease risk, progression or response to treatment. However, they are non-specific and will increase with any inflammation, not just the pathological inflammation associated with the disease.

C-reactive protein (CRP) is produced by the liver in response to inflammatory signals (e.g. IL-6) and binds to PAMPs/DAMPs, such as phosphocholine. It can also bind to C1q to activate the complement cascade (Marnell et al, 2005). Healthy adult CRP levels are approximately 0.8 mg/L (Povoa, 2002) and these levels can increase 1000-fold within 24-48 hours of an inflammatory insult (Volanakis, 2001). A study by Colley et al (1983) found that, following surgery,

there was a 6-8 hour delay before the acute phase proteins CRP and fibrinogen increased in the blood. This was confirmed by Li et al (2004) who found increases in CRP were first measurable at 6 hours in patients receiving renal angioplasty with a stent. They do however disagree on when CRP levels peak in the blood, with Colley et al (1983) reporting 48 hours and Li et al (2004) reporting 24 hours, which could be due to the different surgeries patients underwent (i.e. elective surgeries, such as unilateral hernia repair, against renal angioplasty with a stent). CRP has a half-life of approximately 19 hours and levels will decrease rapidly following resolution of the inflammation (Hofer et al, 2012). Fibrinogen was shown to peak at 96 hours (Colley et al, 1983). An elevated erythrocyte sedimentation rate, i.e. the rate at which erythrocytes sediment in an hour (the amount of clear plasma at the top of the tube is measured), is also considered a marker of inflammation and is often measured alongside CRP. However, although measuring erythrocyte sedimentation rate is an inexpensive and simple test, it is affected by patient gender and age (Olshaker and Jerrard, 1997; Feldman and Sbong, 2014).

As well as indicating acute inflammation, as the result of trauma or infection, CRP can also be used alongside other markers (such as cholesterol) to determine a person's risk of cardiovascular disease, with levels greater than 3 mg/L indicating a high risk of a heart attack or stroke (Ridker, 2003).

Complement

The complement system consists of three activation pathways for 30 plus plasma and membrane proteins, which react in a cascade-like manner, amplifying the response. These pathways result in (a) opsonisation of pathogens (aids phagocytosis), (b) chemoattraction of white blood cells and (c) formation of membrane attack complexes in some bacteria (Dunkelberger and Song, 2009).

Complement proteins are also positive APPs (Jain et al, 2011). Complement proteins C3 and C4 are measured clinically to diagnose and monitor immune complex diseases (such as systemic lupus erythematosus), where a decrease in serum levels is observed (Egner, 2000; Birmingham et al, 2010).

1.3. Inflammatory mediators: reactive oxygen/nitrogen species

As has already been described (section 1.1), recruitment and activation of immune cells, such as macrophages and neutrophils also leads to the production of free radicals and ROS/RNS (see **Table 1.2** for examples). Free radicals are defined as a species containing at least one unpaired electron. The use of the terms ROS and RNS covers both these free radicals and their reactive derivatives that do not have an unpaired electron (Halliwell, 2001).

Table 1.2: Reactive oxygen species produced during inflammation

Examples of ROS and RNS produced during inflammation (Guzik et al, 2003). These ROS and RNS aid in the destruction of pathogens and act as signals for the recruitment of more immune cells. However when produced in large amounts (or when antioxidant mechanisms are compromised) these species can cause modifications of macromolecules in the body, e.g. lipids, DNA and proteins (Pacher et al, 2007).

Free radicals reactive oxygen/nitrogen species	Non-radical reactive oxygen/nitrogen species
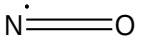 (Nitric oxide)	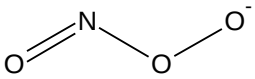 (Peroxynitrite)
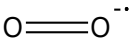 (Superoxide)	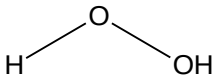 (Hydrogen peroxide)
 (Hydroxyl radical)	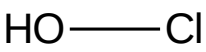 (Hypochlorous acid)

The ROS and RNS generated during inflammation are involved in redox signalling and aid pathogen removal (Winrow et al, 1993; Roos et al, 2003; Dunnill et al, 2015). However, these species are also able to react with, and modify, cellular components such as the fatty acid membrane and proteins. To protect themselves, cells have antioxidant defences which may be enzymatic (e.g. catalase and glutathione peroxidase), or scavengers (e.g. glutathione and

coenzyme Q) (Halliwell, 1996; Rizzo et al, 2010). Oxidative stress is the term used to describe an imbalance between ROS and antioxidant capacity, leading to the oxidative modification of cellular components and tissue damage (Sies, 1997; Halliwell and Whiteman, 2004). Oxidative stress has been linked to many different diseases with an inflammatory component, such as neurodegenerative diseases (Giasson et al, 2000; Butterfield et al, 2006a), cardiovascular pathology (Beckman et al, 1994b; Shishehbor et al, 2003), autoimmunity (Avalos et al, 2007; Szabó-Taylor et al, 2013) and cancer (Reuter et al, 2010; De Sanctis et al, 2014).

Oxidative modifications of proteins can be viewed as just a marker of disease activity. However, there is increasing evidence that oxidative modifications are an active component of the disease, perpetuating the pathology. For example, modifications of proteins may result in a loss or gain of activity, such as; impairment of actin polymerization following oxidation of actin (Dalle-Donne et al, 2001), a decrease in manganese superoxide dismutase enzyme activity following nitration of the enzyme (MacMillan-Crow et al, 1998), increased platelet aggregation following the oxidation of fibrinogen (Azizova et al, 2007) and increased peroxidase activity following the nitration of cytochrome C (Cassina et al, 2000). Another possibility is the generation of an autoimmune response to the altered molecule (Cooke et al, 1997; Griffiths, 2008; Kurien and Scofield, 2008; Ryan et al, 2014). For example, type II collagen modified by ROS can act as an autoantigen in rheumatoid arthritis (Nissim et al, 2005). This is thought to be due to modifications forming neo-epitopes that bypass tolerance and stimulate lymphocytes (Eggleton et al, 2008; Eggleton et al, 2013). It has been suggested that this immune response to the neo-epitope could then lead to the activation of an immune response against the native (unmodified) molecule (Gauba et al, 2011), via the phenomenon of “epitope spreading”.

White blood cell infiltration of a wound (e.g. neutrophils) is at its most rapid in the first 12 hours (Kim et al, 2008) and has been shown to peak at 12 hours post-surgery (Colley et al, 1983). From this, it can be inferred that the respiratory burst and ROS release begins at the site of inflammation within the first 12 hours. As there is a 6-8 hour delay in acute phase protein release (Colley et al, 1983; Li et al, 2004) that does not peak until at least 24 hours (Li

et al, 2004) it can be hypothesised that levels of oxidative stress, and the markers associated with it, will peak earlier than markers associated with the acute phase response.

Numerous studies have investigated whether oxidative stress markers could be used as biomarkers in disease (reviewed in Griffiths et al (2002); Frijhoff et al (2015)) and some of the well-studied markers are discussed in section 1.5.

1.4. Biomarkers of disease

The World Health Organisation describe a biomarker as *"any substance, structure, or process that can be measured in the body or its products and influence or predict the incidence or outcome of disease"* (WHO, 2001). Biomarkers can range from a non-invasive imaging biomarker, e.g. measuring brain atrophy by magnetic resonance imaging, to proteins in bio-fluids, e.g. tau levels in the cerebrospinal fluid (Anoop et al, 2010).

Biomarkers are vital not only in obtaining information on aspects of the disease process but also in drug development, where they can be used to assess the efficacy of treatment. Biomarkers can have clinical utility if they identify human individuals at risk of disease, improve diagnosis of disease or allow monitoring of disease activity. From a practical stand point, a biomarker also needs to be in an easily accessible tissue, something that can be measured on a large scale and economically viable.

A perfect diagnostic biomarker would accurately identify all individuals with the disease AND all individuals without the disease. However, many clinical diagnostic tests often produce false positives (wrongly identifies healthy individuals as diseased) and/or false negatives (wrongly identifies diseased individuals as healthy) (Lalkhen and McCluskey, 2008). How well a test performs is often described in terms of sensitivity and specificity and these may be plotted on a receiver operator characteristics (ROC) curve (**Figure 1.3**).

Sensitivity refers to the test's ability to correctly identify diseased individuals, the higher the sensitivity the lower the rate of false negatives (**Equation 1.1**). Specificity is the test's ability to correctly identify individuals without the disease, the higher the specificity the lower the rate of false positives (**Equation 1.2**). A ROC curve plots sensitivity against 1-specificty, the area under the curve (AUC)

is then calculated to determine the test's overall accuracy, an AUC of 1.0 represents a perfect test and an AUC of 0.5 represents a test that has no ability to discriminate between those with and without disease (**Figure 1.3**) (Lalkhen and McCluskey, 2008).

Equation 1.1:

$$Sensitivity = \frac{True\ positives}{True\ positives + False\ negatives}$$

Equation 1.2:

$$Specificity = \frac{True\ negatives}{True\ negatives + False\ positives}$$

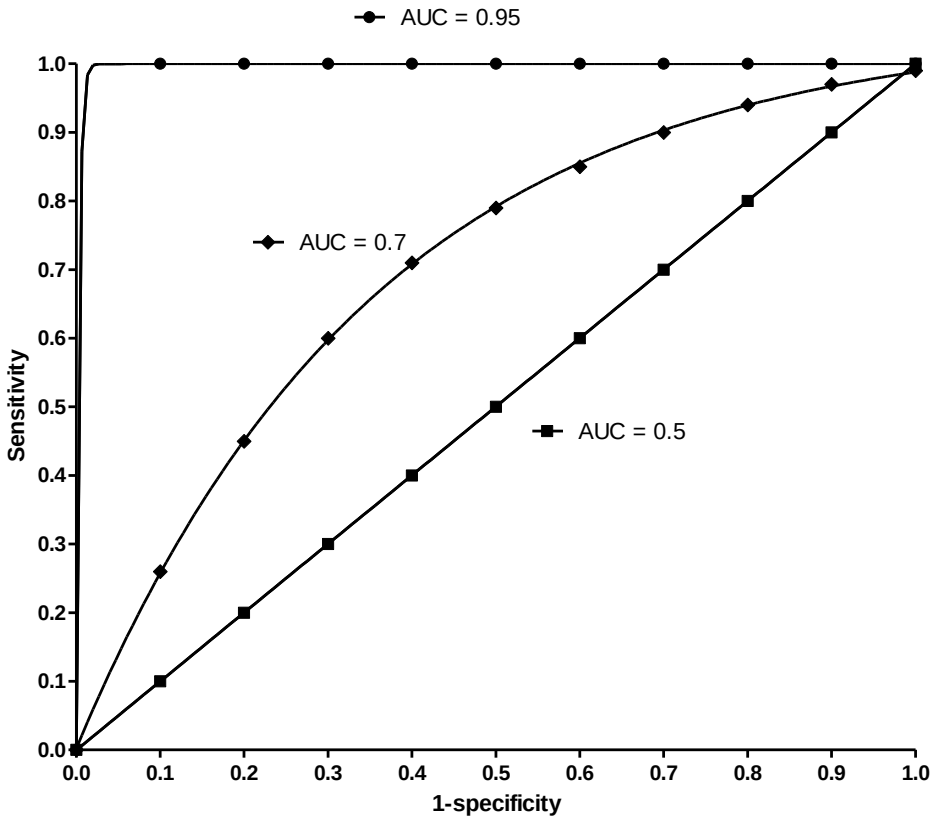

Figure 1.3: Receiver operator characteristics (ROC) curves

ROC curves for an 'excellent' biomarker, area under the curve (AUC) = 0.95, a 'fair' biomarker, AUC =0.7, and biomarker that has no diagnostic ability, AUC =0.5, (Brubaker, 2008; Lalkhen and McCluskey, 2008).

1.4.1. Markers of oxidative stress and their measurement

Several pathologies are associated with oxidative stress. To investigate these associations, measurements of the redox state of a specific tissue or the whole body is required. Due to the transient nature of most ROS and RNS, they cannot be measured directly *in vivo*. Therefore, oxidative stress has been investigated by a few different approaches, such as by measuring the abundance/activity of enzymes that produce ROS/RNS, by measuring antioxidant defences and by measuring ROS/RNS-induced modifications. Below is a brief overview of some oxidative stress markers and their measurement in human inflammatory diseases.

Isoprostanes are primarily formed by the peroxidation of the fatty acid, arachidonic acid and are isomeric with prostaglandins (Rokach et al, 1997). F_2-isoprostanes are considered one of the most reliable biomarkers of oxidative stress *in vivo* as they are chemically stable and specific for lipid peroxidation (Montuschi et al, 2004). It has been suggested that isoprostanes may have a pathophysiological function, as they assert biological activity, e.g. 15-F_{2t}-isoprostane is a potent vasoconstrictor (Montuschi et al, 2004) (**Figure 1.4A**). Immunoassays for isoprostane measurement have been developed commercially but validation with mass spectrometry is advised (Frijhoff et al, 2015). Elevated isoprostanes have been associated with several human diseases, such as cardiovascular disease (Davies and Roberts, 2011) and Alzheimer's disease (Montine et al, 2002).

Protein carbonylation is the result of many reactions that give rise to the formation of aldehyde and ketone moieties on proteins (**Figure 1.4B**). The addition of a carbonyl group may be due to direct oxidation of amino acid residues or via a secondary reaction, such as binding of aldehydic lipid oxidation products (Dalle-Donne et al, 2006a; Frijhoff et al, 2015). The amino acids often affected are lysine, arginine, and proline. These residues are often located at metal binding sites and are thus prone to metal-catalysed oxidation (Stadtman, 1992; Dalle-Donne et al, 2003a). Protein carbonyls are very stable and considered a good marker of oxidative stress (Griffiths, 2000). Carbonyls are usually detected following derivatization with 2,4-dinitrophenylhydrazine (DNP), which can then be detected with an anti-DNP antibody in an ELISA or

with spectrophotometry (Frijhoff et al, 2015). Protein carbonyls have been found to increase in Alzheimer's disease (Sultana et al, 2010), chronic obstructive pulmonary disorder (Kirkham et al, 2011) and with major trauma (Winterbourn et al, 2000). However, they are a broad marker of oxidation rather than a sign of any particular ROS/RNS generation (Dalle-Donne et al, 2003b).

"Thiols" can refer to low molecular weight thiols (e.g. glutathione, **Figure 1.4C**) or thiol groups (-SH) on the amino acid cysteine. Oxidation of cysteines within a protein may affect the protein function; however glutathione (GSH) acts as an antioxidant as it scavenges ROS (forming oxidised glutathione; GSSG) (Frijhoff et al, 2015). The GSH:GSSG ratio has been used as a marker of oxidative stress in several diseases, e.g. paediatric tumours (Zitka et al, 2012), breast cancer (Yeh et al, 2006) and amnestic mild cognitive impairment (Sultana et al, 2008). However, cysteine thiols are unstable as they are readily chemically reduced. Additionally, changes in GSH levels may be due to a nutritional/metabolic imbalance rather than oxidative stress (Frijhoff et al, 2015).

Normal cellular metabolism results in background levels of DNA and RNA oxidation, which are increased following oxidative stress. DNA/RNA oxidation may result in base or sugar modifications, single or double strand breaks or cross-linking with proteins (Cooke et al, 2000; Cooke et al, 2003). Single deoxynucleotides and DNA chains can both be oxidised. The former will not be incorporated into DNA chains and the latter should be removed from the DNA chain by DNA glycosylases (to avoid mutagenic potential) (Cooke et al, 2000). The guanine moiety is particularly vulnerable to oxidation and 8-oxo-7,8-dihydroguanine (8-oxoGua) and 8-oxo-7,8-dihydro-2′-deoxyguanosine (8-oxodG, **Figure 1.4D**) are the most studied of the oxidative lesions caused to DNA (Loft et al, 2012; Frijhoff et al, 2015). Urinary excretion of 8-oxoGua and 8-oxo-dG was positively associated with risk of lung cancer and oestrogen receptor positive breast cancer respectively (Loft et al, 2012; Loft et al, 2013). Urinary excretion of oxidised RNA guanine (8-oxoGuo) has also been shown to predict long-term mortality in those with type 2 diabetes (Broedbaek et al, 2011). These modifications to DNA and RNA are excreted in urine, can be measured by ELISA or HPLC-MS and are stable over time, thus achieving many of the criteria needed from a clinical biomarker (Cooke et al, 2000; Frijhoff et al, 2015).

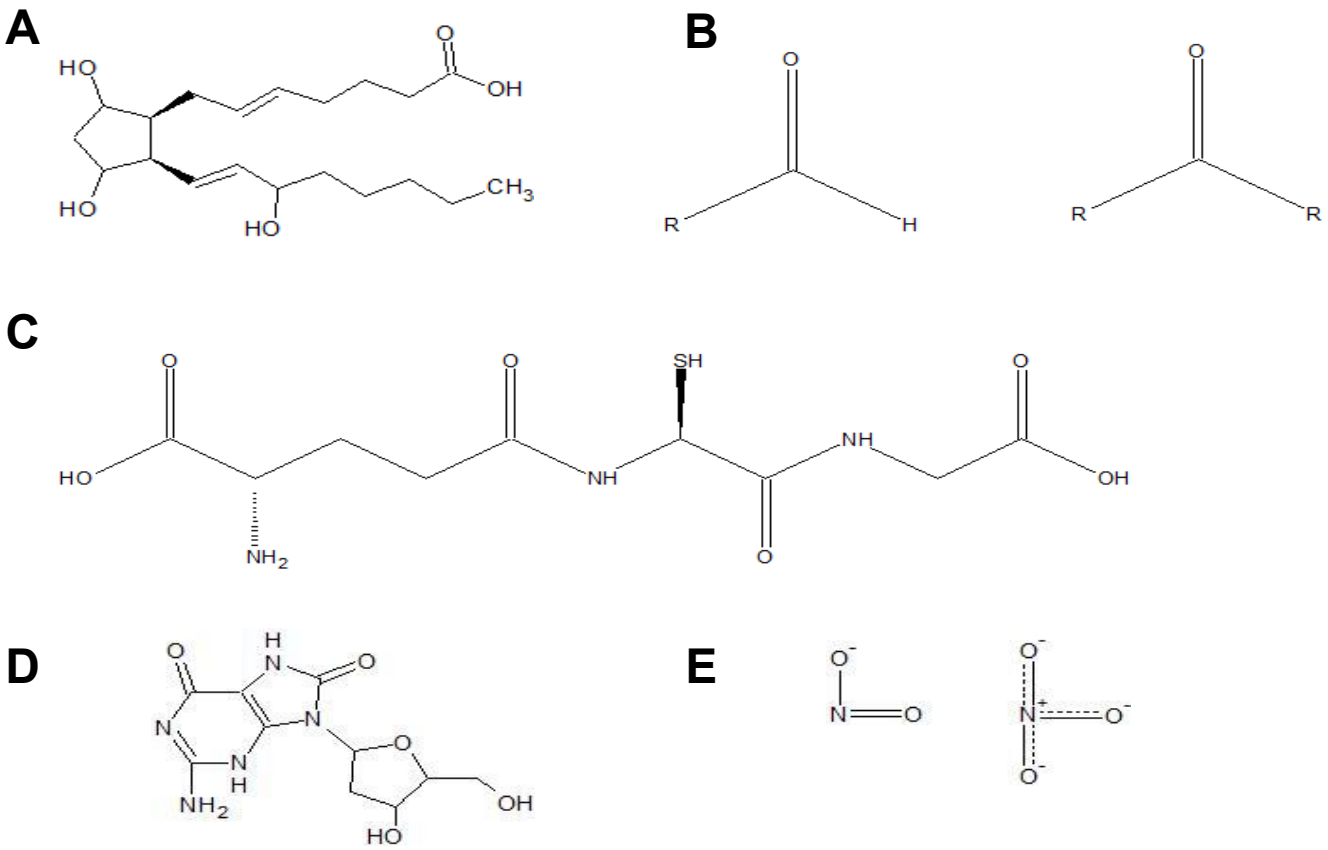

Figure 1.4: Markers of oxidative stress

The above are the chemical structures for the following oxidative stress markers. (A) 15-F_2-isoprostane. (B) Carbonyl (aldehyde and ketone). (C) Glutathione. (D) 8-oxo-7,8-dihydro-2′-deoxyguanosine. (E) Nitrite and nitrate.

Nitrite (NO_2^-) and nitrate (NO_3^-) are often measured as markers of nitric oxide ($^{\bullet}NO$) production (**Figure 1.4E**) (Hood et al, 1998; Kleinbongard et al, 2003). NO_2^- is usually measured by employing the Griess reaction. By reducing NO_3^- to NO_2^-, prior to the Griess reaction, NO_3^- levels can also be measured (Tsikas, 2007). The 'Griess reagents' are sulfanilic acid and α-naphthylamine. Under acidic assay conditions, NO_2^- reacts with sulfanilic acid to form a diazonium ion (**Figure 1.5**). This then couples with α-naphthylamine, creating a red azo dye which can be measured by absorbance (Tsikas, 2007).

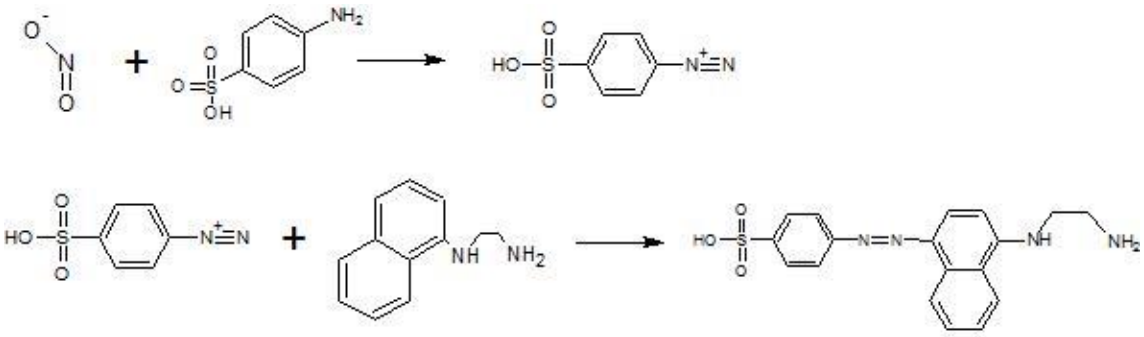

Figure 1.5: Griess reaction for measurement of nitrite.

Nitrite reacts with sulfanilic acid forming a diazonium ion. The diazonium ion then couples with α-naphthylamine to create a red azo dye.

Ozone-based chemiluminescence is considered a more sensitive method than the Griess reaction for the measurement of NO_2^- in biological samples, but is less widely available (MacArthur et al, 2007; Nagababu and Rifkind, 2010). This method measures $^{\bullet}NO$, requiring that both NO_2^- and NO_3^- are chemically reduced prior to measurement. $^{\bullet}NO$ is subsequently reacted with ozone to form "excited state" nitrogen dioxide. As nitrogen dioxide returns to the ground state, a single photon is emitted which is detected and measured, by a photomultiplier tube (**Figure 1.6**), allowing the quantification of NO_2^- or NO_3^- (MacArthur et al, 2007; Piknova and Schechter, 2011).

An additional consideration, when measuring these markers, is that NO_2^- and NO_3^- plasma levels do not just reflect endogenous $^{\bullet}NO$ production but also dietary ingestion of these metabolites (Miller et al, 2012; Ashworth et al, 2015). For example, green leafy vegetables and beetroot are high in NO_3^-. Therefore, it is important to factor diet into the study design and analysis when using these

metabolites as markers of ˙NO production. Additionally, NO_3^- can be reduced to NO_2^- e.g. by NO_3^-reductases in oral bacteria (Doel et al, 2005) and NO_2^- can be reduced to ˙NO e.g. by xanthine oxidase (Zhang et al, 1998). These pathways are discussed further in Chapter 4.

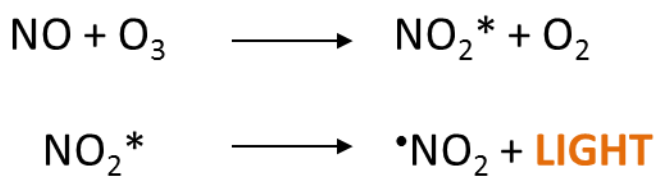

Figure 1.6: Ozone-based chemiluminescence for the measurement of nitrite and nitrate

Nitrite and nitrate are reduced to nitric oxide prior to ozone-based chemiluminescence. Nitric oxide then reacts with ozone to form “excited state” nitrogen dioxide. As the nitrogen dioxide returns to the ground state it releases a photon (light) and this is measured.

1.5. 3-Nitrotyrosine as a marker of nitrative stress in inflammation

Tyrosine (Tyr) nitration is considered a marker of nitrative stress and involves the removal of a hydrogen atom and the addition of a nitro group ($^{-}NO_2$) to the third carbon of the aromatic ring (Bartesaghi et al, 2007), i.e. the carbon adjacent to the hydroxyl group (**Figure 1.7**), the possible mechanisms for this are described later in pathways 1.1. and 1.2. The amino acids tryptophan, histidine and phenylalanine can also be nitrated (Alvarez and Radi, 2003). Nuriel et al (2011) have shown that tryptophan nitration is less common than Tyr nitration due to the different properties of these amino acids, e.g. Trp is more hydrophobic than Tyr, and Tyr nitration is the most studied of these modifications. The addition of the nitro group causes an increase in mass of +45 Da and drop in pKa (from 10 to ~7.5), which can bring a negative charge into a protein (Alvarez and Radi, 2003). Nitration can occur by many pathways but always involves reactive oxygen species and has been described as a two-step process (Souza et al, 2008);

1) Tyr is oxidised resulting in the tyrosyl radical
2) A radical-radical reaction occurs between the Tyr radical and nitrogen dioxide ($^{\bullet}NO_2$)

It is also possible for the Tyr radical to react with $^{\bullet}NO$, followed by further oxidation, to yield nitrotyrosine (Tyr-NO_2) but this pathway has not been well studied (Bartesaghi et al, 2007).

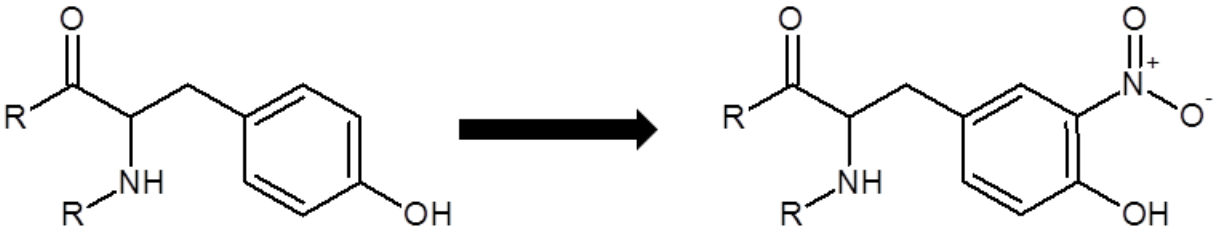

Figure 1.7: Conversion of tyrosine to 3-nitrotyrosine

The removal of a hydrogen atom and the addition of a nitro group ($^{-}NO_2$) to the third carbon of the aromatic ring of tyrosine results in 3-nitrotyrosine. The mechanisms are detailed in pathways 1.1. and 1.2.

One widely studied pathway for nitration is the production of the ROS/RNS peroxynitrite ($ONOO^-$). Peroxynitrite is formed by $^{\bullet}NO$ and $O_2^{\bullet-}$ combining in an exceedingly fast radical-radical reaction (rate constant: 1×10^{10} M^{-1} s^{-1}) meaning that $^{\bullet}NO$ can outcompete the dismutation of $O_2^{\bullet-}$ by superoxide dismutases (SODs) (Radi, 2013). $ONOO^-$ is a nucleophile that can generate secondary free radicals, such as $^{\bullet}NO_2$. $ONOO^-$ has a pKa of 6.8 and, as such, is present in both the anionic and protonated (ONOOH) form *in vivo*, making its reactivity highly pH dependent (Radi, 2013). The nucleophilic reaction of $ONOO^-$ with carbon dioxide increases the formation of Tyr-NO_2 (Alvarez and Radi, 2003) via the adduct nitrosoperoxocarbonate ($ONOOCO_2^-$), which undergoes homolysis to the secondary free radicals $^{\bullet}NO_2$ and carbonate radical ($CO_3^{\bullet-}$) (Peluffo and Radi, 2007). $CO_3^{\bullet-}$ is able to oxidise Tyr, forming a Tyr radical that can then react with the $^{\bullet}NO_2$ (**Pathway 1.1**).

Pathway 1.1: Peroxynitrite mediated tyrosine nitration

i.	$^{\bullet}NO + O_2^{\bullet-}$	$\longrightarrow$	$ONOO^-$	1×10^{10} M^{-1} s^{-1} (Radi, 2013)
ii.	$ONOO^- + CO_2$	$\longrightarrow$	$^{\bullet}NO_2 + CO_3^{\bullet-}$	3×10^{4} M^{-1} s^{-1} (Lymar and Hurst, 1995)
iii.	$CO_3^{\bullet-} + Tyr$	$\longrightarrow$	$Tyr^{\bullet} + HCO_3^-$	1.4×10^{8} M^{-1} s^{-1} (Augusto et al, 2002)
iv.	$Tyr^{\bullet} + {}^{\bullet}NO_2$	$\longrightarrow$	Tyr-NO_2	3×10^{4} M^{-1} s^{-1} (Lepoivre et al, 2005)

For a while, Tyr-NO_2 was believed to be a specific marker of peroxynitrite formation but this has since been disproved (Halliwell, 1997; van der Vliet et al, 1997), with the major alternate pathway cited involving the enzyme myeloperoxidase (MPO – **Pathway 1.2**). MPO is a haem peroxidase produced by immune cells that, in the presence of hydrogen peroxide (H_2O_2) and nitrite (NO_2^-), can catalyse the production of both the tyrosyl radical and $^{\bullet}NO_2$ (Bartesaghi et al, 2007).

Pathway 1.2: MPO mediated tyrosine nitration

i.	$H_2O_2 + MPO$	$\longrightarrow$	$MPO\text{-}I + H_2O$	1.8×10^{7} M^{-1} s^{-1} (Marquez et al, 1994)
ii.	$MPO\text{-}I + NO_2^-$	$\longrightarrow$	$MPO\text{-}2 + {}^{\bullet}NO_2$	2×10^{6} M^{-1} s^{-1} (Burner et al, 2000)
iii.	$MPO\text{-}I + Tyr$	$\longrightarrow$	$MPO\text{-}II + Tyr^{\bullet}$	7.7×10^{5} M^{-1} s^{-1} (Marquez and Dunford, 1995)
iv.	$Tyr^{\bullet} + {}^{\bullet}NO_2$	$\longrightarrow$	Tyr-NO_2	3×10^{4} M^{-1} s^{-1} (Lepoivre et al, 2005)

Pathways 1.1 and 1.2 are both intrinsically linked to inflammation. $^{\bullet}NO$ and $O_2^{\bullet-}$ production are increased during the phagocytic cells' oxidative burst (section

1.3) and thus $ONOO^-$ formation is increased during inflammation (Ischiropoulos et al, 1992). $ONOO^-$ has bactericidal activity (Zhu et al, 1992) but is also a potent oxidant that not only causes Tyr nitration but lipid peroxidation (Radi et al, 1991) and DNA damage (Szabo and Ohshima, 1997). (Szabo and Ohshima, 1997). MPO is released by activated neutrophils and mediates pathogen killing by the production of hypochlorous acid (HOCl), **Pathway 1.3** (Hazen and Heinecke, 1997; Nauseef, 2014). MPO activity has also been found to cause endothelial dysfunction by reducing the bioavailability of $^{\bullet}NO$ (Eiserich et al, 2002). As well as HOCl being involved in 3-chlorotyrosine formation (Domigan et al, 1995), HOCl has also been found to cause a loss in both free and protein-associated Tyr-NO_2 *in vitro* (Whiteman and Halliwell, 1999). The loss occurred in a concentration and time dependent manner (Whiteman and Halliwell, 1999) and, it has been suggested, that this loss is due to the Tyr-NO_2 being chlorinated, to form 3-chloro-5-nitrotyrosine (Curtis et al, 2011). If this loss occurs *in vivo* then levels of Tyr-NO_2 production could be underestimated when HOCl is also being locally generated (Whiteman and Halliwell, 1999).

Pathway 1.3: MPO generation of hypochlorous acid (HOCl) (Marquez et al, 1994)

i.	H_2O_2 + MPO	$\longrightarrow$	MPO-I + H_2O	$1.8 \times 10^7\ M^{-1}\ s^{-1}$
ii.	MPO-I + Cl^-	$\longrightarrow$	MPO-I-Cl^-	$2.2 \times 10^6\ M^{-1}\ s^{-1}$
iii.	MPO-I-Cl^-	$\longrightarrow$	HOCl	$5.2 \times 10^4\ s^{-1}$

When Tyr-NO_2 is measured in human samples it is not possible to tell which of the above pathways are responsible for the nitration detected. Pfeiffer et al (2000) suggested that peroxidase activity may be responsible for more nitration than $ONOO^-$. They showed that, at low concentrations of $ONOO^-$, the formation of dityrosine (a Tyr radical reacting with another Tyr radical) was favoured over Tyr-NO_2 formation and concluded that this may limit the amount of nitration caused by $ONOO^-$ formation *in vivo*. $^{\bullet}NO/O_2^{\bullet-}$ generating systems also produced less nitration than bolus addition of authentic $ONOO^-$ (Pfeiffer et al, 2001). When measuring nitration in activated RAW 264.7 macrophages, an inconsistency between the time course of $^{\bullet}NO/O_2^{\bullet-}$ release and Tyr-NO_2 formation was observed, where $^{\bullet}NO/O_2^{\bullet-}$ peaked far earlier than Tyr-NO_2 formation. Inhibition of nitration by azide and catalase also suggested that peroxidase activity was responsible in this system, rather than $ONOO^-$ (Pfeiffer et al, 2001). When Souza et al (1999) nitrated three proteins of a similar size

(ribonuclease A, lysozyme and phospholipase A2) *in vitro* they found that the nitration agent they used affected which protein was preferentially nitrated. MPO favoured ribonuclease A nitration, whilst $ONOO^-$ favoured phospholipase A2. Bartesaghi et al (2007) observed that $ONOO^-$-mediated protein nitration skews towards Tyr residues deeper in the phosphatidylcholine liposome transmembrane than MPO-mediated nitration of protein residues. They suggested that this is due to the difference in where oxidants are formed, as $ONOO^-$ can undergo homolysis within the membrane but MPO oxidants are produced outside of the liposome.

Both of these pathways can nitrate either free Tyr (free Tyr-NO_2) or Tyr residues within a polypeptide structure (protein-associated Tyr-NO_2). It is hard to determine whether free Tyr is more susceptible to nitration than Tyr residues *in vivo*, as degradation of nitrated proteins will affect free Tyr-NO_2 levels. Free Tyr-NO_2 levels can affect the levels of protein-associated Tyr-NO_2, Eiserich et al (1999) found that culturing cells with free Tyr-NO_2 (50 µM) led to incorporation of the Tyr-NO_2 into α-tubulin, as tubulin can be post-translationally modified by the removal and addition of Tyr to the carboxyl terminus of the protein (MacRae, 1997). However, there is no incorporation of the nitrated free amino acid during protein synthesis, as Tyr-NO_2 cannot be used during this process (Peluffo and Radi, 2007). Nitration of tyrosine residues within a peptide appears to show a level of specificity, as not all proteins are nitrated and of those that are, only a few of the Tyr residues are susceptible to this modification. This does not appear to be dictated by the level of aromatic ring exposure (Souza et al, 1999). The Tyr residue's local environment may affect this selectivity and common characteristics in this environment are: (1) close proximity to an acidic amino acid, (2) the Tyr being positioned on a loop structure and (3) the Tyr being near to a transition metal centre (Ischiropoulos, 2003; Bartesaghi et al, 2007). These factors may influence the local concentration of nitrating agents and their proximity to Tyr residues, for example a metal centre may generate nitrating agents that can nitrate proximal Tyr residues (Ischiropoulos, 2003).

The post-translational modification of proteins by nitration was shown to have multiple effects depending on the protein being studied. These effects range from being a possible physiological signalling mechanism to being an important pathological feature of diseases. Tyr phosphorylation is an important part of

signal transduction pathways and some studies have suggested that Tyr nitration is also part of cellular signalling (Monteiro, 2002; Yakovlev and Mikkelsen, 2010; Jia et al, 2011). For a modification to be considered relevant to cellular signalling pathways it must be reversible and some studies have found signs of a denitrase activity (Kamisaki et al, 1998; Irie et al, 2003; Deeb et al, 2013). Although it is thought to be enzymatic in nature, as the activity is decreased by heat and trypsin treatment, the mechanism for this denitration has not yet been identified, (Irie et al, 2003; Deeb et al, 2013). Additionally, the majority of research describes Tyr-NO_2 as a stable product of $ONOO^-$ formation or MPO activity that accumulates during inflammation (Herce-Pagliai et al, 1998; Dalle-Donne et al, 2006b). As many studies have shown, and continue to show, increased Tyr-NO_2 in disease, and without further evidence of denitration, the hypothesis that Tyr-NO_2 is a cellular signalling mechanism cannot yet be upheld.

There is also evidence to suggest that Tyr-NO_2 acts as a 'signal/tag' for the 20S proteasome, enhancing degradation of modified proteins (Gow et al, 1996; Souza et al, 2000b). If the modified protein does indeed experience a higher rate of turnover than other, non-modified, proteins then this would affect accurate measurement of Tyr-NO_2 formation in tissues. However, increased Tyr-NO_2 levels are observed in many pathologies, suggesting that modification of proteins is occurring at a higher rate than protein turnover. This would also mean that as inflammation subsides, and the rate of formation decreases, the degradation of modified proteins would lead to decreased Tyr-NO_2 levels with recovery and this has been seen in some studies (Ter Steege et al, 1998; Pirro et al, 2007).

Contrary to the above studies, it has also been suggested that nitration of proteins can lead to aggregation of the modified proteins rather than their degradation and removal (Souza et al, 2008). The amount of protein oxidation occurring has been shown to affect whether proteasome degradation occurs, with light damage enhancing degradation and moderate to heavy damage inhibiting the proteasome (Davies, 2001; Shringarpure and Davies, 2002; Dunlop et al, 2009). Aggregation of nitrated proteins has been seen in neurodegenerative diseases, such as Parkinson's (Giasson et al, 2000) and Alzheimer's disease (Reynolds et al, 2005). Whether nitration of proteins is

involved in the disease pathology is unknown, but these studies indicate that oxidative and nitrative stress may be a potential therapeutic target.

Changes to a protein's 3-dimensional structure and chemical properties may also result in a loss of function (Souza et al, 2008) as described for manganese superoxide dismutase (MacMillan-Crow et al, 1998). Increased levels of Tyr-NO_2 have been found within cancers (De Sanctis et al, 2014), with one study suggesting that the nitration of chemokines within the tumour environment hinders their ability to attract tumour specific cytotoxic T cells to the tumour (Molon et al, 2011). However, gain of function has also been observed for some proteins, such as cytochrome c (Cassina et al, 2000) and fibrinogen (Vadseth et al, 2004).

Tyr-NO_2 has also been linked with autoimmunity (section 1.3), as modified proteins can lead to the formation of neo-epitopes that bypass tolerance, i.e. are not recognised by the immune system as self (Eggleton et al, 2008; Ryan et al, 2014). Tyr-NO_2 levels in plasma have been found to correlate with disease severity or activity in patients with the autoimmune conditions rheumatoid arthritis (Misko et al, 2013) and systemic lupus erythematosus (Oates et al, 1999; Khan et al, 2006) and anti-Tyr-NO_2 antibodies have been found in both diseases (Khan and Ali, 2006; Khan and Siddiqui, 2006). These observations led to the suggestion that Tyr-NO_2 may perpetuate the inflammatory response and contribute to the pathogenesis of these diseases rather than just being a consequence of disease.

1.5.1. Measuring 3-nitrotyrosine

In a solution containing only protein, Tyr-NO_2 can be measured by UV-visible spectrometry. Tyr has an absorption peak (lambda max) at 280 nm. However, Tyr-NO_2 displays additional peaks at ~357 nm in acidic solutions and at ~430 nm in basic solutions (Yang et al, 2010). This shift in peak wavelength at different pH values is due to the Tyr-NO_2 either being in its neutral form at low pH or ionized at high pH (De Filippis et al, 2006).

When dealing with more complex samples (e.g. tissue samples), other techniques need to be employed. Published techniques include immunological (as anti-Tyr-NO_2 antibodies can be raised) and analytical chemistry methods,

such as chromatography coupled with various detection systems like mass spectrometry. Both these techniques have advantages and disadvantages: ELISA methods are high throughput, relatively low cost and do not involve extensive sample preparation but have low sensitivity and are semi-quantitative. GC/LC-MS/MS is quantitative, highly sensitive and accurate but is low-throughput, time-consuming and expensive, limiting this method's usefulness in a clinical setting.

A review of reported Tyr-NO_2 levels, in healthy human plasma, is complicated due to the methodological differences between studies and a lack of clarity when reporting the findings. However, when attempting to compare the healthy human plasma levels of Tyr-NO_2, it is clear that the literature is highly varied, as can be seen in **Tables 1.3** and **1.4**.

Table 1.3 details just a small selection of studies measuring Tyr-NO_2 in healthy human plasma. This comparison is limited, as different units have been used across studies making direct comparison near-impossible without further details. Furthermore, results may not be directly comparable for ELISA data as most studies report a standard equivalence rather than the absolute Tyr-NO_2 concentration, but this is rarely mentioned. It is also important to know whether free Tyr-NO_2, protein-associated Tyr-NO_2 or total Tyr-NO_2 is being measured and this is not always clearly stated. The two mass spectrometry studies produced similar results but are only measuring nitrated albumin rather than total protein nitration (Human serum albumin contains 18 Tyr residues (Consortium, 2015), **Table 1.3**). Despite this, nitrated albumin plasma levels of approx. 24 nM are higher than the levels reported for total protein-associated nitration in three of the five ELISA methods (**Table 1.3**). Wayenberg et al (2009) and Wayenberg et al (2011) measured albumin nitration in the plasma of human new-borns by sandwich ELISA and reported results of 7.3 ng nitrated albumin/ml and 3.9 ng nitrated albumin/ml respectively. However, due to the difference in the units used to report the results (i.e. ng/ml for the ELISA and nM for the mass spectrometry) these studies cannot be directly compared.

Table 1.3: A comparison of selected studies in which protein-associated 3-nitrotyrosine levels were measured by ELISA or Mass Spectrometry in the plasma of healthy humans

The studies below are a small example of the literature, selected on the basis that the units allowed direct comparison of the results from healthy (i.e. no disease) control participants. All the selected studies measured protein-associated Tyr-NO_2 in plasma.

Reference	**Method**	**Plasma protein-associated Tyr-NO_2 concentrations as reported in the original paper**	**Plasma protein-associated Tyr-NO_2 concentrations expressed as nM**
Rossner Jr et al (2007)	Non-competitive ELISA	856 ± 1989 nmol/l	860 ± 2000 nM
Sun et al (2007)	Sandwich ELISA	7.9 ± 7 nmol/l	7.9 ± 7 nM
Bo et al (2005)	Sandwich ELISA	Median (range) – 4.78 (0.04–235.7) nmol/ml	4800 nM (range 40 nM – 235.7 µM)
Ter Steege et al (1998)	Sandwich ELISA	Undetectable	(Limit of Detection 2 nM)
Ceriello et al (2001)	Indirect ELISA	Undetectable	(Limit of Detection 10 nM)
Tsikas et al (2003)	GC-MS/MS	24 ± 4 nM nitrated albumin	24 ± 4 nM
Keimer et al (2003)	GC-MS/MS	23.4 nM nitrated albumin	23.4 nM

Other ELISA methods have reported high levels of plasma protein nitration, but these methods were not included in the table because they measured total nitration (i.e. free Tyr-NO_2 is also measured) rather than protein-associated nitration. Inoue et al (2002) used a competitive ELISA to measure total (free and protein-associated) Tyr-NO_2 in healthy humans. This study found levels of 135.4 ± 18.7 nM (35.21 ± 4.87 ng/ml) Tyr-NO_2 in healthy humans, contradicting three of the five ELISA findings in the table. However, these results represent total Tyr-NO_2, not just the protein-associated form and this could explain the higher levels measured. Bekpinar et al (2005) also used a competitive ELISA, to study oxidative and nitrative stress in Behçet's disease. Tyr-NO_2 levels were 3.67 ± 0.05 ng/ml in healthy controls (approx. 13 nM), this is ten times lower than the Inoue et al (2002) findings but comparable to levels of nitrated albumin measured in new-borns (Wayenberg et al, 2009; Wayenberg et al, 2011). If the higher levels in the competitive ELISA studies are the result of free Tyr-NO_2 in the plasma, these studies would still not support the data obtained by mass spectrometry in **Table 1.3**. Separate measures of free Tyr-NO_2 levels in plasma have been obtained by chromatography coupled with several different detection methods, such as mass spectrometry, UV detection and electrochemical detection (**Table 1.4**).

Some investigators have chosen to report the results in relation to total protein or Tyr content, allowing for the proportion of nitration to be assessed across data sets. Additionally, protein concentration may vary between individuals (potentially drastically between those with disease and healthy controls) and reporting the results in terms of total protein or Tyr content can account for this difference.

Table 1.4: A comparison of reported free 3-nitrotyrosine levels in the plasma of healthy humans

The studies below are an example of some of the literature selected on the basis that the units allow direct comparison of the results from healthy (i.e. no pathology) control participants. All the studies measured free Tyr-NO_2 in plasma. (A) Gas chromatography separation, (B) Liquid chromatography separation.

Table 1.4A: Gas chromatography separation

Authors	Method	Plasma free Tyr-NO_2 concentrations as reported in the original paper	Plasma free Tyr-NO_2 concentrations expressed as nM
Schwedhelm et al (1999)	GC-MS/MS[1]	2.8 ± 0.84 nM	2.8 ± 0.84 nM
Keimer et al (2003)	GC-MS/MS[1]	636.0 (153.0) pM[2]	0.64 nM (0.15)
Söderling et al (2003)	GC MS/MS[1]	0.74 ± 0.30 nM	0.74 ± 0.30 nM
Tsikas et al (2003)	GC-MS/MS[1] GC-MS[1]	**GC-MS/MS** Group aged 51 ± 10 years: 1.140 ± 0.727 nM Group aged 25 ± 3 years: 2.677 ± 1.540 nM Male group aged 26 ± 3 years: 0.73 ± 0.53 nM **GC-MS** Group aged 51 ± 10 years: 4.463 ± 4.495 nM Group aged 25 ± 3 years: 5.447 ± 2.783 nM	**GC-MS/MS** Group aged 51 ± 10 years: 1.1 ± 0.73 nM Group aged 25 ± 3 years: 2.7 ± 1.5 nM Male group aged 26 ± 3 years: 0.73 ± 0.53 nM **GC-MS** Group aged 51 ± 10 years: 4.5 ± 4.5 nM Group aged 25 ± 3 years: 5.5 ± 2.8 nM
Pannala et al (2003)	GC-MS[1]	5.44 ± 1.19 nmoles/l	5.4 ± 1.2 nM
Gaut et al (2002a)	EC-NCI GC/MS[1] LC-MS/MS[1]	EC-NCI GC/MS 11 ± 2 nM LC-MS/MS undetectable LOD reported as 39 fmol	**EC-NCI GC/MS** 11 ± 2 nM **LC-MS/MS** Not detected (Limit of Detection 20 nM)

Table 1.4B: Liquid chromatography separation

Authors	Method	Plasma/serum free Tyr-NO_2 concentrations as reported in the original paper	Plasma/serum free Tyr-NO_2 concentrations expressed as nM
Yi et al (2000)	LC-MS/MS[1]	< 4.4 nmol/L	Not detected (Limit of Detection 4.4 nM)
Thornalley et al (2003)	LC-MS/MS[1]	6.5 ± 2.5	6.5 ± 2.5 nM
Ahmed et al (2003)	LC-MS/MS[1]	9.4 ± 0.4 nM	9.4 ± 0.4 nM
Ahmed et al (2005)	LC-MS/MS[1]	<0.4 nmol/l	Not detected (Limit of Detection 0.4nM)
Kaur and Halliwell (1994)	HPLC – UV	Undetectable (serum)	Not detected (Limit of Detection 200 nM)
Fukuyama et al (1997)	HPLC – UV	Undetectable	Not detected (Limit of Detection 600 nM)
Fatouros et al (2004)	HPLC-UV	5.3 ± 0.4 µM (older men)	5300 ± 400 nM
Ohshima et al (1999)	HPLC electrochemical detection	Undetectable	Not detected (Limit of Detection 5 nM)
Kamisaki et al (1996)	HPLC – Fluorescence spectrophotometer	31 ± 6 pmol/ml	31 ± 6 nM
Ohya et al (2002)	853 type amino acid analyzer (Hitachi)	Undetectable (<0.1 nmol/mL)	Not detected (Limit of Detection 100 nM)
Footnotes			
1	Studies took steps to address artefact formation (discussed in the text).		
2	Data expressed as the median. Values in parentheses represent interquartile ranges.		

UV detection has been coupled with chromatography for the detection of free Tyr-NO_2 and these studies often have a high limit of detection (LOD), suggesting low sensitivity (see **Table 1.4B**). For example Fukuyama et al (1997) used HPLC-UV to measure free Tyr-NO_2 in plasma taken from healthy individuals, as well as renal failure patients (separated into those with septic shock and those without). At a wavelength of 274 nm the LOD was 600 nM, this is several orders of magnitude higher than the LOD of methods using tandem MS (MS/MS) and ELISA methods (although it is protein-associated Tyr-NO_2 measured by ELISA). Perhaps unsurprisingly, free Tyr-NO_2 was undetected in healthy plasma. The high LOD did not prevent free Tyr-NO_2 being measured in the renal failure patients, where levels were exceedingly high (118.2 ± 22.0 µM with sepsis and 28.0 ± 12.3 µM without).

Specificity when measuring Tyr-NO_2 in tissue can also be an issue with some detection methods, e.g. Kaur et al (1998) used HPLC coupled to a photodiode array detector to analyse Tyr-NO_2 in brain tissue from various neurological disorders; a peak with the same retention time as Tyr-NO_2 (that was not detected in controls) was produced and could be reduced to aminotyrosine by dithionite (an often used criterion for identifying Tyr-NO_2). However, when mass spectrometry was employed as a detection system it was revealed that this peak was not true Tyr-NO_2 (the compound was not identified). Other detection systems, such as UV and electrochemical detection, were unable to make this distinction, confirming that mass spectrometry is a more specific detection method.

Mass spectrometry is considered the most accurate method to quantify Tyr-NO_2. However, there are still several factors to take into account. For example, Tsikas et al (2003) measured free Tyr-NO_2 in the same samples by either GC-MS or GC-MS/MS and reported levels to be lower with the tandem MS method, e.g. for the age group 51 ± 10 years the results for MS vs. MS/MS were 5.5 ± 2.8 nM and 1.1 ± 0.73 nM respectively (**Table 1.4A**).

A principal consideration when measuring Tyr-NO_2 by mass spectrometry is artefact formation during acidic sample preparation (Frost et al, 2000; Yi et al, 2000). Yi et al (2000) compared liquid and gas chromatography (LC and GC) and concluded that LC was less likely to lead to artificial formation due to a less

extreme pH during sample processing. However, Tsikas and Caidahl (2005) suggested that this means compromising on sensitivity, and that the methodological steps needed to improve sensitivity to a GC standard would increase the risk of artefact formation, thus removing its advantage over the GC analysis. Gaut et al (2002a) also compared two methods (electron capture negative chemical ionization-GC/MS and LC-electrospray ionization MS/MS) and found the GC/MS to be not only 100-fold more sensitive than LC-MS/MS but also less time-consuming; generation of Tyr-NO_2 during analysis was found to be negligible for both methods. However, Duncan (2003) suggested that Gaut et al (2002a) were mistaken in their conclusion and that the 'failings of the LC assay' were due to the system they used, rather than LC being less sensitive for Tyr-NO_2 measurement. Duncan (2003) recommended a triple quadrupole system for improved sensitivity. Other methods employed to prevent artefact formation include: avoiding acidic conditions (Frost et al, 2000) and removing NO_2^-, NO_3^- and Tyr from the sample prior to GC-MS/MS sample preparation (Schwedhelm et al, 1999).

Some mass spectrometry studies do not assess the Tyr-NO_2 of the entire plasma proteome, for example only looking at albumin (Keimer et al, 2003; Tsikas et al, 2003). This is presumably done because of the low abundance of Tyr-NO_2 in serum/plasma (Radi, 2004) and a desire to remove a lot of unmodified Tyr from the sample so that Tyr-NO_2 can be detected by the MS/MS (discussed further in Chapter 5, section 5.4). Therefore, these results are not truly representative of the serum nitration levels as they may be missing large portions of the Tyr-NO_2 present in the proteome. ELISAs however, are able to measure whole samples, without any extensive sample preparation (or risk of artefact formation). Coupled with lower cost and higher throughput this makes ELISA a more appealing method than MS/MS for measuring large numbers of clinical samples.

Many different sample types have been used when measuring Tyr-NO_2 in samples, e.g. plasma/serum (Shishehbor et al, 2003; Misko et al, 2013), synovial fluid (Kaur and Halliwell, 1994), cerebrospinal fluid (Tohgi et al, 1999; Korolainen and Pirttilä, 2009), urine (Tsikas et al, 2012), exhaled breath condensates (Hanazawa et al, 2000; Bodini et al, 2006) and tissue biopsies (Kaminsky et al, 1999; Sultana et al, 2006). These studies demonstrate that

Tyr-NO_2 is formed in many different tissue types *in vivo,* of which many are accessible in a clinical setting with minimal invasiveness. This has led to the suggestion that Tyr-NO_2 could be measured as a marker of oxidative stress, for prognosis or disease monitoring, in clinical studies.

This thesis expands on the above studies by measuring Tyr-NO_2, along with other inflammatory/oxidative stress markers, in four inflammatory settings: (1) inflammation as a result of trauma/tissue injury (i.e. surgery), (2) NO_3^- supplementation in smokers (low level, persistent inflammation) and non-smokers, (3) an acute, infective inflammatory response (i.e. sepsis), and (4) a pathology with a chronic inflammatory component (i.e. Alzheimer's disease).

1.5.2. Oxidative/nitrative stress following surgery, an example of acute inflammation

Inflammation and oxidative stress are known to occur following surgery and oxidative stress has been the subject of investigation as a factor affecting recovery (Rosenfeldt et al, 2013). This is of particular importance in surgery that involves ischaemia-reperfusion (e.g. abdominal aortic aneurysm and transplantation), where excessive ROS generation, such as $O_2^{\bullet-}$, has been shown to cause tissue damage (Kaminski et al, 2002; Bonder et al, 2004; Granger and Kvietys, 2015).

Ischemia is a reduction in blood flow to a tissue, resulting in hypoxia, and reperfusion is the return of normal blood flow to the affected area. Both of these stages can cause tissue damage, termed ischaemia-reperfusion injury (Dorweiler et al, 2007; Kalogeris et al, 2012). During the hypoxic period of ischaemia, anaerobic metabolism is utilised, decreasing cellular pH and rapidly depleting ATP, resulting in decreased active transport of calcium leading to calcium overload in the cell (**Figure 1.8**) (Carden and Granger, 2000; Kalogeris et al, 2012). If prolonged, necrosis of the ischaemic tissue occurs, making prompt return of blood flow vital. However, this reperfusion also causes damage. Reperfusion injury is thought to be due to many factors including generation of substantial amounts of ROS and a large inflammatory response (**Figure 1.8**) (Carden and Granger, 2000; Kalogeris et al, 2012).

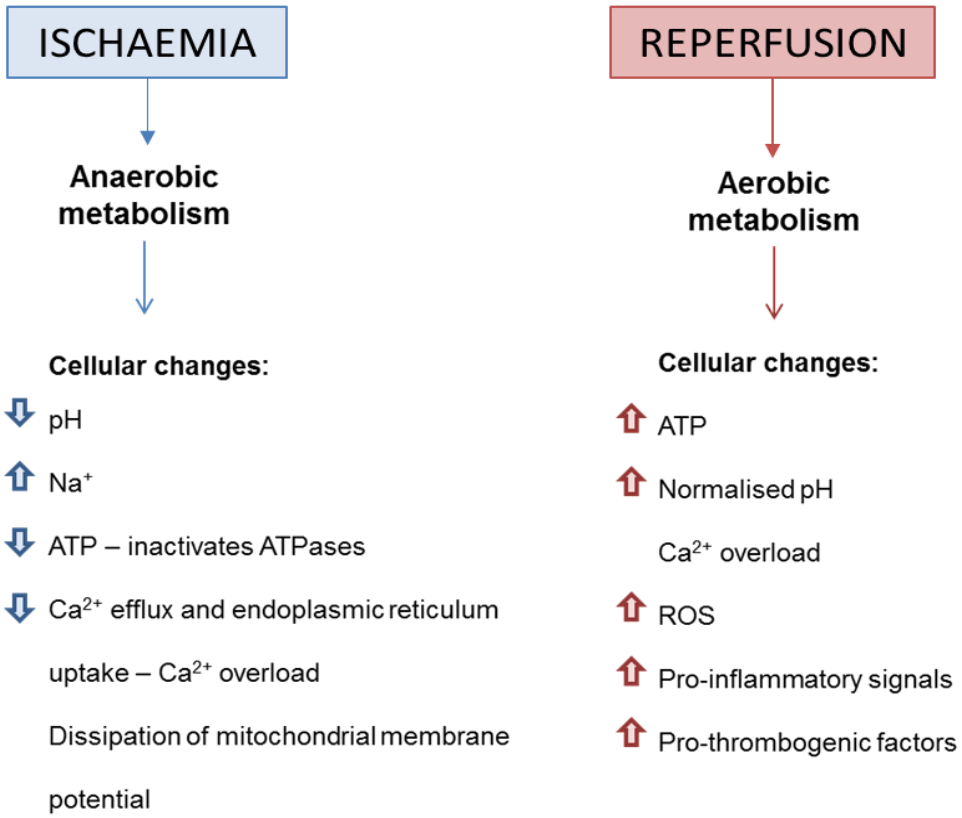

Figure 1.8: Cellular changes arising from ischemia and reperfusion

Ischemia gives rise to anaerobic metabolism and disruption of cell processes that can lead to cell death. However, reperfusion can also cause damage to the cells.

$^{\bullet}NO$, $O_2^{\bullet -}$, and $ONOO^-$ have all been cited as influencing the myocardial damage observed following an ischaemia-reperfusion injury event in cardiovascular surgery (Zweier and Talukder, 2006; Venardos et al, 2007). $^{\bullet}NO$ is increased by two pathways during this process: NOS activation, i.e. eNOS (activated by haemodynamic stimuli) and iNOS (induced following the activation of macrophages), and the chemical reduction of NO_2^- by xanthine oxidase (XO) (Zweier and Talukder, 2006). $O_2^{\bullet -}$ is produced by NADPH oxidase in infiltrating polymorphonuclear cells (PMN) and by uncoupling of NOS, observed when arginine or BH4 are depleted (Zweier and Talukder, 2006). As well as acting as chemoattractants for more PMNs, these free radicals form $ONOO^-$ (Pathway 1.1). It has been suggested that, at physiological concentrations, $ONOO^-$ is potentially cardioprotective during reperfusion as it decreases PMN adhesion and XO activity (Nossuli et al, 1998; Lee et al, 2000). However, $ONOO^-$ can also modify many cellular targets, such as inducing protein nitration, as previously mentioned (Pathway 1.1). Following ischaemia-reperfusion injury,

increased nitration has been measured in rat heart tissue (Bas et al, 2012) and human plasma proteins (Troxler et al, 2004; Zhao et al, 2005; Hui et al, 2012).

Clinical human studies, using therapies targeting oxidative stress induced by surgery, have shown that high doses of antioxidants can decrease tissue damage or improve recovery time (Bartels et al, 2004; Arato et al, 2010; Leong et al, 2010). Tyr-NO_2 may be beneficial in these studies as a marker of protein modification linked to $^{\bullet}NO$ production.

Measurement of Tyr-NO_2 post-surgery is discussed further in chapter 3.

1.5.3. Oxidative/nitrative stress in smokers, an example of low-level chronic inflammation

The presence of inflammation and oxidative stress induced by smoking has been demonstrated in many studies. Smokers have an accumulation of neutrophils and macrophages in their airways (Kuschner et al, 1996; van der Vaart et al, 2004; Mehta et al, 2008; Mortaz et al, 2010), as well as increased pro-inflammatory signals (Rastrick et al, 2013; Wiegman et al, 2015). Increased serum levels of peripheral blood cells, such as neutrophils, are also seen in smokers compared to non-smokers (Martins et al, 2013). Additionally, isolated peripheral blood cells from smokers were found to produce more H_2O_2 than non-smoker cells (Tanni et al, 2012). Mortaz et al (2010) found that cigarette smoke induces TLR9 signalling in isolated human neutrophils; *in vivo,* this signalling would lead to further recruitment of neutrophils. However, Mehta et al (2008) suggested that, although there is an influx of immune cells, these cells had decreased phagocytic and respiratory burst functions. They suggested that this is part of the reason why smokers are vulnerable to recurrent infections.

Increased markers of oxidative stress have also been measured in smokers, compared to non-smokers, e.g. the lipid oxidation product malondialdehyde (Isik et al, 2007; Waseem et al, 2012). van der Vaart et al (2004) studied the effects of acute smoking and found that there was an increase in exhaled $^{\bullet}NO$ and 8-isoprostane, as well as an increase in $O_2^{\bullet-}$ and H_2O_2 in bronchoalveolar lavage fluid. This was accompanied by a brief decrease in blood NO_2^- and NO_3^-. Decreased antioxidant capacity has also been measured in smokers compared

to non-smokers, i.e. a decrease in serum superoxide dismutase, catalase and glutathione peroxidase (Waseem et al, 2012).

Histone deacetylase 2 (HDAC2) was found to be significantly nitrated in the peripheral lung tissue of smokers compared to non-smokers and it was shown that nitration increased proteasomal degradation (Osoata et al, 2009). HDAC2 lowers inflammatory gene expression and decreased expression in peripheral lung tissue has been observed in chronic obstructive pulmonary disease (COPD), a disease where a strong inflammatory response is seen in the airways (Barnes, 2009). Smoking is widely linked to COPD, a leading cause of morbidity and mortality worldwide (Mannino and Buist). It has also been suggested that COPD has an autoimmune component (Agustí et al, 2003). Kirkham et al (2011) found that cigarette smoke forms carbonyl adducts on proteins and that COPD patients had both an increase in carbonyl modified proteins, in the lung and circulation, and the presence of autoantibodies against carbonyl modified proteins. As has already been mentioned, a link between proteins with oxidative modifications and autoimmunity has been established (Griffiths, 2008; Ryan et al, 2014) and as such, smoking-induced protein modifications (in addition to carbonyl adducts) could be an important factor in COPD pathology.

1.5.4. Oxidative/nitrative stress in sepsis, as an example of an infective inflammatory disease

Sepsis is an example of an acute infective inflammatory disease. In essence, sepsis is a systemic host response to infection that is maladaptive (Vincent and Abraham, 2006); involving a dysfunctional level of pro-inflammatory cytokines in the circulation followed by a later immunosuppressive stage, caused by an increase in anti-inflammatory cytokines (**Figure 1.9**). This immunosuppressive stage has been described as a compensatory anti-inflammatory response syndrome and leaves patients vulnerable to a secondary infection (Adib-Conquy and Cavaillon, 2008).

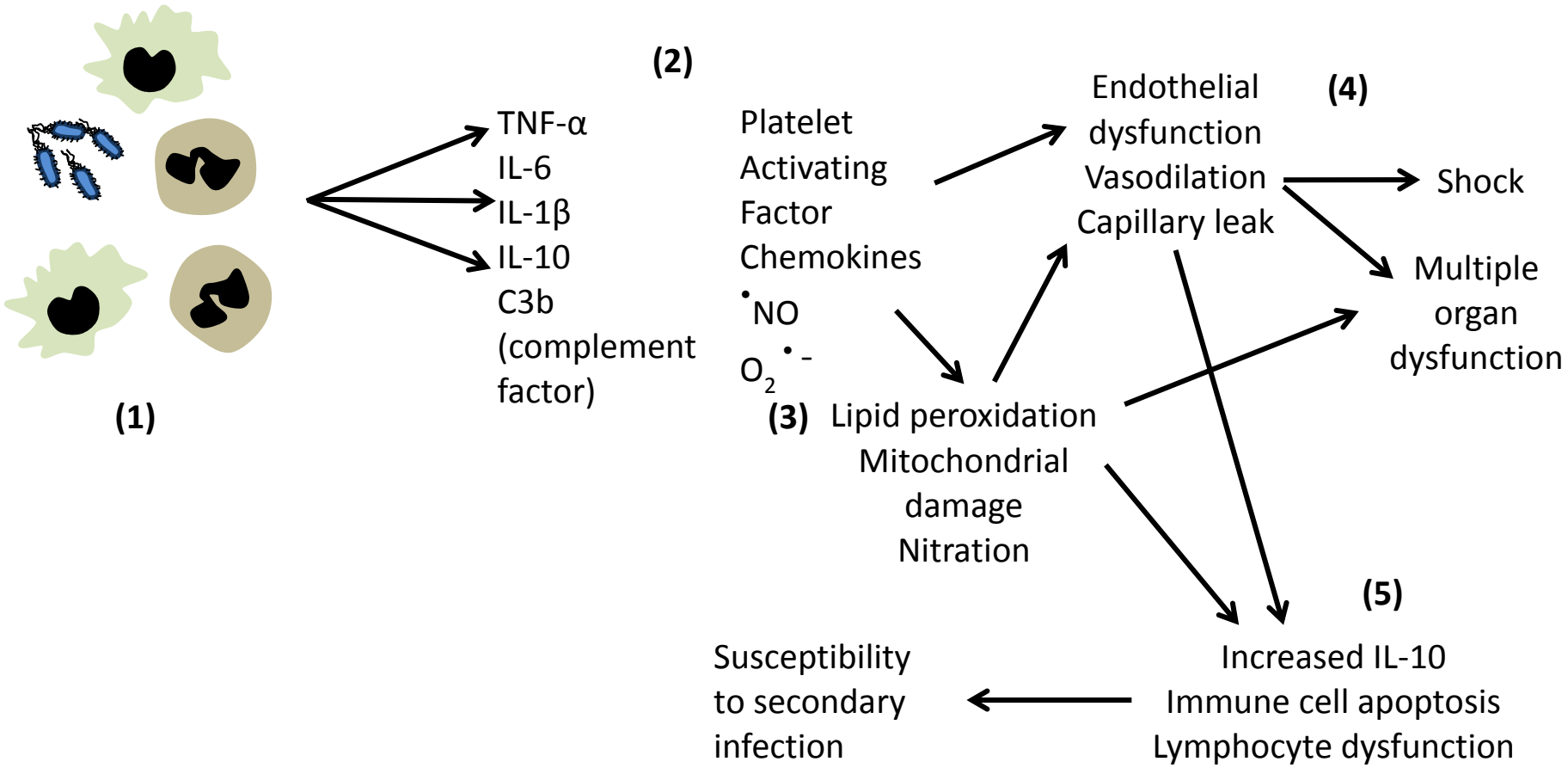

Figure 1.9: Sepsis disease progression

Sepsis is maladaptive systemic response to infection, some of the stages and mediators are described above. (1) Innate immune cells (macrophages and neutrophils shown) respond to an infection (a bacterial infection is shown but it can be viral or fungal). (2) Release of cytokines, chemokines and ROS into the circulation. (3) ROS mediated damage. (4) Tissue damage, organ dysfunction and hypotension. (5) Compensatory anti-inflammatory response.

A 2006 database review (Harrison et al, 2006) of sepsis in England, Wales, and Northern Ireland revealed that '*the number of admissions to UK critical care units with severe sepsis within the first 24 hours of admission is increasing'* going from 23.5 % in 1996 to 28.7 % in 2004. Despite a decrease in mortality over this time there was an increase in the total number of deaths (~9,000 to ~14,000) (Harrison et al, 2006). The pathology of sepsis is highly complex and heterogeneous and there has been much debate over the definition and diagnosis criteria of sepsis, with only 17% of physicians agreeing on any single definition in a 2004 survey (Vincent et al, 2009).

Diagnosing sepsis clinically is far from simple. To begin with, the inflammatory response is comparable to a sterile inflammatory response initiated by trauma, burns, pancreatitis, etc., in which no infection is involved (and thus antimicrobials are ineffective as a treatment). Sepsis is not confined to one type of organism (i.e. the pathogen may be viral, bacterial or fungal) or to one origination point (i.e. infection may occur anywhere in the body) (Vincent and Beumier, 2013). The progression, and outcome, of the response will vary depending on the microorganism present and individual characteristics of the patient (e.g. age, co-morbidity, etc.) (Vincent et al, 2009). All these factors make finding one defining marker of disease next to impossible. Instead, diagnosis depends on multiple signs and markers.

The British Medical Journal Best Practice sets out diagnostic criteria of sepsis based on the consensus of a 2001 conference (Levy et al, 2003). Sepsis is considered if at least 2 of the following are present in conjunction with infection:

- Hypothermia (<36°C) or hyperthermia (>38.3°C)
- Tachycardia (>90 beats per minute)
- Tachyponea (>20 breaths per minute)
- PCO_2 <4.3 kPa (32 mmHg)
- Hyperglycaemia in the absence of diabetes (>6.66 mmol/L)
- Acutely altered mental state
- White blood cell count <4 or >12 x 10^9/L

The “cytokine storm” produced during sepsis is both an excessive release of pro-inflammatory cytokines, in response to infection, and an extreme counteractive release of anti-inflammatory cytokines (Chaudhry et al, 2013; Schulte et al, 2013). Increased IL-6 has shown a correlation with disease severity ($r = 0.63$, $p < 0.001$, Damas et al (1992)) and persistent overproduction of IL-10 is considered a risk factor for a fatal outcome (Chaudhry et al, 2013). A pilot study by (Lukaszewski et al, 2008) measured mRNA expression levels for a panel of cytokines (IL-1β, IL-6, IL-8, IL-10, TNFα, FasL and CCL2) *prior* to diagnosis of sepsis in intensive care unit patients (ICU - these patients have a higher risk of sepsis) and ICU patients without complications (i.e. no sepsis). With this data, they were able to produce a successful neural network model for predicting which ICU patients would develop sepsis. This is one of the few studies that measured markers prior to sepsis diagnosis and, as the effectiveness of antimicrobial therapy rapidly decreases following the onset of sepsis (Kumar et al, 2006; Weiss et al, 2014), identifying biomarkers to allow for earlier diagnosis is a vital area of research.

The acute phase proteins CRP and procalcitonin have both been studied as potential markers of sepsis (Pierrakos and Vincent, 2010). CRP is a well-known inflammatory marker routinely measured in clinical settings and has been studied as a potential marker for differentiating sepsis from systemic inflammatory response syndrome with an area under the curve of 0.94 (Sierra et al, 2004). However, some have reported that its ability to distinguish between patients with infection and patients with a sterile inflammatory response is not discriminatory (Lavrentieva et al, 2007). Increased procalcitonin concentrations have been associated with bacterial infections (Delévaux et al, 2003) and some studies suggest that procalcitonin is superior to CRP at indicating infection during systemic inflammatory response syndrome (Luzzani et al, 2003; Uzzan et al, 2006; Kibe et al, 2011). However, some meta-analysis studies have suggested that procalcitonin still has a low-to-moderate diagnostic performance for the identification of sepsis (Jones et al, 2007; Tang et al, 2007). As a prognostic marker, procalcitonin is superior to CRP due to the fact that levels decrease far quicker (Standage and Wong, 2011).

As previously discussed, the inflammatory response leads to the recruitment of immune cells and the generation and release of ROS/RNS. Sepsis is no

exception to this and extensive evidence of oxidative stress has been observed in sepsis (Martins et al, 2003; Santos et al, 2012). This oxidative stress has been linked to endothelial dysfunction, aiding progression to septic shock (Azevedo et al, 2006; Huet et al, 2011) and damage to mitochondria, leading to dysfunction and multiple organ failure – severe sepsis (**Figure 1.9**) (Victor et al, 2004; Castellheim et al, 2009). This suggests that oxidative stress is not only a result of sepsis but also a pathological feature, which can cause a serious deterioration in the patient's condition.

High amounts of free radical generation (e.g. $^{\bullet}NO$ and $O_2^{\bullet-}$) and MPO release would increase Tyr-NO_2 formation and free Tyr-NO_2 has indeed been found to be greatly elevated during sepsis (Fukuyama et al, 1997; Ohya et al, 2002). Nitration can affect protein function (Radi, 2012) and this too may contribute to disease progression. For example, nitration of manganese superoxide dismutase (a mitochondrial enzyme) results in a loss of function and thus an accumulation of $O_2^{\bullet-}$ and further oxidative damage (MacMillan-Crow et al, 1998; Moreno et al, 2011).

The presence of Tyr-NO_2 in sepsis means it could potentially be used as a biomarker for this disease. Indeed, some have suggested that free Tyr-NO_2 in plasma is associated with sepsis prognosis (Ohya et al, 2002). This is discussed further in Chapter 5.

1.5.5. Oxidative/nitrative stress in Alzheimer's disease; a chronic disease with an inflammatory component

As life expectancy improves, many countries now have to deal with the health consequences of an ageing population, one of which is an increasing prevalence of dementia (Sosa-Ortiz et al, 2012). In 2010 it was estimated that 35 million people worldwide had dementia (Sosa-Ortiz et al, 2012), with Alzheimer's disease (AD) making up approximately 70% of this group (Zhu and Sano, 2006). The second largest sub-group is vascular dementia (VaD). However, it is thought that a 'mixed' dementia (AD with cerebrovascular disease) sub-group is underestimated in the population (Kalaria, 2002).

AD is characterised by three pathological changes in the brain – intracellular neurofibrillary tangles (containing the microtubule-associated protein tau),

extracellular amyloid-β plaques and loss of synapses (Sultana et al, 2006; Reynolds et al, 2007; Reyes et al, 2011), changes that can only be observed post-mortem. Neuronal loss and widespread atrophy are also observed (Fox et al, 2001). A transition step between healthy ageing and AD is mild cognitive impairment and this condition is often studied to observe early physical changes in AD (Cenini et al, 2008).

Neuroinflammation is known to occur in AD and is now being viewed as an important pathological factor in disease progression (Heneka et al, 2015). The central nervous system has resident innate immune cells (microglia and astrocytes) that are activated by DAMPs such as amyloid plaques (Heppner et al, 2015) (**Figure 1.10**). The neurofibrillary tangles and plaques can also activate complement pathways and dementia is associated with increased levels of cytokines and chemokines that may be released by neurons, as well as the resident immune cells (Akiyama et al, 2000).

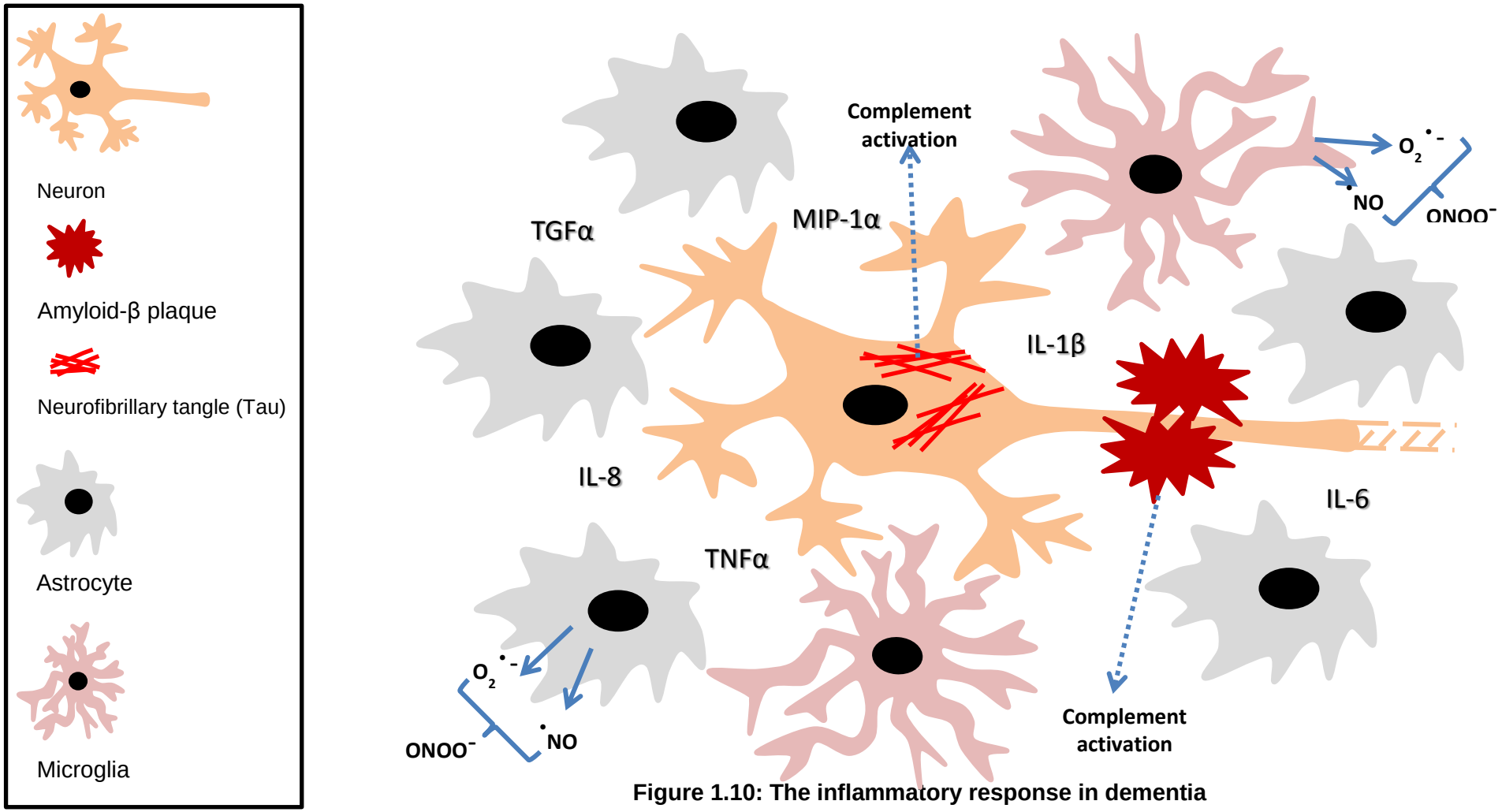

Figure 1.10: The inflammatory response in dementia

Amyloid-β acts as a DAMP that activates the brain immune cells; microglia and astrocytes. Once activated these cells release cytokines, chemokines and ROS. Neurofibrillary tangles (containing tau) and amyloid plaques can both activate complement pathways. Neurons can also release cytokines, chemokines and ROS.

An altered antioxidant status has been implicated in dementia. Decreased circulating levels of antioxidants have been associated with poor memory (Perkins et al, 1999), while increased dietary intake of antioxidants is linked with an improved cognitive performance (Masaki et al, 2000). However, prospective studies looking at dietary intake of antioxidants and AD risk have had mixed results, such as a decreased risk regardless of genotype (Engelhart et al, 2002), decreased risk only in those that are not a carrier of apolipoprotein E4 gene (Morris et al, 2002) and no decreased risk at all (Luchsinger et al, 2003). A two year controlled clinical study (double-blind, placebo-controlled, randomised and multicentre), treating 'moderate' AD patients with high dose vitamin E (2000 IU/day) was performed (Sano et al, 1997). Although the treatment group saw a significant delay in time to the primary outcomes (progression to severe AD and death), there was no impact on the rate of cognitive decline. Praticò (2008) carried out a review, of clinical studies using antioxidant treatments, and made the important point that many studies failed to measure markers of oxidative burden in the patients and as such, it is unknown whether the antioxidant drugs were decreasing oxidative stress in the central nervous system.

The species involved in Tyr-NO_2 formation are present in the AD brain, e.g. $^{\bullet}NO$ is produced by neuronal (nNOS), endothelial (eNOS) and inducible (iNOS) nitric oxide synthase (Law et al, 2001). Superoxide dismutase (SOD) activity was found to be reduced in the AD brain (Marcus et al, 1998). As mentioned earlier (see section 1.1), SOD is responsible for dismutating $O_2^{\bullet -}$ to H_2O_2 and therefore a loss of activity will lead to an increase in available $O_2^{\bullet -}$ which, in the presence of $^{\bullet}NO$, will lead to $ONOO^-$ formation leading to nitration of proteins within the brain (Good et al, 1996; Castegna et al, 2003; Butterfield et al, 2007b). An increased expression of MPO has also been observed in the AD brain (Green et al, 2004), where MPO appeared to be localised to amyloid plaques. Active MPO catalyses the nitration of tyrosine residues in the presence of NO_2^- and H_2O_2 (section 1.5, pathway 1.2).

An increase in Tyr-NO_2 has been observed in AD brains when compared to control subjects (Good et al, 1996; Castegna et al, 2003; Sultana et al, 2006; Butterfield et al, 2007b; Sultana et al, 2007; Reed et al, 2009). Nitrated tau was observed in tangles, with evidence that this could occur early in the disease (Butterfield et al, 2007b). However, it has been suggested that tau nitration may

have a physiological role, possibly in neuron differentiation (Cappelletti et al, 2004).

Nitration of other proteins may affect neuronal survival. For example, nitration of the pro-apoptotic protein p53 is suggested to play a part in neuronal cell death (Cenini et al, 2008). This protein showed significantly more nitration in specific cerebral regions of Alzheimer's brains compared to age-matched controls without a history of dementia, an observation not made in samples from patients with mild cognitive impairment (Cenini et al, 2008). Nitration of certain enzymes in neurons could also affect the enzymatic function, altering important cellular processes such as glucose metabolism and cell survival (Sultana et al, 2006).

Dildar et al (2010) reported that serum Tyr-NO_2 concentrations were no different in AD patients when compared to control subjects and that this modification might only be observable in the brain. However, the accurate measurement of Tyr-NO_2 in plasma/serum is currently a matter of debate, as there are widely varying levels being reported between research groups (discussed in section 1.5.1). The method used by Dildar et al (2010) was a commercial sandwich ELISA kit with a limit of detection of 2 nM. Even if we assume that plasma Tyr-NO_2 is indeed increased in this pathology, during preparation the samples were diluted and, given that Tyr-NO_2 is suspected to be present in very low concentrations in plasma, this method may have been too insensitive to detect Tyr-NO_2. Tyr-NO_2 in dementia is discussed further in Chapter 6.

Animal models play a key role in biomedical research, aiding in target discovery and validation of therapeutic approaches. Transgenic animal models express foreign DNA, e.g. human genes. This technique has been used to produce mice with pathological hallmarks of AD pathology, allowing researchers to understand some of the mechanisms and the disease progression (Houdebine, 2007). There are several mouse models for AD that exhibit some, though not all, AD pathology (Morrissette et al, 2009; Elder et al, 2010). Mouse models of AD are discussed further in Chapter 6, section 6.1.

Oxidative stress is observed in the brain of AD mouse models, with some studies suggesting that this is an important factor in disease pathology rather than a consequence of plaque and tangle formation (Matsuoka et al, 2001; Praticò et al, 2001; Kanamaru et al, 2015). Models of AD have the benefit of

allowing the time course of the disease to be studied, not just the final hallmarks of pathology. For instance, Praticò et al (2001) measured urinary, plasma and brain lipid peroxidation levels over several time points in a transgenic mouse model (Tg2576) and found that isoprostane levels increased prior to the amyloid-β plaque deposition (8 and 12 months respectively). They concluded that this indicates oxidative stress helps drive AD pathology rather than being a result of the amyloid-β plaque formation. Supporting this hypothesis is the study by Kanamaru et al (2015), in which an AD mouse model was crossed with a mouse model that exhibits increased oxidative stress. It was found that the double transgenic had plaque pathology earlier than the AD single transgenic model, implying that oxidative stress accelerates the AD-like pathology. Based on the idea that oxidative stress is important in driving AD pathology, Lim et al (2001) tested the effect of the antioxidant curcumin on a mouse model of AD. They found that both low and high doses reduced the levels of oxidised proteins and plaque burden, in brain tissue, compared to untreated mice.

Although these studies suggest that oxidative stress is central in AD progression the results cannot be extrapolated to humans, due to both species differences and the fact that mice do not exhibit the full range of AD pathology. However, oxidative stress remains an interesting area for therapeutic targeting and biomarkers of oxidative stress could help determine the efficiency of interventions.

1.5.6. Further inflammatory conditions where 3-nitrotyrosine may have clinical utility

Various studies have reported the production of Tyr-NO_2 in diseases involving an inflammatory response and below are a selection of studies that have focused on whether Tyr-NO_2 is (or has the potential to be) a clinically relevant biomarker.

Gastrointestinal inflammatory conditions

Intestinal inflammation is observed in inflammatory bowel diseases, i.e. Crohn's disease (CD) and ulcerative colitis (UC). In CD and UC, Tyr-NO_2 has been detected using semi-quantitative immunohistochemical studies, with little or no staining observed in non-inflamed or control tissue (Dijkstra et al, 1998; Perner

et al, 2001). Plasma Tyr-NO_2 in CD and UC has not been reported, but has been reported in coeliac disease, another inflammatory intestinal disorder (Ter Steege et al, 1998). In the latter study, Tyr-NO_2 was measured using an ELISA method, where a decrease in protein-associated Tyr-NO_2 was observed following a gluten-free diet.

For clinical purposes, quantitatively assessing a biomarker in an accessible human tissue such as plasma is preferable to using gut biopsies for qualitative immunohistochemical studies. Therefore, before Tyr-NO_2 can be considered as a biomarker in gastrointestinal inflammatory disorders it first needs to be determined that the plasma concentrations of Tyr-NO_2 are: (a) elevated during episodes of inflammation and (b) decreased following clinically successful therapeutic intervention. The study on coeliac disease (Ter Steege et al, 1998) demonstrates, in principle, that plasma protein-associated Tyr-NO_2 concentrations may fall in response to treatment and thereby reflect disease activity, but follow-up studies are needed.

Systemic lupus erythematosus

Systemic lupus erythematosus (SLE) is an autoimmune disease and involves chronic systemic inflammation. The fluxes of ROS/RNS, such as $O_2^{\bullet -}$, $^{\bullet}NO$ and hydroxyl radical are known to increase in SLE (Khan et al, 2006; Wang et al, 2010). Interestingly, in addition to an increase in protein nitration, anti-Tyr-NO_2 antibodies have been reported in the serum of SLE patients (Khan and Siddiqui, 2006) and such antibodies are also being investigated as a possible biomarker in this disease. Wang et al (2010) used an ELISA to compare serum Tyr-NO_2 concentrations to disease activity score ("SLE Disease Activity Index", n=72) and found levels were significantly higher in patients with a disease activity score greater than six (n=44). Avalos et al (2007) suggested that oxidative stress is more likely to be associated with renal dysfunction than disease activity score. Stein (2010) also suggested that renal function should be taken into account, along with smoking status and obesity, when examining potential oxidative stress measures in SLE.

If the correlation between serumTyr-NO_2 concentration and disease activity can be replicated in further large clinical studies, then Tyr-NO_2 could potentially be used as a tool for monitoring disease activity in response to therapy. Moreover,

if an available ELISA method can be shown to be sensitive enough to detect these changes, this would allow high-throughput analysis of patient samples. However, it is still unclear whether the measurement of plasma Tyr-NO_2 concentrations provides clinical insight into therapeutic efficacy that is more informative than the existing clinical criteria.

Rheumatoid arthritis

Rheumatoid arthritis (RA) involves an autoimmune inflammatory reaction within synovial joints, which leads to the chronic destruction of the cartilage and bone which underlies the synovium (Stamp et al, 2012). Tyr-NO_2 staining was observed in immunohistochemical staining of the synovium from RA patients (Mapp et al, 2001; Sandhu et al, 2003) as well as within RA plasma/serum (Kaur and Halliwell, 1994; Misko et al, 2013). Quantification of Tyr-NO_2 in aspirated samples of knee-joint synovial fluid has demonstrated the importance of selecting the correct methodology when measuring Tyr-NO_2, as the concentrations reported in RA (Kaur and Halliwell, 1994), using HPLC-UV, could not be confirmed by LC-MS/MS (Yi et al, 2000). The latter study reported Tyr-NO_2 to be undetectable in RA synovial fluid. HPLC using electrochemical detection has been confounded by an artefact that co-eluted with Tyr-NO_2 in human brain tissue (Kaur et al, 1998) and this may also be an issue with other tissue samples when not using MS to provide an unequivocal structural identification of the Tyr-NO_2 analyte.

As well as an increased plasma concentration of Tyr-NO_2 in RA patients, compared to healthy control participants, studies have demonstrated a fall in plasma Tyr-NO_2 concentration following treatment with various drugs (Nemirovskiy et al, 2009; Misko et al, 2013). Nemirovskiy et al (2009) have shown a fall in plasma Tyr-NO_2 concentrations in animal models of arthritis following administration of experimental iNOS inhibitors. Within human subjects, Misko et al (2013) reported a lowering of plasma Tyr-NO_2 concentrations after 6 months of anti-TNF treatment (3774 pg/ml to 2955 pg/ml, n=18), as well as a correlation with other RA markers (e.g. the acute phase protein CRP and matrix metalloproteinase-3). The method employed was LC-MS/MS and total Tyr-NO_2 was measured (i.e. both protein-associated and free Tyr-NO_2). The drop in plasma Tyr-NO_2 concentration was also associated with a change in the RA

disease activity score (DAS28-3 CRP). However, this does not provide any more clinically useful information than measuring CRP and future work should focus on what new information Tyr-NO_2 can provide, if any.

Chronic obstructive pulmonary disease

Chronic obstructive pulmonary disease (COPD) involves an abnormal inflammatory response in the lungs that becomes chronic and has been shown to be coupled with systemic inflammation (Chung and Adcock, 2008). White blood cells accumulate in the small airways and alveolar destruction is, in part, caused by neutrophils and macrophages. This damage causes the release of DAMPs and further inflammation (Barnes, 2004; O'Donnell et al, 2006; Chung and Adcock, 2008). The associated oxidative stress is also thought to cause activation of pro-inflammatory transcription factors, such as NF-κB (Rahman and Adcock, 2006). Increased oxidative stress in COPD may be the result of increased MPO levels. Zhu et al (2014) performed a meta-analysis and found sputum MPO levels were higher in COPD patients, compared to controls, and increased further during exacerbations. MPO is measured as a marker of neutrophil activity and could be a potential novel therapeutic target (Zhu et al, 2014). Increases in MPO could cause an increase Tyr-NO_2 levels, which could then potentially be measured as a marker of MPO activity. However, consideration must also be given to the observed *in vitro* decrease in Tyr-NO_2 levels in the presence of HOCl, another product of MPO activity (**Section 1.5**) (Whiteman and Halliwell, 1999).

The majority of research into Tyr-NO_2 in COPD has been done by immunostaining techniques (Ichinose et al, 2000; Sugiura et al, 2003; Ricciardolo et al, 2005; Rytila et al, 2006) with Tyr-NO_2 staining determined to be greater in the later stages compared to early stages and controls (smokers). Of those studies that have used semi-quantitative methods (i.e. ELISA) Ricciardolo et al (2005) found free Tyr-NO_2 to be higher in bronchoalveolar lavage fluid in severe COPD, compared with mild/moderate COPD and patients with normal lung function and Footitt et al (2016) found sputum Tyr-NO_2 to be higher in COPD compared to non-smoking control participants. This suggests Tyr-NO_2 has potential as a marker of oxidative stress in COPD but further work

with quantitative methods is needed before firm conclusions can be drawn from Tyr-NO_2 measurements in this disorder.

Cardiovascular Disease

Atherosclerosis has an inflammatory component, with immune cells such as macrophages being active at the site of the atherosclerotic plaque (Chinetti-Gbaguidi et al, 2011). Many studies have found nitrated proteins within the plaque tissue (Beckman et al, 1994b), e.g. LDL (Leeuwenburgh et al, 1997) and high MPO levels are associated with cardiovascular disease (Loria et al, 2008; Roman et al, 2010).

Some studies have investigated whether plasma/serum concentrations of Tyr-NO_2 change in response to statin therapy for cardiovascular disease. Shishehbor et al (2003) reported an association (from a study using LC-MS/MS) between the concentration of plasma protein-associated Tyr-NO_2 and coronary artery disease (defined as documented myocardial infarction, coronary artery bypass graft surgery, percutaneous coronary intervention or a stenosis of 50% or greater in a major coronary vessel), as well as a reduction in plasma Tyr-NO_2 following statin treatment. This lowering effect was concluded to be independent of the fall in lipid parameters and CRP. Pirro et al (2007) also reported a fall in plasma protein-associated Tyr-NO_2 (using an ELISA) following rosuvastatin treatment in hypercholesterolemia. A drop in plasma protein-associated Tyr-NO_2 concentrations, following statin treatment, being observed by two different studies and methods (LC-MS/MS and ELISA) suggests that Tyr-NO_2 has potential as a biomarker for disease monitoring following therapeutic intervention in cardiovascular disease. The former method offers high assay specificity and replication but the latter method suggests that a semi-quantitative high-throughput assay is also applicable in these circumstances. However, as with many of the other diseases mentioned, further clinical studies are needed to confirm that Tyr-NO_2 meets the requirements of a clinical biomarker (i.e. high sensitivity and specificity, section 1.4).

Tyr-NO_2 has also been associated with coronary artery disease in pre-diabetes. A prospective study by Chu et al (2012) reported an increase in plasma Tyr-NO_2 concentration (measured via ELISA), two hours after an oral glucose tolerance test. In those with an abnormal glucose tolerance plasma Tyr-NO_2

levels were significantly higher in those with coronary artery disease compared to those without. Many studies have also been conducted to assess whether there is an association between circulating Tyr-NO_2 concentration and endothelial dysfunction (an important part of cardiovascular disease pathology) in diabetes (Mihm et al, 2000; Ceriello et al, 2007; Ceriello et al, 2008).

In conclusion, the issue of which method to employ for the determination of Tyr-NO_2 in the high-throughput analysis of clinical samples needs be addressed, as mass spectrometry is not yet feasible for high-throughput analysis and other methods in the literature suffer from methodological flaws or cannot be properly assessed due to a lack of detailed methodological information (Duncan, 2003). When measuring protein-associated Tyr-NO_2, another factor that needs to be investigated is the effect of protein turn-over rate on protein-associated Tyr-NO_2 concentration. A fall in protein-associated Tyr-NO_2 concentration will only be measurable if the nitrated protein is degraded in parallel with a decrease in disease activity. As mentioned in section 1.5 there is evidence that nitration of certain proteins can enhance proteolytic degradation (Grune et al, 1998; Souza et al, 2000a) or inhibit it (Davies, 2001; Dunlop et al, 2009).

Validation of oxidative stress modifications as useful biomarkers in disease has been hindered by methodological flaws.Tyr-NO_2 is no exception to this and this topic has been reviewed (Griffiths et al, 2002; Tsikas and Caidahl, 2005; Tsikas and Duncan, 2014; Frijhoff et al, 2015). There is still much work to be done in assessing Tyr-NO_2 as a clinically useful biomarker, with more clinical studies (e.g. randomised drug trials and prospective cohort studies) assessing sensitivity and specificity needed in particular. However, findings so far – at least in relation to some inflammatory diseases – have been encouraging, with some studies showing that plasma Tyr-NO_2 levels correlate with disease activity (e.g. high Tyr-NO_2 levels were seen in patients with a high SLE disease activity index (Wang et al, 2010)) and are decreased following successful therapeutic interventions (e.g. as seen with statin treatment in cardiovascular disease (Shishehbor et al, 2003)). The question of whether Tyr-NO_2 is any more informative, in clinical terms, than other markers that are already available, e.g. CRP, is still to be addressed.

Other post-translational modifications of proteins have been used clinically to aid diagnosis, prognosis or disease monitoring. For example, the presence of antibodies, in serum, to citrullinated proteins can aid diagnosis of rheumatoid arthritis (Schellekens et al, 2000; Luban and Li, 2010). Citrullination is a post-translational modification caused by peptidylarginine deiminase enzymes, that converts arginine residues to citrulline residues (Vossenaar and van Venrooij, 2004). In diabetes, glycated haemoglobin can be used to assess/monitor a person's glycaemia levels over the preceeding 120 days, an erythrocyte's average lifespan (Bunn, 1981; Goldstein et al, 2004; Nathan et al, 2007). Glycation of haemoglobin is an effectively irreversible non-enzymatic modification and the glycation is directly proportional to the glucose concentration in the surrounding area (Goldstein et al, 2004).

1.6. Hypothesis and Aims

The main hypothesis, which forms the basis of the following research project, is that Tyr-NO_2 is a clinically relevant biomarker of inflammation.

Within this project the aims have been to:

1. Develop and validate a new sensitive ELISA method for the high-throughput analysis of protein-associated Tyr-NO_2 in human samples (Chapter 3).
2. Measure $^{\bullet}NO$ metabolites and protein-associated Tyr-NO_2 in serum to assess nitrative stress following an acute inflammatory response, i.e. after surgery (Chapter 3).
3. To determine whether high dietary NO_3^- ingestion by smokers leads to an increase in nitrative stress-induced post-translational modifications of proteins (Chapter 4).
4. Compare protein-associated Tyr-NO_2 to CRP as a marker of inflammation in patients post-surgery and assess its clinical utility in the diagnosis of patients that developed post-surgery sepsis (Chapter 5).
5. Measure $^{\bullet}NO$ metabolites and protein-associated Tyr-NO_2 in brain tissue to assess nitrative stress in dementia (Chapter 6).

Chapter 2
General Methods

Materials and methods used throughout this project are detailed within the following sections and will be referred to throughout this thesis.

2.1. Materials

Phosphate buffered saline (PBS; 10mM) (P5368), RIPA buffer, protease inhibitor cocktail, bovine serum albumin (BSA) fraction V, bromophenol blue sodium salt, sodium dodecyl sulfate (SDS), Ponceau S, N,N,N′,N′-tetramethylethylenediamine (TEMED), β- mercaptoethanol, methanol, hydrogen peroxide (H_2O_2), manganese (IV) oxide (MnO_2), dithiothreitol (DTT), vanadium chloride and hydrochloric acid (HCl) were purchased from Sigma-Aldrich (Gillingham, UK).

Glycine, Tris base, zinc sulfate ($ZnSO_4$), glacial acetic acid, Tween-20 and ammonium persulfate (APS) were from Fisher Scientific (Loughborough, UK).

The protein-free blocking buffer, bicinchoninic acid (BCA) assay reagents, pH indicator paper and “PageRuler” pre-stained protein ladder were from Thermo-Fisher Scientific (Cramlington, UK).

The TGX FastCast acrylamide kit (12%) and nitrocellulose membrane (0.45 µm) were from Bio-Rad (Hemel Hempstead, UK).

The protein carbonyl enzyme immunoassay (EIA) kits were from Biocell Corporation Ltd (Auckland, NZ).

Coomassie Brilliant Blue was from LKB Produkter (Stockholm, Sweden).

All buffers and reagents were made up in deionised, ultrapure H_2O (ddH_2O, 18.2 MΩ/cm) unless otherwise stated.

2.1.1. Antibodies

Table 2.1: Details of the antibodies used in the ECL ELISA and western blotting

Antigen	Host	Conjugation	Type	Supplier (product number)	Lot number	ELISA dilution	Western Blot dilution
Nitrotyrosine	Mouse	-	Monoclonal	Cambridge Biosciences 189542	0426640-1	1 µg/ml	
			Monoclonal		0460908-1		1:1,000
Nitrotyrosine	Mouse	Biotin	Monoclonal	Cambridge Biosciences 10006966	0448074-1	2 µg/ml	
Actin	Rabbit	-	Polyclonal	Cambridge Biosciences A300-485A	A300485A-2		1:5,000
Mouse IgG	Goat	IRDye680RD	Polyclonal	LiCor 926-68070	C40312-02		1:15,000
Rabbit IgG	Goat	IRDye800CW	Polyclonal	LiCor 926-32211	C40325-02		1:15,000
Mouse IgG	Goat	IRDye800CW	Polyclonal	LiCor 925-32210	C40826-04		1:15,000
Rabbit IgG	Goat	IRDye680RD	Polyclonal	LiCor 925-68071	C41022-02		1:15,000
Biotin	n/a	IRDye800CW	*Streptavidin*	LiCor 925-32230	C50226-03		1:5,000

2.2. Samples

Serum: 4ml clotted blood sample was collected at each time point. These were centrifuged and the serum stored frozen as a single aliquot (2.0-2.5 ml) at DSTL (further details in sections 3.2.1 and 5.1).

Plasma: Blood was collected in 5ml EDTA vacutainers and spun at *350 g* for 20 minutes, the plasma supernatant was then collected and frozen.

Human brain tissue homogenates were collected and lysed by the South West Dementia Brain Bank (further details in section 6.1).

Forebrain and cerebellum tissue samples from the brain of transgenic (n=24) and wild-type mice (n=14) were collected and snap frozen, then stored at -80°C until lysis (further details in section 6.1).

Plasma, serum and brain samples were stored at -80°C until use. Further preparation was method dependent.

2.3. Determination of protein concentration

The bicinchoninic acid (BCA) assay (Thermo Fisher, Cramlington, UK) was used to determine the protein concentration of samples (range 0.06 – 2 mg/ml). The BCA assay uses the Biuret reaction (reduction of copper (II) to copper oxide (I), in alkali conditions, by the peptide bond), which is then followed by the formation of a complex between copper oxide (I) and BCA. This produces a deeper purple colour than the Biuret reaction alone and has an absorbance maximum at 562 nm (Smith et al, 1985). Bovine serum albumin (BSA) in H_2O was used for a 6 point standard curve with a range of 0.06 – 2.00 mg/ml. The sample was diluted in H_2O as necessary to fit within this range (e.g. plasma/serum was diluted 1 in 100).

Clear, flat bottom, 96-well microtiter plates (Sterilin, Fisher Scientific, Loughborough UK) were used and 25 µl of the sample/standard was mixed with the 200 µl BCA reagent - if the sample volume was limited 10 µl sample was used (altering the assay working range to 0.125 – 2 mg/ml). The plate was then covered and incubated at 37°C for 30 minutes before measuring the absorbance on a Fluostar Optima plate reader (BMG Labtech, Ortenberg,

Germany), with a 550-10 excitation filter. Calculated concentrations were then multiplied by the samples dilution factor. A typical standard curve from this assay is shown in **Figure 2.1**.

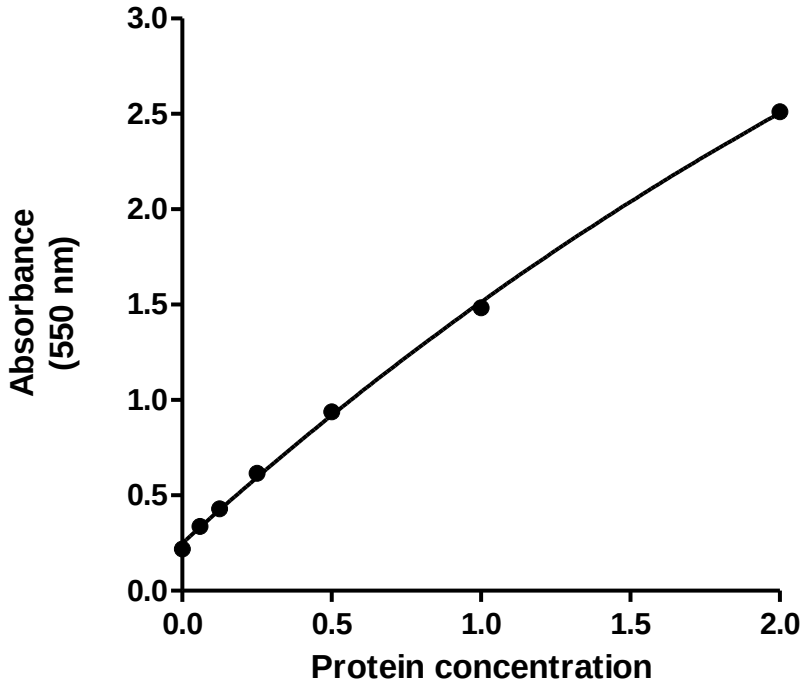

Figure 2.1: BCA assay standard curve

Bovine serum albumin was used as the protein standard at a range of 0.06 – 2.00 mg/ml

2.4. SDS-PAGE (sodium dodecyl sulfate polyacrylamide gel electrophoresis)

Denaturing and reducing conditions were used during SDS-PAGE to separate sample proteins by mass. Samples were denatured by addition of Laemmli buffer and heating. Laemmli buffer contains SDS and a reducing agent. SDS is both denaturing and an ionic detergent that binds evenly to proteins, giving them all an equivalent negative charge and allowing separation by mass only in the gel. β-mercaptoethanol or DTT were used as a reducing agent; breaking the

disulphide bonds so that proteins are no longer in their tertiary or quaternary structures.

Samples then underwent electrophoresis; this process uses a positive charge to draw the proteins through the pores in the polyacrylamide gel. A 12% acrylamide gel was used as this has a small pore size, allowing low molecular weight proteins to be resolved. The gel was then either stained with Coomassie stain or used for a western blot.

2.4.1. Preparation of gels

Bio-Rad (Hemel Hempstead, UK) FastCast acrylamide kits and mini-protean plates were used according to the manufacturers instructions to make 1.5 mm thick gels with 10 wells. Resolving gel was 12% acrylamide and stacking gel 4% acrylamide. Kit instructions were followed using the listed reagents (n = number of gels): *Stacking gel* – 1.5 ml x *n* Stacker A, 1.5 ml x *n* Stacker B, 3 µl x *n* TEMED and15 µl x *n* 10% fresh ammonium persulfate (APS). *Resolving gel* – 4 ml x *n* Resolver A, 4 ml x *n* Resolver B, 4 µl x *n* TEMED, 40 x *n* 10% fresh APS.

2.4.2. Sample preparation

Sample protein concentration was determined by the BCA assay (see section 2.1) and the required volume (for 60 µg protein per well) was calculated and mixed with 8 µl of 5x Laemmli buffer (Laemmli, 1970), the volume was made up to 40 µl with H_2O. Samples were then boiled at 99°C for 5 minutes and all 40 µl were applied to the track.

Composition of 5x Laemmli buffer: 200 mM Tris (pH 6.8), 10% SDS, 50% Glycerol, pinch of bromophenol blue (to colour) and H_2O to required volume. *And one of the following reducing agent (added immediately prior to use)*: 100 mM dithiothreitol or 1% β-mercaptoethanol.

2.4.3. Electrophoresis

Gels were placed in a Mini Trans-Blot cell (Bio-Rad Hemel Hempstead, UK) and the middle reservoir filled with 1x SDS running buffer. Once it was confirmed that there was no leaking, the tank was then half filled with SDS-running buffer and samples were loaded into the wells. The first well was loaded with 4 µl pre-stained protein marker. This marker contained proteins of known molecular weights (10 – 170 kDa) that had been stained so that their progress down the

gel could be observed (**Figure 2.2**). This marker was used to estimate the molecular weight of protein bands obtained from the samples.

The PowerPac HC (Bio-Rad Hemel Hempstead, UK) voltage was set to a constant 70V for the first 20 minutes as proteins passed through the stacking gel. This voltage was then increased to a constant 100V until the loading dye reached the end of the gel (approximately 90 minutes). The electrophoresis was then stopped and the gel removed from the tank.

Composition of 10x SDS running buffer: 0.25 M Tris base, 1.92 M glycine, 1% SDS and H_2O to required volume.

2.5. Coomassie staining

To visualise protein bands the SDS-PAGE gel was dyed with Coomassie Brilliant Blue dye (G25). The staining solution contains methanol, to fix proteins by stopping diffusion through the gel, and acetic acid. Within this acidic buffer Coomassie can bind to residues within proteins.

Composition of 1L Coomassie Brilliant Blue staining solution: 500 ml Methanol, 100 ml Glacial acetic acid, 400 ml H_2O and 2.5 g Coomassie Brilliant Blue.

The gel was incubated in the dye for 2 hours. A de-staining solution (the same as the staining solution but without Coomassie Brilliant Blue) was then used to remove any of the non-bound dye, after an hours incubation, the destain solution was refreshed and then incubated overnight. All incubations were at room temperature with gentle rocking.

The gel was imaged on a LiCor Odyssey CLx (LI-COR Biosciences UK Ltd Cambridge, UK). By comparing band position to the pre-stained protein marker a rough estimate of molecular weight for each protein band was achieved.

This gel image can then be compared to blot images obtained from western blots or bands of interest can be excised from stained gels for mass spectrometry analysis. An example gel is seen in **Figure 2.2**, this gel contained a molecular weight marker, human brain tissue samples and nitrated bovine serum albumin (this acted as a positive control in tandem western blots).

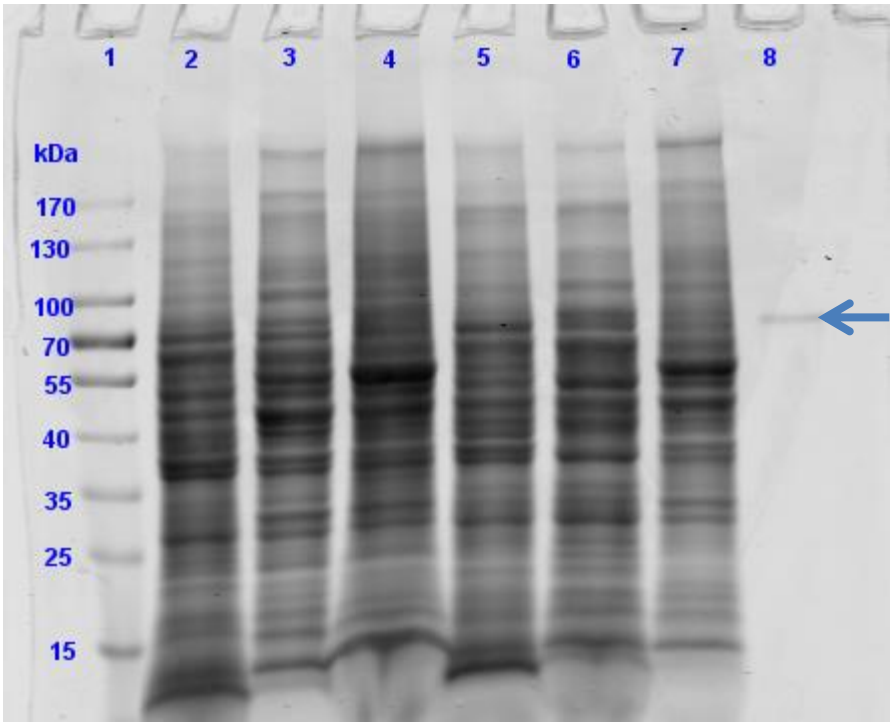

Figure 2.2: A Coomassie stain of brain samples run on an SDS-PAGE gel

Track 1: molecular weight marker. Tracks 2-7 contain 60 µg human brain tissue homogenate. Track 8: nitrated bovine serum albumin (blue arrow, purchased from Sigma Aldrich, Gillingham UK).

2.6. Western blotting

Western blotting uses antibodies to probe for a certain target antigen within a sample, following the transfer of proteins from the SDS-PAGE gel to a membrane. This technique was described and named by Burnette (1981) and the main principles of the procedure have not changed since.

2.6.1. Transfer

Transfer from the SDS-PAGE gel to the membrane (nitrocellulose 0.45 µm) was performed using the 'wet' tank electrotransfer method. With this method, a transfer 'sandwich' was created in which the gel and nitrocellulose membrane were placed between two sheets of filter paper and transfer pads (all pre-soaked in cold transfer buffer). It is important to remove air bubbles between the gel and membrane before transfer as they will interfere with the process; a roller

was used for this. The sandwich was then placed in a Mini Trans-Blot cell (Bio-Rad Hemel Hempstead, UK), with the membrane closest to the anode, along with an ice block and magnetic stirrer. A lot of heat is generated during the transfer process and this can melt the gel. Therefore, the tank was kept cold throughout. The tank was filled with cold transfer buffer and the PowerPac HC (Bio-Rad Hemel Hempstead, UK) constant current set to 0.35 A, the gel was set to transfer for 60 minutes. Transfer of the pre-stained protein marker from the gel to the membrane was used as a marker of a successful transfer.

Gels were stained with Coomassie (section 2.4) after transfer to confirm that proteins had effectively migrated out of the gel.

Composition of transfer buffer: 50 mM Tris base, 40 mM glycine, 20% methanol, 0.1% SDS and H_2O up to required volume.

2.6.2. Blocking the membrane

The nitrocellulose membrane has a high affinity for protein and therefore would bind the antibodies if not 'blocked' first. Protein-free blocking buffer was used, rather than the common BSA blocking solution, as nitrated tyrosine could be expected to be present in albumin. The blocking component of this protein-free buffer is proprietary but it was able to efficiently block the membrane. This step was performed overnight at 4°C with gentle rocking.

2.6.3. Antibody incubation

The antibodies listed previously (**Table 2.1**) were used, with actin (a cytoskeletal protein present in all cells) as a loading control marker. The anti-actin antibody binds to the γ-actin isoform (Uniprot P63261, MW 41,793 Da), with some cross-reactivity for β-actin (Uniprot P60709, MW 41,737).

The secondary antibodies are conjugated to fluorophores that emit in near-infrared (NIR) wavelengths (700 and 800 nm). These fluorophores produce a signal directly proportional to the antigen and are stable over time.

The primary and secondary antibodies were both incubated at room temperature for one hour with gentle agitation.

2.6.3.1. Western blot controls

Nitrated BSA was used as a positive control, to verify antibody binding. This was either commercial or nitrated in-house using peroxynitrite (see section 2.8).

2.6.4. Imaging

For imaging the LiCor Odyssey CLx system was used (LI-COR Biosciences UK Ltd Cambridge, UK), this platform has an infrared laser for excitation of the NIR fluorophores. The Image Studio Lite (LI-COR Biosciences UK Ltd Cambridge, UK) software was then used to analyse the images. This software allows for the image to be edited (e.g. cropped, flipped, brightened) without changing the actual signal intensities (numerical data) collected so that comparisons between bands are valid.

Nitrotyrosine bands were quantified by expression as a ratio of the actin signal. An example of a typical blot and quantification can be seen in **Figure 2.3**.

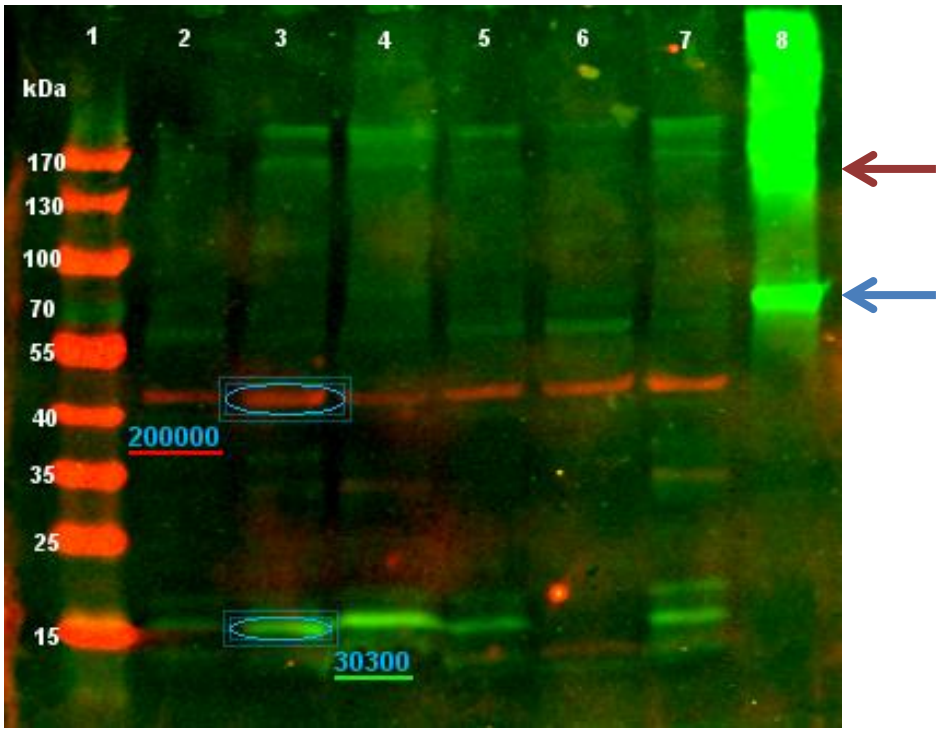

Figure 2.3: An example of a NIR western blot

Red bands are actin positive and green bands nitrotyrosine positive. Signal intensity quantification is shown for the two circled bands. Track 1 molecular weight marker. Tracks 2-7 contain 60 µg human brain tissue homogenate. Track 8 nitrated bovine serum albumin monomer (blue arrow) and nitrated aggregate (red arrow) (Enzo Life Sciences, New York USA).

2.7. Mass Spectrometry

Details of the applicable sample digestion protocols can be found in the relevant chapters. The following HPLC-MS/MS protocol was used for all mass spectrometry.

Digested peptide mixtures were separated by liquid chromatography on an Ultimate 3000 system (Dionex, UK). A C18RP pre-column (C18 PepMapTM, 5 µm, 5 mm x 0.3 mm i.d. Dionex, UK) was used for capturing and desalting peptides, by washing for 4 min with 2% aqueous acetonitrile (0.1% formic acid) at 30 µL/min. A C18 nano-HPLC column (C18 PepMapTM, 5 µm, 75 µm i.d. x 150 mm, Dionex, UK) was then used for separation with a gradient elution running from 2% to 45% aqueous acetonitrile (0.1% formic acid) over an hour. The final wash step then ran from 45 % to 90 % aqueous acetonitrile (0.1% formic acid) in 1 min. The system was then washed with 90% aqueous

acetonitrile (0.1% formic acid) for 5 min and then equilibrated with 2% aqueous acetonitrile (0.1% formic acid).

A 5600 Triple TOF mass spectrometer was used for mass spectrometry analysis (Sciex, Warrington UK). Peptide ionization was achieved with a spray voltage set at 2.4 KV, a source temperature of 150ºC; declustering potential was set at 50 V with a curtain set at 15 V. Scans were collected using survey high resolution TOF MS mode in positive mode 400 to 1200 da for 200 ms. Information-dependent acquisition was used to collect MS/MS data, with the following criteria: the 10 most intense ions with +2 to +5 charge states and a minimum intensity of 500 counts-per-second were chosen, using dynamic exclusion for 20 s, 250 ms acquisition time and rolling collision energy.

The data analysis is detailed for each project in individual chapters.

2.8. Protein carbonyl enzyme immunoassay

Protein carbonyls were measured with an enzyme immunoassay (EIA) kit (Biocell PC test, NZ) which utilises derivatization by dinitrophenylhydrazine (DNP) and an anti-DNP antibody.

Kit instructions were followed for high protein concentration samples (i.e. serum) and room temperature incubations were performed at 21°C.

The serum was incubated with a DNP solution for 45 min before dilution in an EIA buffer; the samples were then used to coat the plate overnight. The plate was then blocked before incubation with a biotinylated anti-DNP antibody. Streptavidin-HRP and chromatin reagent were then used for colour development. Absorbance was measured at 450 nm, using the Fluostar Optima plate reader (BMG Labtech, Ortenberg, Germany). A typical standard curve can be seen in **Figure 2.4**.

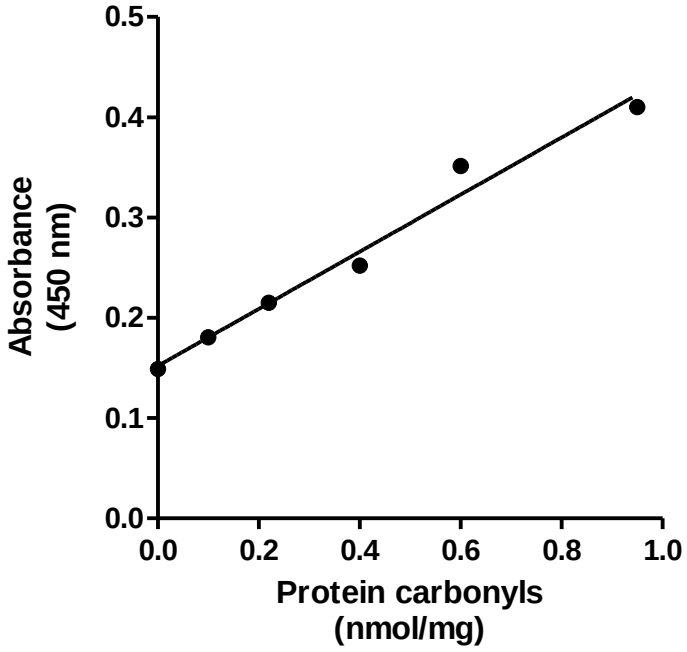

Figure 2.4: Protein carbonyls standard curve

Oxidised protein standards in the range 0.10 – 0.95 nmol/mg protein were used in the protein carbonyl assay.

2.9. Peroxynitrite synthesis

Peroxynitrite was synthesised as a nitrating agent for *in vitro* experiments, according to the method described by Beckman et al (1994a). Solutions were cold and all steps were performed using glass beakers on ice. Three solutions (each 50 ml) were made: (1) 0.6 M $NaNO_2$, (2) 0.7 M acidified H_2O_2 (0.6 M HCl) and (3) 1.2 M NaOH. Stock H_2O_2 concentration was measured (Spectra Max M2^e, Molecular Devices, USA) prior to use; 3 ml of 100x diluted solution was placed into a quartz cuvette and the absorbance was read at 240 nm (extinction coefficient 43.6 M^{-1} cm^{-1} (Hildebrandt and Roots, 1975)).

The acidified H_2O_2 was quickly poured into the $NaNO_2$, immediately followed by the NaOH. This results in a yellow solution of diluted peroxynitrite. MnO_2 (~15 mg) was added to deplete excess H_2O_2 and the solution was then filtered and frozen at -20°C. The top layer of this frozen solution was concentrated peroxynitrite that thaws rapidly, this layer was collected and aliquoted for later use. Concentrations of 200 – 210 mM were routinely achieved when measuring

the absorbance at 302 nm (extinction coefficient 1670 M^{-1} cm^{-1} (Hughes and Nicklin, 1968). The aliquots were kept at -20°C for up to 3 months (-80°C for longer storage) and the concentration was checked upon defrosting (**Equation 2.1**). Aliquots were used within 30 minutes of defrosting.

Equation 2.1:

$$Molar\ concentration = \frac{Absorbance}{Extinction\ coefficient}\ x\ dilution$$

2.9.1. Nitration of protein

A BSA solution of 2 mg/ml was generated in a bicarbonate based nitration buffer. The solution was exposed to 3 mM peroxynitrite (stock diluted to 30 mM with H_2O), whilst being gently vortexed. The pH of the solution was then checked using pH indicator paper (pH 0-14, Fisher Scientific, Loughborough UK), to ensure that a neutral pH had been retained. Successful nitration could be observed by a change in colour of the solution from clear to a faint yellow. Nitration was measured, at pH 10, on a Cary 300 UV-Vis spectrophotometer (Agilent Technologies LDA UK Limited, Cheshire UK), using the extinction coefficient 428nm = 4200 $M^{-1}cm^{-1}$ (van der Zee et al, 1977). An example spectrum can be seen in **Figure 2.5**.

Composition of nitration buffer: 100 mM Potassium phosphate (KH_2PO_4) and 25 mM Sodium bicarbonate ($NaHCO_3$).

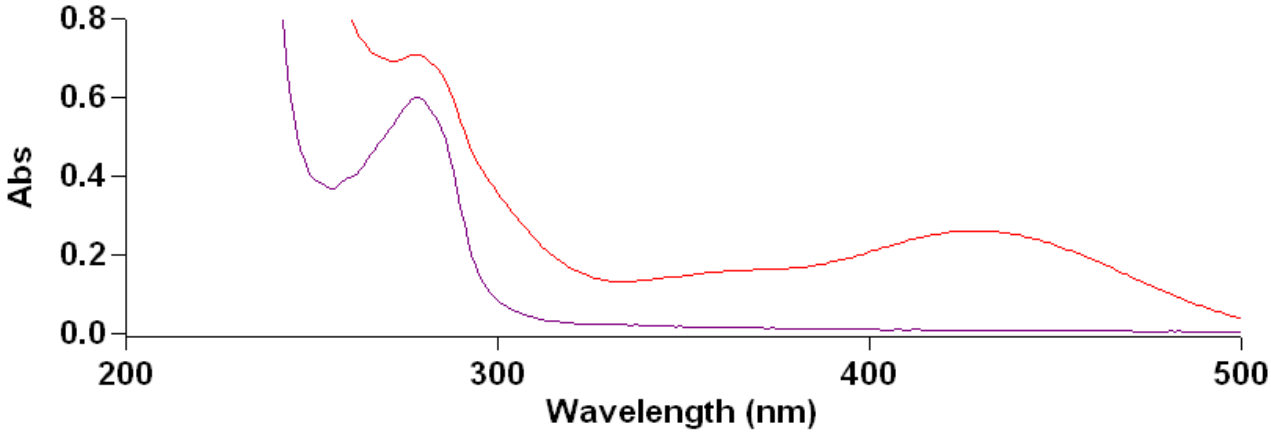

Figure 2.5: UV-visible spectrophotometry spectra of native and nitrated BSA

The spectra of native BSA (purple) and nitrated BSA (red) were recorded at wavelengths between 200 and 500 nm (pH 10). Polypeptides show a peak at 280 nm and nitrotyrosine a peak at 428 nm.

2.10. Ozone-based chemiluminescence (NO_2^- and NO_3^- measurement)

Nitrite (NO_2^-) and nitrate (NO_3^-) were measured using a Sievers •NO analyser (Sievers NOA 280; Analytix, UK). This method involves the reduction of NO_2^- and NO_3^- to •NO which then reacts with ozone to produce luminescence, this light was then measured by a photomultiplier tube. An example of the time trace is shown in **Figure 2.6**.

Five known concentrations of sodium nitrite (0.2 – 10 µM) and sodium nitrate (0.5 – 20 µM) were used as standards for NO_2^- and NO_3^- respectively. Samples were deproteinized prior to measurement using 0.5 M NaOH and 10% zinc sulfate ($ZnSO_4$). The ratio was always 1:2:2 (sample: NaOH: ZnSO4), a sample dilution factor of 5, with at least 100 µl sample being used. After addition of NaOH and $ZnSO_4$, samples underwent a brief vortex before incubation at room temperature for at least 15 minutes. Samples were then centrifuged at 17,500 *g* for 5 minutes and the supernatant analysed.

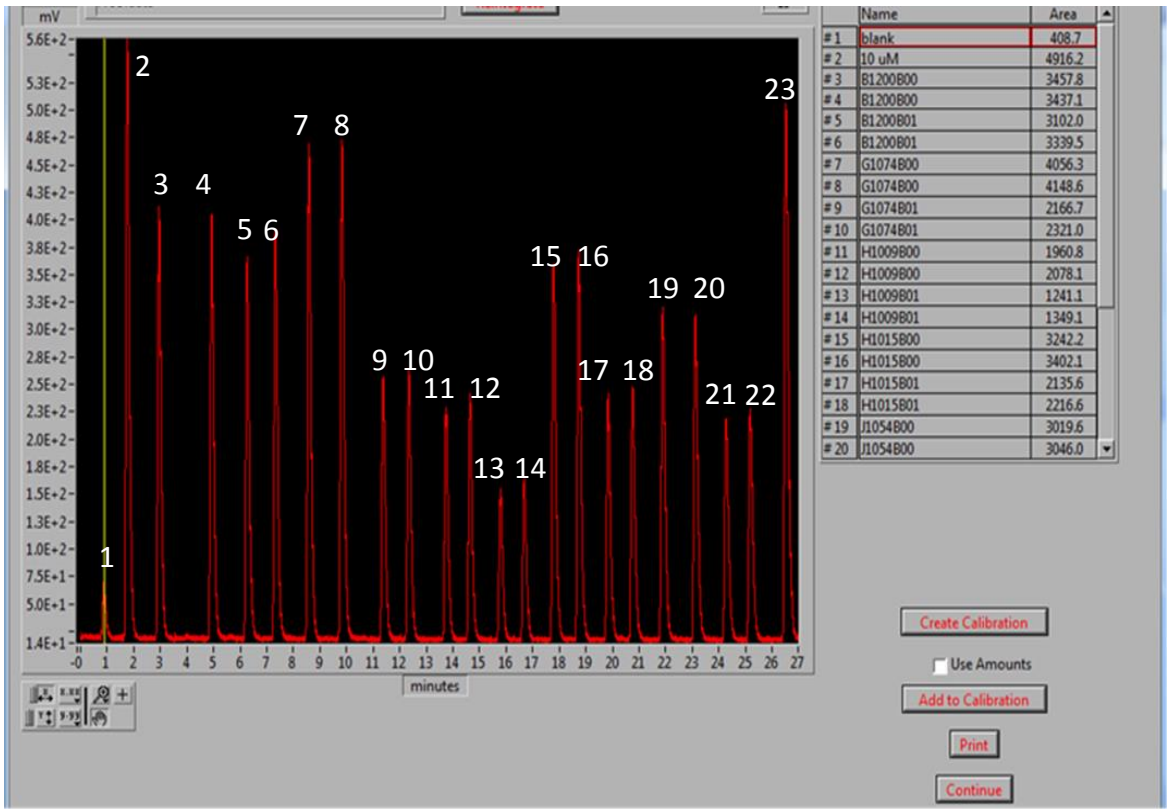

Figure 2.6: Time trace for ozone based chemiluminescence, measuring nitrate in serum samples.

Each peak represents an injection of a sample and the area of this peak was calculated for comparison to a standard curve. Injection 1 was the blank, injections 2 and 23 were a 10 µM NO_3^- standard, injections 3-22 were serum samples in duplicate (i.e. 10 samples).

Aliquots (100 µl) of the deproteinised samples were refluxed in a reaction chamber with 1 ml 0.3 M sodium iodide and 4 ml glacial acetic acid (at 35°C) for NO_2^- measurement, or with 4ml 0.1 M vanadium III chloride /1M HCl (at 95°C) for NO_3^- measurement.

Chapter 3
Validation of a new electrochemiluminescence ELISA for the measurement of protein-associated 3-nitrotyrosine

3.1. Introduction

As discussed in Chapter 1 (section 1.5) the formation of Tyr-NO_2 in human tissues/bio-fluids is associated with several pathologies which involve a strong inflammatory component. For example, plasma protein-associated Tyr-NO_2 concentrations have been shown to be increased in patients with systemic lupus erythematosus (Khan et al, 2006), celiac disease (Ter Steege et al, 1998) and cardiovascular disease (Shishehbor et al, 2003; Eleuteri et al, 2009), when compared to controls (in the aforementioned papers, 'controls' being individuals with no clinical signs of disease). This is perhaps unsurprising given that the two most cited initiators of nitration - peroxynitrite (Skatchkov et al, 1997; Kuhn et al, 2004) and myeloperoxidase (Gaut et al, 2002b; Sun et al, 2007) - are both increased in inflammatory conditions.

This has led to the suggestion that Tyr-NO_2 could be measured as a marker of oxidative stress in clinical studies. Some studies have shown that Tyr-NO_2 correlates with disease activity (Ohya et al, 2002; Wang et al, 2010) and decreases following treatment (e.g. with the cholesterol reducing drugs statin and rosuvastatin in cardiovascular conditions, Shishehbor et al (2003); Pirro et al (2007)).

Evidence supporting oxidative stress modifications as useful biomarkers in disease has been hindered by a fragmented literature and Tyr-NO_2 is no exception to this (Frijhoff et al, 2015). There have been two main approaches to quantifying Tyr-NO_2 levels *in vivo*, high-throughput ELISA's and highly sensitive GC/LC-MS/MS. Both of these methods have advantages and disadvantages: ELISA methods are high throughput, less costly and do not involve extensive sample preparation but have low sensitivity and are semi-quantitative. GC/LC-MS/MS is quantitative, highly sensitive and accurate but is low-throughput, time-consuming and expensive - limiting this method's usefulness in a clinical setting.

When measuring Tyr-NO_2 there are two major methodological issues to consider: (1) low concentrations of the analyte and (2) artefactual formation of Tyr-NO_2 during sample processing (Yi et al, 2000). Mass spectrometry measurement of Tyr-NO_2 is considered to be the 'gold standard', and offers the greatest sensitivity, but also has the biggest risk of Tyr-NO_2 formation during sample preparation.

For the measurement of a large number of clinical samples an ELISA is a more practical method, but for a Tyr-NO_2 ELISA to be successful the drawbacks of this method need to be addressed. Despite a wealth of studies utilising ELISAs for Tyr-NO_2 measurement in clinical samples, the literature contains inconsistent methodologies and results (as discussed in Chapter 1, section 1.5.1). For example, along with differences in ELISA design (indirect, competitive and sandwich) the standard has also varied; Ter Steege et al (1998) used nitrated plasma, where others have used nitrated BSA (BSA-NO_2) (Khan et al, 1998; Bo et al, 2005; Weber et al, 2012). These ELISA methods have reported drastically different values of Tyr-NO_2, in the plasma of healthy controls, from undetectable, with a LOD of 0.2 nM (Ter Steege et al, 1998), to >4000 nM (Bo et al, 2005). Additionally, there is an ambiguity in reported results, as many results are reported as absolute concentrations when they are in fact standard equivalents. For the authors to report an absolute concentration the exact amount of nitrated Tyr residues in the protein standard must be known. However, often all that is known/reported is the concentration of the nitrated protein standard. Therefore, the presented results are equivalent to the protein concentration, not the Tyr-NO_2 content. Earlier studies have reported the development of ELISA's for Tyr-NO_2 (Ter Steege et al, 1998; Sun et al, 2007; Weber et al, 2012) and commercial Tyr-NO_2 assays are widely available. However, an obstacle still to be addressed is poor sensitivity, in that these ELISAs are often unable to detect Tyr-NO_2 in a high proportion of human serum samples.

Therefore, a high-throughput assay based on a highly sensitive electrochemiluminescence (ECL) platform has been developed for Tyr-NO_2 measurement. The base of an ECL ELISA plate contains carbon electrodes which transmit the electrical current to the antibody/antigen complex. The streptavidin tag is conjugated to a ruthenium complex which undergoes redox

cycling, following electrical stimulation, resulting in the production of light (**Figure 3.1**).

In the present study, our developed ELISA, for protein-associated Tyr-NO_2, was applied to serum samples from patients undergoing major elective surgery, with serum being collected prior to and one day after the surgery as an exemplar of the acute inflammatory response in humans.

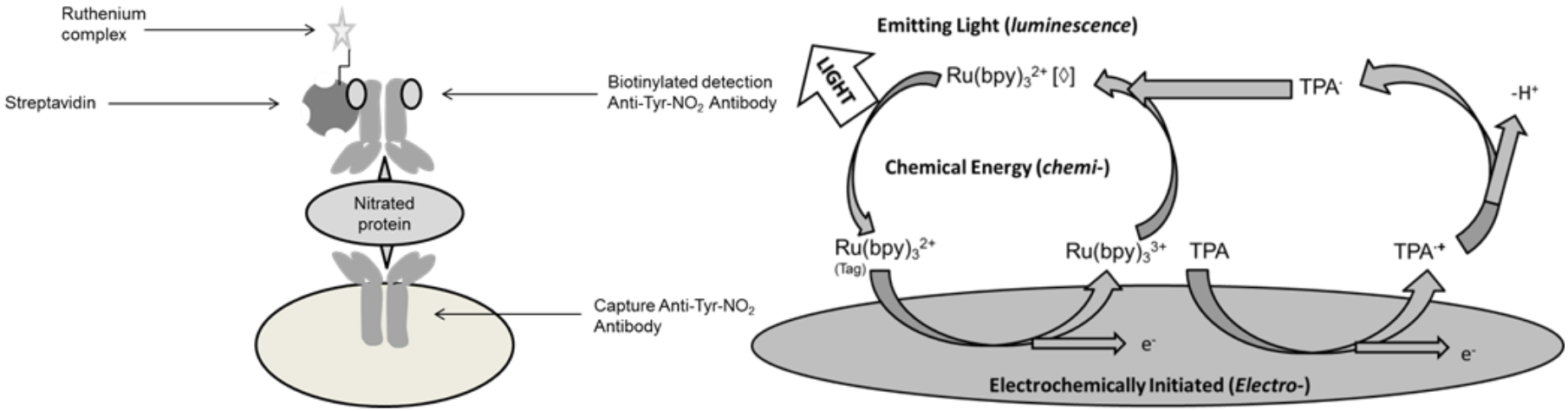

Figure 3.1: Electrochemiluminescence ELISA schematic

A sandwich ELISA was utilised for the measurement of protein-associated Tyr-NO_2. The tag is a ruthenium complex that produces light upon electrical stimulation. Tripropylamine (TPA) is within the Read buffer and is a co-reactant for light generation.

3.2. Materials and methods

3.2.1. Patient serum samples

The serum samples were collected in a study approved by the NRES Committee South Central (REC ref 06/Q1702/152) and prior informed consent to take part in the study was obtained from each individual.

A clotted blood sample was collected at each time point, these were centrifuged and the serum was frozen.

Serum was collected from 35 individuals (18 male, 17 female; 59 ± 13 years old) prior to major elective surgery and again 24 hours after surgery.

3.2.2. Additional samples

The assay was also applied to lysed blood cells. These additional samples were:

- Erythrocytes and monocytic cells isolated from healthy human blood (all volunteers gave informed consent, and this study was approved by the Institutional Research Ethics Committee - approval number 2014/781).
- U937 cells, a histiocytic lymphoma cell line (Sigma-Aldrich, Gillingham UK. ECACC supplied, Lot 11D008).

3.2.3. Materials

Ultra-pure water was used for buffer preparations throughout. The following reagents were used in addition to those listed in Chapter 2, section 2.1: acetonitrile, iodoacetamide, trypsin (proteomics grade), RIPA buffer, protease inhibitor cocktail and Percoll (lot 10226958) (Sigma Aldrich, Gillingham UK). Dextran (batch DB4311) was from Pharmacosmos, Holbæk, Denmark. Methanol (analytical reagent grade), ammonium bicarbonate (analytical reagent grade), Formic acid 99% , foetal bovine serum (FBS, lot 41F6547K) and HyClone™ antibiotic-antimycotic solution (Lot J140011) were purchased from Fisher Scientific, Loughborough, UK. Dulbecco's modified Eagle's medium (DMEM), high glucose DMEM, and L-glutamine were obtained from Lonza, Wolverhampton UK.

The details of the two anti-nitrotyrosine (biotinylated and non-biotinylated) antibodies can be found in **Table 2.1** (Chapter 2, section 2.1.1). Blocking buffer A (BSA), SULFO-TAG-labelled streptavidin and Read Buffer T 4x was purchased from Meso Scale Discovery (MSD), Maryland, USA. Nitrated bovine serum albumin (BSA-NO_2) (Enzo Life Sciences, New York, USA).

We used standard bind single spot 96 well plates (MSD, Maryland USA) and an electrochemiluminescence Sector Imager 2400 (MSD, Maryland USA).

3.2.4. Validation of the assay

LLOQ and CV:

The lower limit of quantification (LLOQ) was defined as the lowest standard with a mean accuracy of 80 – 120% and a duplicate variation of <20%.

The coefficient of variation (CV) was determined by preparing and measuring the same sample multiple times within and across plates (n=8). CV% = (standard deviation/mean) x 100.

The inter-assay CV for room temperature incubations compared to a constant 25°C (Jeio Tech Lab Companion SI-300R shaking incubator, Seoul Korea) was also assessed.

The variation between sample duplicates, at low concentrations of Tyr-NO_2, was also determined.

Recovery and linearity:

A plasma sample was spiked with 1 nM nitrated BSA (BSA-NO_2) and diluted to four different concentrations (1 in 2, 1 in 5, 1 in 10 and 1 in 20) to determine the linearity and recovery of the assay.

Antibody specificity:

Pre-incubation of the detection antibody and spiking of the sample, with free Tyr-NO_2, was performed to assess the antibodies binding affinities.

Comparison of mass spectrometry and ELISA:

BSA (2 mg/ml) in a bicarbonate buffer (25 mM $NaHCO_3$ and 100 mM KH_2PO_4) was exposed to 11 mM peroxynitrite (synthesised according to the method described by (Beckman et al, 1994a)) to cause nitration of tyrosine residues (Chapter 2, section 2.8). Half of this solution was then exposed to 1 mM sodium dithionite to chemically reduce the nitro groups to amino groups (Nikov et al, 2003).

Native (unmodified), nitrated and chemically reduced BSA samples were then analysed by SDS-PAGE (as described in Chapter 2, section 2.3; β-mercaptoethanol was used as the reducing agent) and the bands excised and trypsin digested based on a previously described protocol (Shevchenko et al, 2006). Mass spectrometry (MS/MS) analysis involved high pressure liquid chromatography (Dionex, UK) coupled to a 5600 Triple TOF mass spectrometer (Sciex, Warrington UK) and is detailed in Chapter 2, section 2.6.

The generated data was then analysed with Mascot Daemon statistical software v 2.3.2 (MatrixScience, 2014) with the following settings applied:

Digestion enzyme: Trypsin
Fixed modifications:

- Carbamidomethyl (C) (formed by the iodoacetamide)

Variable modifications:

- Oxidation (M) Nitro (Y) Amino (Y)

Instrument type: ESI QUAD TOF
Taxonomy: Mammalian
Charge: 2+, 3+ and 4+
Fragment mass tolerance: 0.5 Da

Peptides were then further examined using Peak View (Version 1.0 (ABSCIEX)); this was to examine their extracted ion chromatograms (XIC). For this, the m/z of the peptides containing either unmodified tyrosine, nitrotyrosine or aminotyrosine were entered, along with an XIC range width of 0.1.

Analysis of this data was based on the assumption that modified peptides would be measured with the same sensitivity as the unmodified forms, and therefore

the results are an approximation of the nitration occurring. To manually confirm the analysis by Mascot, the following criteria were applied: peaks with intensities below 1.0×10^4 were excluded and peaks without the mono-isotopic peak were excluded as an artefact. The peptide sequence was then confirmed by *de novo* sequencing. For the remaining peaks, the intensities were recorded allowing calculation of the total peptide intensity (unmodified + modified) and the percentage contribution for each modification calculated.

3.2.5. ELISA method

Buffers

Blocking buffer (3% blocker A in PBS), dilution buffer (1% blocker A in PBS), washing buffer (0.05% Tween-20 in PBS) and 2x Read buffer (50% Read buffer T4x, 50% H_2O). The primary antibody was diluted in PBS (1 µg/ml). The BSA-NO_2 standard (10 nM), secondary antibody (2 µg/ml) and streptavidin (1:500) were prepared in dilution buffer.

Standard preparation

Commercial BSA-NO_2 was aliquoted into 1000 nM stock solutions (reconstituted with distilled water) prior to use. A 1000 nM stock was then diluted with dilution buffer to 10 nM to form the top point of the standard curve. Dilutions (2.5-fold) were used for the next six standards and dilution buffer was used as a blank (standard range 0.04 nM – 10 nM).

Serum preparation

Serum samples were defrosted (stored at -80°C) and centrifuged at 14,000 *g* for 15 minutes at 4°C, to pellet any debris. The serum was kept cool and diluted 1 in 5 with dilution buffer immediately prior to use.

ELISA protocol

Primary antibody (non-biotinylated) was placed into each well of the plate and then incubated at 4°C overnight. The plate was then blocked with 150 µl blocking buffer at 25°C for one hour with gentle agitation (these were the conditions for all further incubations). Each standard/sample (25 µl) was added to the relevant well, with quadruplicate repeats of each, and incubated. A biotinylated secondary antibody was used alongside a streptavidin tag coupled to a ruthenium complex. Read buffer (150 µl, 2x concentration) was placed into each well and the plate immediately read on the MSD Sector Imager 2400.

The standard curve was plotted and the sample concentrations calculated from these known values. Results were expressed as BSA-NO_2 equivalents.

3.2.6. Additional methods

Protein concentration was determined by the BCA assay (Chapter 2, section 2.2). Protein carbonyl content was measured using a commercial enzyme immunoassay kit (Chapter 2, section 2.7). C-reactive protein (CRP) was measured by myself at the Clinical Chemistry department at the Royal Devon and Exeter (RD&E) Hospital, using a standard clinical assay - an immunoturbidimetric assay on a Roche Cobas automated analyser (Roche Diagnostics, West Sussex UK), with a range of 0.3 – 350 mg/L. In order to perform this assay, serum was placed in a reaction cuvette with latex particles coated with a monoclonal anti-CRP antibody. Any aggregates formed by the binding of CRP to these particles were determined turbidimetrically. Due to the low volume of serum available, the CRP test was carried out on a smaller volume than usually applied (when doing routine clinical analyses) but preliminary tests run by Emily Brewer (RD&E Hospital) confirmed that the volume (50 µl) was suitable for testing.

NO_2^- is oxidised to NO_3^- in the presence of oxyhaemoglobin (Kim-Shapiro et al, 2005). As serum was collected rather than plasma, this meant that NO_2^- and haemoglobin had a longer amount of time to react. Therefore, only NO_3^- concentrations were evaluated. NO_3^- concentration was measured by ozone-based chemiluminescence (Chapter 2, section 2.9).

During collection clinical information was recorded for some of these samples (e.g. white blood cell count).

3.2.7. Cell culture and isolation

U937 cells were cultured in DMEM supplemented with 10% FBS, 4 mM L-glutamine, and an antibiotic/antimycotic solution (100 units penicillin, 100 µg streptomycin and 0.25 µg amphotericin B).

For the separation of cells from blood, the following protocol was used (Shaw et al, 2011): whole blood (5ml) was collected into EDTA tubes and centrifuged (20 minutes, 350*g*), and the plasma removed. Red blood cell sedimentation was achieved by incubating the cells with dextran (6% w/v), for 30 minutes, room temperature. Further separation of cells into mononuclear and polymorphonuclear cell types was then accomplished using a discontinuous

Percoll gradient (81: 68: 55%). Centrifugation through the gradient (20 minutes, 720*g*, 4°C) resulted in mononuclear cells being retained at the upper boundary (between the 68 and 55% Percoll) and polymorphonuclear cells at the lower boundary (between the 68 and 81% Percoll).

All cells were lysed in order to measure cellular protein nitration. For this, RIPA buffer with a protease inhibitor cocktail was used according to the manufacturer's instructions. Lysate protein content was measured by BCA assay (Chapter 2, section 2.2).

3.2.8 Statistical analysis

Data sets were tested for a normal distribution using the Shapiro-Wilk's test and the appropriate parametric (two-way ANOVA) or non-parametric test (Wilcoxon matched pairs and Kruskal-Wallis) selected accordingly.

3.3. Results

Optimisation and validation of the assay

The combination, and concentration, of antibodies for the assay had already been determined (see **Section 2.1.1, Table 2.1**).

The results from assays run at 25°C were more consistent than assays run at room temperature (**Table 3.1**).

Table 3.1: Temperature dependent variation in the ECL ELISA

The standard deviation (SD) at room temperature was far higher than when the assay was run at a consistent 25°C.

	Tyr-NO_2 (BSA-NO_2 equivalents; nM)					
	#1	**#2**	**#3**	**#4**	**Mean**	**SD**
Room temperature	1.899	2.578	1.810	0.155	**1.610**	**1.03**
25°C	1.778	1.885	1.745	1.247	**1.664**	**0.28**

The CV was determined, at 25°C, for within the assay (intra-assay CV 6.5%) and between days (inter-assay CV 11.3%) (**Table 3.2**). The LLOQ was 0.04 nM BSA-NO_2, the highest standard used was 10 nM BSA-NO_2.

Table 3.2: Determination of ECL ELISA intra- and inter-assay CV

The mean and SD of 8 replicates was determined to calculate the CV ((SD/mean) x100).

	Tyr-NO_2 (BSA-NO_2 equivalents; nM)										
	#1	**#2**	**#3**	**#4**	**#5**	**#6**	**#7**	**#8**	**Mean**	**SD**	**CV%**
Intra-assay	1.87	1.80	1.83	1.58	1.82	1.65	1.66	1.88	**1.8**	**0.1**	**6.5**
Inter-assay	2.5	2.67	2.77	2.18	2.45	2.19	2.02	2.67	**2.4**	**0.3**	**11.3**

Control plasma samples, spiked with BSA-NO_2, revealed that low concentrations of Tyr-NO_2 (i.e. near the LLOQ) had higher replicate variation than samples with higher concentrations (i.e. midway on the standard curve), percentage variation 13.8 and 6.1% respectively. As plasma levels of Tyr-NO_2 are known to be low, in healthy individuals, the variation of duplicate and quadruplicate measurements, of healthy human plasma (average concentration 0.09 ± 0.06 nM Tyr-NO_2 (BSA-NO_2 equivalents; nM)), were compared (**Table 3.3**). Variation of <20% was achieved more often with quadruplicate measurement than duplicate variation. Therefore, quadruplicate measurement was selected for analysis of plasma/serum samples in the ECL ELISA.

Table 3.3: Table comparing duplicate and quadruplicate measurement variation in the ECL ELISA

Plasma samples from healthy volunteers were analysed in the ECL ELISA (average concentration 0.09 ± 0.06 nM Tyr-NO_2 (BSA-NO_2 equivalents; nM)). Quadruplicate measurement produced variation of less than 20% more often than did duplicate measurement.

Plasma sample	Duplicate variation (%)	Quadruplicate variation (%)
1	*20.6*	11.1
2	*21.8*	*37.8*
3	7.6	14.6
4	18.2	15.5
5	*32.3*	*42.5*
6	19.2	12.7
7	*39.7*	17.1
8	*120.4*	12.5

The average linearity and recovery were 0.998 ± 0.001 (n=3) and 106 ± 3% (n=4), respectively (**Table 3.4**). A 1 in 5 dilution was selected for sample analysis of serum as a balance between maximising the signal in low concentration samples whilst only needing a low volume of sample.

Table 3.4: Linearity and recovery for a spiked plasma sample in the ECL ELISA

Plasma was spiked with 1 nM BSA-NO_2 and diluted to 4 different concentrations for determination of linearity and recovery.

	#1	#2	#3	#4	Mean
Linearity (R^2)	0.9987	0.9996	0.9969		**0.9984**
Recovery (%)	107	103	108	109	**106**

Pre-incubation of the secondary antibody with free Tyr-NO_2 inhibited the ELISA ($p = 0.03$, Kruskal-Wallis test, n=3). However, when Tyr-NO_2 and BSA-NO_2 were competing within the assay, inhibition of the signal did not reach significance, despite the concentration of free Tyr-NO_2 being in excess of the protein associated Tyr-NO_2 (free Tyr-NO_2 would inhibit the assay signal due to the 'sandwich' design needing two epitopes), suggesting that the antibody has a higher affinity for the protein associated Tyr-NO_2. Unmodified BSA was not inhibitory (the antibody dilution buffer contains unmodified BSA).

This method offers far more sensitivity than a colorimetric ELISA (**Figure 3.2**), due to a lower background.

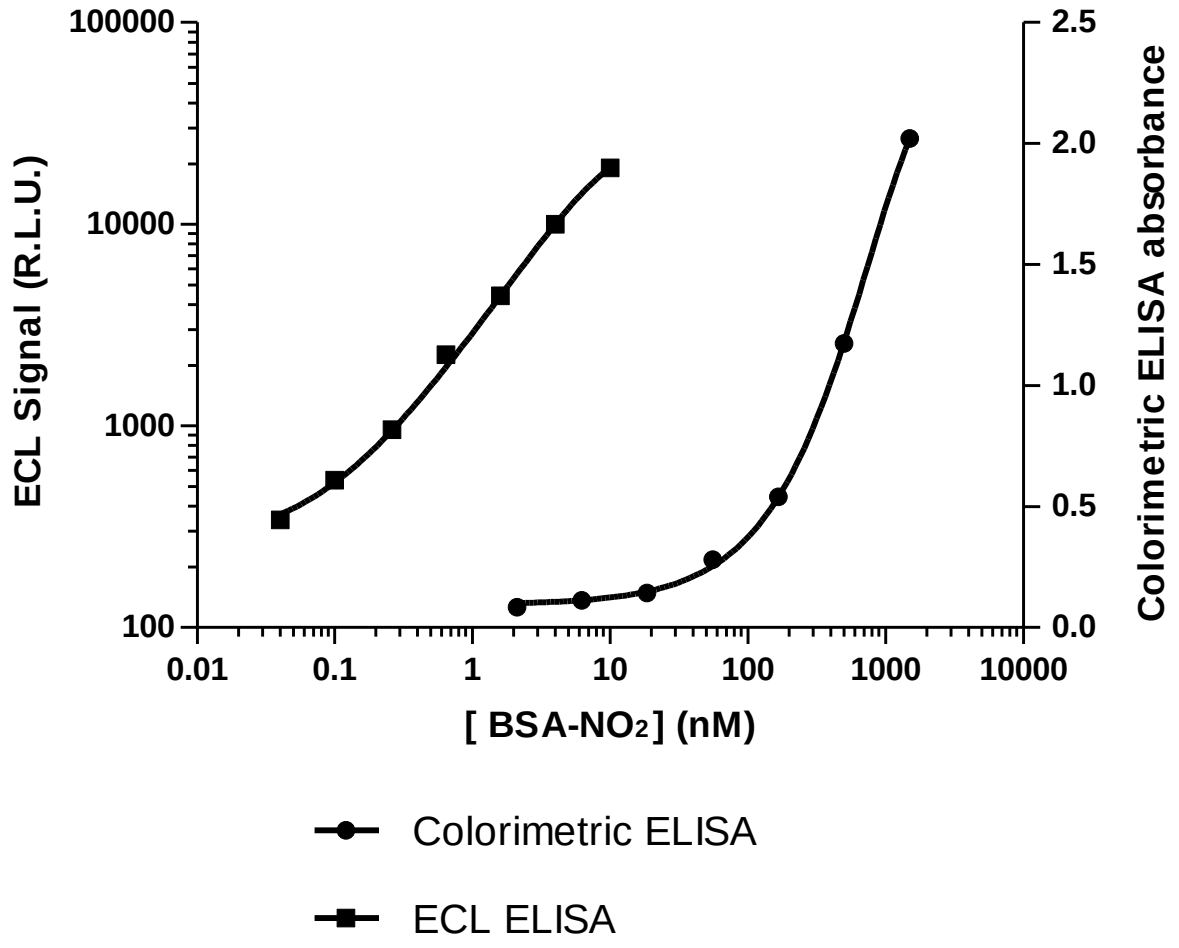

Figure 3.2: ECL ELISA vs. Colorimetric ELISA

The limit of detection of the ECL ELISA was lower than that of the colorimetric ELISA; a more relevant physiological range was also covered. R.L.U. relative light units. BSA-NO_2, nitrated BSA.

Comparison to mass spectrometry

In a preliminary experiment, three BSA samples (native, nitrated and chemically reduced) were analysed by mass spectrometry and ECL ELISA (**Figure 3.3**). The percentage modification for 3 peptide sequences (residues confirmed to be nitrated by *de novo* sequencing) was determined by mass spectrometry for comparison to the ECL ELISA data. The data (n=1) shows an increase in Tyr-NO_2 in the peroxynitrite exposed sample compared to the native sample in both methods. A decrease in signal was then seen for the dithionite treated (reduced) sample (**Figure 3.3**), although the mass spectrometry still shows a higher level of nitration than seen in the native BSA sample. The BSA standard was also analysed and the three confirmed Tyr-NO_2 residues are highlighted in **Figure 3.4**.

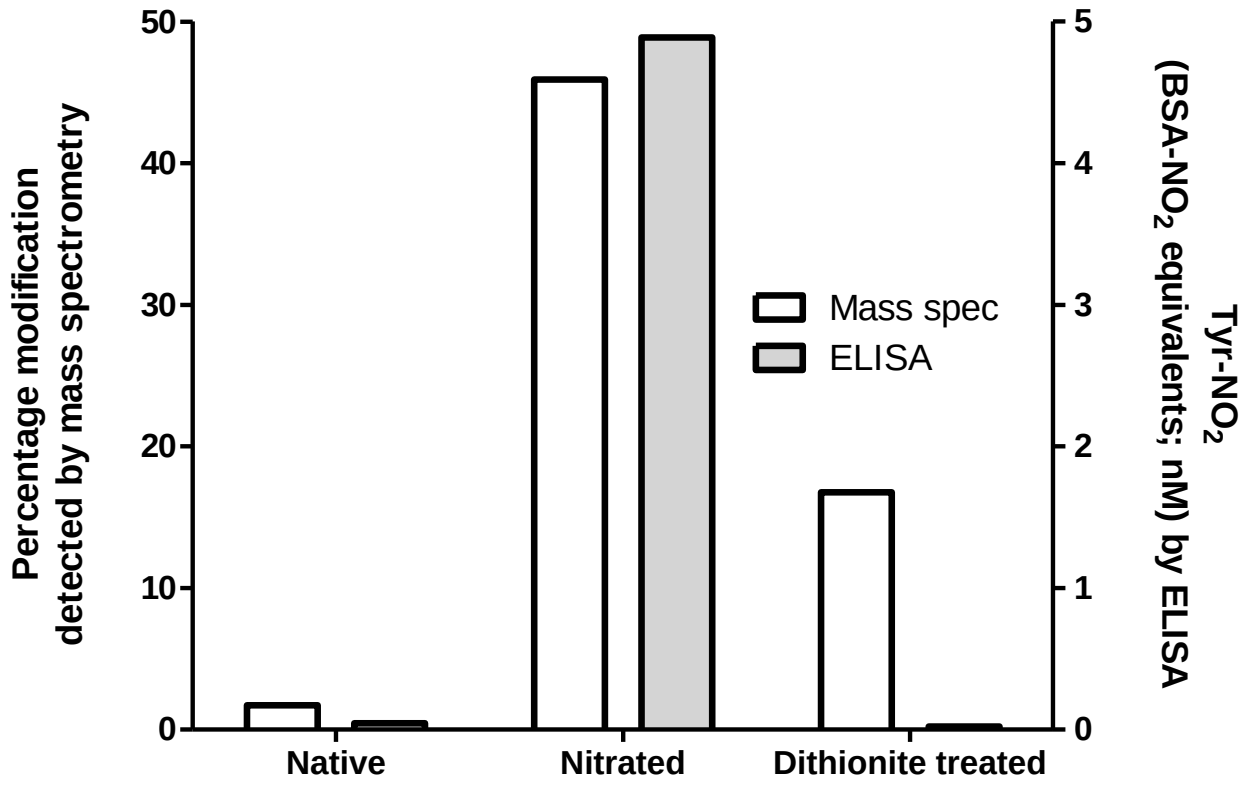

Figure 3.3: A comparison of mass spectrometry with the ECL ELISA

The same three BSA samples (see section 3.2.4) were analysed by mass spectrometry and ECL ELISA to see if there was agreement in relative nitration levels (n=1).

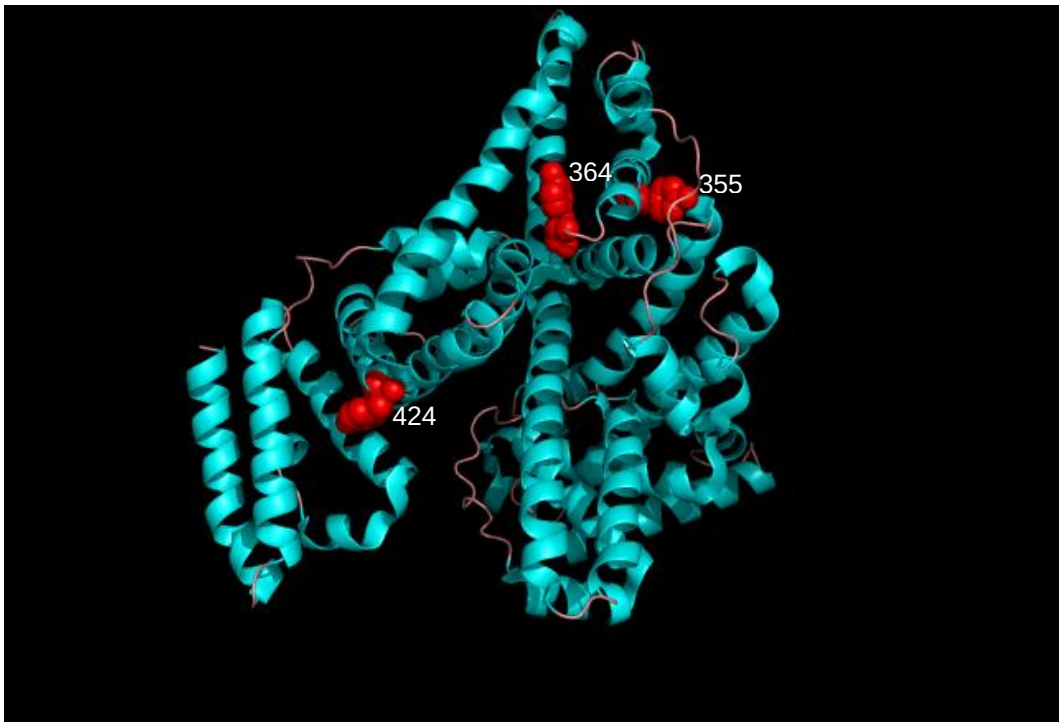

Figure 3.4: Tertiary positions of nitrated residues in the BSA standard

The figure represents a 3D model of BSA. Tyrosine residues confirmed to be nitrated by mass spectrometry (see section 3.2.4) are highlighted in red, blue coils represent alpha helices and pink strands are random coils. BSA contains 21 Tyr residues, approximately 70% of these residues are buried and 30% exposed. Of the Tyr residues highlighted above Tyr 355 and Tyr 364 are both buried and Tyr 424 is exposed.

Application of the ECL ELISA to pre- and post-surgery serum samples

Due to natural variations in protein concentration, and a statistically significant ($p<0.01$, Wilcoxon matched pairs) fall in protein concentration post-surgery, results were normalised to protein content and expressed as fmol BSA-NO_2 equivalents/mg protein.

A statistically significant ($p<0.05$, Wilcoxon matched pairs) increase in serum Tyr-NO_2 was seen post-surgery (**Figure 3.5**), median (IQR): 0.59 (0 – 1.3) and 0.97 (0 – 1.7) Tyr-NO_2 fmol BSA-NO_2 equivalents/mg protein for pre- and post-surgery respectively.

Median serum CRP levels increased significantly following surgery ($p<0.0001$, Wilcoxon matched pairs).

Median serum protein carbonyls increased significantly following surgery ($p<0.05$, Wilcoxon matched pairs).

Some of the samples had data on the white blood cell populations in the blood ($n = 40$, both days combined). A significant increase was seen in total neutrophil population number ($p<0.001$, two-way ANOVA).

Median (IQR) serum NO_3^- concentrations before surgery were 41.3 (29.1 – 62.2) µM and a statistically significant (Wilcoxon matched pairs, $p=0.0002$) decrease in the median was observed post-surgery; median (IQR) post-surgery 28.8 (17.7 – 49.7) µM.

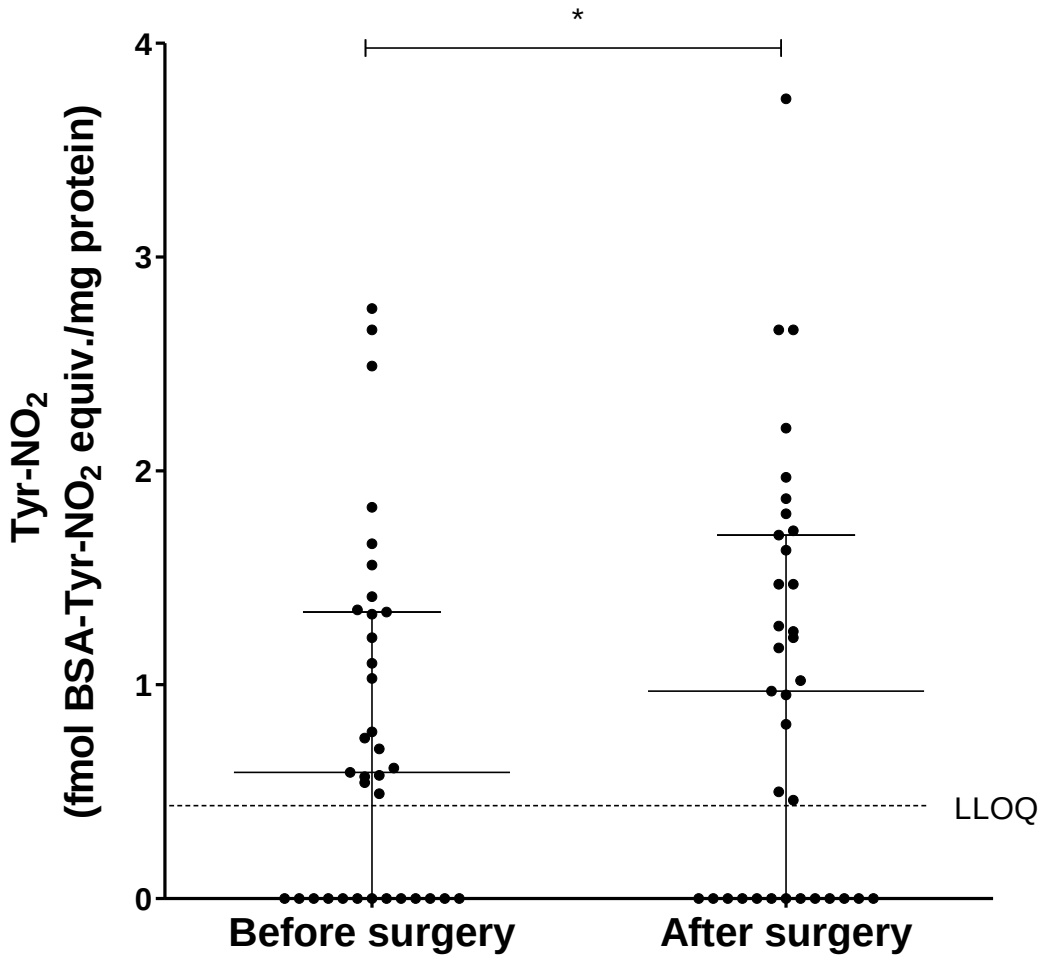

Figure 3.5: Median serum nitration levels before and after surgery

The Tyr-NO_2 was measured as per the protocol described in section 3.2.5. **The** median and inter-quartile range are shown (n=35). Serum nitration levels increased following major elective surgery (*p= 0.02, Wilcoxon matched pairs).

Tyr-NO_2 levels in additional samples

Cellular levels of Tyr-NO_2 were investigated to determine whether this fraction of blood is more susceptible to nitration than the plasma/serum. Levels of Tyr-NO_2 were far higher in cellular samples compared to the serum, with the highest levels being observed in the cell line U937 (**Figure 3.6**). There was poor separation of polymorphonuclear cells during cell isolation, so Tyr-NO_2 was not measured for this cell population.

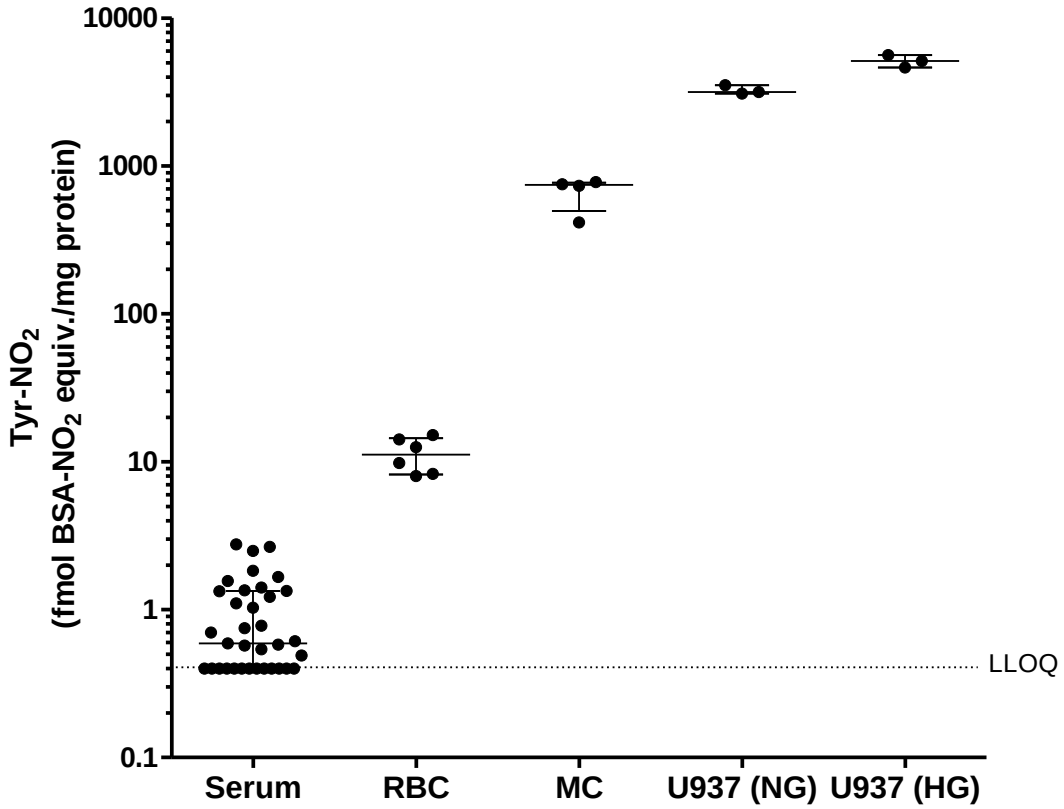

Figure 3.6: A comparison of 3-nitrotyrosine levels in serum and blood cells

Levels of nitration were far lower in the serum compared to cellular samples. Tyr-NO_2 was measured as per the protocol in section 3.2.5. Cells collected as per protocol in section 3.2.7. RBC (red blood cells), MC (mononuclear cells) and U937 cells (histiocytic lymphoma cell line) at a normal glucose (NG - 5.6 mM) and high glucose (HG – 24 mM) concentration. A log scale has been used for the y-axis, samples that had undetectable Tyr-NO_2 were plotted at the LLOQ so as to appear on this log scale.

3.4. Discussion

A sensitive ECL ELISA was developed for the measurement of Tyr-NO_2 in bio-fluids, this assay has an improved LLOQ compared to existing colorimetric ELISAs (LLOQ 0.04 nM BSA-NO_2, **Figure 3.2**) as well as good linearity, recovery, and specificity. The importance of performing incubations at 25°C was shown by comparing the assay variation at room temperature and at 25°C (**Table 3.1**). Agreement on measurement of nitration between methods was seen between the ECL ELISA and mass spectrometry for the native and nitrated BSA. However, this experiment was only done once and needs to be repeated to confirm the level of agreement between the methods. The two methods showed disagreement for the relative nitration of the chemically reduced BSA, this may have been due to the mass spectrometry being more sensitive but could also have been the result of residual dithionite affecting the ECL ELISA performance.

The ECL ELISA was applied to the measurement of Tyr-NO_2 in serum from patients undergoing major elective surgery, with samples collected before and after surgery. This gave us paired samples for before and after an inflammatory insult (as confirmed by CRP levels and neutrophil count). NO_3^- concentration was measured as another marker of $^{\bullet}NO$ production and, despite the initiation of an inflammatory response and an increase in Tyr-NO_2, the median concentration of NO_3^- significantly decreased following the surgery. However, this NO_3^- concentration decrease may be accounted for by dilution of the blood, such as by intravenous fluids, following surgery. A change in oxidative stress status was confirmed by measuring serum protein carbonyl levels. As has already been discussed, in Chapter 1 (section 1.5.2), a rise in oxidative stress post-surgery has been linked with tissue damage and recovery time (Kaminski et al, 2002; Rosenfeldt et al, 2013). As the ROS required for Tyr-NO_2 formation have been implicated in ischaemia-reperfusion injury (Zweier and Talukder, 2006), protein nitration may be an ideal marker of ROS production following surgery.

Multiple sample types were also measured by this new ECL ELISA, showing the versatility of the assay. These results also show that Tyr-NO_2 levels are far higher in cellular samples compared to circulating serum levels. The highest

results by far were in unstimulated U937 cells, this is a cell line grown at atmospheric oxygen concentrations, and could, therefore, be considered to be in a constant state of oxidative stress (Halliwell, 2003).

Tandem mass spectrometry (MS/MS) is considered to be the 'gold-standard' method for measuring Tyr-NO_2 as the method is highly accurate and can quantify absolute Tyr-NO_2 concentration (Tsikas and Caidahl, 2005; Ryberg and Caidahl, 2007; Tsikas and Duncan, 2014). However, this method is not suitable for the analysis of a lot of samples (such as in a clinical setting) as it is time-consuming (low-throughput) and expensive. ELISA methods address these issues but are only semi-quantitative and not as accurate.

Commercial ELISA assays for measuring Tyr-NO_2 are available but are unlikely to be sensitive enough to detect the low levels of Tyr-NO_2 present in serum. Some studies using this kind of assay do report Tyr-NO_2 levels to be undetectable in healthy human plasma (Ter Steege et al, 1998; Ceriello et al, 2001). However, other studies have reported levels far higher than those observed here, even in health (i.e. the absence of inflammation), see Chapter 1, section 1.5.1, Table 1.3 (Bo et al, 2005; Rossner Jr et al, 2007). This discrepancy cannot be explained with any certainty, but a few possibilities for these contradictory results are differences in methodology, antibody binding, the standards used and/or the reporting style (e.g. absolute Tyr-NO_2 concentration or standard equivalents).

The wide variation in the baseline (i.e. before surgery) serum nitration levels (median (IQR): 0.048 (0 – 0.102) nM BSA-NO_2 equivalents) was thought to be due to the range of medical conditions and general heterogeneity of the sample group. There was also a significant (Wilcoxon matched pairs, $p = 0.007$) drop in serum protein concentration following surgery; this was most likely due to the use of intravenous fluids during recovery. To account for this change in protein concentration Tyr-NO_2 levels were adjusted for protein concentration. When this was done, a statistically significant difference (**Figure 3.5**) was observed between pre- and post-surgery samples, which was not seen prior to the protein adjustment.

Increased oxidative stress (and nitration) may also lead to an enhanced degradation of modified proteins. When the degradation of proteins modified by

oxidative stress has been investigated, the 20S proteasome has been found to be largely responsible (Davies, 2001; Jung et al, 2014) and peroxynitrite modified proteins are degraded faster than unmodified protein (Gow et al, 1996; Souza et al, 2000b). When Souza et al (2000b) exposed Cu-Zn superoxide dismutase to $ONOO^-$ nitration of a single Tyr residue was determined to be the only structural modification, and degradation by the proteasome was enhanced. This suggests that nitrated proteins are marked for degradation and therefore more likely to be removed than non-nitrated proteins. Based on this, it seems reasonable to speculate that the measured protein-associated Tyr-NO_2 underrepresents the actual level of nitration. However, it should be noted that when oxidative stress becomes excessive proteins may cross-link and aggregate, preventing them from being degraded and may even bind to and inhibit the proteasome (Davies, 2001; Shringarpure and Davies, 2002).

Radák et al (2003) measured Tyr-NO_2 daily in people doing a super-marathon, an extreme exercise that induces an inflammatory reaction. The authors noted an increase in serum Tyr-NO_2 from baseline to day one of the race but then levels reached a plateau, despite the increasing intensity of the race. They theorised that this was due to nitration and degradation reaching equilibrium. However, they did not mention measuring the protein concentration of the serum over the course of the race (intense exercise can cause proteinuria), or correction of their results for protein content. If a drop in protein concentration was seen with each day then adjustment for protein would have shown nitration levels increasing rather than remaining constant. However, few studies in the literature do this and it may account for some of the discrepancies in results between studies. Weber et al (2012) suggested that all samples should be diluted to the same protein concentration prior to measurement. This was highlighted as a methodological issue (as protein concentration may affect assay performance) but would also act as a way of normalising the samples to a single protein concentration.

This study was limited by the large variety of pathologies and surgeries encountered within the sample population. Additionally, the patient numbers for any one type of surgery were too small to allow analysis of whether a particular surgery type is associated with significantly higher levels of Tyr-NO_2. The blood cell populations were only harvested from healthy volunteers. It is therefore

unknown what happens to the levels of Tyr-NO_2 in blood cells following surgery/inflammation. A further study with fewer patient groups, but with large sample numbers for each pathology/surgery, and collection of both serum and blood cells, would address these issues.

3.5. Conclusion

The ECL ELISA described was able to detect Tyr-NO_2 in many of the samples, although even with its improved sensitivity some samples were below the LLOQ. The assay was also able to measure a statistically significant increase in serum Tyr-NO_2 following activation of an inflammatory response (i.e. by surgery).

The assay has attempted to not only improve sensitivity but to produce and report a valid and robust way to measure Tyr-NO_2. However, there is room for further improvement of the assay, such as the reporting of results as BSA-NO_2 equivalents rather than as an absolute Tyr-NO_2 concentration. This is a flaw found in many reported ELISA results and needs to be addressed for published research to be accurately compared.

3.6. Acknowledgements

Pre- and post-surgery serum samples were provided by Dr R Lukaszewski (Defence Science and Technology Laboratory).

Human blood was collected from healthy volunteers by Dr Stephen Bailey, Sport and Health Science University of Exeter.

Mass spectrometry was performed with the aid of Professor A Pitt, Dr C Spickett and Dr K Tveen-Jensen (Aston University).

Nitrated BSA residues, in the ECL ELISA standard, were mapped on to a 3D model with the aid of Dr Michail Isupov and Professor Jennifer Littlechild (University of Exeter, College of Life and Environmental Sciences).

CRP measurement was performed with the aid of Emily Brewer and Dr Tim McDonald (Royal Devon and Exeter NHS Foundation Trust).

Chapter 4
3-Nitrotyrosine levels in plasma and saliva from healthy human volunteers following nitrate supplementation

4.1. Introduction

Nitrite (NO_2^-) and nitrate (NO_3^-) are often used as biomarkers of $^{\bullet}NO$ production (Chapter 1, section 1.4.1) (Kleinbongard et al, 2003; Tsikas, 2004). However, NO_2^- and NO_3^- in the diet affect the concentrations of NO_2^- and NO_3^- in the blood (Kelly et al, 2014). It is also now thought that the reactions shown in **Figure 4.1** can proceed in the reverse direction, meaning the traditional nitric oxide synthase (NOS) pathway for $^{\bullet}NO$ production is not the only means of producing $^{\bullet}NO$, e.g. dietary NO_3^- could lead to $^{\bullet}NO$ production (Duncan et al, 1995).

Ingestion of NO_3^- has previously been viewed as harmful, leading to strict regulations on the NO_3^- content of water supplies (Johnson and Kross, 1990; McKnight et al, 1999). However, there is now evidence to suggest that ingesting high levels of NO_3^- may also have beneficial effects (e.g. lowering of blood pressure (Lundberg et al, 2006)) and it is thought these effects rely on the reduction of NO_3^- to $^{\bullet}NO$ (Gilchrist et al, 2010).

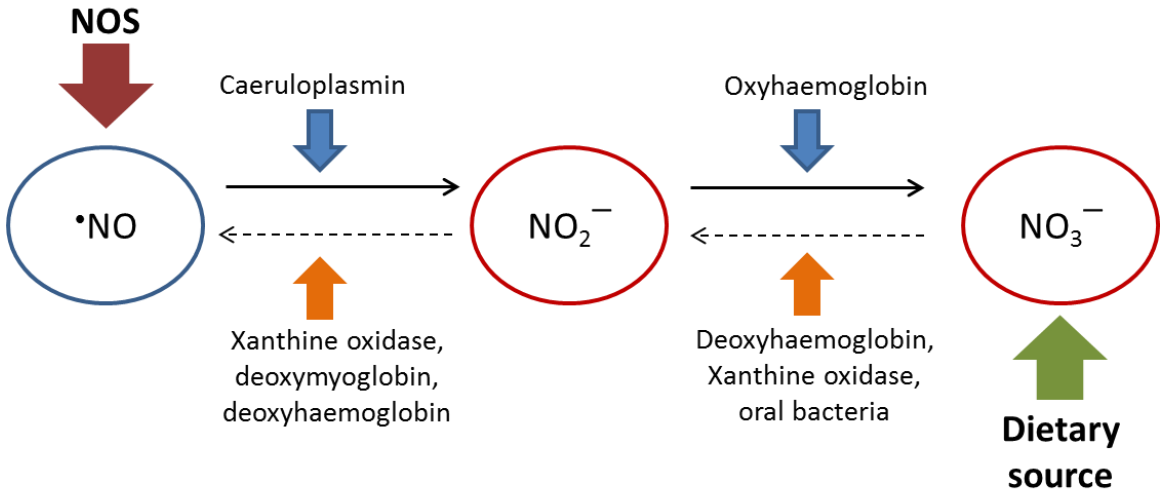

Figure 4.1: Nitric oxide metabolism

$^{\bullet}NO$ can be formed by NOS enzymes and oxidised to NO_2^- and NO_3^-. Alternatively NO_3^- ingested in the diet can be reduced to NO_2^- and $^{\bullet}NO$ by NO_3^- and NO_2^- reductases respectively (Duncan et al, 1995; Zhang et al, 1998; Cosby et al, 2003; Doel et al, 2005; Shiva et al, 2007).

Several studies have shown that NO_3^--rich dietary supplementation can enhance sports performance in healthy participants by reducing the oxygen cost of submaximal exercise and improving exercise tolerance (reviewed by Jones (2014) and Affourtit et al (2015)). The NO_3^- itself is thought to be inert but ingestion leads to an increase in plasma NO_2^- concentration, for example through the NO_3^- reductase activity of bacteria in the mouth (Duncan et al, 1995; van der Vliet et al, 1997; Doel et al, 2005). The NO_2^- generated by NO_3^- reductase activity is then depleted during exercise (Larsen et al, 2007; Kelly et al, 2014). Several mechanisms by which NO_2^-can affect exercise performance have been suggested, such as augmented vasodilation in contracting muscles through the generation of $^{\bullet}NO$ from NO_2^- by deoxyhaemoglobin (Cosby et al, 2003), deoxymyoglobin (Shiva et al, 2007) or xanthine oxidase (Zhang et al, 1998). In the hypoxic conditions of exercising muscles, this will be enhanced, whereas the classical $^{\bullet}NO$ production pathway (i.e. NOS) will be impaired, as oxygen is required for this pathway. However, supplementation in individuals with diseases such as diabetes and COPD has not shown a significant effect on the oxygen cost of mild exercise (Shepherd et al, 2015a; Shepherd et al, 2015b).

Oldreive et al (2001) found that a NO_3^--rich meal did not increase plasma Tyr-NO_2 levels in healthy non-smoking participants. However, neutrophil count and serum MPO levels have been found to be higher in smokers compared to non-smokers (Andelid et al, 2007; Martins et al, 2013). As has been previously described (in Chapter 1, section 1.5) MPO can utilise NO_2^- as a substrate, leading to the formation Tyr-NO_2 (detailed in **Pathway 4.1**). It could, therefore, be hypothesised that smokers ingesting high amounts of NO_3^- may have increased serum Tyr-NO_2 formation.

Pathway 4.1: Tyrosine nitration in the presence of NO_2^- and MPO

i.	H_2O_2 + MPO	$\longrightarrow$	MPO-I + H_2O	1.8×10^7 M^{-1} s^{-1} (Marquez et al, 1994)
ii.	MPO-I + NO_2^-	$\longrightarrow$	MPO-II + $^{\bullet}NO_2$	2×10^6 M^{-1} s^{-1} (Burner et al, 2000)
iii.	MPO-I + Tyr	$\longrightarrow$	MPO-II + Tyr$^{\bullet}$	7.7×10^5 M^{-1} s^{-1} (Marquez and Dunford, 1995)
iv.	Tyr$^{\bullet}$ + $^{\bullet}NO_2$	$\longrightarrow$	Tyr-NO_2	3×10^4 M^{-1} s^{-1} (Lepoivre et al, 2005)

Studies have shown that post-translational modifications (PTMs) can lead to the formation of neo-epitopes (Karsdal et al, 2010). These epitopes may not be recognised as 'self' by the immune system and thus, can elicit an immune response and auto-antibodies (reviewed by Ryan et al (2014)). An example of PTMs creating neo-epitopes is citrullination via the catalysed conversion of arginine to citrulline in RA. Arginine is converted to citrulline by removal of the imine group and this is catalysed by peptidylarginine deiminases (György et al, 2006). Within RA patient tissues, citrullinated proteins are a target for autoantibodies and this has become an important factor in the diagnosis of the disease (Luban and Li, 2010). Autoantibodies that bind nitrated proteins have been observed in the autoimmune conditions RA and SLE (Khan and Ali, 2006; Khan and Siddiqui, 2006). Therefore, conditions that increase nitration of proteins could potentially also increase a person's risk of auto-antibody production. As NO_3^--rich supplements are becoming increasingly popular, it is important to determine whether NO_3^- ingestion increases PTMs.

NO_2^- concentrations in the saliva of healthy humans have been measured at 30-210 µM (van der Vliet et al, 1997), and these levels rise significantly following NO_3^- ingestion; as mentioned above, this is due to NO_3^- reduction by the oral microflora (Duncan et al, 1995; van der Vliet et al, 1997; Doel et al, 2005). One possible fate for this NO_2^- is a reaction catalysed by peroxidases, such as MPO, in the saliva (Takahama et al, 2003). Takahama et al (2003) observed H_2O_2/ NO_2^--dependent nitration of salivary proteins *in vitro* and suggested that this reaction could happen *in vivo* during an immune response. Klebanoff (1993) also suggested that the reaction of MPO/H_2O_2 and NO_2^- (**Pathway 4.1**) may increase bactericidal activity, although he notes that under certain conditions (*in vitro*) NO_2^- inhibits the antibacterial activity of MPO (e.g. high [MPO] with low pH). Although nitration of bacterial proteins could aid host defences (Takahama et al, 2003), the nitration of host proteins could potentially alter protein function (Radi, 2012). Additionally, the NO_2^- that is swallowed will become acidified in the stomach and increase the bactericidal activity of gastric acid through the generation of reactive nitrogen intermediates that have cytotoxic properties (Dykhuizen et al, 1996; McKnight et al, 1999).

There has been little research into salivary nitration *in vivo*, although Ueshima et al (2007) measured protein-associated levels of Tyr-NO_2, and concluded that

the levels of protein-associated Tyr-NO_2 in saliva do not interfere with the measurement of Tyr-NO_2 in sputum from COPD and asthmatic patients; they found 0.02 ± 0.01 pmol/ml protein-associated Tyr-NO_2 in saliva from COPD patients.

In light of the above mentioned concerns that NO_3^--rich supplements may increase nitration, particularly in smokers, and that this can create neo-epitopes that are not recognised by the immune system, the plasma and salivary Tyr-NO_2 levels in smokers/non-smokers, who had been administered a NO_3^--rich supplementation (beetroot juice), were measured.

4.2. Methods

4.2.1. Study design

The study used a cross-over design (**Figure 4.2**) so that each participant ingested both the supplement (NO_3^--rich beetroot juice, 70 ml containing 4.2 mmol NO_3^-) and the placebo (NO_3^--depleted beetroot juice, 70 ml containing 0.04 mmol NO_3^-). The depletion of NO_3^- from beetroot juice was done using Purolite resin (Gilchrist et al, 2014)). Physiological measures, such as blood pressure and exercise performance, were taken along with blood and saliva being collected for analysis. Blood was collected in a 5 ml EDTA vacutainer and spun at *350 g* for 20 minutes. The plasma supernatant was then collected and frozen. Saliva was collected by direct void into a container for 5 minutes. Subjects were asked to keep a consistent diet throughout the study and samples were collected at the start to establish baseline levels. Subjects were then randomly assigned a condition (placebo or supplement) for 6 days. The juice was taken twice a day (morning and evening) for 5 days and then 140 ml (i.e. two doses) was consumed 2 hours before collection of samples on the sixth day. A 7-10 day washout period separated the two conditions. The smokers were determined to have normal blood pressure, normal respiratory function, healthy body mass index and a similar aerobic fitness to the non-smokers. There were 17 volunteers (non-smokers n=8, smokers n=9) with 8 females (4 non-smokers) and 9 males (4 non-smokers). The mean age of all participants was 24 (range 18-37) years overall, the mean age within each group was also 24 years (non-smokers 18-32 years, smokers 18-37 years). All volunteers gave informed consent, and this study was approved by the Institutional Research Ethics Committee (approval number 2013/539 (rev2)).

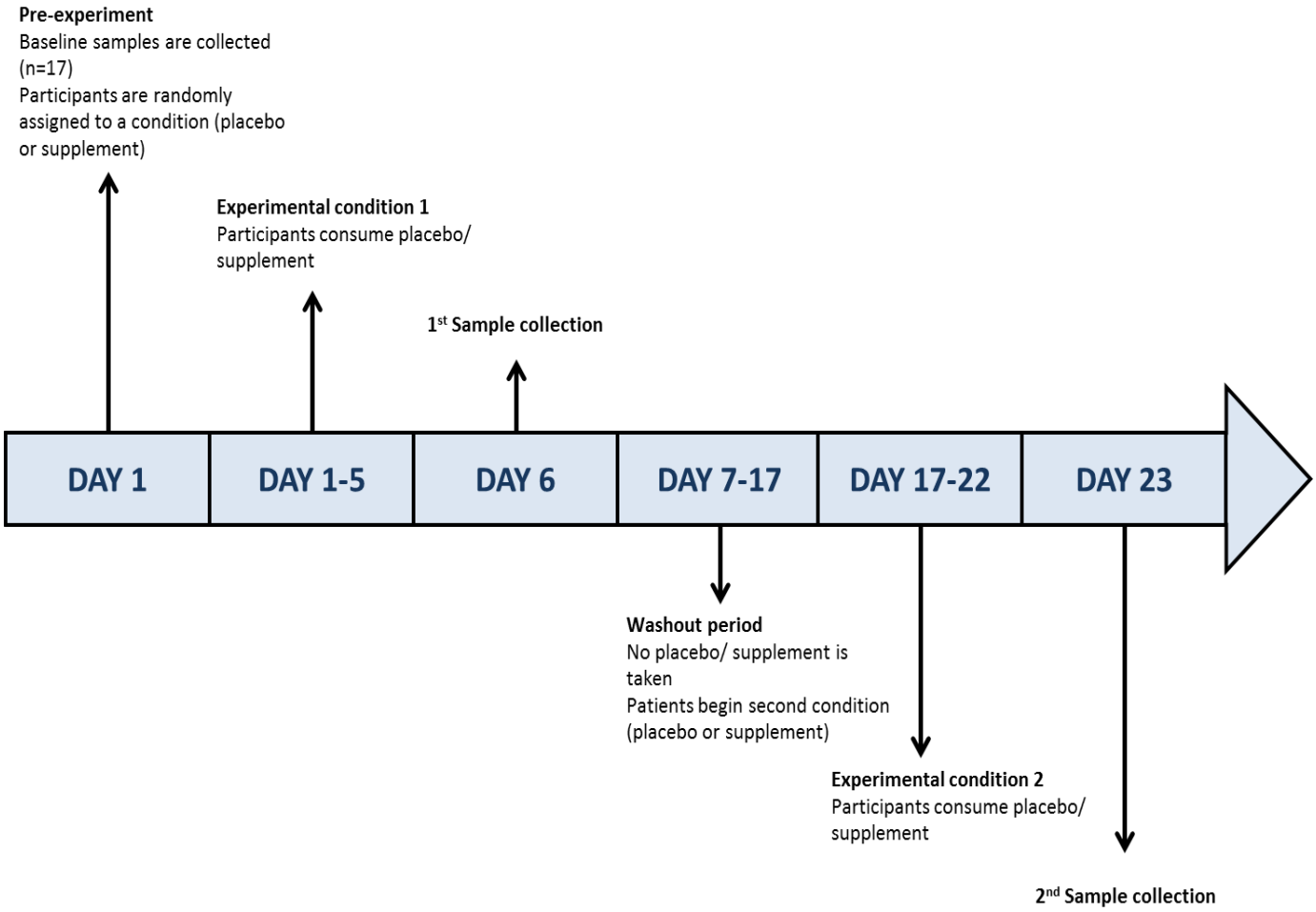

Figure 4.2: Nitrate supplementation cross-over study design

All participants provided samples prior to the study and were then either given the placebo (NO_3^--depleted beetroot juice) or supplement (NO_3^--rich beetroot juice) and samples were taken again. The participants were then switched to the opposite treatment and samples collected again.

4.2.2. Electrochemiluminescence-based ELISA for 3-nitrotyrosine

The protocol described in Chapter 3 (section 3.2.5) was used to measure Tyr-NO_2. Plasma was diluted 1 in 5, with dilution buffer, and measured in quadruplicate. Saliva was diluted 1 in 2, with dilution buffer, and measured in duplicate. Both were corrected for protein content as determined by the BCA assay (Chapter 2, section 2.2).

4.2.3. Assays of nitrite, nitrate, thiocyanate and asymmetric dimethylarginine

Dr Stephen Bailey (University of Exeter Sport and Health Science) also collected data on plasma and saliva concentrations of: NO_2^- and NO_3^- (using ozone-based chemiluminescence (see Chapter 2, section 2.9)), thiocyanate (using the König reaction (Tsuge et al, 2000)) and plasma asymmetric dimethylarginine (using a competitive enzyme immunoassay (Immundiagnostik, 2009)).

4.2.4. Statistical analysis

Nonparametric tests were applied for the statistical analysis of the data (Wilcoxon matched pairs, Freidman test and Mann-Whitney test) unless the Shapiro-Wilk test indicated that the data were normally distributed (parametric test – paired and unpaired t test).

4.3. Results

4.3.1. Plasma

There was no statistically significant difference in the median plasma nitration levels between the non-smokers and smokers prior to supplementation: median (IQR) 0.92 (0.67-1.34) and 1.28 (0.77-2.35) Tyr-NO_2 fmol BSA equiv./mg protein in the non-smokers and smokers respectively (Mann-Whitney p=0.44, **Figure 4.3A**). There was also no statistically significant difference in plasma Tyr-NO_2 levels between non-smokers and smokers after NO_3^--rich supplementation: median (IQR) 0.97 (0.57-1.92) and 1.13 (0.69-2.23) Tyr-NO_2 fmol BSA equiv./mg protein in the non-smokers and smokers respectively (Mann-Whitney p=0.37, **Figure 4.3B**).

There was no statistically significant change in median plasma Tyr-NO_2 levels when comparing pre-experiment and post NO_3^--rich supplementation for either non-smokers or smokers (**Figure 4.4**). There was also no statistically significant difference between the median levels prior to supplementation and after placebo (NO_3^--depleted) supplementation for either subject group.

Although both groups showed a statistically significant increase in mean plasma NO_2^- and NO_3^- concentration following NO_3^--rich supplementation (p=0.007 and 0.0009 for non-smokers and smokers respectively, paired t-test) (**Figure 4.5**) the post-supplementation concentrations were lower in the smokers compared to the non-smokers (unpaired t-test: NO_3^- p = 0.005, and NO_2^- p= 0.04).

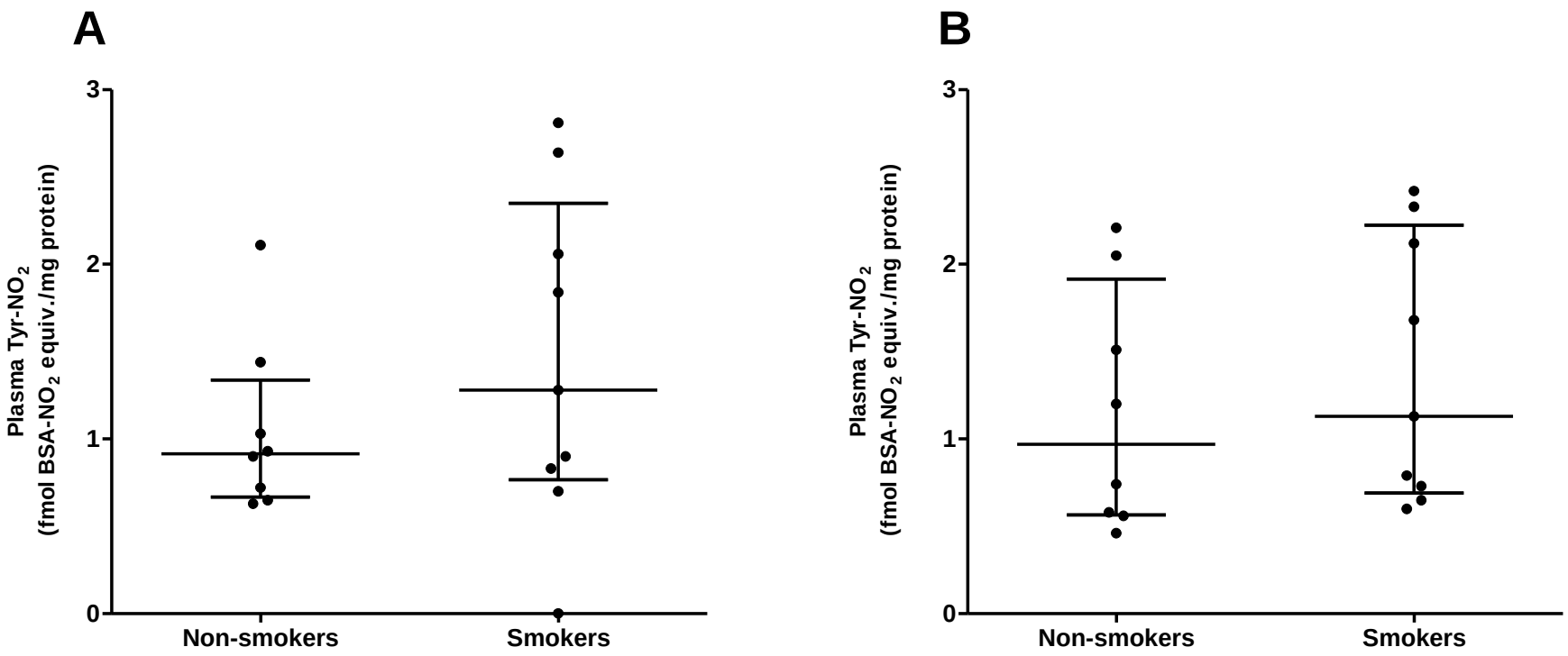

Figure 4.3: 3-Nitrotyrosine levels in the plasma from healthy non-smokers and smokers before and after nitrate-rich beetroot supplementation

The NO_3^--rich supplementation protocol was as described in section 4.2.1. The plasma Tyr-NO_2 levels were measured as described in Chapter 3, section 3.2.5. The median and IQR values are shown. Non-smokers n=8 and smokers n=9. (A) Non-smokers and smokers before beetroot supplementation (Mann-Whitney, p=0.44) and (B) Non-smokers and smokers after NO_3^--rich beetroot supplementation (Mann-Whitney, p=0.37). There was no statistically significant difference between the median levels of Tyr-NO_2 in the two subject groups either prior to supplementation or after NO_3^--rich beetroot supplementation.

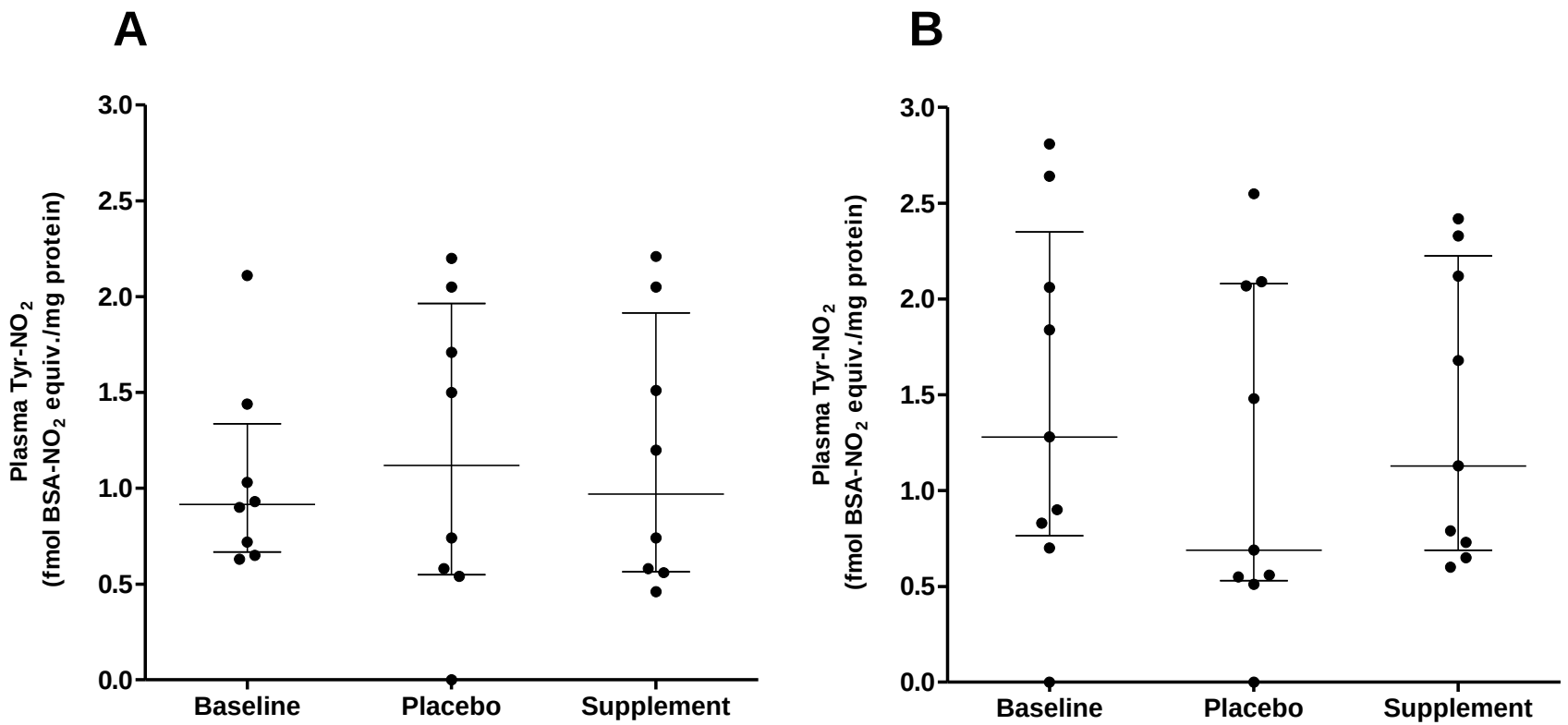

Figure 4.4: Non-smoker's and smoker's plasma 3-nitrotyrosine levels before and after each supplementation condition

The supplementation protocol was as described in section 4.2.1. The plasma Tyr-NO_2 was measured as described in Chapter 3, section 3.2.5. Non-smokers n=8 and smokers n=8, median and IQR shown. (A) Non-smokers (Freidman test p= 0.53) and (B) Smokers (Freidman test p= 0.05). Neither of the subject groups showed a statistically significant change in median plasma Tyr-NO_2 levels with NO_3^--depleted or NO_3^--rich supplementation.

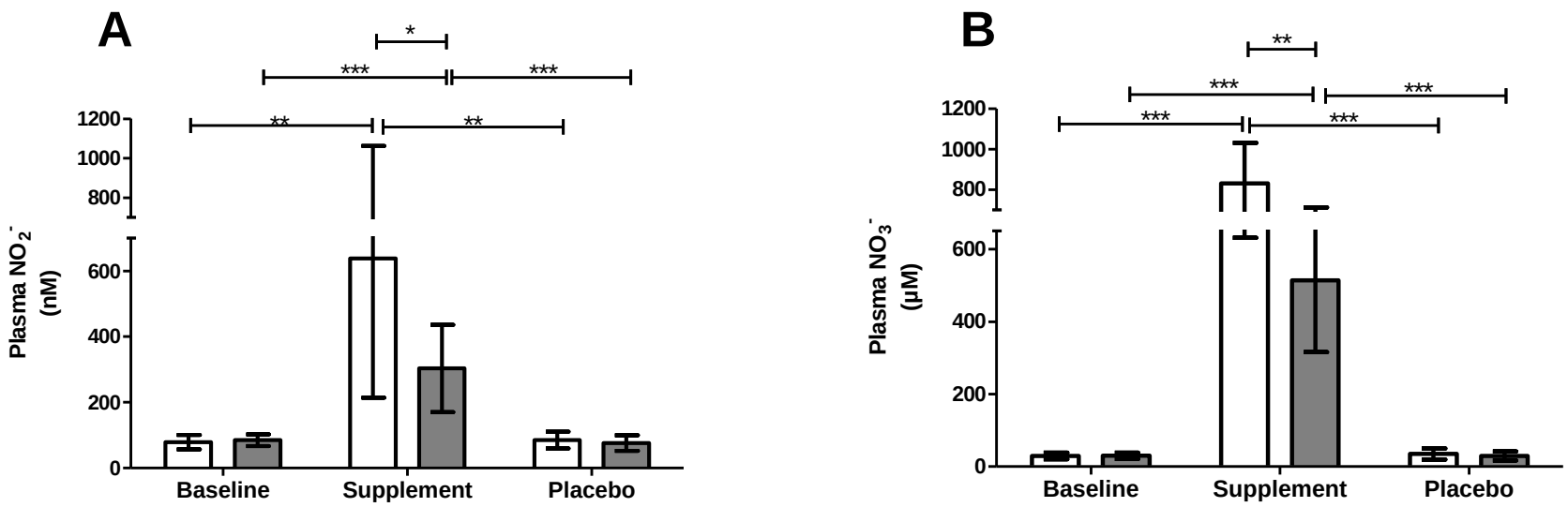

Figure 4.5: Plasma nitrite and nitrate concentrations, in non-smoker's and smoker's, before and after nitrate-rich beetroot supplementation

The NO_3^--rich supplementation protocol was as described in 4.2.1, and the salivary NO_2^- and NO_3^- was measured as described in Chapter 2, section 2.9. The mean and SD are shown. Open bars represent the non-smokers (n=8), filled (grey) bars represent the smokers (n=9). (A) Plasma NO_2^- concentration increased significantly in both groups following supplementation but not with placebo (**p<0.01, ***p<0.001, repeated measures ANOVA). After supplementation the smokers had lower concentrations than non-smokers (*p<0.05, unpaired t test). (B) Plasma NO_3^- also increased with supplementation in both groups but not with placebo (**p<0.01, ***p<0.001 – repeated measures ANOVA). After supplementation the smokers had lower concentrations than non-smokers (**p<0.01, unpaired t test). The data shown was collected by Dr S Bailey.

4.3.2. Saliva

There was no statistically significant difference in the median saliva nitration levels between the non-smokers and smokers prior to NO_3^--rich supplementation (Mann-Whitney p=0.71, **Figure 4.6A**) or after the NO_3^--rich supplementation (Mann-Whitney p=0.23, **Figure 4.6B**).

With non-smokers there was a decrease in salivary Tyr-NO_2 when comparing baseline with post-supplementation (Friedman test p=0.03): median and (IQR) 0.57 (0.09 – 1.07) and 0.21 (0.03 – 0.52) Tyr-NO_2 pmol BSA equiv./mg protein for baseline and post-supplementation respectively (**Figure 4.7A**). The smokers had no significant change with NO_3^--rich supplementation (Friedman test p=0.08) (**Figure 4.7B**). However, a statistical difference was seen with post-testing when comparing the placebo supplementation and the real supplementation in the smokers (Dunn's multiple comparison test p<0.05): median (IQR) 0.86 (0.33 – 1.57), 0.995 (0.80 – 1.87) and 0.49 (0.33 – 0.64) Tyr-NO_2 pmol BSA equiv./mg protein for baseline, placebo and real supplement respectively. There was no difference between the placebo and baseline Tyr-NO_2 levels in either group.

There was an increase in mean salivary NO_2^- concentration for both groups following supplementation (p=0.004 and 0.0002 for non-smokers and smokers respectively, ANOVA repeated measures) (**Figure 4.8A**). The levels of NO_3^- also increased following supplementation in both groups (p<0.0001 for non-smokers and smokers, ANOVA repeated measures). However, the mean concentration was lower in smokers compared to non-smokers (p=0.046, Mann-Whitney test) (**Figure 4.8B**).

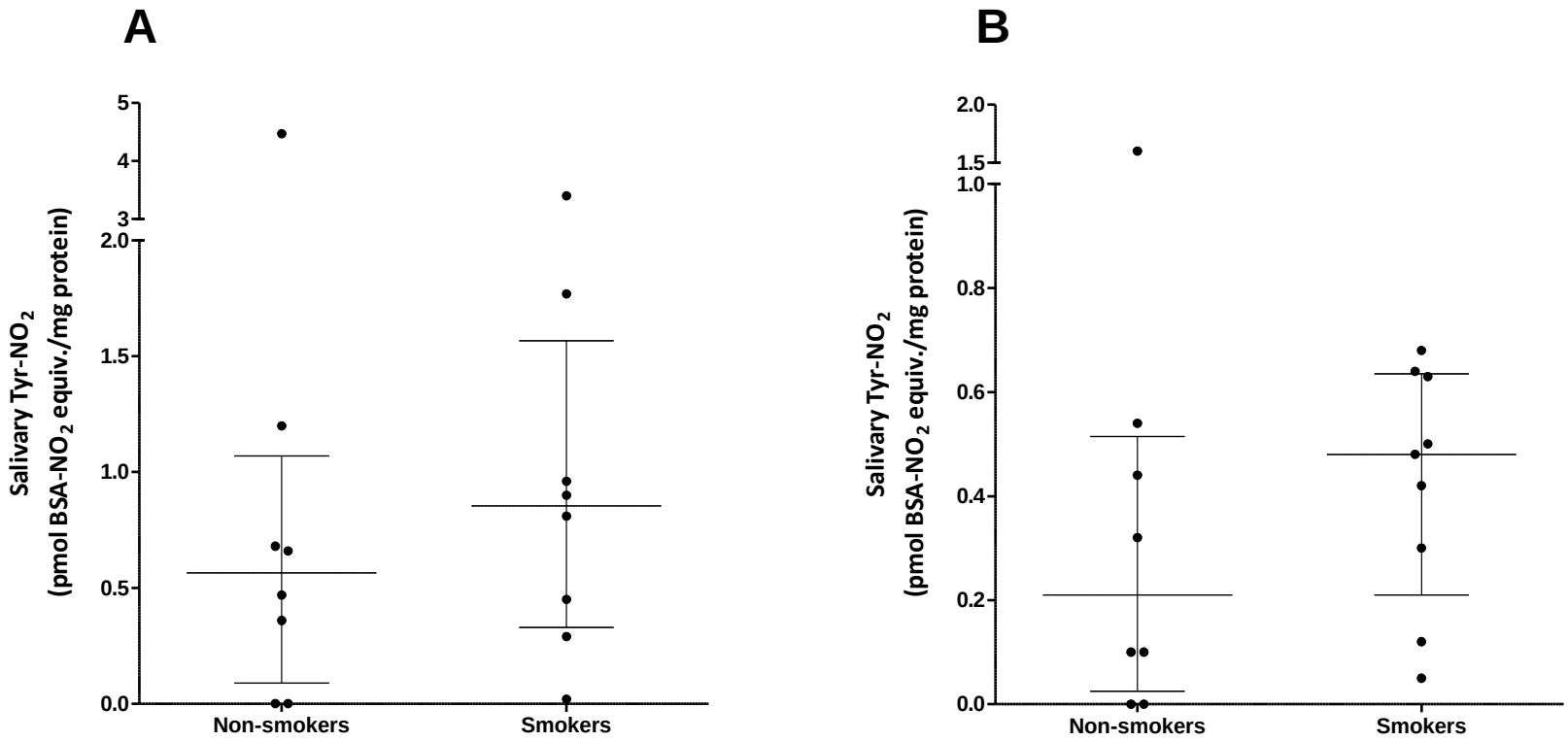

Figure 4.6: 3-Nitrotyrosine levels in the saliva from healthy non-smokers and smokers before and after nitrate-rich beetroot supplementation

The NO_3^--rich supplementation protocol was as described in section 4.2.1, and the salivary Tyr-NO_2 was measured as described in Chapter 3, section 3.2.5. The median and IQR values are shown: (A) before supplementation - n=8 for each group (Mann-Whitney p=0.71), and (B) after supplementation - non-smokers n=8, smokers n=9 (Mann-Whitney p=0.23). There was no difference between the two subject groups in either condition.

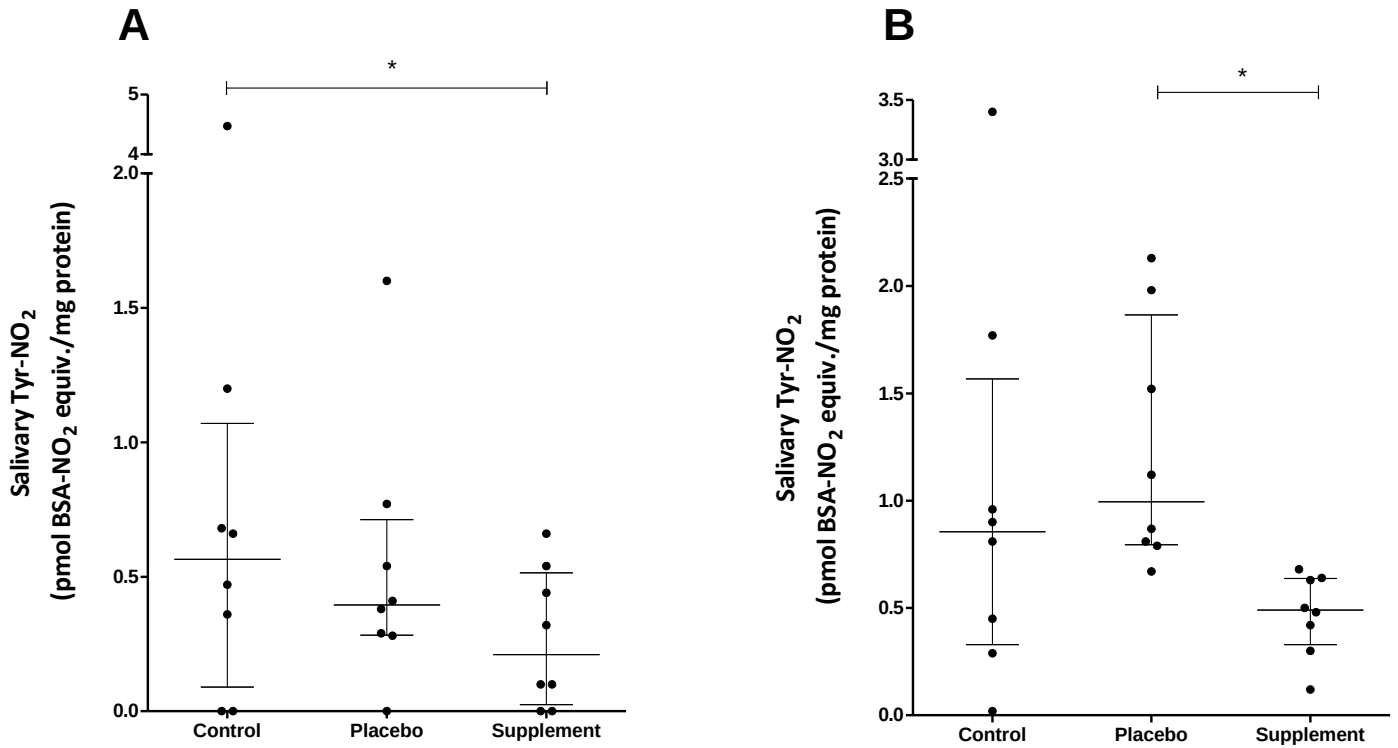

Figure 4.7: Non-smoker's and smoker's saliva 3-nitrotyrosine levels before and after each supplementation condition

The NO_3^--rich supplementation protocol was as described in section 4.2.1, and the salivary Tyr-NO_2 was measured as described in Chapter 3, section 3.2.5. The median and IQR shown values are shown. (A) In non-smokers there was a significant decrease in Tyr-NO_2 levels following supplementation, n=8 (Friedman test *p=0.03). (B) Smokers showed a trend towards a decrease in saliva Tyr-NO_2 levels, but this was not statistically significant, n=8 (Friedman test p=0.08). However, the post-test showed a statistically significant difference between the placebo group and the supplement (Dunn's multiple comparison test $p<0.05$).

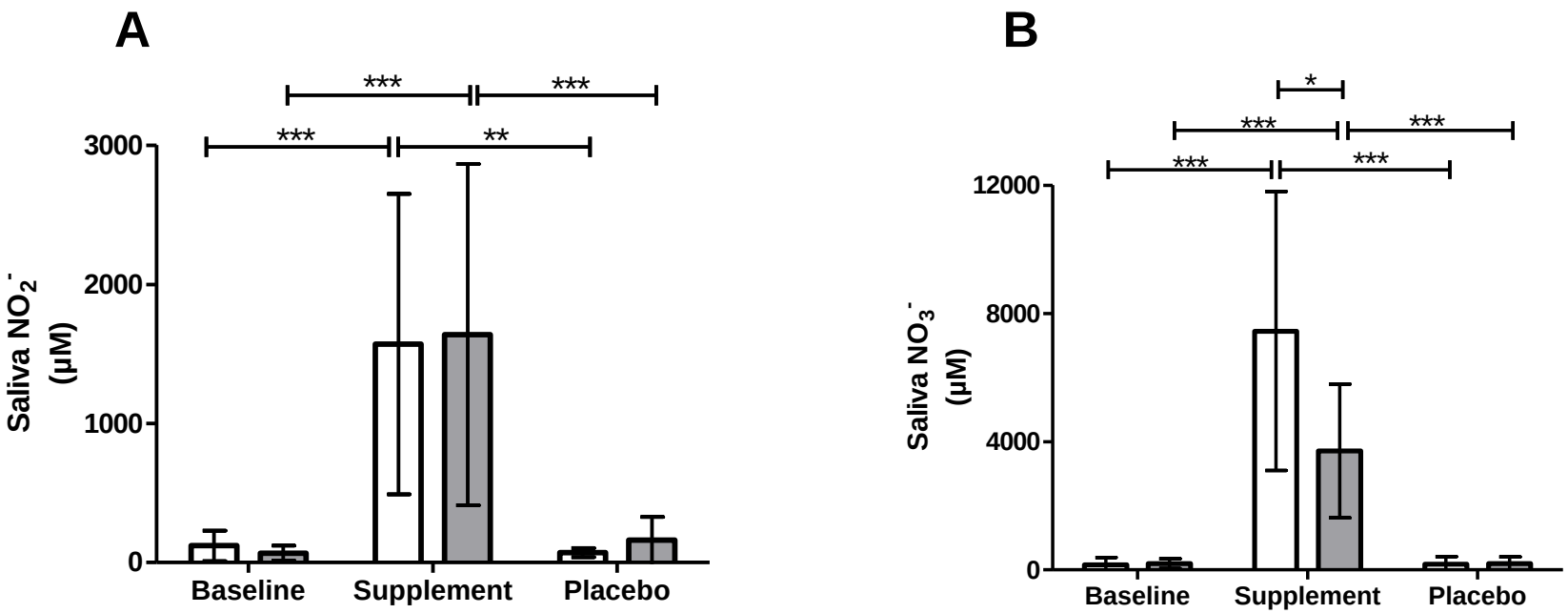

Figure 4.8: Salivary nitrite and nitrate concentrations, in non-smoker's and smoker's, before and after nitrate-rich beetroot supplementation

The NO_3^--rich supplementation protocol was as described in section 4.2.1, and the salivary NO_2^- and NO_3^- was measured as described in Chapter 2, section 2.9. The median and IQR values are shown. Open bars represent the non-smokers (n=8), filled (grey) bars represent smokers (n=9). (A) Salivary NO_2^- concentrations showed a statistically significant increase following supplementation in both groups but not with the placebo (**p<0.01, ***p<0.001, ANOVA repeated measures). (B) Salivary NO_3^- concentrations also showed a statistically significant increase in both groups but not with placebo (***p<0.001, ANOVA repeated measures). However, smokers had a lower salivary NO_3^- concentration than non-smokers (*p<0.05, Mann-Whitney test). The data was collected by Dr S Bailey.

4.3.3. Correlations

There were no statistically significant correlations between plasma nitration and plasma NO_2^- or NO_3^- or salivary NO_2^- or NO_3^- levels.

Plasma thiocyanate negatively correlated with plasma NO_3^- concentration (Spearman's rank correlation r = -0.50, p= 0.04, **Figure 4.9A**) as did salivary thiocyanate and salivary NO_3^- concentration (Spearman's rank correlation r = -0.52, p= 0.03, **Figure 4.9B**).

Salivary Tyr-NO_2 negatively correlated with salivary NO_2^- (Spearman's rank correlation r -0.37, p= 0.008) and this significance was maintained following the Bonferroni correction (p= 0.04) (**Figure 4.10A**). A statistically significant negative correlation between salivary nitration and plasma NO_2^- was also maintained after the Bonferroni correction (Spearman's rank correlation r -0.34, p = 0.01 after Bonferroni correction) (**Figure 4.10B**).

There were no statistically significant correlations between salivary Tyr-NO_2 and NO_3^- levels in either plasma or saliva.

Plasma and salivary Tyr-NO_2 levels did not show a statistically significant correlation with each other.

Salivary thiocyanate showed a statistically significant correlation with salivary Tyr-NO_2 (Spearman's rank correlation r = 0.4, p = 0.005) (**Figure 4.11**). There was no correlation between plasma thiocyanate and plasma Tyr-NO_2.

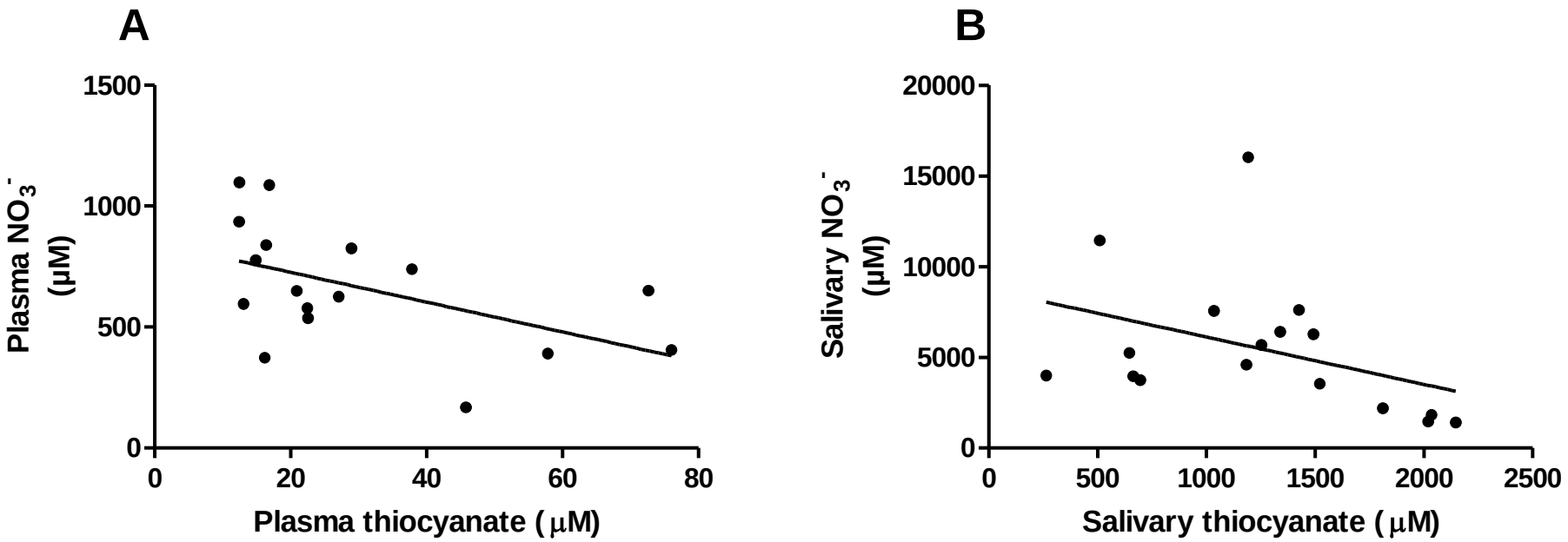

Figure 4.9: Inverse correlation of thiocyanate concentrations with nitrate concentrations in plasma and saliva

NO_3^--rich supplementation and thiocyanate measurement was performed as described in section 4.2.1. (A) Correlation between plasma thiocyanate and plasma NO_3^- showed a statistically significant negative correlation (Spearman's rank correlation r = -0.50, p= 0.04), and (B) correlation between salivary thiocyanate and salivary NO_3^- showed a statistically significant negative correlation (Spearman's rank correlation r = -0.52, p= 0.03). The data shown was collected by Dr S Bailey.

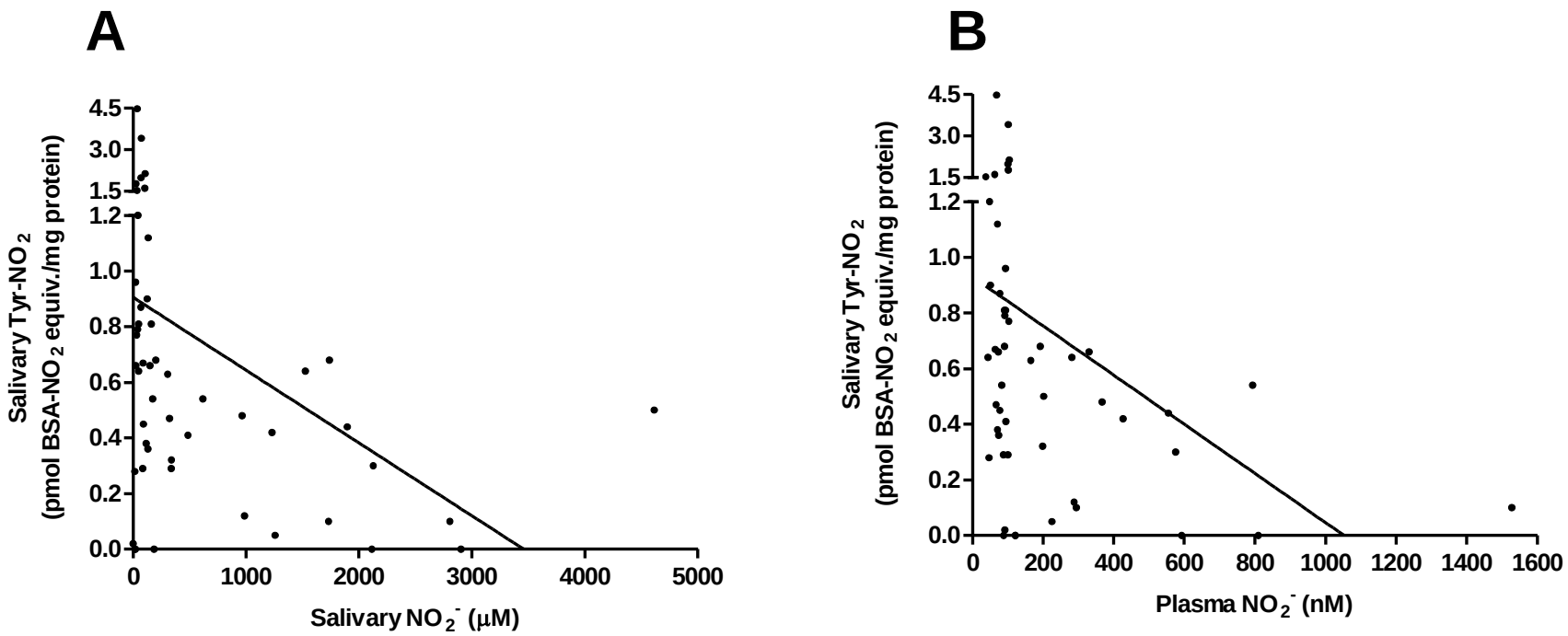

Figure 4.10: Inverse correlation of salivary 3-nitrotyrosine levels with salivary and plasma nitrite concentrations

The NO_3^--rich supplementation protocol was as described in section 4.2.1. Tyr-NO2 was measured as described in Chapter 3, section 3.5.2. (A) Correlation between salivary Tyr-NO_2 levels and salivary NO_2^- concentrations showed a statistically significant negative correlation (Spearman's rank correlation r = -0.37, p= 0.04), and (B) correlation between salivary Tyr-NO_2 levels and plasma NO_2^- concentrations showed a statistically significant negative correlation (Spearman's rank correlation r= -0.34, p= 0.01). Nitrite and nitrate data were collected by Dr S Bailey.

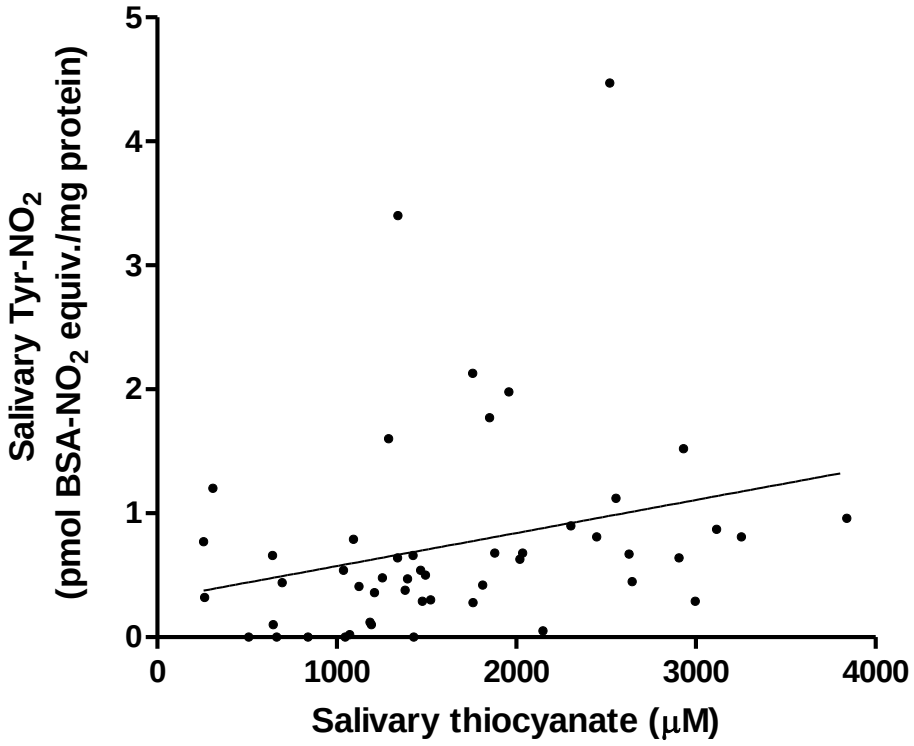

Figure 4.11: Correlation between salivary thiocyanate concentrations and salivary 3-nitrotyrosine levels

Thiocyanate was measured as described in section 4.2.1. There was a statistically significant positive correlation between salivary thiocyanate concentrations and Tyr-NO_2 levels (Spearman's rank correlation r = 0.4, p= 0.005). Thiocyanate data were collected by Dr S Bailey.

4.4. Discussion

NO_3^- is reduced to NO_2^- in the mouth by microflora-associated NO_3^- reductases (Doel et al, 2005) and NO_2^- can be further reduced to $^{\bullet}NO$ (Zhang et al, 1998; Cosby et al, 2003; Shiva et al, 2007; Ferguson et al, 2013). As both $^{\bullet}NO$ and NO_2^- are involved in Tyr-NO_2 formation it is possible that high NO_3^- ingestion could lead to increased protein nitration. Oxidative PTMs of proteins can create neo-epitopes that are not recognised as 'self' and lead to the production of auto-antibodies (Griffiths, 2008; Ryan et al, 2014), and anti-Tyr-NO_2 antibodies have been linked with the auto-immune conditions rheumatoid arthritis and systemic lupus erythematosus (Khan and Siddiqui, 2006). Smoking has been linked to increased carbonylation of proteins, which in turn has been suggested to be a contributing factor in a possible auto-immune response in COPD (Kirkham et al, 2011).

This study sought to determine whether ingesting high amounts of NO_3^- affected the Tyr-NO_2 levels in plasma and saliva, particular with regards to smokers. Smokers could potentially have higher levels of Tyr-NO_2 formation following ingestion of NO_3^- due to increased inflammatory activity, including higher levels of serum MPO (Andelid et al, 2007; Martins et al, 2013).

Within this study, the median plasma Tyr-NO_2 levels were comparable in the two groups (non-smokers and smokers) prior to NO_3^--rich supplementation, as were the plasma NO_2^- and NO_3^- concentrations. Once baseline samples were collected, a cross-over study design was used so that participants went through both experimental conditions (**Figure 4.2**). These conditions involved the ingestion of either NO_3^--rich beetroot juice or NO_3^--depleted beetroot juice. This study was carried out under double-blind conditions to avoid bias.

The plasma Tyr-NO_2 data collected here (**Figure 4.3**) is in agreement with Oldreive et al (2001) and Pannala et al (2003) in that high dietary NO_3^- intake does not increase plasma Tyr-NO_2 in non-smokers. Plasma NO_2^- concentrations increase with NO_3^- ingestion and, as both MPO levels (Martins et al, 2013) and H_2O_2 production are thought to be increased in the blood of smokers (Tanni et al, 2012), the substrates and catalysts for Tyr-NO_2 formation are present. However, the data collected here have shown that smokers do not have a statistically significant increase in median plasma Tyr-NO_2 following

NO_3^- rich supplementation. It is possible that other reactions involving NO_2^- or H_2O_2 are more likely, or that the increased levels of MPO do not translate to increased activity of the enzyme. Although, there was an increase in plasma NO_2^- and NO_3^- concentration following NO_3^--rich supplementation the smokers did not have the same level of increase in NO_2^- and NO_3^- as non-smokers (**Figure 4.5**), this may be due to increased levels of thiocyanate in smokers.

Thiocyanate is an anion produced during detoxification of hydrogen cyanide, found in cigarettes, and salivary concentrations of thiocyanate have been used as a marker for smoking frequency/duration (Galanti, 1997; Aggarwal et al, 2013). Thiocyanate and NO_3^- have been shown to have an antagonistic relationship for secretion in saliva (Edwards et al, 1954) that is suspected to be due to both anions competing for the same receptor. This competition would mean higher thiocyanate levels would result in less NO_3^- uptake and a negative correlation for both plasma and salivary thiocyanate with NO_3^- confirm this (**Figure 4.9**).

The values for plasma NO_2^- concentration, in healthy individuals without supplementation, obtained by different studies have varied substantially, e.g. 322 nM (Lauer et al, 2001) and 43 nM (Wylie et al, 2016b). Although there is wide variation, several studies have measured concentrations close to 100 nM (Larsen et al, 2007; Thompson et al, 2015; Wylie et al, 2016a), and the mean concentration within this study, for all participants, was 82 nM. Recorded concentrations of plasma NO_3^- have not varied as greatly, with many in the range of 25-40 µM (Lauer et al, 2001; Larsen et al, 2007; Thompson et al, 2015; Wylie et al, 2016b) and the mean concentration in this study was 30 µM. The variation in NO_2^- concentration but not NO_3^- may be due to the rapid reduction of NO_2^- to NO_3^- by haemoglobin in whole blood (Moshage et al, 1995), meaning that different collection methods may have led to different lengths of exposure of NO_2^- to haemoglobin. Differences in detection method may also influence the results obtained.

Like the plasma, the salivary NO_3^- concentrations were significantly higher in the non-smokers, compared to the smokers (**Figure 4.8B**). However, the salivary NO_2^- concentrations following supplementation did not differ between

participant groups, though both displayed a vast increase from baseline (**Figure 4.8A**). Bojić et al (2004) found that the rate of reduction in the NO_2^-/ NO_3^- ratio, by oral bacteria, decreased with increasing NO_3^- concentration and concluded this could be attributed to enzyme saturation by NO_3^-. Therefore, the extra NO_3^- in the saliva of the non-smokers, compared to the smokers, may make no difference to the NO_2^- levels as the enzyme is already saturated. As there is no statistically significant difference in the salivary NO_2^- concentrations between the groups it would be expected that plasma NO_2^- concentrations would also be comparable, between the two groups. However, as already mentioned, the median plasma NO_2^- concentration was lower in the smokers than the non-smokers (**Figure 4.5A**). This may be due to the large variation observed, for salivary concentrations, as the median, though not significantly lower, is lower for the smokers and a higher participant number may have led to a significant difference in salivary NO_2^- levels between non-smokers and smokers. Alternatively, thiocyanate is a potent catalyst of nitrosation under acidic conditions (Boyland and Walker, 1974; Moriya et al, 2002), therefore, in the smokers, more of the swallowed NO_2^- may be utilised in this reaction decreasing the amount absorbed into the blood. Nitrosation of secondary amines in the diet is considered carcinogenic (Hill et al, 1973; Mirvish, 1995). Therefore, if the increased thiocyanate in smoker's saliva leads to increased nitrosamine formation following NO_3^- rich supplementation, this would have serious health consequences. As mentioned, NO_2^- is rapidly reduced to NO_3^- in whole blood (Moshage et al, 1995) but it is unlikely that this has only been a factor affecting samples from smokers.

There have not been as many studies reporting salivary NO_2^- and NO_3^- concentrations but as with the plasma, there is variation seen. Pannala et al (2003) report salivary NO_2^- levels of 249-483 µM and NO_3^- levels of 204-392 µM in the hours after a low NO_3^- meal. Doel et al (2004) measured children's salivary NO_2^- and NO_3^- levels and found them to be approx. 100 µM and 1,500 µM respectively. Sukuroglu et al (2015) looked at patients with periodontal disease on different treatments and reported salivary NO_2^- and NO_3^- levels of 2.9-7.1 µM and 372-478 µM respectively. The average results of this study were 93 µM NO_2^- and 183 µM NO_3^-. Obvious variances in these studies are participant age and the absence of periodontal disease, and this could account

for some of the discrepancy. Another factor is saliva collection, Doel et al (2004) used swabs, Sukuroglu et al (2015) used Lashley cups (parotid gland saliva) and Pannala et al (2003) and this study collected saliva by direct void into a container over 5 minutes. However, the results here show lower levels of salivary NO_2^- than Pannala et al (2003) (93 µM and 249-483 µM respectively) but the NO_3^- levels are comparable to the lower end of the Pannala et al (2003) studies range (183 µM for this study and 204-392 µM for (Pannala et al, 2003)).

Salivary Tyr-NO_2 levels were also far higher (pmol range) than the levels measured in the plasma (fmol range) despite the lower protein concentration. This may be due to the higher NO_2^- levels in saliva compared to plasma (approx. 1000-fold) as well as peroxidase activity within the saliva. The oral cavity contains MPO, released from leukocytes, and salivary peroxidase, released from the saliva glands (Ihalin et al, 2006). Additionally, any inflammation in the gums (e.g. periodontal disease) will increase MPO activity (Cao and Smith, 1989). Ueshima et al (2007) reported 0.02 ± 0.01 pmol/ml protein-associated Tyr-NO_2 in saliva. This level is roughly a hundred times lower than the average level found here (mean 1.69 pmol/ml for both smokers and non-smokers at baseline). However, there were several methodological differences that make a direct comparison dubious. For instance Ueshima et al (2007) looked solely in COPD patients, who had recently had sputum collected, the samples then underwent extensive sample preparation for measurement by HPLC-electrochemical detection.

There was no difference in salivary nitration between the non-smokers and smokers (Mann-Whitney $p>0.05$, **Figure 4.6**) before or after supplementation. However, following ingestion of NO_3^--rich beetroot juice, both subject groups had decreased salivary Tyr-NO_2 levels; this was only statistically significant in the non-smokers (Freidman test $p<0.05$, **Figure 4.7A**). However, when the placebo group was compared to the supplement group a significant difference was seen in the smokers as well (Dunn's multiple comparison test $p<0.05$, **Figure 4.7B**). A significant change in salivary Tyr-NO_2 between the post-placebo levels and post-supplement levels but not between baseline levels and post-supplement levels is likely due to the placebo samples being less varied than the baseline samples.

The fact that the Tyr-NO_2 levels in the placebo condition (NO_3^--depleted beetroot juice) did not differ from baseline levels of Tyr-NO_2, suggests that it is not components/antioxidants, other than NO_3^-, found in the beetroot juice that are responsible for the Tyr-NO_2 decrease. The reason for the decreased nitration following NO_3^- ingestion is hard to explain; an increase (or no change) was expected. Logically a decrease must be the result of either anti-oxidant activity or decreased inflammation; although increased turn-over of modified proteins is also an option, this seems unlikely.

Ingestion of NO_3^- has been shown to cause an increase in exhaled $^{\bullet}NO$ due to the salivary production of $^{\bullet}NO$ (Zetterquist et al, 1999). It has been hypothesised that salivary production of $^{\bullet}NO$, following ingestion of dietary NO_3^-, protects the oral cavity and gut from infection (Duncan et al, 1995) and Doel et al (2004) have shown that significantly fewer dental caries are observed in those with high salivary NO_3^-. It could, therefore, be hypothesised that the NO_3^--rich supplementation increased salivary $^{\bullet}NO$ production, which has then decreased the number of pathogenic bacteria in the mouth and thus diminished any inflammation and ROS formation e.g. $O_2^{\bullet -}$ and H_2O_2. This, in turn, would mean less Tyr-NO_2 formation as these species are needed alongside the NO_2^- and $^{\bullet}NO$ for nitration to occur.

A correlation of Tyr-NO_2 levels with thiocyanate concentrations (Spearman $p<0.01$) was seen when all groups/conditions were combined (**Figure 4.11**). Thiocyanate has been shown to decrease the antimicrobial activity of MPO (Ihalin et al, 1998). This lends support to the suggestion that Tyr-NO_2 levels are connected to oral pathogenic bacteria levels and the associated inflammation. Further studies are needed, investigating MPO levels/activity in the saliva, along with other inflammatory markers, to see if they are indeed affected by a week of high NO_3^- ingestion.

4.5. Conclusion

Ingestion of a NO_3^--rich supplementation resulted in a significant increase in plasma and saliva NO_2^- and NO_3^- concentration for both groups. However, after supplementation, there was a difference between non-smokers and smokers for plasma NO_2^- and NO_3^- and saliva NO_3^-, where the smokers were found to have significantly lower concentrations of each. This is thought to be due to the higher levels of thiocyanate in the smokers, which can compete with the NO_3^- anion for secretion in the saliva.

The levels of Tyr-NO_2 in healthy plasma were near the limit of quantification and appear to be unaffected by high NO_3^- ingestion, regardless of whether the participant was a smoker or non-smoker. Salivary Tyr-NO_2 levels are far higher than plasma levels and were unexpectedly seen to decrease with NO_3^- ingestion in smokers. The reason for this is unknown but may be due to increased $^{\bullet}NO$ production protecting the oral cavity from pathogens and reducing inflammation. The fact that there is no increase in plasma Tyr-NO_2 and a decrease in saliva Tyr-NO_2 suggests that NO_3^--rich supplementation, in smokers, does not risk an increase in potentially auto-immune PTMs of self-proteins.

4.6. Acknowledgements

This study was carried out in collaboration with Dr Stephen Bailey (University of Exeter, Sport and Health Science), who designed the nitrate supplementation study and collected the samples.

Chapter 5
A time-course study of serum 3-nitrotyrosine levels before and after surgery, comparing patients who developed sepsis with those who did not

5.1. Introduction

Oxidative stress has been implicated in sepsis; examples of ROS/RNS-induced processes in sepsis are lipid peroxidation, mitochondrial damage and cytotoxicity (Victor et al, 2004). It has been hypothesised that this damage is a contributing factor in the organ dysfunction seen in severe sepsis (see Chapter 1, section 1.5.4 for definition) (Victor et al, 2004; Castellheim et al, 2009). ˙NO is thought to play a role in the hypotension observed in septic shock and preclinical studies have been performed using non-specific NOS inhibitors (i.e. they don't target a specific isoform). For example, a randomised, double blind, placebo controlled study examining the effects of NG monomethyl-L-arginine (*L*-NMMA) in humans with septic shock found that *L*-NMMA improved the blood pressure of the patients (Petros et al, 1994). However, they also noted a fall in cardiac output that needed to be investigated in larger studies. A randomized, double-blind, placebo-controlled multicentre study using the inhibitor NG-methyl-L-arginine hydrochloride also found blood pressure was improved by non-selective NOS inhibition (Watson et al, 2004). However, large clinical trials were abandoned due to an increase in mortality in those receiving the drug, possibly as a result of decreased cardiac output (López et al, 2004). Although lower concentrations of the inhibitor did show an improvement in mortality rates the study of NOS inhibitors in sepsis has decreased since the large clinical trials were abandoned. Inhibitors that selectively target iNOS have shown encouraging results in animal models of sepsis/septic shock (Kadoi and Goto, 2004; Stahl et al, 2010; Su et al, 2010) but, as far as we are aware, this has not yet been investigated in humans with septic shock.

As previously described (see Chapter 1, section 1.5.), ˙NO undergoes a radical-radical reaction with $O_2^{\bullet -}$ to form the ROS, peroxynitrite ($ONOO^-$). $ONOO^-$ can modify several molecules (e.g. DNA, lipids, enzymes, etc.). An example is manganese SOD: nitration of this mitochondrial enzyme causes a loss of function, leading to accumulation of $O_2^{\bullet -}$ in mitochondria (Salvemini and Cuzzocrea, 2002). As $O_2^{\bullet -}$ is not effectively removed this nitration leads to

increased formation of $ONOO^-$ and further oxidative modifications (Salvemini and Cuzzocrea, 2002). Since mitochondrial dysfunction may be a significant contributor to organ dysfunction (Castellheim et al, 2009), we suggest that reactive oxygen species, like $ONOO^-$, are a factor in sepsis. We also postulated that – whilst therapies directed towards the prevention of nitrative stress might be difficult to implement in clinical practice – there could be scope for using measures of nitrative stress, such as Tyr-NO_2, in the diagnosis and/or monitoring of sepsis. For example, some researchers have suggested that the concentration of free Tyr-NO_2 in plasma is associated with sepsis prognosis (Ohya et al, 2002). As nitration is a rapid chemical reaction which modifies proteins that are already present, nitrated Tyr may also represent a marker that is measurable in the plasma long before other currently-used inflammatory markers, such as CRP, which must be synthesised by hepatocytes in response to inflammatory signals. As discussed in Chapter 1 (section 1.5.4), sepsis is associated with a high mortality rate and improved/quicker diagnosis is needed in order to improve therapeutic efficiency.

Surgery is a risk factor for septicaemia. In the USA, post-surgery sepsis made up 30% of all sepsis patients (Vogel et al, 2009). As part of a collaborative project with the Defence Science and Technology Laboratory (DSTL), serum samples from a cohort of 51 patients, 26 of whom developed post-surgery sepsis, were analysed using the new ECL ELISA (as described in Chapter 3). The aim of this study was (a) to determine if protein-associated Tyr-NO_2 was increased in patients with post-surgery sepsis, compared with patients without post-surgery sepsis and (b) to determine whether measurement of Tyr-NO_2 is a useful addition to the existing set of diagnostic tests and clinical measurements currently used to establish the diagnosis of sepsis.

5.2. Materials and Methods

5.2.1. Sample details

Serum samples were provided by DSTL as 100 µl aliquots. The samples were collected as part of a study approved by the NRES Committee South Central (REC ref 06/Q1702/152) and informed consent to take part in the study was obtained from each individual.

Serum was collected prior to major elective surgery and then each day subsequently until whichever of the following occurred first:

i. Hospital discharge
ii. Seven days post-surgery
iii. Sepsis diagnosis

Where available, patient blood test results (e.g. white blood cell count) were also provided by DSTL. Information on patient group, age and gender are detailed in **Table 5.1**.

Table 5.1: Patient information

	No post-surgery sepsis	**Post-surgery sepsis**
Age in years (mean ± SD)	65 ± 8.6	64 ± 10.1
Gender	12 female, 13 male	10 female, 16 male

Samples from 51 patients (each with one pre-surgery and at least one post-surgery sample) were analysed. The patients were split into two groups: those with no post-surgery sepsis, i.e. controls, and those with post-surgery sepsis.

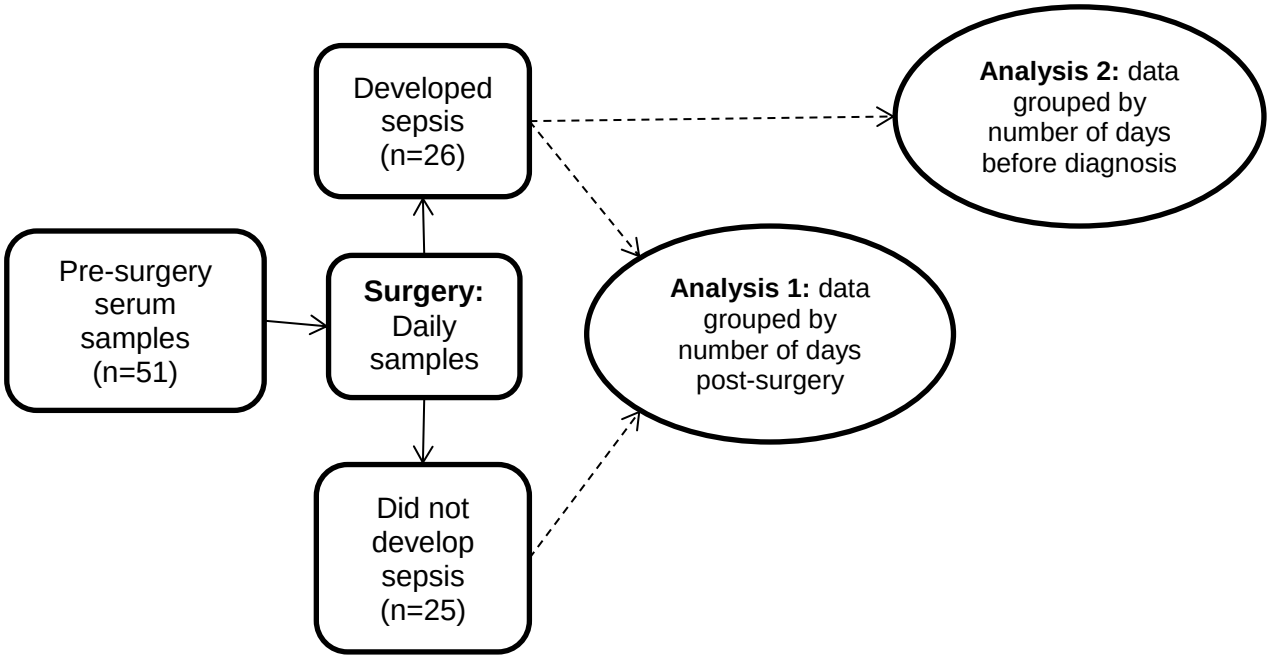

Figure 5.1: Serum samples, grouping and analysis

Those patients who developed sepsis were diagnosed at different time-points post-surgery, e.g. some were diagnosed two days after surgery, and others were diagnosed five days after surgery (**Table 5.2**). Therefore, during statistical analysis samples were either grouped in terms of 'days post-surgery' or 'days prior to diagnosis'. For analysis 2 (**Figure 5.1**), samples were matched with control samples which were at the same time point in terms of the number of days since surgery.

Table 5.2: Post-surgery sepsis patient's diagnosis time points.

The delay between surgery and sepsis diagnosis was variable and is summarised in the table.

Days post-surgery that sepsis diagnosis occurred	2	3	4	5	6	7	8
Number of patients diagnosed on this day	7	5	4	3	2	4	1

5.2.2. Electrochemiluminescence-based ELISA for 3-nitrotyrosine

The Tyr-NO_2 content was determined by the ECL ELISA (described in Chapter 3, section 3.2.5). Samples were diluted 1 in 5 and measured in quadruplicate. The protein content was measured using the BCA assay (Chapter 2, section 2.2) and the Tyr-NO_2 levels adjusted to give values expressed as fmol BSA-NO_2 equivalents/mg protein.

5.2.3. Mass spectrometry

A subgroup of 10 samples was analysed by mass spectrometry (ESI-QUAD-TOF-MS/MS). Mass spectrometry is the gold standard measurement for Tyr-NO_2. Therefore, we wished to compare the ECL ELISA with mass spectrometry to assess whether the two results were in agreement. The samples selected were from both sepsis and control patients with pre-surgery and post-surgery time points.

In-solution digestion was performed (detailed in the following sections) to prepare these samples for mass spectrometry analysis. All incubations were at room temperature unless otherwise stated.

5.2.3.1. Materials

Along with the reagents detailed in Chapter 2 (section 2.1), the following were used for preparation of the samples for mass spectrometry.

Acetonitrile and iodoacetamide were from Sigma Aldrich (Gillingham, UK). Methanol (analytical reagent grade), acetic acid (1M lab solution), acetone (99+%, extra pure) and formic acid 99% were from Fisher Scientific (Loughborough, UK). Rapigest was purchased from Waters (Hertfordshire, UK). Trypsin Gold was from Promega (Southampton, UK).

5.2.3.2. Protein precipitation

Serum (10 µl) was mixed with ice cold acetone (40 µl), briefly vortexed and then incubated for an hour (-20°C). The solution was then spun at 14,000 *g* (10 minutes) to pellet the precipitated protein. The supernatant was discarded and remaining acetone was left to evaporate from the uncapped tube.

5.2.3.3. Preparation for digestion

The protein pellet was then suspended in 50 mM Tris, 0.1% Rapigest, pH 8.4 (100 µl). The pellet was fully re-suspended and the pH checked (via pH paper). Tris (5 µl, 50 mM), containing 194 mM DTT, (pH 8.4) was then added before vortexing the samples and incubating (1 hour). After this, 20 µl of 50 mM Tris, containing 184 mM iodoacetamide (pH 8.4), was added and the samples were mixed gently before incubation for 1 hour in the dark. Tris (20µl, 50 mM), containing 194 mM DTT, pH 8.4 was then added and the samples were again incubated for 1 hour.

Samples were then diluted to approx. 50 µg in 100 µl of 50 mM Tris pH 8.4, followed by the addition of 2.5 µl of trypsin (reconstituted in 50 mM acetic acid) to achieve a ratio of 1:20 (trypsin: protein). This mixture was then incubated at 37°C (24 hours) to digest.

After digestion samples underwent centrifugal evaporation (Jouan RC 10.22) until dried. The dry samples were then stored at -20°C until analysis.

Prior to mass spectrometry analysis samples were suspended in 25µl of eluent A (98% acetonitrile and 0.1% formic acid).

Mass spectrometry was carried out according to the protocol in Chapter 2, section 2.6. Analysis of the data was performed using Progenesis QI (Nonlinear Dynamics, Newcastle upon Tyne, UK), Mascot Daemon statistical software v2.3.2 (Matrix Science, London, UK) and Peak View v1.0 (AB SCIEX, Cheshire, UK).

Progenesis QI was used to compare samples by aligning the total ion chromatograms, to compensate for the between-run variation, and quantified relative abundance of the peptides (including sequences suspected to be nitrated). The software also accessed online databases (i.e. Swiss-Prot (Consortium, 2015)) to identify the proteins in the sample. A report was then produced detailing the relative abundance of each protein with a statistical analysis comparing the different time points for each sample.

Mascot Daemon (MatrixScience, 2014) was also used to search Swiss-Prot for protein identifications. However, this software can only be used to analyse one

sample in isolation, rather than comparing peptides across samples. This software provided data on the ion score (score of how reliable the data is), nitrated peptides and retention time. This data was then used to look at extracted ion chromatograms and spectra, for *de novo* sequencing, using the Peak View (ABSCIEX) software.

5.2.4. Serum CRP measurement

CRP was measured by an immunoturbidimetric assay, as described in Chapter 3, section 3.2.6.

5.2.5. Statistical analysis

Normality of the data was tested using the Shapiro-Wilk test and determined to be non-parametric ($p<0.01$). Therefore, the Mann-Whitney test, Wilcoxon matched pairs and Spearman rank correlation tests were chosen for comparison of the data sets.

A Receiver Operating Characteristic (ROC) analysis allowed calculations of the area under the curve (AUC). Sensitivity/specificity of the data sets was also determined.

5.3. Results

5.3.1. Increased serum Tyr-NO_2 post-surgery

Figure 5.2 shows that the median levels of serum Tyr-NO_2 were increased following major elective surgery, compared to pre-surgery levels (median (IQR): pre-surgery 1.74 (0.59 – 4.79) and post-surgery 3.00 (1.01 – 7.15) fmol BSA-NO_2 equiv./mg protein. Wilcoxon matched pairs p=0.007). This supports results previously reported (Chapter 3, section 3.3). The sepsis and non-sepsis groups were combined for the analysis shown in **Figure 5.2**.

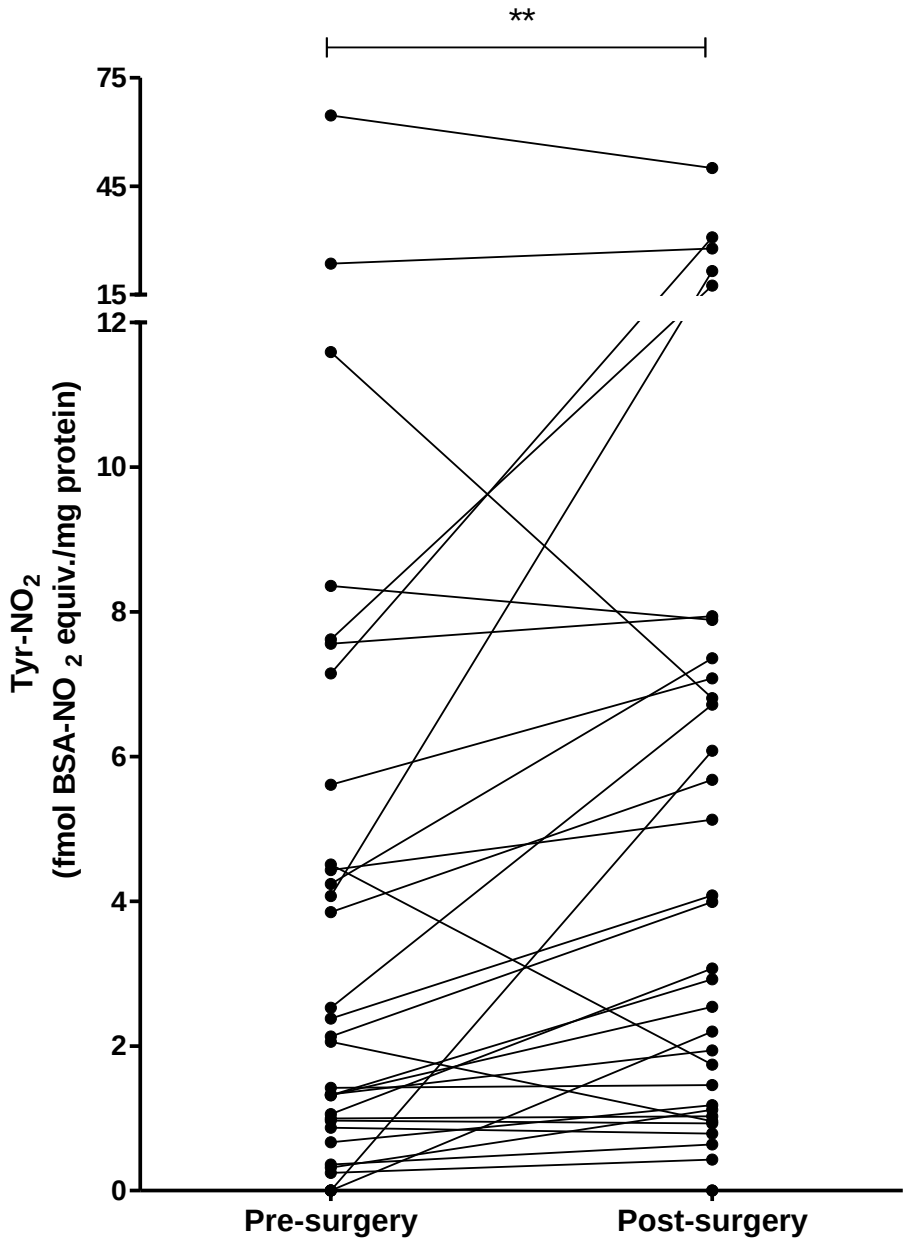

Figure 5.2: Pre- and one day post-surgery serum levels of 3-nitrotyrosine

Tyr-NO_2 was measured as described in Chapter 3, section 3.2.5.The figure represents the combined data from both sepsis patients and control patients (n=34). The median and inter-quartile range (IQR) values are shown. A significant increase in median Tyr-NO_2 levels was observed 24 hours post-surgery (Wilcoxon matched pairs, **p=0.005).

5.3.2. Changes in serum Tyr-NO_2 over time

When comparing all time points (**Figure 5.3**) there were no statistically significant differences in the median levels of serum Tyr-NO_2 over the time course for either group (Kruskal-Wallis $p>0.05$). The median serum Tyr-NO_2 levels were generally higher in those patients who went on to develop sepsis, than in those patients who did not develop sepsis, but this did not reach significance (Mann-Whitney, $p>0.05$). Sepsis patients peaked at day 5 post-surgery (5.46 fmol BSA-NO_2 equiv./mg protein) compared to the non-sepsis control group which peaked at day 1 post-surgery (2.37 fmol BSA-NO_2 equiv./mg protein).

The time course was also plotted in terms of days prior to diagnosis (**Figure 5.4**), with controls matched according to the number of days post-surgery that the sepsis patients had reached when diagnosis occurred. The post-surgery sepsis group had an increase in median serum Tyr-NO_2 prior to diagnosis, compared to pre-surgery levels, with the peak occurring one day prior to diagnosis (**Figure 5.4B**). However, there was no statistically significant difference between the time points (Kruskal-Wallis $p=0.29$). The matched controls also had an increase in median serum Tyr-NO_2 levels but this peaked in those matched for 3 days before diagnosis, i.e. closer to the surgery (**Figure 5.4A**). The levels of serum Tyr-NO_2 were significantly higher in the sepsis group one day before diagnosis; median values of 4.5 and 1.2 fmol BSA-NO2 equiv./mg protein for sepsis and controls respectively (Mann-Whitney, $p=0.04$).

Individual Tyr-NO_2 level time courses, for each patient, can be seen in appendix 1.

Serum Tyr-NO_2 levels pre-surgery and pre-diagnosis were analysed further in the following sections, with a comparison to CRP concentrations.

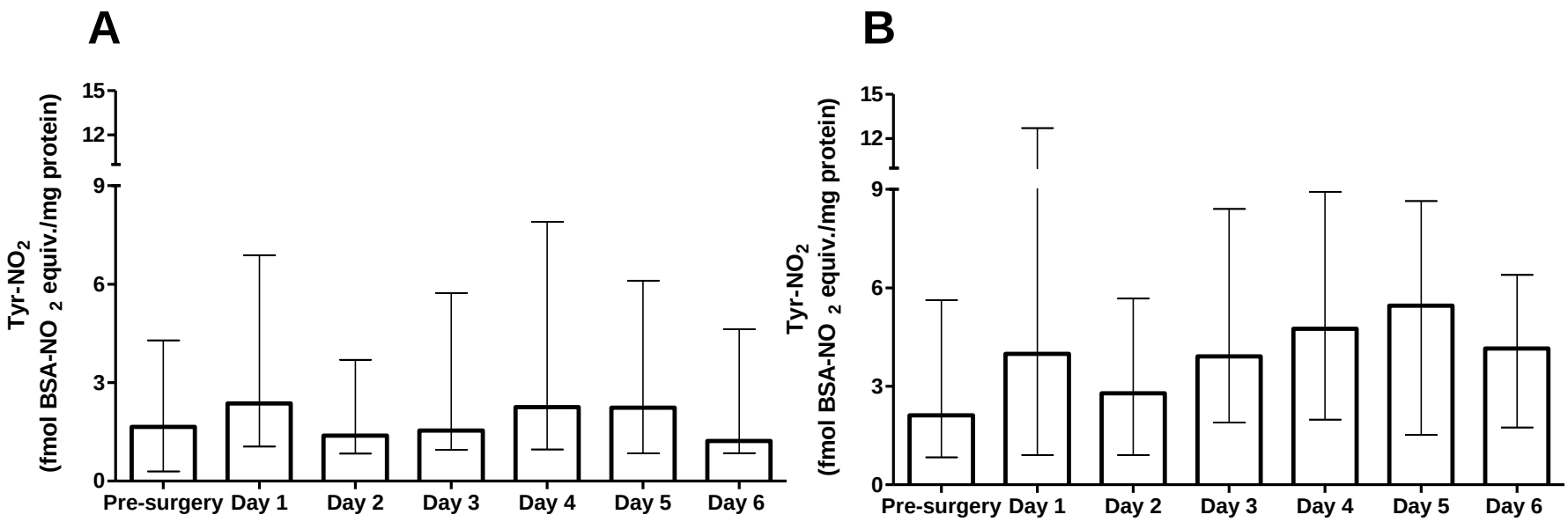

Figure 5.3: Post-surgery time course of serum of 3-nitrotyrosine in patients with and without post-surgery sepsis

Tyr-NO_2 was measured by the protocol described in Chapter 3, section 3.2.5. The median and IQR values are shown for each day in the two groups. (A) In the case of patients who did not develop post-surgery sepsis (n=25), there was no statistically significant difference between the median values of each time point (Kruskal Wallis p=0.77). Tyr-NO_2 levels peaked at one day post-surgery. (B) In the case of patients who developed post-surgery sepsis (n=26), there was no statistically significant difference between the median values of each time point (Kruskal Wallis p=0.50). Tyr-NO_2 levels peaked at day five post-surgery.

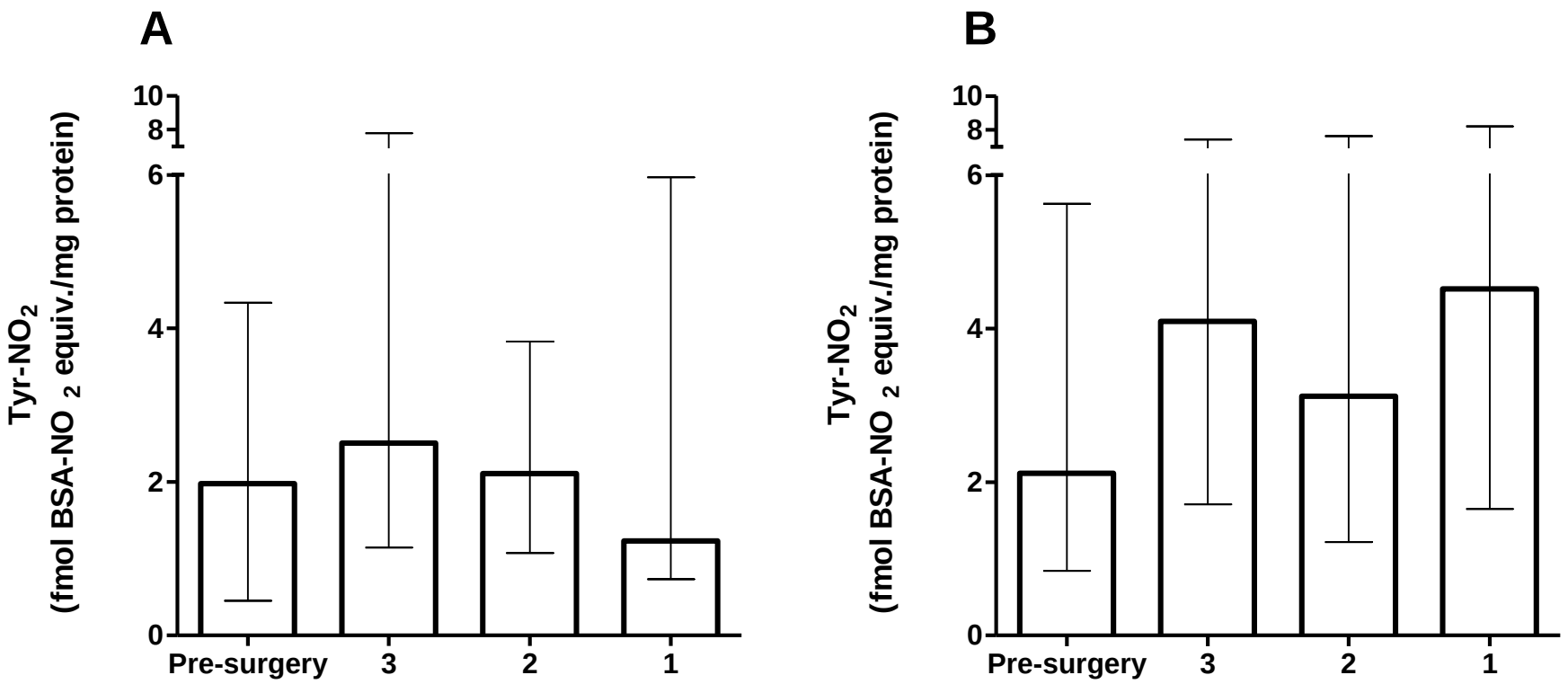

Figure 5.4: Pre-diagnosis time course for serum 3-nitrotyrosine in those patients with post-surgery sepsis and their matched controls

Tyr-NO_2 was measured by the protocol described in Chapter 3, section 3.2.5. The median and IQR values are shown for each day in the two groups. The patients who did not develop sepsis (controls) were matched according to the number of days post-surgery the sepsis patients had reached when diagnosis occurred. (A) No post-surgery sepsis (Kruskal Wallis p=0.67) and (B) Post-surgery sepsis (Kruskal Wallis p=0.29).

To compensate for the variation in total levels and individual differences the absolute change and percentage change were also analysed. The absolute change in serum Tyr-NO_2 from pre-surgery to the day before diagnosis was determined to be non-significant (**Figure 5.5A**). Absolute change median (IQR): control patients without post-surgery sepsis 0.66 (-0.01 – 1.45) and post -surgery sepsis patients 1.91 (0.02 – 3.55) fmol BSA-NO_2 equiv./mg protein (Mann-Whitney p=0.06). Percentage change was also non-significant, control patients without post-surgery sepsis 24.3% (-5.5 – 39.1) and post -surgery sepsis patients 49.7% (0 – 200) increase (Mann-Whitney p=0.17, **Figure 5.5B**).

As all groups were expected to have an increase in Tyr-NO_2 following surgery, due to the ensuing tissue damage, the serum Tyr-NO_2 from day one post-surgery to the day before diagnosis was also determined (**Figure 5.6**). When assessing absolute change the control patients (no post-surgery sepsis) showed a decrease in median Tyr-NO_2 levels and the post-surgery sepsis patients an increase in median, but this did not reach significance: median change (IQR) -0.6 (-2.4 – -0.1) and 0.1 (-0.2 – 6.1) fmol BSA-NO_2 equiv./mg protein change in Tyr-NO_2, for control and sepsis patients respectively (Mann-Whitney, p=0.052).However, percentage change in Tyr-NO_2 levels, over this time period, was statistically significant: median (IQR) -27.2% (-59.5 - -9.0) and 1.4% (-7.8 – 210) for control patients and post-surgery sepsis patients respectively (Mann-Whitney, p= 0.02).

The highest serum Tyr-NO_2 levels, for all post-surgery time points, for control patients (no post-surgery sepsis) and post-surgery sepsis patients were 21.59 and 64.60 fmol BSA-NO_2 equiv./mg protein respectively. The median peak levels were 2.2 (1.1 – 7.2) and 6.1 (2.4 – 11.2) fmol BSA-NO_2 equiv./mg protein for control and sepsis patients respectively, these medians were not significantly different (Mann-Whitney, p = 0.086).

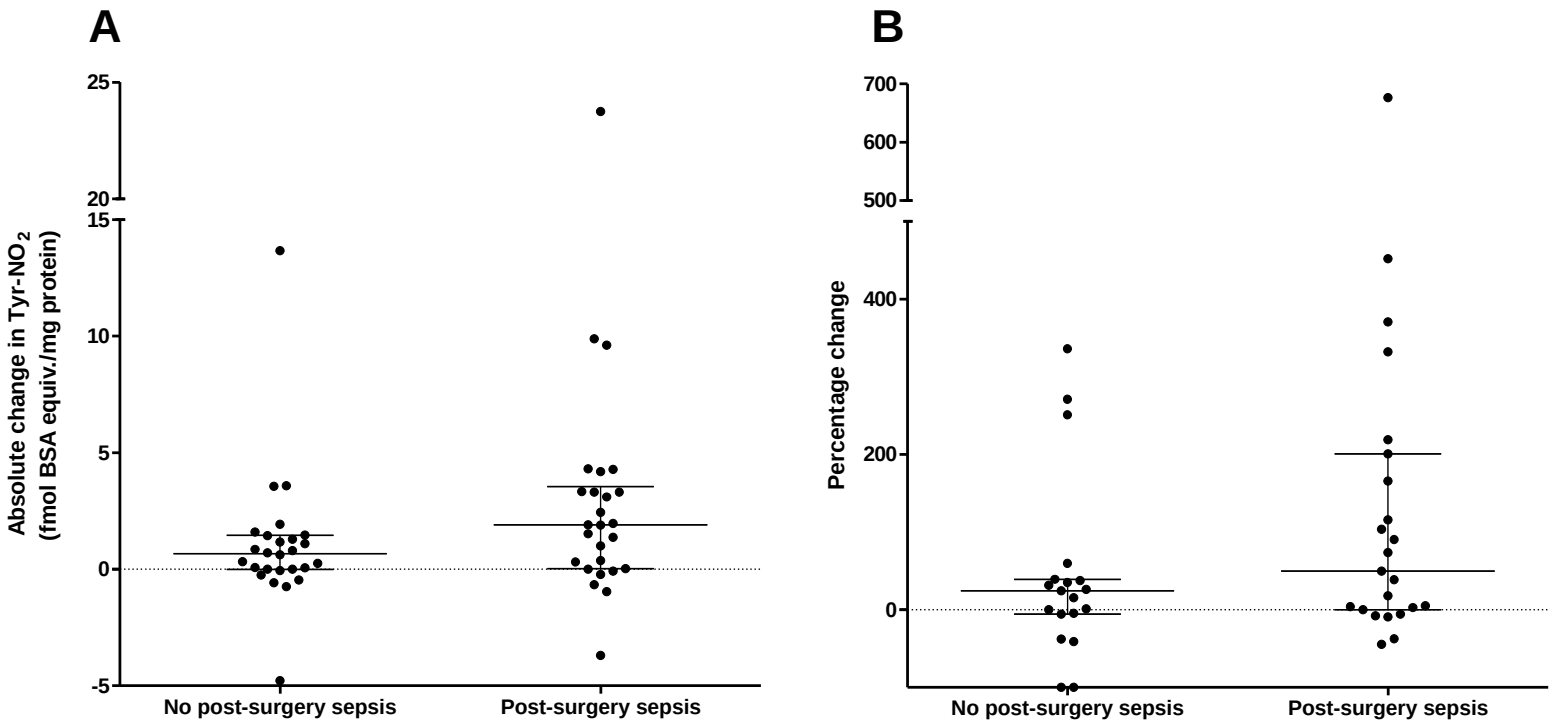

Figure 5.5: Absolute and percentage change in serum 3-nitrotyrosine from pre-surgery levels to one day before diagnosis

Tyr-NO_2 was measured by the protocol described in Chapter 3, section 3.2.5. The patients who did not develop sepsis (control group) were matched to sepsis patients by the number of days post-surgery the sepsis patients were when diagnosed. The median and IQR values are shown. (A) Those that developed sepsis (n=26) did show a higher absolute median increase compared to those that did not (n=26), however this was not statistically significant (Mann Whitney, p=0.06). (B) The percentage increase from pre-surgery levels was not statistically higher in the post-surgery sepsis (n=23) group compared to the control group (n=19) group (Mann Whitney, p=0.17).

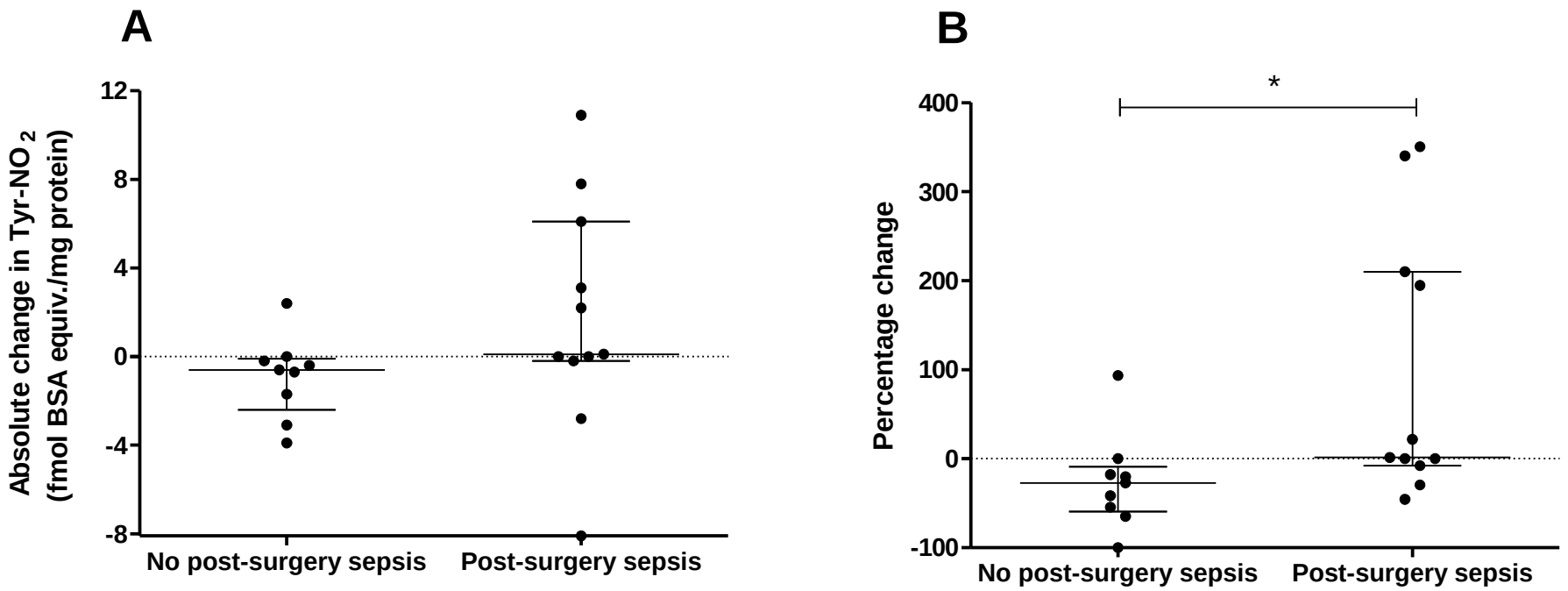

Figure 5.6: Absolute and percentage change in serum 3-nitrotyrosine from day one post-surgery levels to one day before diagnosis

Tyr-NO_2 was measured by the protocol described in Chapter 3, section 3.2.5. The patients who did not develop sepsis (control group) were matched to sepsis patients by the number of days post-surgery the sepsis patients were when diagnosed. The median and IQR values are shown. (A) The post-surgery sepsis group (n=11) show a median increase in serum Tyr-NO_2 levels and the control group (n=9) a median decrease, but this was not statistically significant (Mann Whitney, p=0.052). (B) The percentage change over this time was statistically significant (Mann Whitney, *p=0.02).

5.3.3. Serum 3-nitrotyrosine levels and CRP concentrations pre-surgery

There was no statistically significant difference in the pre-surgery serum Tyr-NO_2 levels when comparing patients who went on to develop sepsis with those who did not (**Figure 5.7**, Mann-Whitney p=0.53). The median (IQR) values were 1.66 (0.3-4.3) and 2.33 (0.9-5.1) fmol BSA-NO_2 equiv./mg protein for the control and sepsis group respectively. Two patients in the sepsis group had very high levels of pre-surgery serum Tyr-NO_2 (64.6 and 23.6 fmol BSA-NO_2 equiv./mg protein); both these patients had a gastrectomy, one patient died from sepsis, whilst the outcome of the second is unknown.

In the present study, serum CRP (mg/L) levels were above the reported normal value of 0.8 mg/L (0.3-1.7) (median and IQR) (Povoa, 2002) prior to surgery. In our study, the serum CRP concentration measured in patients was: 5.00 (1.00-14.00) mg/L. Additionally, the median levels of CRP pre-surgery in the sepsis group were significantly higher than in the non-sepsis (control) group: 8.5 and 2 mg/L respectively (**Figure 5.8A**, Mann-Whitney p = 0.013).

A ROC analysis of pre-surgery serum CRP (mg/L) gave an AUC of 0.7 (**Figure 5.8B**). The individuals mentioned above (in **Figure 5.7**), with high serum Tyr-NO_2 levels, were not amongst those with exceptionally high serum CRP concentrations (12 and 3 mg/L) and at the optimal cut-off (>6.5mg/L, 57.7% sensitivity and 60.8 % specificity) CRP levels would only have detected one of these patients. When serum CRP was adjusted for serum protein (i.e. mg CRP/mg protein x 10^5) values were still significantly different but the p value was increased and the AUC was decreased (Mann-Whitney p=0.047, AUC = 0.66, **Figure 5.9**).

Pre-surgery Tyr-NO_2 levels did not correlate with age or differ between genders. There was a positive correlation between Tyr-NO_2 and CRP (mg/mg protein x 10^5) (r=0.22, p=0.003) when all data points were pooled into one group. When data were separated into patients who developed sepsis and patients who did not, there was no correlation between pre-surgery Tyr-NO_2 and pre-surgery CRP, in either group.

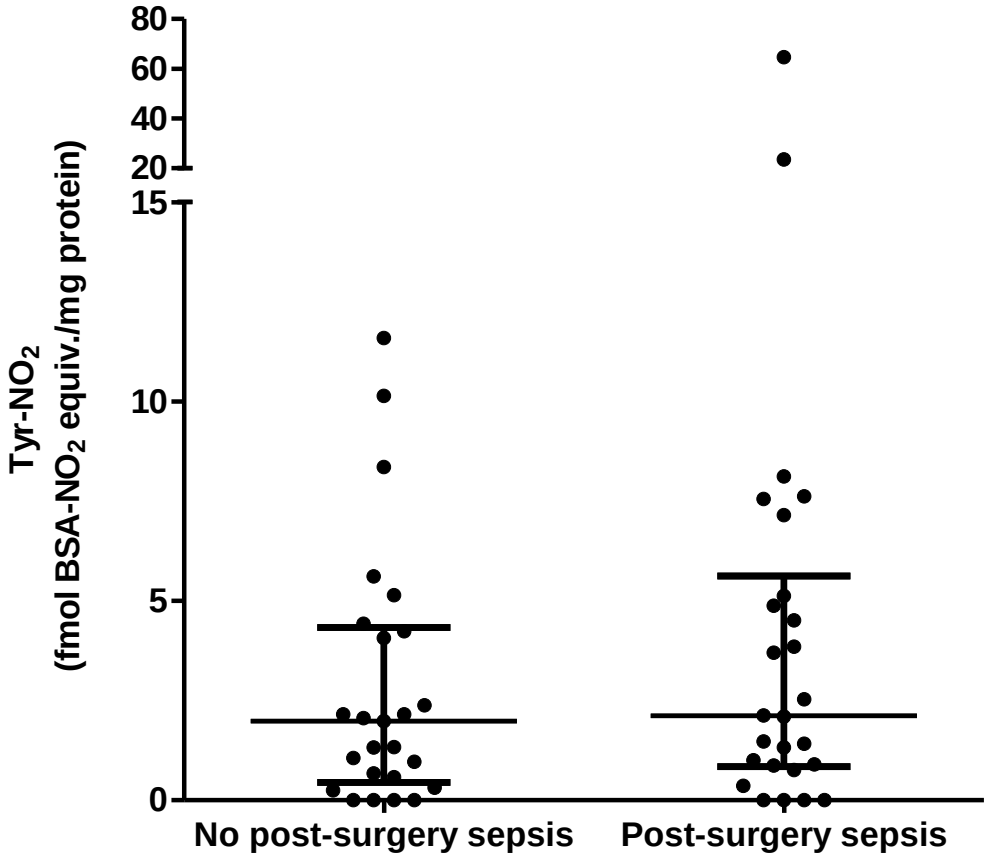

Figure 5.7: Pre-surgery 3-nitrotyrosine levels in patients with and without a diagnosis of post-surgery sepsis

Tyr-NO_2 was measured as described in Chapter 3, section 3.2.5.The median and IQR values are shown. There was no statistically significant difference between the median serum Tyr-NO_2 levels in patients without a post-surgery sepsis diagnosis (n=25) and the median serum Tyr-NO_2 levels of patients with a post-surgery sepsis diagnosis (n=26) (Mann-Whitney, p=0.53).

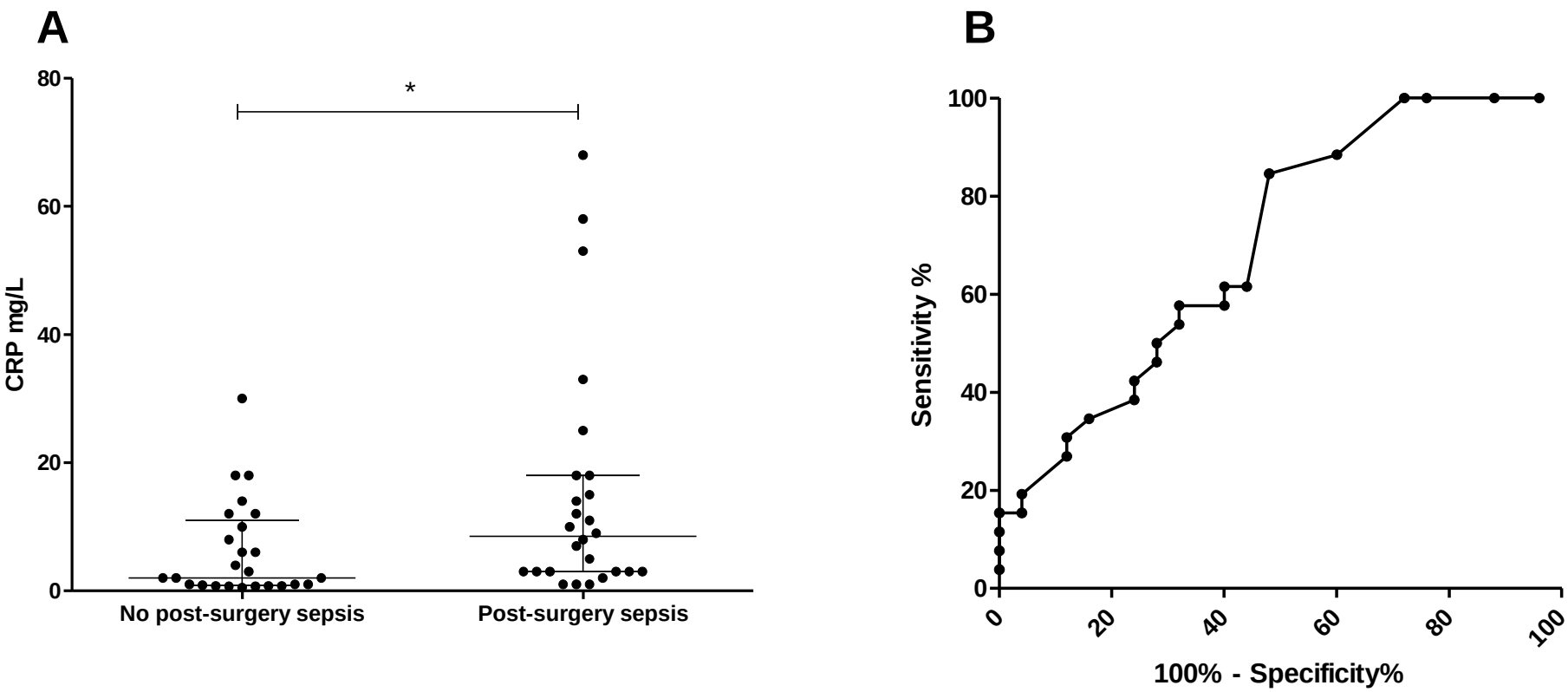

Figure 5.8: Pre-surgery CRP (mg/L) concentration in patients without, and patients with, a post-surgery sepsis diagnosis and ROC analysis

CRP was measured by the protocol described in Chapter 3, section 3.2.6. (A) The median and IQR values are shown. The median pre-surgery level of CRP was significantly higher in patients who developed post-surgery sepsis (n=26) compared to the median pre-surgery level of CRP in those who did not (n=25) (Mann-Whitney, *p=0.01). (B) ROC analysis of pre-surgery CRP levels (AUC=0.7).

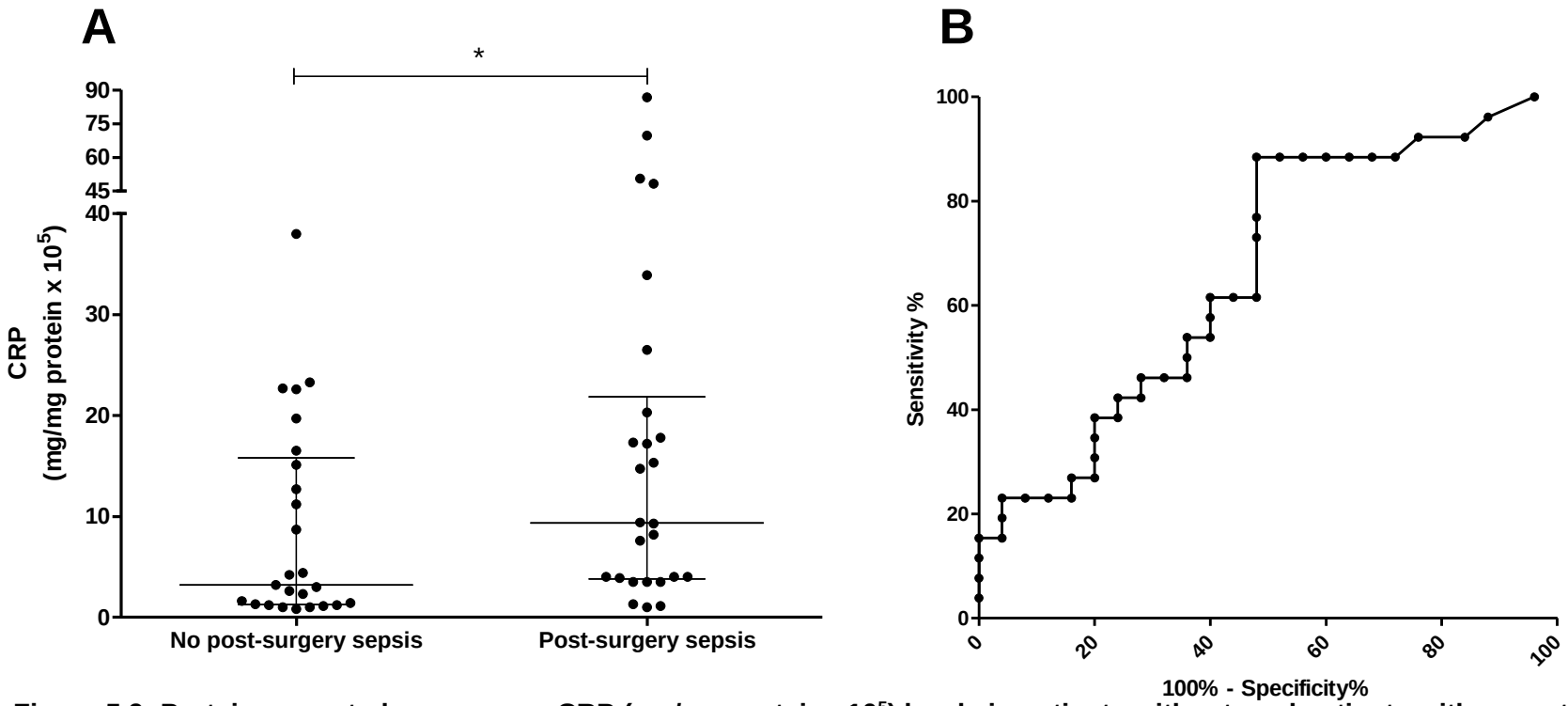

Figure 5.9: Protein corrected pre-surgery CRP (mg/mg protein x10^5) levels in patients without, and patients with, a post-surgery sepsis diagnosis and ROC analysis

CRP was measured by the protocol described in Chapter 3, section 3.2.6 and adjusted for total serum protein concentration. (A) The median and IQR values are shown. The median pre-surgery levels of CRP was significantly higher in patients who developed post-surgery sepsis (n=26) compared to the median pre-surgery level of CRP in those who did not (n=25) (Mann-Whitney, *p=0.047). (B) ROC analysis of pre-surgery CRP levels (AUC=0.66).

5.3.4. Serum Tyr-NO_2 levels and CRP concentrations prior to diagnosis

One day prior to diagnosis:

Median serum Tyr-NO_2 levels showed a statistically significant increase in the post-surgery sepsis group, one day prior to diagnosis, compared to the non-sepsis control group (matched by the number of days post-surgery sepsis patients were when diagnosed), with median values of 4.5 and 1.2 fmol BSA-NO_2 equiv./mg protein, respectively (**Figure 5.10A**, Mann-Whitney p=0.02). ROC analysis of Tyr-NO_2 levels one day prior to diagnosis produced an AUC of 0.69 and a p-value of 0.027 (**Figure 5.10B**). A cut-off value of ≥1.935 fmol BSA-NO_2 equiv./mg protein gave a sensitivity of 79.2% and a specificity of 58.3%. When this cut-off was used the assay was able to predict 19/25 sepsis cases that were later diagnosed clinically. When assessing both false negative and false positive results, Tyr-NO_2 had an accuracy of 70%.

Serum CRP (mg/L) was also significantly higher in the sepsis group one day prior to diagnosis (**Figure 5.11A**, Mann-Whitney, p<0.0001) and gave an AUC of 0.89 and p-value <0.0001 (**Figure 5.11B**). At the optimal cut-off (>109.5 mg/L) only three sepsis patients would fail to be diagnosed (87.5% sensitivity and 88.5% specificity). The overall predictive accuracy (i.e. the percentage that were neither false negative or false positive) was 88%.

When adjusted for serum protein concentration (CRP mg/mg protein x 10^5) the AUC was increased to 0.9 (a cut-off >168.4 CRP mg/mg protein x 10^5 gave 95.8% sensitivity and 62.6% specificity), and 1/25 sepsis patients would have been a false negative (overall accuracy 92%).

Two days prior to diagnosis:

Two days prior to diagnosis Tyr-NO_2 serum levels did not show a statistically significant increase in the sepsis group compared to the non-septic control patient group: the median (IQR) values in the two groups were 3.12 (1.22–7.64) and 2.17 (0.85 – 3.58) fmol BSA-NO_2 equiv./mg protein respectively (Mann-Whitney, p=0.21) (**Figure 5.12A**). However, median CRP concentrations were still significantly higher in the sepsis group compared to the non-sepsis control patient group: median (IQR) 347.2 (202.9 – 411.9) and 90.9 (53.8 – 215.4) mg CRP/mg protein x10^5 respectively (Mann-Whitney, p=0.0007) (**Figure 5.12B**).

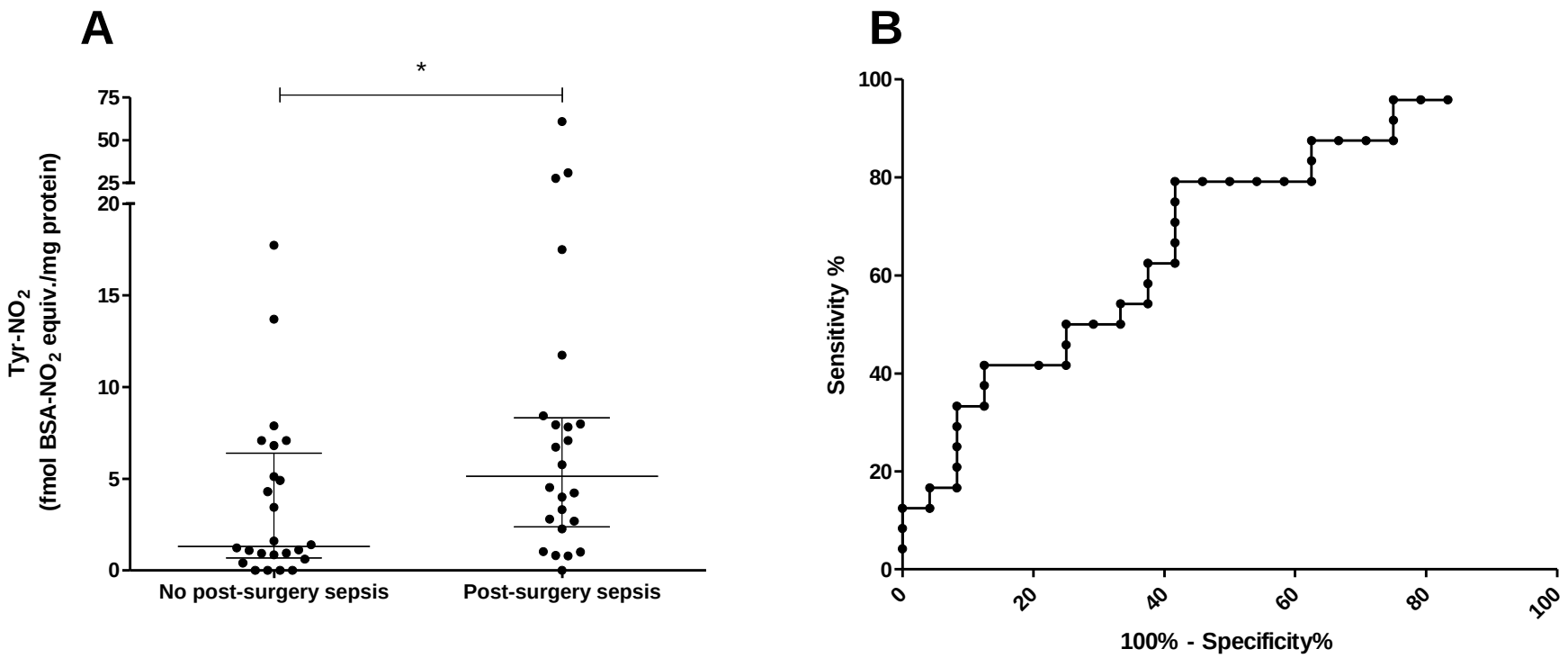

Figure 5.10: Predictive ability of serum 3-nitrotyrosine levels to detect sepsis, one day prior to sepsis diagnosis

Tyr-NO_2 was measured by the protocol described in Chapter 3, section 3.2.5. Patients who did not develop sepsis (control group) were matched to sepsis patients by the number of days post-surgery the sepsis patients were when diagnosed. (A) The median and IQR values are shown. Median nitration levels were significantly higher in the patients who developed post-surgery sepsis (n= 24) compared to those who did not (n=24) (Mann-Whitney, *p=0.02). (B) ROC analysis of Tyr-NO_2 levels one day prior to diagnosis (AUC=0.69).

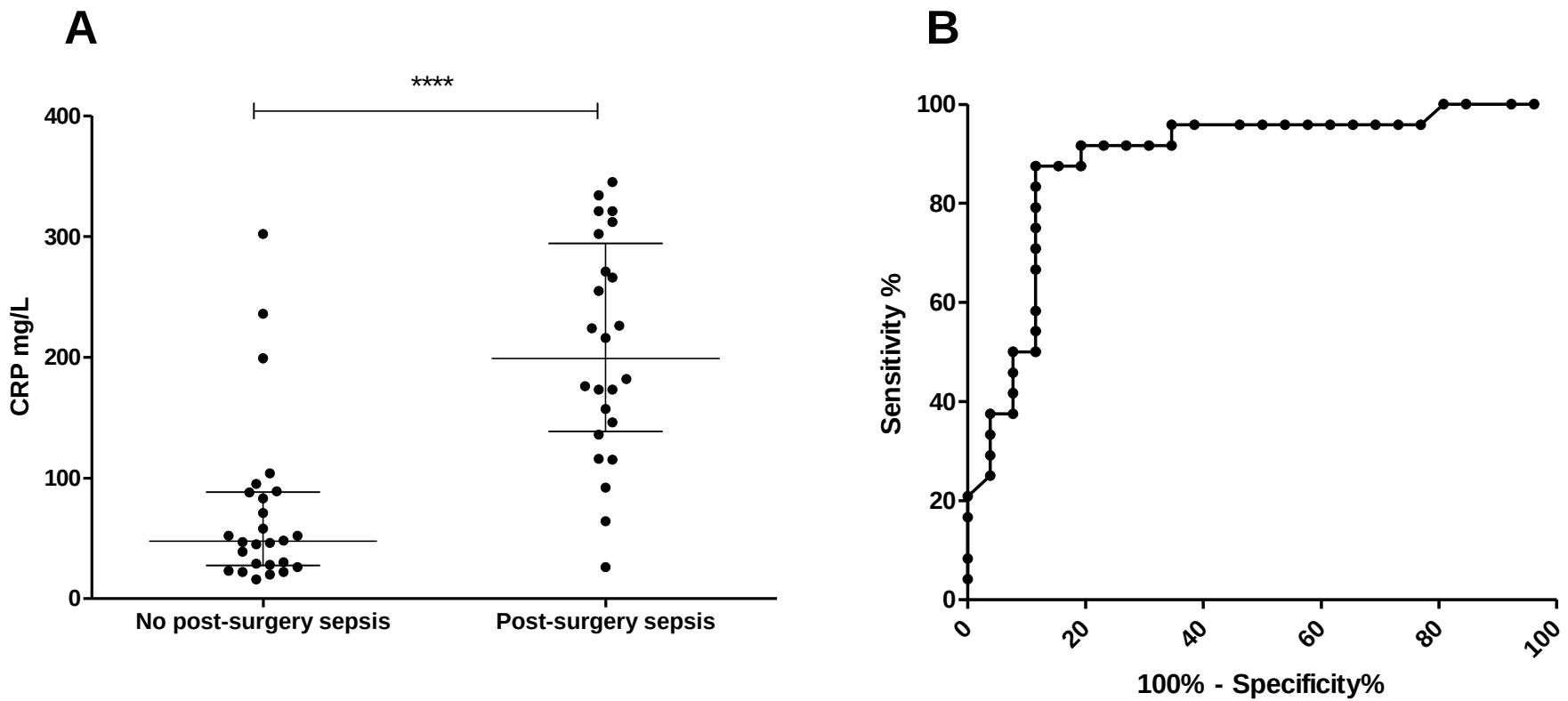

Figure 5.11: Predictive ability of serum CRP concentrations to detect sepsis, one day prior to diagnosis

CRP was measured by the protocol described in Chapter 3, section 3.2.6. The patients who did not develop sepsis (control group) were matched to the sepsis patients by the number of post-surgery the sepsis patients were when diagnosed. (A) The median and IQR values are shown. Serum CRP concentrations were significantly higher in the sepsis group (n=24) compared to the control group (n=25) (Mann-Whitney, ****p<0.0001). (B) ROC analysis of CRP concentrations one day prior to diagnosis (AUC=0.89).

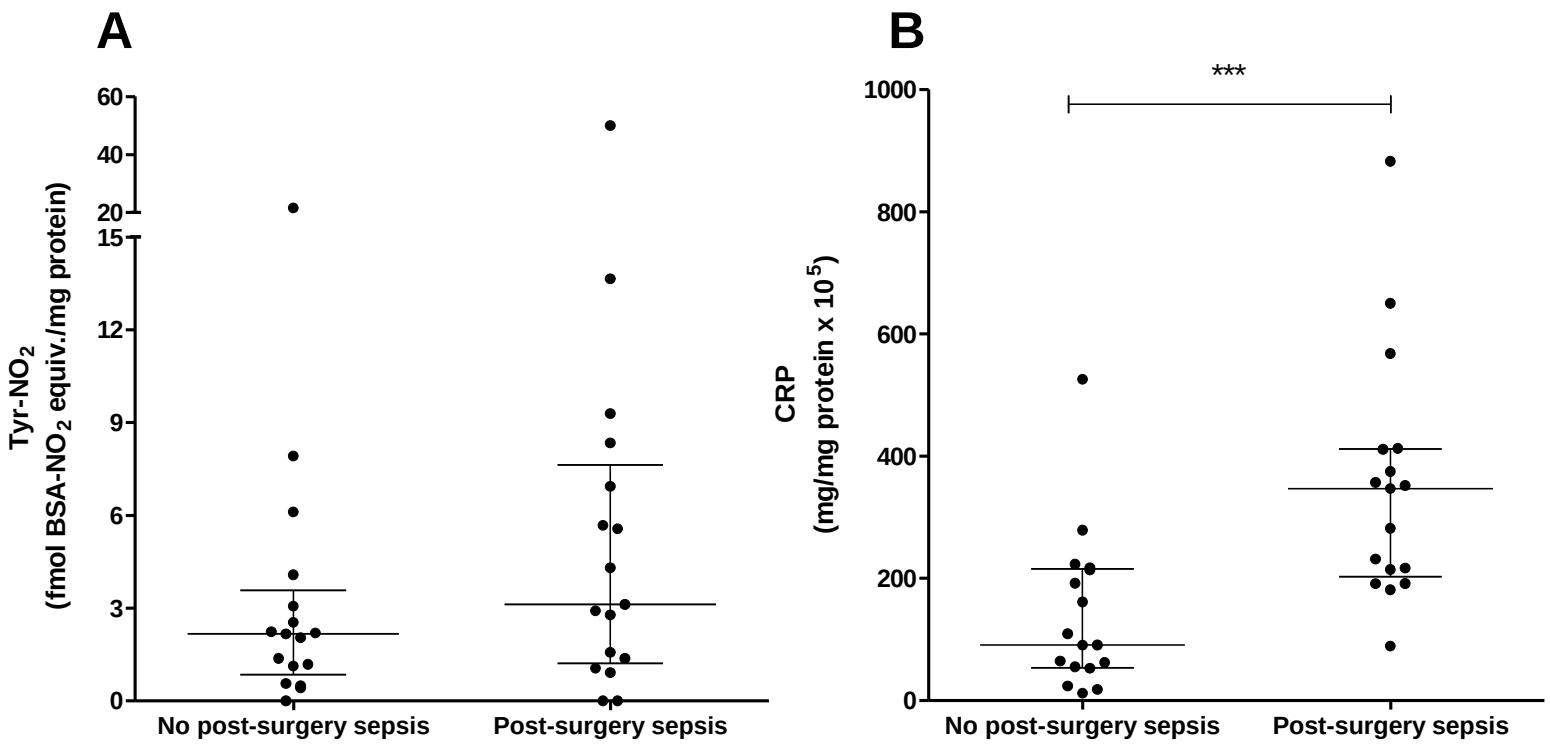

Figure 5.12: Serum 3-nitrotyrosine levels and CRP concentrations in sepsis patients, two days prior to diagnosis, compared with matched patients who did not develop sepsis

Tyr-NO_2 was measured by the protocol described in Chapter 3, section 3.2.5. CRP was measured by the protocol described in Chapter 3, section 3.2.6. The patients who did not develop sepsis (control group, n=17) were matched to sepsis patients (n=17) by the number of days post-surgery the sepsis patients were when diagnosed. Median and IQR values are shown. (A) There was no statistically significant difference in median serum Tyr-NO_2 levels, between the two groups, two days prior to diagnosis (Mann-Whitney, p=0.21). (B) Serum CRP concentrations were significantly higher in the sepsis group compared to the control group (Mann-Whitney, ***p=0.0007).

5.3.5. White blood cell counts

Serum Tyr-NO_2 levels did not show a statistically significant correlation with total white blood cell count (WBC), neutrophil count or monocyte count in either the sepsis group or in the non-sepsis group, or when the groups were combined.

One of the clinical signs of sepsis is a WBC <4 or >12 (x 10^9/L). To assess the sensitivity and specificity of this parameter the data was converted into a score of one for any value <4 or >12, with WBC values 4-12 being assigned a score of zero. This produced an AUC of 0.7 (p=0.034) for WBC one day prior to diagnosis.

5.3.6. Combining parameters

The scoring system above was then extended to incorporate the Tyr-NO_2 and CRP (mg/mg protein x 10^5) values so that the parameters could be combined for ROC analysis. The cut-off points discussed for each individual assay were used for scoring, with levels above the relevant cut-off scoring a value of one and below the cut-off scoring a value of zero. Therefore, a patient could have any score from 0 – 3 (**Table 5.3**).

Table 5.3: Parameter scoring system

Patients were scored depending on their levels of three parameters (Tyr-NO_2 levels, CRP levels and WBC count) one day prior to diagnosis.

Parameter	Score
≥1.94 Tyr-NO_2 (fmol BSA-NO_2 equiv./mg protein)	1
≥168 mg CRP/mg protein x 10^5	1
<4 or >12 x10^9/L WBC count	1
Range of possible scores	0 - 3

This combining of parameters gave an AUC of 0.86 (p<0.001), improving the sensitivity and specificity of the results from Tyr-NO_2 alone or WBC alone but

detracting sensitivity and specificity obtained from the results of the CRP (mg/mg protein alone x 10^5) test alone, which (as mentioned above) gave an AUC of 0.9.

When this scoring system was applied to just WBC and Tyr-NO_2 levels an AUC of 0.73 (p=0.02) was achieved, meaning that these two parameters provided better sensitivity and specificity when combined than when either was used alone. When the only parameters scored were Tyr-NO_2 levels and CRP concentration the AUC of 0.82 was produced (p=0.0001). Again this improved on using only Tyr-NO_2 levels but decreased the sensitivity and specificity of CRP concentrations alone.

5.3.5.1. Net reclassification index (NRI)

The NRI score determines whether the addition of a marker improves a test's prediction performance. Within this analysis, Tyr-NO_2 was added to CRP (mg/mg protein alone x 10^5) to assess whether combining parameters improved the prediction of patients who would develop sepsis from samples collected one day prior to diagnosis.

Equation 5.1: Net reclassification index

$$\frac{\boldsymbol{n\ of\ correctly\ reclassified}}{\boldsymbol{total\ n}} - \frac{\boldsymbol{n\ of\ incorrectly\ reclassified}}{\boldsymbol{total\ n}} = \boldsymbol{NRI\ score}$$

When combining the CRP test with the Tyr-NO_2 test it was seen that the Tyr-NO_2 correctly reclassified 3 patients, one day prior to diagnosis. However, combining the tests also incorrectly reclassified 13 patients, resulting in an NRI score of -0.2 (**Equation 5.1**). This means that the prediction of which patients would develop sepsis with CRP plus Tyr-NO_2 test produced results 20 % worse than when just the CRP test was used.

5.3.7. Mass spectrometry analysis of 3-nitrotyrosine in sepsis

The mass spectrometry analysis was performed using the Progenesis QI software. This software provides relative quantification by comparing protein expression and nitration over the time-points for each patient. However, the Progenesis QI algorithm was only able to identify a few nitrated residues from

data with low scores (suggesting peptide sequencing may be inaccurate). No statistical changes over the time-course could be seen for either patient group (i.e. sepsis or control), see **Table 5.4**.

Table 5.4: Nitrated proteins identified by Progenesis QI

The identified proteins each contained one sequence predicted to be nitrated.

Patient	Nitrated proteins
Sepsis patient U1577	Metastasis-associated in colon cancer protein (MACC1) Polycomb protein SUZ12 (SUZ12)
Sepsis patient B1164	Double stranded RNA binding protein, staufen homolog (STAU2)
Control patient L1292	Complement C5 (CO5)
Control patient L1287	Complement C3 (CO3) Metastasis-associated in colon cancer protein (MACC1)

It was assumed that this result was due to the low percentage of Tyr-NO_2 in the sample. Therefore, the samples were analysed again using pseudo multiple reaction monitoring (MRM) and the Mascot and Peak View software. Pseudo MRM is a targeted approach for particular m/z values of selected peptides (m/z for parent and nitrated peptide). Peptide sequences from serum albumin (the most abundant protein in serum) were targeted. The targeted peptides are detailed in **Table 5.5** and were selected based on previous work conducted as part of this project (see Chapter 3). However, when using this approach no nitration of these residues was detected in the serum samples.

Table 5.5: Peptide sequences in serum albumin targeted by pseudo MRM MS/MS

The m/z of the unmodified (parent) and nitrated (modified) peptide were targeted during pseudo MRM. Nitration adds a mass of 45 Da, this is then divided by the charge state to determine the m/z difference for the modified peptide, compared to the parent peptide.

Location in HSA sequence	Amino acid sequence	m/z (charge)
106-117	ETY(NO_2)GEMADCCAK	Parent 717.8994 (+2) Modified 740.3494
161-168	YLY(NO_2)EIAR	Parent 464.2955 (+2) Modified 486.7955
287-298	Y(NO_2)ICENQDSISSK	Parent 722.4044 (+2) Modified 744.9044
348-360	DVFLGMFLY(NO_2)EYAR	Parent 812.4903 (+2) Modified 834.9903
469-490	RMPCAEDY(NO_2)LSVVLNQLCVLHEK	Parent 840.1748 (+3) Modified 855.1748
508-524	RPCFSALEVDETY(NO_2)VPK	Parent 637.7175 (+3) Modified 652.7175

5.4. Discussion

The British Medical Journal Best Practice sets out the diagnostic criteria for systemic inflammatory response syndrome (SIRS) based on the consensus of a 2001 conference (Levy et al, 2003). Two of these criteria need to be met for a SIRS diagnosis, and infection must be present for a sepsis diagnosis.

Diagnosis criteria:

- Hypothermia (<36°C) or hyperthermia (>38.3°C)
- Tachycardia (>90 beats per minute)
- Tachyponea (>20 breaths per minute)
- PCO_2 <4.3 kPa (32 mmHg)
- Hyperglycaemia in the absence of diabetes (>6.66 mmol/L)
- Acutely altered mental state
- White blood cell count <4 or >12 x 10^9/L

As the criteria for SIRS are non-specific (and will be met by many within the intensive care unit), and as infection cannot always be confirmed, other biomarkers are needed to determine which treatment is necessary (Vincent et al, 2009). CRP and procalcitonin are both used clinically but both have questionable specificity (Pierrakos and Vincent, 2010), and differing baselines between individuals. This makes changes in time more relevant than a single value (Vincent et al, 2011). In a 2010 review of studies looking at sepsis biomarkers, 3370 studies were found, in which researchers examined 178 different markers (Pierrakos and Vincent, 2010); this is a far larger pool of potential markers than found in many other diseases, emphasising the complex nature of this disease.

The primary aim of this study was to determine whether serum Tyr-NO_2 levels were higher in those with post-surgery sepsis, compared to those without. Samples were collected from patients prior to, and for several days after, major elective surgery and split into two groups; those without post-surgery sepsis (n=25) and those with post-surgery sepsis (n=26). Previous studies, showing that free Tyr-NO_2 is elevated in sepsis, obtained the samples at one time point from patients already diagnosed with septic shock, i.e. sepsis plus hypotension and did not measure the protein-associated form of Tyr-NO_2 (Fukuyama et al,

1997; Ohya et al, 2002). Therefore, these results did not show whether protein-associated Tyr-NO_2 was elevated, or if any nitration could be observed prior to sepsis diagnosis as reported here. As can be seen in **Figure 5.3** the median levels of serum Tyr-NO_2 were higher in the post-surgery sepsis group for all post-surgery time points. Though, due to the large variation in values, there wasn't a significant difference between the groups at any post-surgery time point. However, when the time points were changed from days post-surgery to days prior to diagnosis a significant difference was observed one day prior to diagnosis, with levels being higher in the post-surgery sepsis group compared to their matched controls (median and IQR 5.15 (2.38-8.32) and 1.3 (0.79-5.55) fmol BSA-NO_2 equiv./mg protein respectively, **Figure 5.10**). Median levels were also higher at two and three days before diagnosis (**Figure 5.4**) but this did not reach significance. Absolute and percentage change was also analysed. When day one post-surgery was compared to one day before diagnosis a significant difference in the percentage change for the post-surgery sepsis and their matched controls was observed (**Figure 5.6**), as the control group was decreasing between these time points and the sepsis group was increasing between these time points. This data shows, for the first time, that sepsis patients have increased nitrative stress prior to sepsis diagnosis. In the case of post-surgery sepsis, serum Tyr-NO_2 can be seen to rise in the days following surgery whereas matched controls subjects have a reduction in nitrative stress (following the peak observed immediately post-surgery). Another study that has looked at pre-diagnosis markers of sepsis was Lukaszewski et al (2008) who measured the daily mRNA levels of the cytokines IL-1β, IL-6, IL-8, IL-10, TNFα, FasL and CCL2 in intensive care unit patients following high risk procedures. Using a neural network they were able to achieve a predictive accuracy of 94.55% with these 7 markers.

A delay (even of a few hours) in anti-microbial treatment was found to affect sepsis survival rates (Kumar et al, 2006; Weiss et al, 2014), therefore looking at potential markers prior to clinical diagnosis is vitally important in developing ways to identify sepsis early and improve mortality rates. Therefore, this study also sought to determine if serum Tyr-NO_2 could be a potentially useful addition to the clinical markers of sepsis, i.e. aid a quicker and more accurate diagnosis. There was no difference in the pre-surgery levels of Tyr-NO_2 between the two

groups, suggesting no pre-surgery prognostic value. However, two of the sepsis patients did have very high pre-surgery levels of serum Tyr-NO_2 (**Figure 5.7**). Both these patients were having a gastrectomy (removal of part or all of the stomach). These levels could reflect a high level of inflammation associated with their illnesses, or possibly the beginnings of an infection that would develop into sepsis; a control patient (i.e. did not develop sepsis) who had a gastrectomy had undetectable Tyr-NO_2.

As was also seen in Chapter 3 (section 3.3) there was a wide range in pre-surgery Tyr-NO_2 levels (0 - 64.6 fmol BSA-NO_2 equiv./mg protein) and this is probably due to the heterogeneous nature of the medical conditions within the studied patient population. Ideally, this confounding factor would be removed by studying a population with the same medical condition, and undergoing the same operation. However, this would not accurately reflect the highly heterogeneous nature of sepsis.

The CRP levels observed at the pre-surgery time-point were higher than would be seen in healthy individuals (healthy median 0.8 mg/L (Povoa, 2002)), i.e. if there was no acute phase response, as the patients in the present study had a wide variety of diseases. A small, but statistically significant ($p<0.05$), difference was seen between the two groups at this pre-surgery time point: the median and IQR for the sepsis group was 8.5 (3-18) mg/L and the corresponding values for the control (non-sepsis) group were 2.0 (0.85-11) mg/L) (**Figure 5.9**). This could potentially be an indication that these patients were in an inflammatory state that predisposed them to sepsis following surgery. Fransen et al (1999) and Boeken et al (1998) found that a high pre-operative CRP was a strong predictor of post-operative infection, in patients undergoing cardiac surgery. Fransen et al (1999) suggested that this could be due to pre-existing chronic inflammation dysregulating the immune system in the post-operative period, and thereby increasing the risk of infection. High pre-operative CRP has also been indicated as a marker of poor prognosis in cancer related surgeries (Crumley et al, 2006; Zahlten-Hinguranage et al, 2006; Steffens et al, 2012; Steffens et al, 2013). The CRP (mg/L) levels for the two subjects with high pre-surgery Tyr-NO_2 were 3 and 12 mg/L. Therefore, the former subject may not have raised any concerns about their pre-operative state, based on CRP (mg/L)

alone (cut off >6.5 mg/L), but the Tyr-NO_2 levels would have been indicative of high levels of inflammation.

A significant increase in Tyr-NO_2 was observed one day after surgery ($p<0.01$), when compared to pre-surgery levels, with the two groups combined (median and IQR: pre-surgery 1.7 (0.59 – 4.79) and post-surgery 3.0 (1.01-7.15) Tyr-NO_2 fmol BSA-NO_2 equiv./mg protein). However, when the groups were separated into no post-surgery sepsis (control) and post-surgery sepsis, significant differences only remain for the control group (control $p=0.036$ and sepsis $p=0.055$). If the sepsis patients were experiencing a dysregulated immune response prior to surgery (as suggested by Fransen et al (1999) with regard to high pre-operative CRP) then a possible explanation for the smaller increase in the sepsis group could be that the pathways, for Tyr-NO_2 formation, are not as quickly activated post-surgery in these patients as they are in controls. This would cause the control group to have a larger increase in nitration one day post-surgery compared to those that would go on to develop sepsis.

Ohya et al (2002) suggested that free Tyr-NO_2 levels in plasma had prognostic value in predicting survival, but this was based on a low patient number (n=12). In our study, the samples from one day prior to sepsis diagnosis were analysed with control samples matched by the number of days after surgery. As mentioned the median serum protein-associated Tyr-NO_2 levels were significantly higher for the sepsis patients compared to non-sepsis controls (**Figure 5.10**). This is consistent with the fact that the sepsis patients had an ongoing/worsening inflammatory response as a result of infection, in addition to tissue damage caused by the surgery. Whilst in the non-sepsis control patients there is a resolution of the inflammation, purely related to surgery-associated tissue damage, as they recover from the surgery (although the time course for resolution will vary with medical condition/surgery undertaken). Patient outcome was only known for a subset of patients and therefore the prognostic potential of serum Tyr-NO_2 could not be assessed. Serum CRP concentrations were also significantly higher one day prior to diagnosis (**Figure 5.11**, $p<0.0001$) and 14 out 24 (58%) of patients had a WBC count <4 or >12 x 10^9/L. Tyr-NO_2 levels were not correlated with WBC count but Tyr-NO_2 and CRP (mg/mg protein x

10^5) showed a weak positive correlation (r =0.22, p<0.01) when all data points were pooled into one group.

ROC analysis was performed for each of these indicators (i.e. Tyr-NO_2, CRP and WBC) alone and in combination to assess the indicators potential as a diagnostic tool (determined by the AUC). When analysed alone, the AUC's for each assay were: Tyr-NO_2 = 0.69, CRP = 0.88 and WBC = 0.7. Brubaker (2008) defined a diagnostic test with an AUC of 0.5-0.75 as 'fair' and 0.75-0.92 as 'good' (0.92-0.97 is 'very good' and >0.97 is 'excellent'). With these categories, Tyr-NO_2 and WBC were 'fair' diagnostic tools and CRP was a 'good' diagnostic tool. When the parameters were scored (see **Table 5.3**), and combined an AUC of 0.86 was produced. Therefore combining the three factors failed to improve upon the 'good' rating of CRP alone. The NRI score also indicated that combining Tyr-NO_2 and CRP reduced the diagnostic potential of CRP by 20%. CRP levels have previously been measured in a prospective study to differentiate SIRS from sepsis, where an AUC of 0.94 was seen (Sierra et al, 2004). The Sierra et al (2004) study also had a much lower CRP mg/L cut-off (80 mg/L) than seen here (109.5 mg/L), this is probably due to our control group having background inflammation, from the surgery, and therefore, a higher cut-off was needed to differentiate between the groups. Other studies have suggested that CRP is of limited use for differentiating between those with and without infection when a high background inflammatory state is present, such as seen with burn patients (Lavrentieva et al, 2007; Barati et al, 2008).

Due to the fact that Tyr-NO_2 formation is strongly associated with immune/inflammatory pathways (e.g. $O_2^{\bullet -}$ production and MPO activation) it would be expected that Tyr-NO_2 levels would increase vastly in sepsis. However, although the median Tyr-NO_2 level in sepsis is higher than the non-sepsis controls, across all days, the only time-point at which this is significant is one day prior to diagnosis. This lack of a significant difference is due, in part, to the large variation in levels observed; indeed, some patients had non-detectable Tyr-NO_2 prior to diagnosis. One possible explanation for this is the compensatory anti-inflammatory response that can occur in sepsis, where anti-inflammatory cytokines are up-regulated, lymphocyte number is reduced and an immunocompromised state is created (Adib-Conquy and Cavaillon, 2008; Ward et al, 2008). During this state, neutrophils have a lowered rate of phagocytosis

and intracellular microbicidal activity (Adib-Conquy and Cavaillon, 2008) which would be connected with a decreased release of MPO. If free radical production is also limited, there would be very little possibility of Tyr-NO_2 formation. However, low WBC count was not correlated with low serum nitration so it is likely other factors are involved in determining the serum Tyr-NO_2 levels.

Capillary leak is also observed as part of sepsis and this involves the loss of proteins from the blood into the interstitial space (Yang et al, 2014), making the adjustment of Tyr-NO_2 for serum protein concentration an important factor. However, it may be that the loss of serum albumin (the most abundant serum protein) in this way also results in a loss of a large proportion of the nitrated tyrosine.

Mass spectrometry data was unable to provide robust data on the relative amount of nitration, or in which proteins nitration occurred. A few low-abundance proteins were highlighted as containing Tyr-NO_2 by Progenesis QI (see **Table 5.4**) the scores from these hits were low suggesting they may not be true hits. The proteins identified are also doubtful, for example, all but the complement proteins are intracellular proteins, so would not be expected in the serum. Additionally, far more nitration (and within more abundant proteins) was expected. It is suspected that the inability of the analysis to detect nitrated peptides is due to the fact the number of nitrated Tyr residues compared to the number of non-nitrated residues in the sample is very small (around 1 in 10,000 (Radi, 2004)). Additionally, there would have been many sequenced peptides that did not contain Tyr at all. This means the modified peptides are hidden by the greatly more abundant unmodified peptides and may not get sequenced. The low efficiency of mass spectrometry in detecting low abundance PTMs was discussed by Zhao and Jensen (2009), and enrichment of the modified peptides is often required. Therefore, any future work to identify Tyr-NO_2 in human serum would require that the nitrated peptides be separated from the non-nitrated peptides (e.g. by affinity chromatography) prior to mass spectrometry analysis. Such separation procedures would, in themselves, provide additional challenges to obtaining quantitative data.

A targeted pseudo MRM MS/MS approach, in which only serum albumin peptides were analysed, was used in an attempt to filter out a large amount of

the non-nitrated peptide sequences. However, nitrated sequences could still not be identified. This could be due to there still being too much non-modified peptide as albumin is the most abundant protein in the serum (approx. 55% (Anderson and Anderson, 2002). On the other hand, it might have been expected that albumin would be the most nitrated protein due to this high abundance and the significant content of Tyr residues within its polypeptide sequence.

This study was limited by the measurement of only one oxidative stress marker. Consequently, it is unknown whether other markers of oxidative stress act in a similar manner to Tyr-NO_2 prior to sepsis diagnosis, following surgery, or if they follow another pattern. A further study should therefore measure a panel of oxidative stress markers, such as carbonyls and isoprostanes, over the time course as well as Tyr-NO_2.

5.5. Conclusion

As far as we know this is the first time oxidative stress has been measured in sepsis patients prior to diagnosis. The results show that oxidative stress is measurable in the days prior to diagnosis and, that a significant difference is seen at the time point one day before diagnosis, with the patients who went on to develop sepsis having higher levels of Tyr-NO_2 than patients who did not develop sepsis (matched by number of days post-surgery).

The patient group analysed here was highly heterogeneous in terms of medical conditions and surgeries undertaken. This confounding factor likely contributes towards the wide variation in results and overlap between groups for all markers. To improve the study of sepsis it has been suggested that the patient groups need to be graded, in order to achieve more homogenous populations. For this, the PIRO model has been put forward (Vincent et al, 2006; Howell et al, 2011; Granja et al, 2013). The PIRO model categorises patients based on four factors: Predisposition (e.g. age, pre-existing conditions), Infection (e.g. site and whether hospital or community acquired), Response (e.g. temperature, heart rate, cardiac output, etc.) and Organ dysfunction (Vincent et al, 2009; Howell et al, 2011; Granja et al, 2013). Using this model to score patient populations appears to have better predictive value for mortality and intensive care unit stay than other scoring systems, i.e. APACHE II (acute physiology and chronic health evaluation) (Vincent et al, 2009). In the present study, it was observed that serum Tyr-NO_2 was not as sensitive a marker for sepsis as CRP. However, separation of patients into more homogenous groups using the PIRO model, may lead to more informative results being achieved.

This project had some methodological problems in that a new antibody lot number did not perform correctly and this greatly reduced the number of samples in the cohort (we were unable to obtain data for approximately 100 collected patient samples). A larger number of samples would have allowed for stratification of samples into groups based on factors such as surgery being undertaken or patient outcome, whilst still maintaining a large enough *n* number for robust statistical analysis.

Despite this heterogeneity the present study did, as mentioned, show that sepsis patients had significantly higher levels of Tyr-NO_2 than controls one day

before diagnosis. This confirms that the aberrant inflammatory response, seen in sepsis, causes increased oxidative/nitrative stress. Nitration can then lead to dysfunction of the affected proteins and further pathology.

5.6. Acknowledgements

Serum samples were provided by Dr R Lukaszewski (Defence Science and Technology Laboratory).

Mass spectrometry was performed with the aid of Professor A Pitt, Dr C Spickett and Dr K Tveen-Jensen (Aston University).

CRP measurement was performed with the aid of Emily Brewer and Dr Tim McDonald (Royal Devon and Exeter NHS Foundation Trust).

Chapter 6
Nitration in the brain tissue of Alzheimer's disease models and patients

Alzheimer's disease (AD) is characterised by histopathological features, such as senile amyloid plaques and neurofibrillary tangles (Sultana et al, 2006; Reynolds et al, 2007; Reyes et al, 2011) and neuroinflammation can be initiated by both the amyloid plaques and neurofibrillary tangles (Akiyama et al, 2000; Heppner et al, 2015) this is described in Chapter 1 (section 1.5.5). The clinical diagnosis of AD is mostly reliant on the exclusion of other causes for the decline in cognitive function/dementia and will still only result in a diagnosis of either possible or probable AD (McKhann et al, 2011). Neural imaging and cerebrospinal fluid (CSF) biomarkers are, at the moment, insufficient for a definitive diagnosis and post-mortem neuropathological examination is required (McKhann et al, 2011). Additionally, when a probable AD diagnosis is given the disease is at a neuropathologically advanced stage, however, it is believed that new drugs will be most effective in the early stages when neurodegeneration can be slowed, before a severe loss in cognitive function has occurred (Hampel et al, 2010). For this reason biomarkers are needed to improve early detection of the disease.

Transgenic mouse AD models have been developed to aid understanding of what causes this disease, the underlying pathology, testing of potential therapeutic strategies and for preclinical testing. These models tend to use mutations found in familial AD (Morrissette et al, 2009), such as the *Swedish mutation*, which is a double mutation found in a Swedish family that results in increased production of amyloid-β (Haass et al, 1995). Many models exhibit amyloid pathology but some transgenic lines have been crossed to produce mice with both amyloid-β plaques and neurofibrillary tangles. However, it has proved difficult to produce a model which displays the full range of AD pathology (Elder et al, 2010). As has already been discussed in the introduction (Chapter 1, section 1.5.5) oxidative stress has been observed in the brain of mouse AD models, and is thought to accelerate the AD pathology observed (Lim et al, 2001; Praticò et al, 2001; Kanamaru et al, 2015). Lim et al (2001) found that a ˙NO scavenger (curcumin) reduced the plaque burden seen in the

brain tissue. This suggests that ˙NO may be an important factor in AD pathology.

All three NOS isoforms are expressed in the human brain, i.e. neuronal (nNOS), endothelial (eNOS) and inducible (iNOS) (Law et al, 2001). The expression/activity of NOS, along with the role of ˙NO, in AD has been extensively studied but inconsistent results have been seen. Norris et al (1996) found nNOS mRNA levels were not significantly different in those with AD compared to controls with no sign of neurological disease. Yew et al (1999) also measured mRNA for nNOS and found that in AD patients the number of neurons expressing nNOS mRNA goes down but, those neurons expressing the mRNA produce more than seen in non-demented control tissue. However, mRNA expression is not the same as protein activity. Dorheim et al (1994) found that NOS activity in the brain microvessels is increased with AD, they also observed an increase in the expression of both the constitutive (endothelial and neuronal) and inducible NOS compared to the brains of non-demented controls.

To determine ˙NO production in the human brain many have measured NO_2^-, NO_3^- or NO_2^- plus NO_3^- (NO_x). Kuiper et al (1994) and Navarro et al (1996) both measured NO_2^- and NO_3^- in the CSF as a way of assessing the ˙NO production, in the central nervous system, of living AD patients. Kuiper et al (1994) found that levels of these metabolites were lower in the CSF compared to the plasma and suggested that, as they are anions, they do not freely pass through the blood brain barrier. NO_2^- concentrations were not found to be significantly different in AD but NO_3^- concentrations were significantly lower in the CSF of AD patients compared to controls free of neurodegenerative disease. However, Navarro et al (1996) measured NO_3^- in plasma and CSF and found no significant difference between AD and controls. DiCiero Miranda et al (2000) measured NO_x concentration in post-mortem brain tissue and found that they were lower in those with AD compared to non-demented aged controls. Whether ˙NO production is neurotoxic or neuroprotective is a matter of debate as ˙NO is a neurotransmitter and can be anti-inflammatory (Law et al, 2001). Malinski (2007) suggests that ˙NO is cytoprotective in the absence of $O_2^{\bullet -}$, as mentioned (Chapter 1, section 1.5) these radicals react to form $ONOO^-$ which is far more reactive than ˙NO. SOD activity has been found to be reduced in the AD brain (Marcus et al, 1998). SOD is responsible for

dismutation of $O_2^{\bullet -}$ to H_2O_2, therefore, a loss of activity will lead to an increase in available $O_2^{\bullet -}$. Additionally, NOS can become uncoupled, for example due to decreased levels of its cofactor tetrahydrobiopterin – as seen in AD (Foxton et al, 2007) – and produce $O_2^{\bullet -}$ instead of $^{\bullet}NO$. Tyr-NO_2 can be formed, as a result of $ONOO^-$ production, and has been shown to be associated with fibrillar amyloid-β in mouse models of AD (Matsuoka et al, 2001). Tyr-NO_2 has also been observed in human AD brain tissue (Good et al, 1996; Hensley et al, 1998; Calabrese et al, 2006; Butterfield et al, 2007b).

Two studies were conducted assessing nitrative stress in AD brain tissue.

(1) Brain tissue samples from transgenic mouse AD models were analysed for Tyr-NO_2 content to test whether Tyr-NO_2 could be measured in these models. The number of samples was limited so this project was performed to determine whether a further investigation with greater numbers was warranted. Two transgenic mouse models were used during this study, Tas-TPM and Tau35. Tas-TPM is a double transgenic created by cross-breeding two transgenic lines, TAS10 and TPM. These parent models express human amyloid precursor protein and Presenilin-1 respectively, each of these genes contain established mutations in familial AD (AlzForum, (n.d)). As a result of these mutations the mice develop extensive amyloid pathology but they do not develop neurofibrillary tangles (AlzForum, (n.d)). The Tau35 mice express low levels of a disease-related fragment of human tau, to mimic tauopathy in mice (Wray et al, 2008). Tauopathy covers several neurodegenerative diseases with hyperphosphorylated/aggregated tau, AD is the most common of these (Williams, 2006) and insoluble tau is a large part of neurofibrillary tangles (Hanger and Wray, 2010).

(2) A pilot study measuring products of $^{\bullet}NO$ production in the human AD brain was conducted. The aim of the study was to determine whether there was an increase in nitrative stress in the AD brain, if there was then this would be the rationale behind measuring nitration in other tissues that are accessible prior to death (e.g. CSF and blood).

6.1. Materials and Methods

Mouse samples

Forebrain and cerebellum tissue samples from the brain of transgenic (n=24) and wild-type mice (n=14) were collected and snap frozen, then stored at -80°C.

The samples were thawed and homogenised using a 1% SDS lysis buffer (100 mM NaCl, 10 mM Tris (hydroxymethyl) methylamine (pH 7.6), 1 mg/ml aprotinin, PMSF and 1% SDS) and a Retsch Mixer Mill 400. For homogensitation, the samples were weighed and lysis buffer added at a 5 µl/mg tissue ratio (300 µl buffer was used if this was the greater volume), samples were then incubated on ice for at least 20 minutes. Two magnetic beads were then used for homogenisation at 25 hertz/second, in 30-second bursts until the sample was determined to be homogenised by visual inspection. The sample was then pulse centrifuged and the supernatant transferred to a fresh 1.5 ml micro-centrifuge tube. Protein concentration of samples was determined by BCA (Chapter 2, section 2.2), with a 1 in 20 dilution, samples were then stored at -80°C until ready for Tyr-NO_2 measurement.

Human samples

Human brain tissue homogenates were prepared by the South West Dementia Brain Bank (SWDBB). Samples were collected under Brains for Dementia Research (BDR) ethics with the informed consent of the individual or a close relative.

Tissue was collected from the frontal lobe of frozen hemispheres of 15 Alzheimer's disease, 15 vascular dementia (VaD) and 15 non-dementia controls (45 samples in total). The tissue was kept on ice throughout the process. 1% SDS lysis buffer (as above) was used at an approximate ratio of 1ml per 200 mg tissue.

Approx. 200 mg of tissue was homogenised in a Precellys 24 Homogeniser (Stretton Scientific Ltd, Derbyshire UK) using 2.3 mm ceramic beads. The samples were homogenised at 3000 *g* for 15 seconds, then left for 3 minutes on ice before the process was repeated. The samples were stored at -80°C until collection.

After collection, from SWDBB, samples were defrosted and centrifuged at 14,000 *g* for 10 minutes and the supernatant placed in 100 µl aliquots and stored at -80°C until analysis.

6.1.1. Electrochemiluminescence-based ELISA for 3-nitrotyrosine

Tyr-NO_2 content of the tissue was measured by the ECL ELISA (Chapter 3, section 3.2.5) with a 1 in 10 dilution. As the components of the lysis buffer can interfere with the signal produced by the ELISA (**Figure 6.1**) the standard curve was run with an equivalent concentration of lysis buffer to the samples (i.e. 0.1%).

The tissue levels of Tyr-NO_2 were found to be far higher than serum/plasma levels. As the assay showed improved reproducibility, with regards replicate variation, at Tyr-NO_2 levels midway on the standard curve (see Chapter 3, section 3.3) the brain samples were run with duplicate measurements, rather the quadruplicate measurements used for the serum/plasma.

The intra-assay CV for brain tissue was calculated due to all human samples being run on two plates, making within assay variation more relevant than between assay variation. The intra-assay CV was determined by preparing the same human brain sample 8 times and measuring these preparations within one plate.

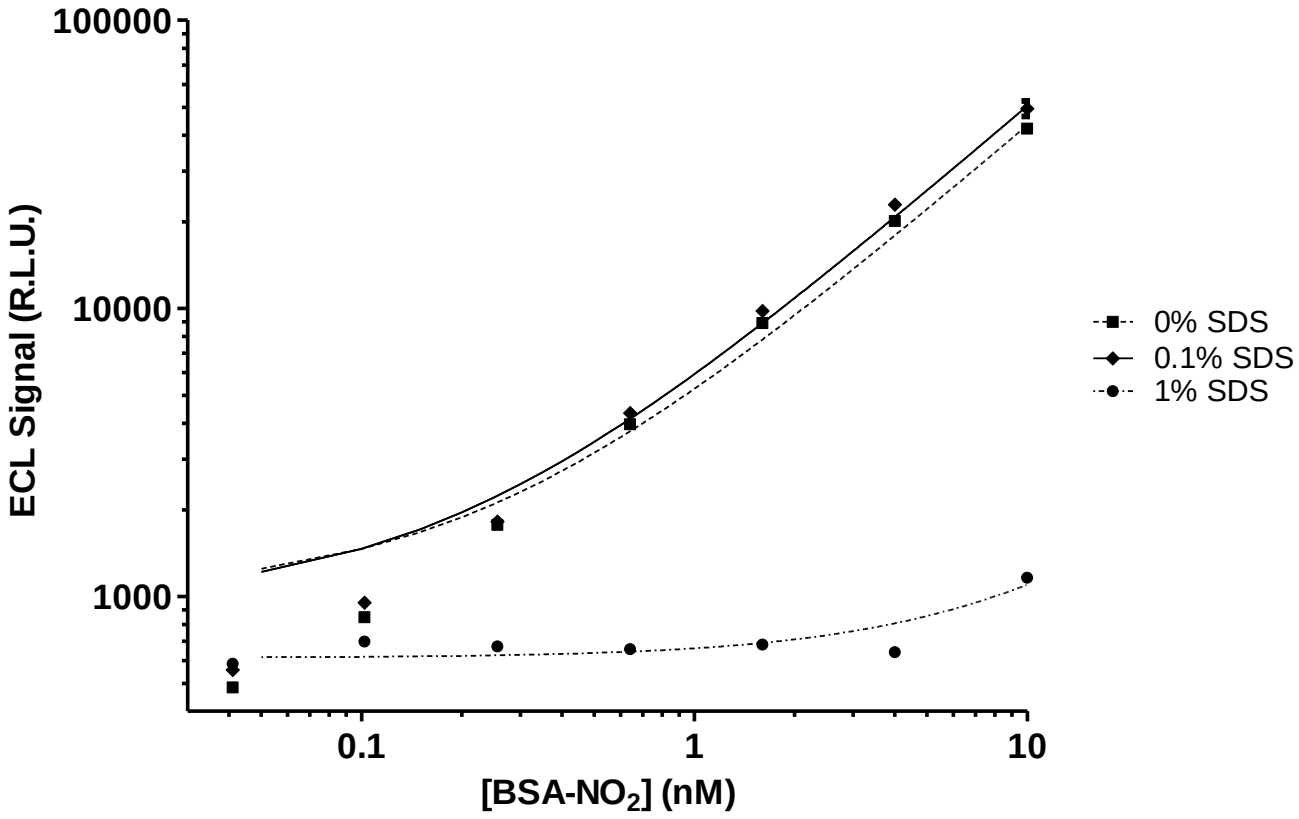

Figure 6.1: Loss of ECL ELISA signal from BSA-NO_2 in the presence of 1% SDS

Nitrated BSA was diluted in dilution buffer containing different amounts of SDS, 1% SDS resulted in a complete loss of ECL signal (n=1). However, a concentration of 0.1% SDS did not result in any signal loss from BSA-NO_2. R.L.U. Relative light units (arbitrary).

6.1.2. Near infra-red western blotting for nitrated proteins

Western blotting for Tyr-NO_2 was performed to determine (A) the molecular weight of the nitrated proteins and, (B) if there was a different pattern of nitration between groups.

Western blotting for Tyr-NO_2 was performed (as described in Chapter 2, section 2.5) to determine the molecular weight of the nitrated proteins. DTT was used as the reducing agent and 60 µg of protein was loaded per lane. Actin was used as the loading control with an IRDye680RD (red fluorescence) anti-rabbit secondary antibody (Chapter 2, Table 2.1).

Mouse samples

A biotinylated anti-nitrotyrosine antibody and a streptavidin IRDye800CW (green fluorescence) secondary antibody were used for detection of Tyr-NO_2 (Chapter 2, Table 2.1).

Human samples

The mouse non-biotinylated anti-nitrotyrosine antibody and anti-mouse IRDye800CW (green fluorescence) secondary antibody was used for detection of Tyr-NO_2 and the anti-actin and anti-rabbit IRDye680RD for the loading control (red fluorescence) (Chapter 2, Table 2.1).

Gels for Coomassie staining (protocol described in Chapter 2, section 2.4) were run simultaneously so that bands could be excised for mass spectrometry analysis. Quantification of the band signal was done using the LiCor Studio Lite software analysis tool. The ratio of the Tyr-NO_2 signal to the actin signal was then calculated.

6.1.3. Mass spectrometry

Human samples

To identify proteins in the nitrated bands mass spectrometry was performed. For this, seven bands corresponding to Tyr-NO_2 positive staining were cut from a Coomassie gel and digested (**Figure 6.12**). The actin positive band was also cut out to confirm that the anti-actin antibody was binding to actin.

6.1.3.1. Materials

In addition to the materials listed in Chapter 2 (section 2.1) the following reagents were used to prepare samples for mass spectrometry analysis.

Acetonitrile and iodoacetamide and trypsin (proteomics grade), were from Sigma-Aldrich (Gillingham, UK). Ammonium bicarbonate (analytical reagent grade) and Formic acid 99% were from Fisher Scientific (Loughborough, UK).

6.1.3.2. In-gel digest

Relevant bands were excised from a Coomassie-stained gel using a clean scalpel. Bands were cut into several pieces (approximately 1mm wide) and placed in a 1.5 ml microcentrifuge tube. All incubations were at room temperature unless otherwise stated.

Firstly, gel bands were washed (500 µl, 100 mM ammonium bicarbonate) and the tubes incubated on a tube roller (30 minutes). The wash solution was discarded and a second wash performed (500 µl, 50% acetonitrile 100 mM ammonium bicarbonate), this wash was then discarded. Samples were reduced with 150 µl of 100 mM ammonium bicarbonate and 10 µl 45 mM DTT (incubated for 30 minutes at 60°C). Samples were cooled to room temperature, then alkylated (10 µl 100 mM iodoacetamide) and incubated in the dark (30 minutes).

The solvent was then removed and the samples washed (500 µl, 50% acetonitrile 100 mM ammonium bicarbonate). The wash was discarded and the gel pieces shrunk (50 µl acetonitrile, approximately 10 minutes incubation), the solvent was removed and the samples were dried under centrifugal evaporation (Jouan RC 10.22).

A trypsin vial was re-suspended in 25 mM ammonium bicarbonate and used to rehydrate gel pieces (just enough to allow gel pieces to swell to the original size, approximately 25 µl). The gel pieces were then covered in 25 mM ammonium bicarbonate and incubated at 37°C overnight, while digestion took place.

The tubes were then pulse centrifuged to pellet the gel pieces and the supernatant transferred to a fresh microtube. The gel pieces were incubated (20

µl, 5% formic acid) for 20 minutes at 37°C, 40 µl acetonitrile was then added for a further 20 minutes. The samples were pulse centrifuged again and the supernatant collected and combined with the previously collected supernatant. This combined solution was then dried down using a centrifugal evaporator (Jouan RC 10.22) and stored at -20°C until analysis.

Prior to mass spectrometry analysis samples were suspended in 25 µl of eluent A (98% acetonitrile and 0.1% formic acid).

6.1.3.4. Mass spectrometry analysis

Mass spectrometry (MS/MS) analysis involved high pressure liquid chromatography (HPLC) coupled to a 5600 Triple TOF mass spectrometer.

The samples were eluted over a 45 minute gradient on a C18 nano-HPLC column. Scans were collected for 200 ms. Information dependent acquisition was used to collect MS/MS data (10 most intense ions), as described in Chapter 2 (section 2.6).

The generated data was then analysed with Mascot Daemon statistical software v 2.3.2 (Matrix Science, London, UK) with the following settings applied:

Digestion enzyme: trypsin
Fixed modifications:

- Carbamidomethyl (C) (formed by the iodoacetamide)

Variable modifications:

- Oxidation (M)
- Nitro (Y)

Instrument type: ESI QUAD TOF
Taxonomy: Human
Charge: 2+, 3+ and 4+
Fragment mass tolerance: 0.5 Da

6.1.4. Ozone-based chemiluminescence (NO_2^- and NO_3^- measurement)

Measurement of NO_2^- and NO_3^- in human brain samples was performed by Dr Miranda Smallwood (University of Exeter Medical School) as per the protocol in Chapter 2 (section 2.9), with the following adaptations: 200 µl of homogenate was deproteinised (dilution of 1 in 5). This means that there was 0.2% SDS in the samples and the standards were run with this concentration as well. Samples were analysed in duplicate. As this analysis was done over several days the between assay variation was determined (inter-assay CV 6.1%).

6.1.5. Statistical analysis

Following a test of normality (Shapiro-Wilk), non-parametric (Mann-Whitney, Kruskal-Wallis and Spearman's r correlation) or parametric (one way ANOVA and two- way ANOVA) testing was applied. Bonferroni correction was applied to cases of multiple correlations against the same data set.

6.2. Results

6.2.1. Mouse brain 3-nitrotyrosine levels

When measuring the overall nitration levels by ELISA there was a statistically significant difference between the wild-type (WT) and transgenic (Tg) mice (models and brain regions combined; Mann-Whitney p=0.044), with the Tg mice having a higher median value: median (IQR) 1.04 (0.72 – 1.53) and 1.36 (1.07 – 1.97) Tyr-NO_2 pmol BSA equiv./mg protein for WT and Tg mice respectively (**Figure 6.2**).

A comparison of the two models (Tas-TPM and Tau35), showed that the Tau35 Tg mice had a higher median Tyr-NO_2 value, but this did not reach statistical significance and animal numbers were low (Tas_TPM WT n=16, Tau35 WT n=3, Tas_TPM Tg n= 5 and Tau35 Tg n=12, Kruskal-Wallis p=0.066) (**Figure 6.3**).

The forebrain and cerebellum regions were compared in the WT and Tg mice (models combined) but no statistically significant differences were seen between regions or between Tg and WT mice within each brain region (**Figure 6.4**).

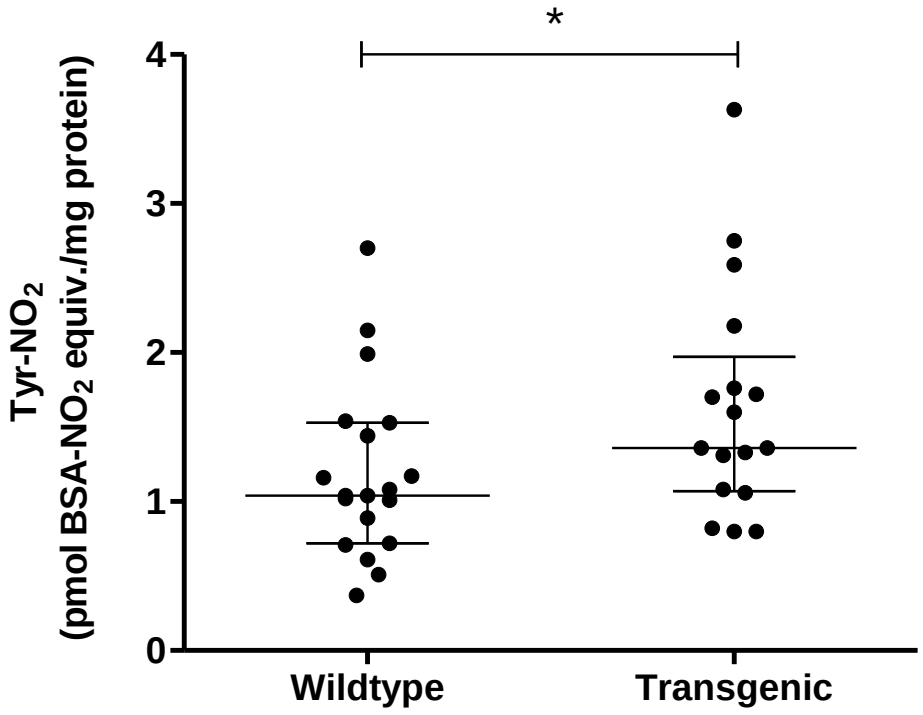

Figure 6.2: Brain tissue nitration: wildtype versus transgenic mice

The median and IQR values are shown. Tyr-NO_2 was measured in duplicate by ECL ELISA as described in section 6.1.1. Mouse models are described in section 6.1. Transgenic mice (n=17) had a statistically significant increase in median nitration compared to wildtype mice (n=18) (Mann-Whitney, *p=0.044).

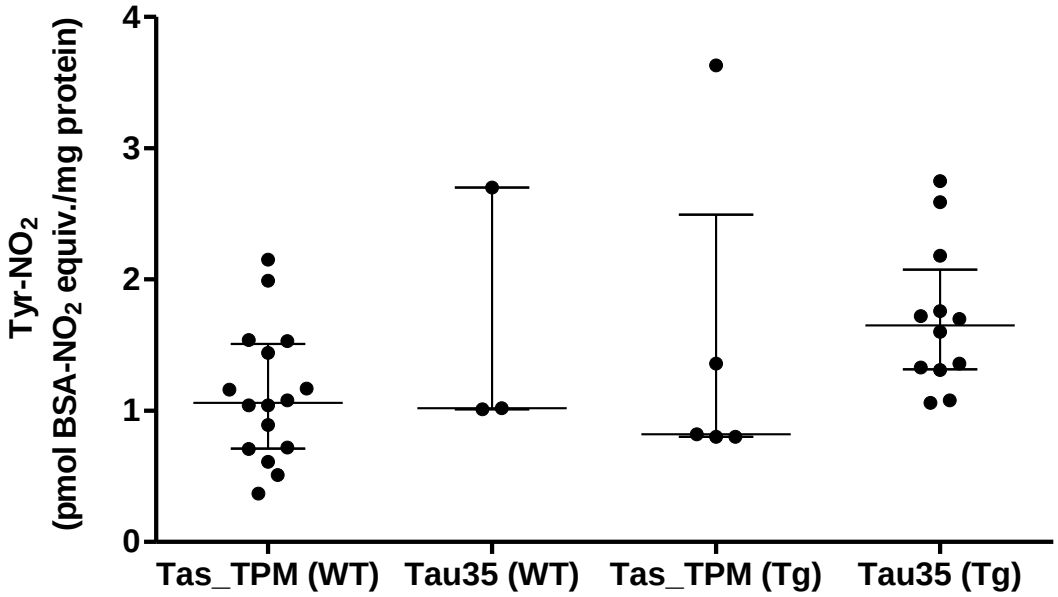

Figure 6.3: A comparison of brain tissue nitration in two transgenic mouse models of Alzheimer's disease

The median and IQR values are shown. Tyr-NO_2 was measured in duplicate by ECL ELISA as described in section 6.1.1. Transgenic mouse models are described in section 6.1. The two models were split into Tg and WT samples, this meant the number of samples in some groups was small (Tas_TPM WT n=16, Tau35 WT n=3, Tas_TPM Tg n= 5 and Tau35 Tg n=12). Tau35 Tg mice showed the highest median levels of nitration but this was not significant (Kruskal-Wallis, p= 0.066).

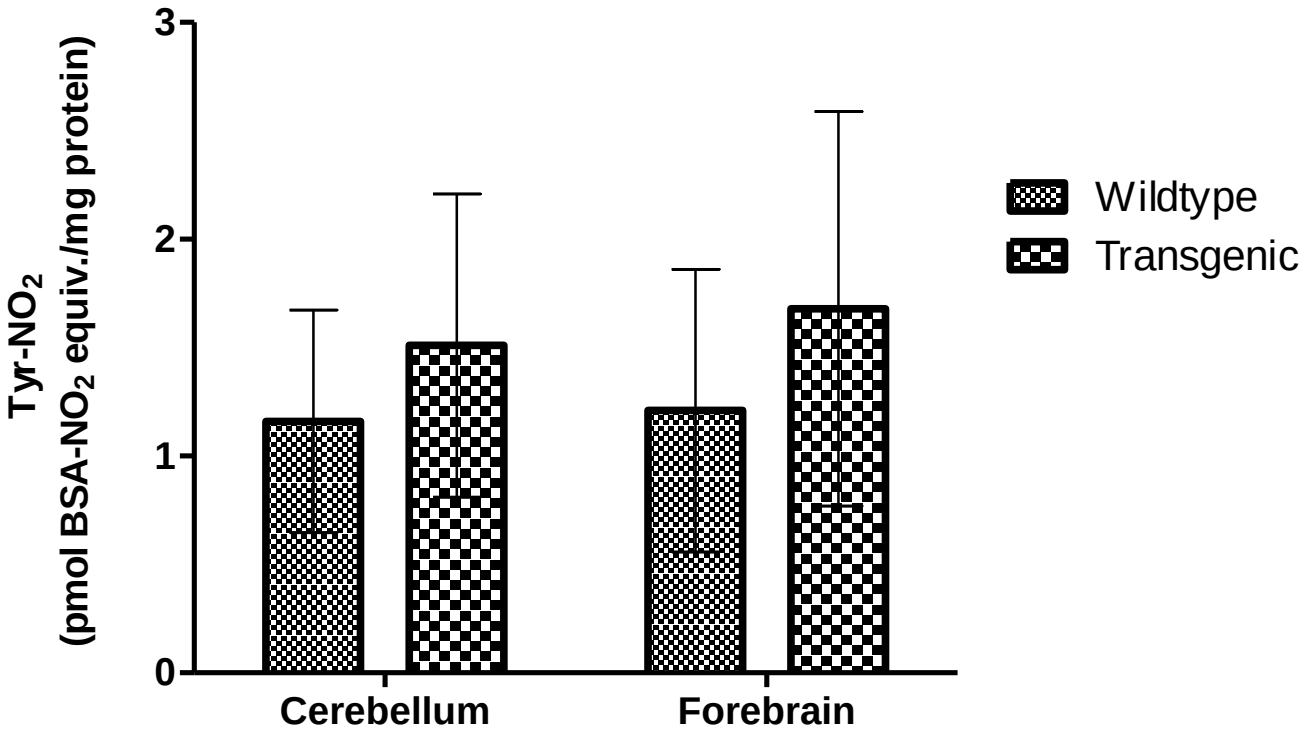

Figure 6.4: 3-Nitrotyrosine levels in the cerebellum and forebrain of wildtype and transgenic mice

The median and IQR values are shown. Tyr-NO_2 was measured in duplicate by ECL ELISA as described in section 6.1.1. Mouse models are described in section 6.1. There were no significant differences between brain region median nitration levels for WT or Tg mice (two-way Anova p=0.82. Cerebellum wildtype n=7 and transgenic n=5. Forebrain wildtype n=12 and transgenic n=8).

6.2.2. Nitrated proteins in mouse brain tissue

Western blots were performed to determine the number, and molecular weight, of nitrated proteins in the mouse brain tissue. However, the results were affected by the presence of endogenous biotin, which is possibly associated with carboxylases, leading to inappropriate binding of the secondary streptavidin antibody. Nevertheless, when comparing a blot with the primary anti-Tyr-NO_2 to a blot run without the primary antibody (this blot showed the false binding of the streptavidin), it was observed that the low molecular weight bands were not false positives (i.e. not endogenous biotin) as they were not present on the second blot (**Figure 6.5**).

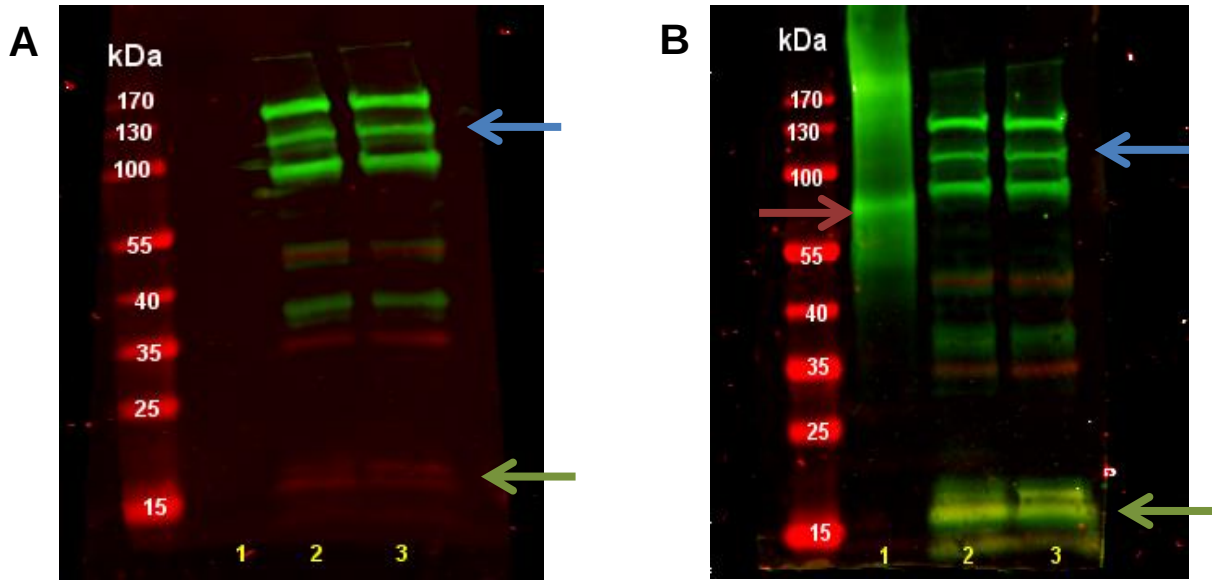

Figure 6.5: Western blot for nitrated proteins in mouse brain tissue

Western blotting protocol described in section 6.1.2. green = nitrotyrosine, red = actin. A biotinylated Ab was used to avoid cross reactivity with mouse proteins. However, there was endogenous biotin in the brain tissue (blue arrows) and a blocking step is needed prior to Ab incubation. Lane 1 positive control; BSA-NO_2 (red arrow), Lane 2 and 3 transgenic mice cerebellum brain samples (A) Blot without an anti-Tyr-NO_2 Ab and (B) blot with an anti-Tyr-NO_2 Ab. The green bands present in B but not A (green arrows) are thought to be true Tyr-NO_2 staining but further work is needed.

6.2.3. Human 3-nitrotyrosine levels

Intra-assay CV (n=8) was calculated by dividing the SD, of the concentration, by the mean, of the concentration, and multiplying by 100 (**Table 6.1**). Intra-CV was 6.36%.

Table 6.1: Determination of intra-assay CV for brain tissue analysis

	#1	#2	#3	#4	#5	#6	#7	#8	Mean	SD	CV
Concentration (nM)	5.19	4.80	4.75	4.62	4.42	4.33	4.37	4.42	4.61	0.29	**6.36**

The Tyr-NO_2 levels were adjusted for sample protein concentration and the median and IQR determined for each group (**Figure 6.6**). No statistically significant differences were observed between these median values (Kruskal-Wallis p=0.97): median (IQR) AD 0.29 (0.19-0.57); VaD 0.36 (0.18-0.40) and non-demented controls 0.3 (0.22-0.55) Tyr-NO_2 pmol BSA-NO_2 equiv./mg protein.

Brain NO_3^- was found to positively correlate with Tyr-NO_2 (Spearman's r = 0.42, p= 0.03) (**Figure 6.7**). NO_2^- did not correlate with Tyr-NO_2 (Spearman's r = 0.31, p= 0.19).

When examining the patient data no association could be found between Tyr-NO_2 levels and patient age, gender, tissue pH or post-mortem interval.

Nitration in the mouse brain tissue was significantly higher than in the human brain tissue: median (IQR) 1.24 (0.98 – 1.71) and 0.32 (0.21 – 0.45) Tyr-NO_2 pmol BSA equiv./mg protein respectively (**Figure 6.8**).

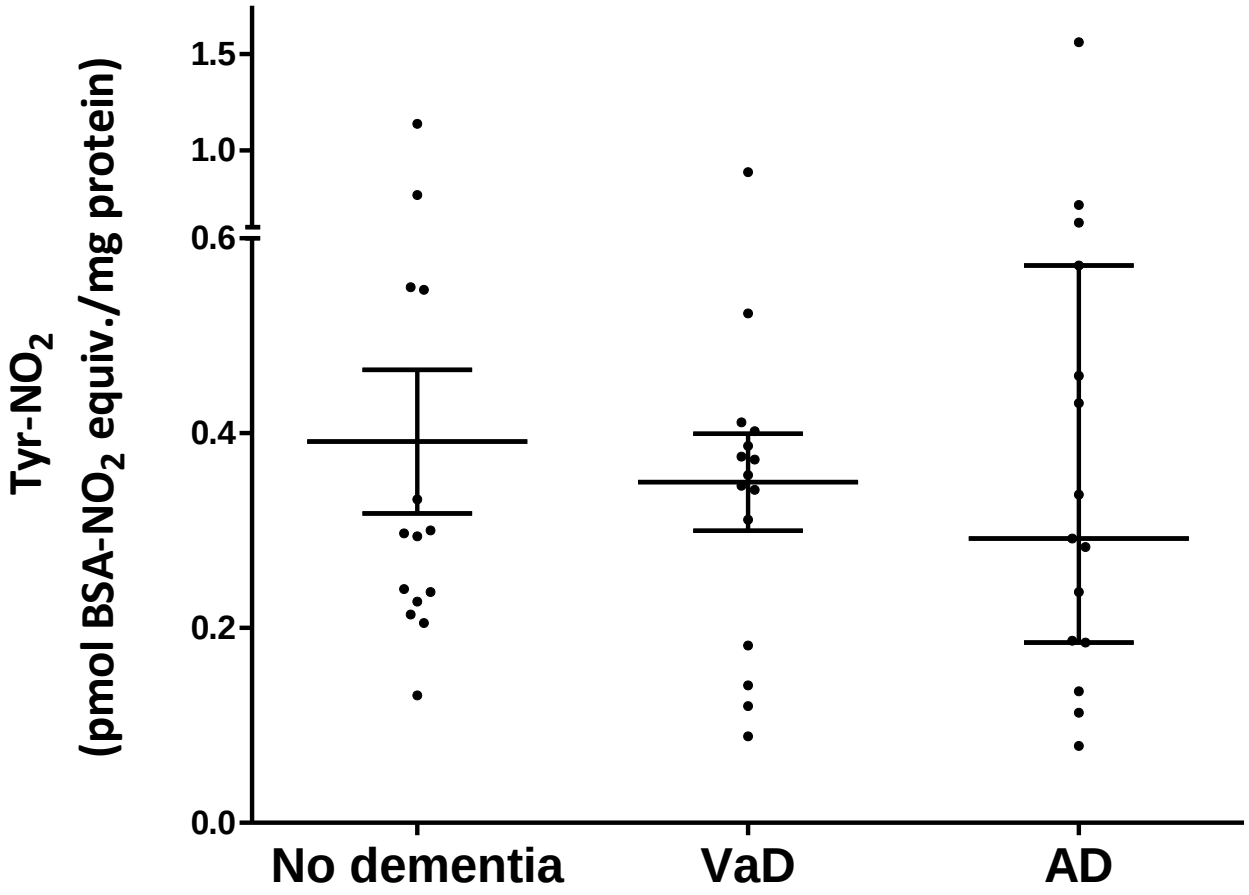

Figure 6.6: 3-Nitrotyrosine levels in brain tissue from human dementia and dementia free control volunteers.

Data represents median and IQR values. Tyr-NO_2 was measured in duplicate by ECL ELISA as described in section 6.1.1. All groups showed high variability in Tyr-NO_2 levels (all n=15) and the median values were not statistically different (Kruskal-Wallis test $p>0.05$).

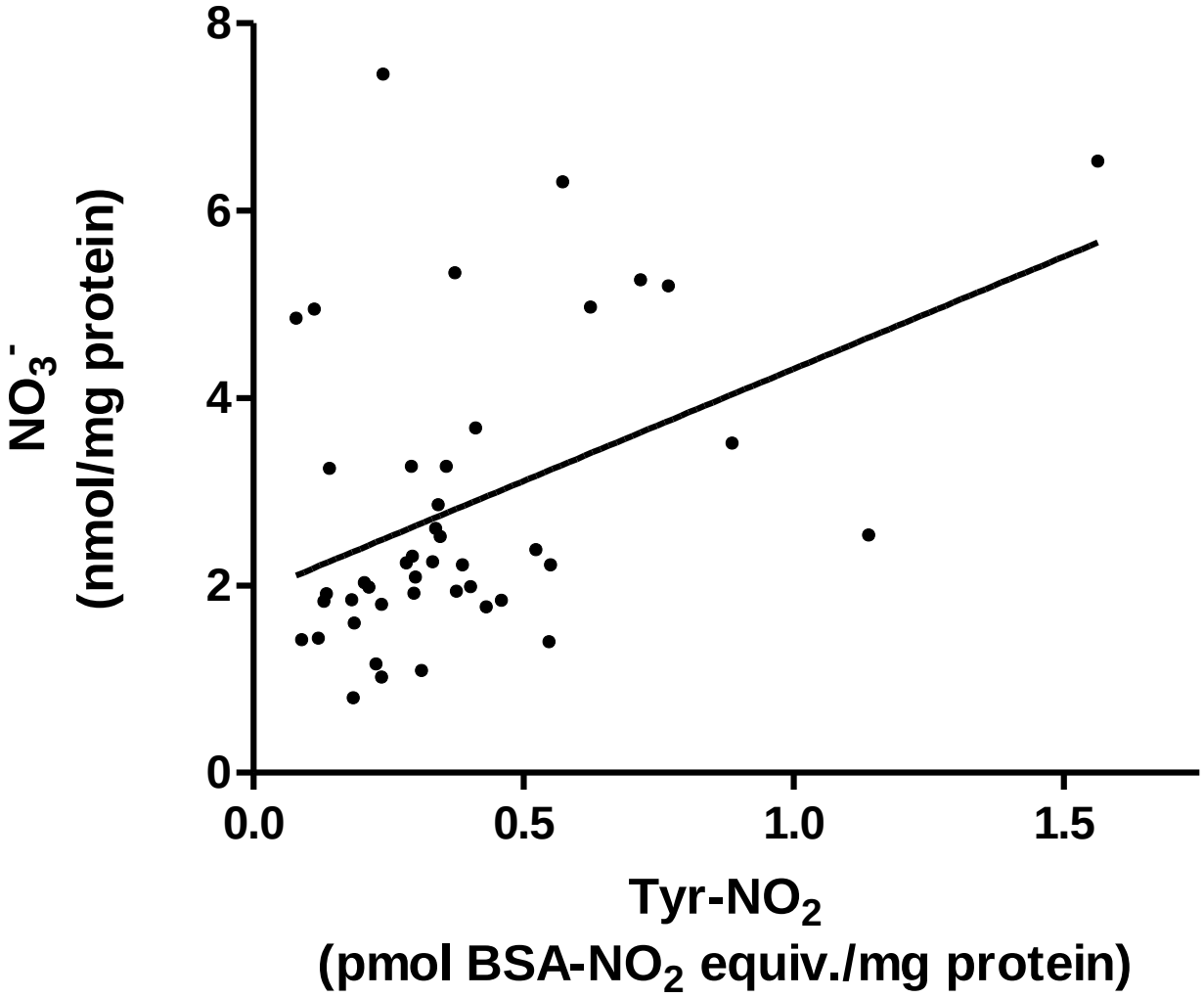

Figure 6.7: Correlation between 3-nitrotyrosine and nitrate concentration in brain tissue from human dementia patients and dementia free control volunteers

NO_3^- was measured by ozone-based chemiluminescence as described in section 6.1.4. and Tyr-NO_2 in duplicate by ECL ELISA as described in section 6.1.1. n=45. NO_3^- positively correlated with Tyr-NO_2, p = 0.03 (with Bonferroni correction) and r = 0.42 (Spearman's rank correlation).

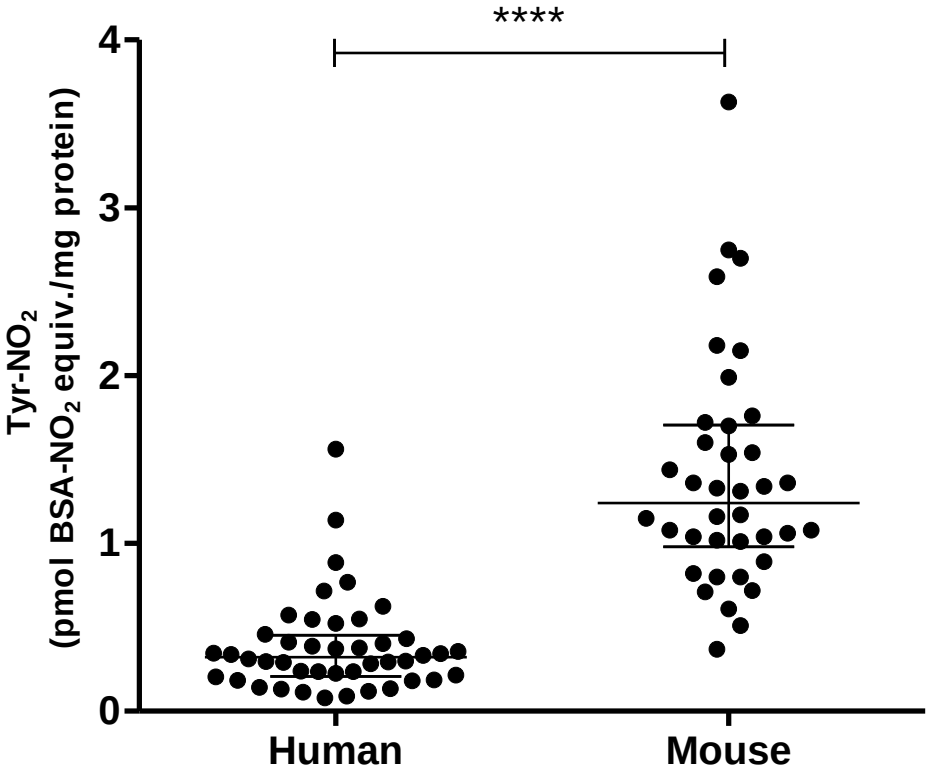

Figure 6.8: A comparison of median 3-nitrotyrosine levels in human and mouse brain tissue

The median and IQR values are shown. Tyr-NO_2 was measured in duplicate by ECL ELISA as described in section 6.1.1. Human samples are as described in section 6.1. and mouse models in section 6.1. The mouse brain Tyr-NO_2 levels (n=38) were far higher than the Tyr-NO_2 levels in the human brain samples (n=44) (Mann-Whitney ****$p<0.0001$).

6.2.4. Nitrite and nitrate levels in human brain tissue

Mean brain NO_2^- levels were significantly different between the 3 groups (One-way ANOVA, p= 0.03) with AD significantly higher than non-demented controls, but there was no difference between VaD and either of the other groups (mean ± SD): AD 0.12 ± 0.05; VaD 0.11 ± 0.03 and non-demented 0.09 ± 0.03 nmol/mg protein (**Figure 6.9A**).

There were no statistically significant differences between groups for median NO_3^- levels (Kruskal-Wallis, p= 0.65): AD 2.6 (1.8-4.9); VaD 2.4 (1.9-3.3) and non-demented controls 2.1 (1.8-2.3) nmol/mg protein (**Figure 6.9B**). NO_3^- and NO_2^- positively correlated (Spearman's rank correlation r = 0.53, p= 0.001) (**Figure 6.10**).

There were no correlations between NO_2^- or NO_3^- with patient age, gender, tissue pH or post-mortem interval.

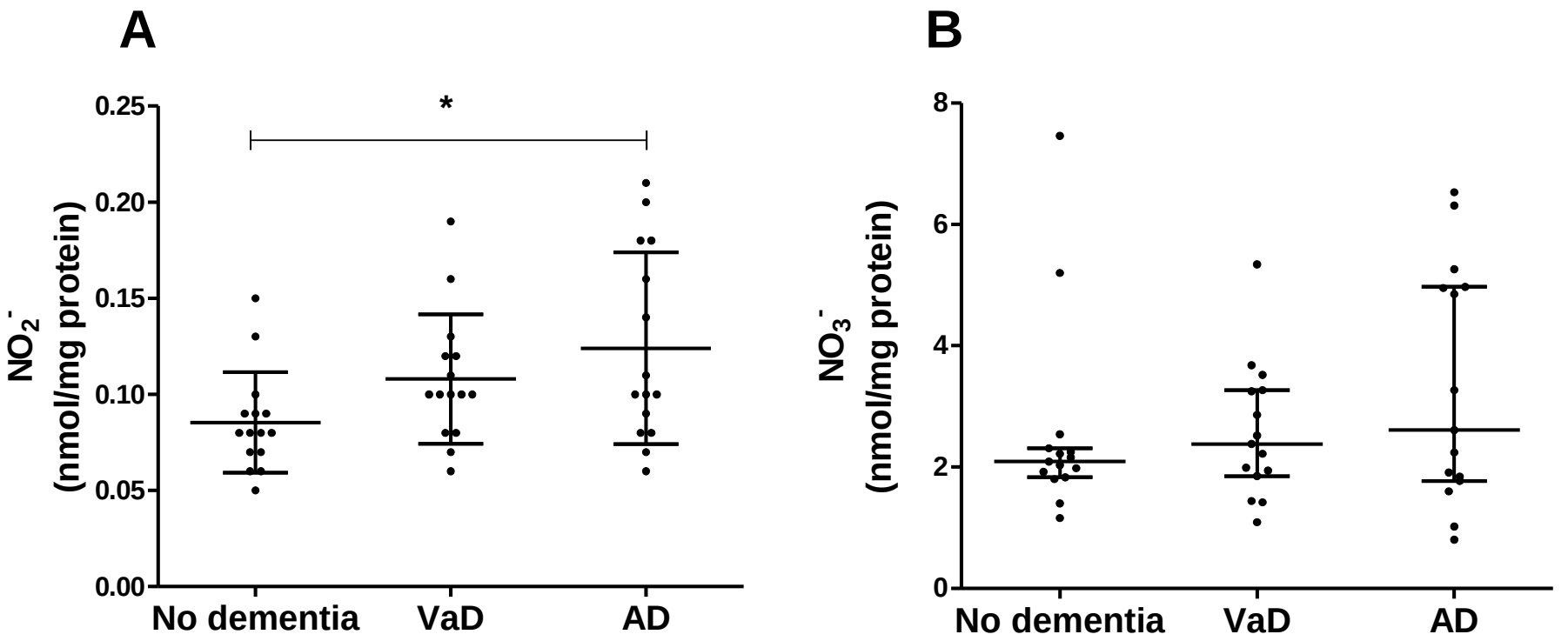

Figure 6.9: Nitrite and nitrate levels in human brain tissue from dementia patients and dementia free control volunteers

NO_2^-/ NO_3^- levels were measured by ozone-based chemiluminescence as described in section 6.1.4. and corrected for protein. Data represents median and IQR values, n=15 in each group. (A) NO_2^- median level showed a statistical difference, *p=0.03 (Kruskal-Wallis test), post-hoc testing (Dunn's Multiple Comparison test) showed the difference to be between the AD and control group. (B) No significant differences were found between groups for NO_3^- levels (Kruskal-Wallis, p= 0.65).

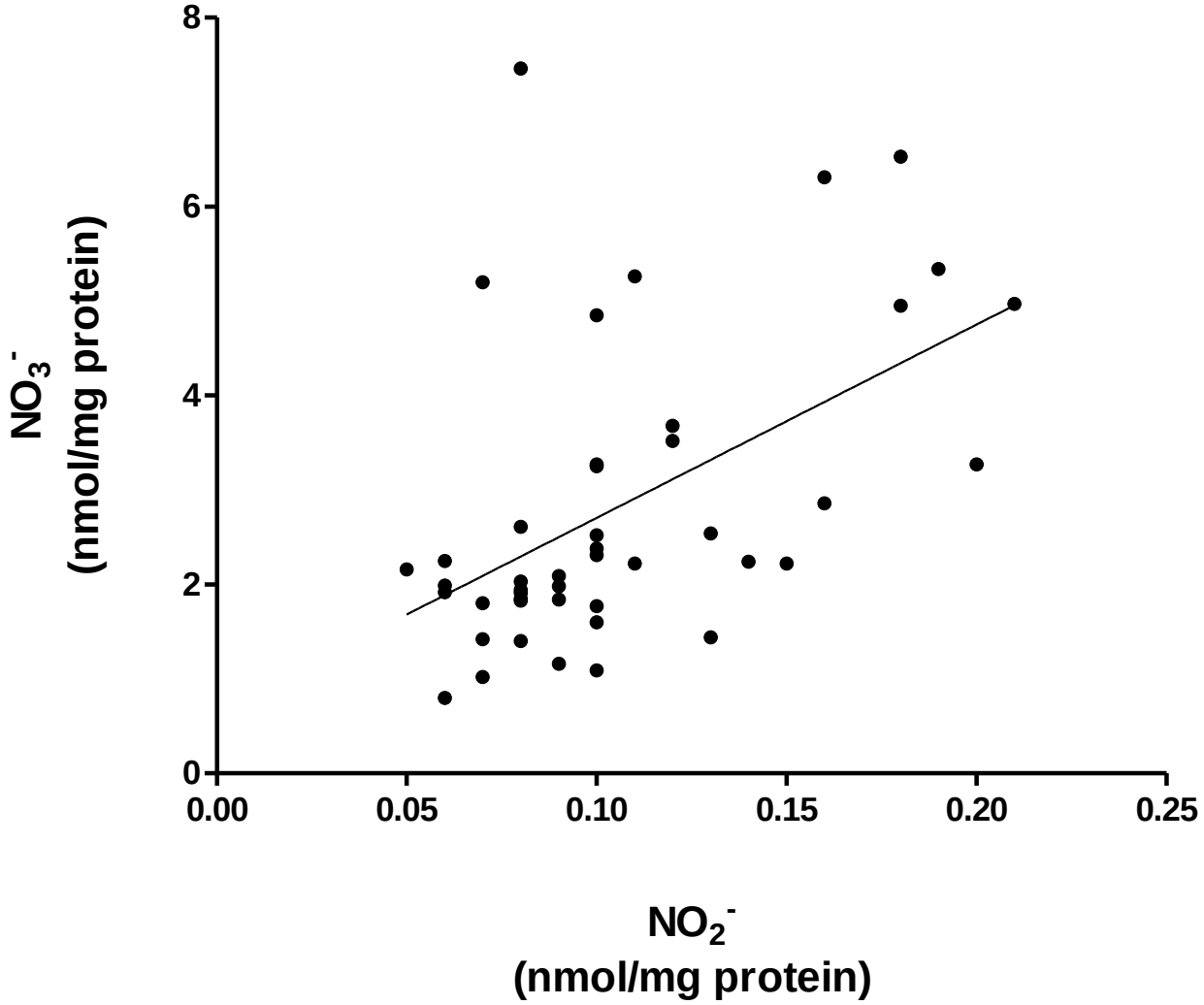

Figure 6.10: Correlation of nitrate with nitrite in human brain tissue samples from dementia patients and dementia free control volunteers

NO_2^- and NO_3^- levels were measured by ozone-based chemiluminescence as described in section 6.1.4. n=45. A statistically significant positive correlation between NO_2^- and NO_3^- was observed, p = 0.001 (with Bonferroni correction) r = 0.53 (Spearman's rank correlation).

6.2.5. Nitrated proteins in human brain tissue

Western blotting did not reveal any qualitative differences between the three groups (**Figure 6.11**). Bands at ~15 and ~18 kDa were nearly always present and semi-quantitative analysis was performed for these bands by calculating the ratio of the Tyr-NO_2 signal to actin signal for each sample. However, neither showed a statistically significant difference between groups (Kruskal-Wallis, p=0.06 and 0.4 for the 15 kDa and 18 kDa bands respectively). Suspected actin cleavage was observed but there was no significant difference, in the signal for the cleaved fragments, between the groups (Kruskal-Wallis, p=0.74).

6.2.6. Mass spectrometry analysis of human brain tissue

Due to the crude nature of the samples, numerous proteins were identified within each Tyr-NO_2 positive band, these results were organised by the most abundant proteins (emPAI) and the reliability of the MS data assessed (**Table 6.2 A-G**). The ion score produced by the Mascot software is the *"calculated probability that the observed match between the experimental data and the database sequence is a random event*" With scores >50 indicating identity or extensive homology at the p= 0.05 cut off (MatrixScience, 2014).

The actin positive band MS/MS results reported actin as the most abundant protein (ion score of 14,579), confirming that the anti-actin antibody is binding appropriately and, that the Mascot Daemon software is able to correctly identify the proteins in the gel bands. **Table 6.2 A-G** represents the bands A-G, indicated in **Figure 6.12.** The top 10 proteins, based on emPAI score, for each band is listed; emPAI is a score of protein abundance in the sample. Within **Table 6.2 A-G** the results have been assessed further using the following criteria: (1) Is the molecular weight of the identified protein in line with the band's position on the coomassie gel? (2) Is the identified protein present in adult brain tissue? And (3) Is the ion score high in relation to the other proteins identified? For this last criteria the ion scores were placed in numerical order (not shown) and the cut-off for removing the lowest 5% determined (ion score >775). For each of the three criteria met a score of one was given, resulting in a score range of 0-3, with 3 indicating the highest confidence score. Information on protein location, Tyr content and function was obtained from the UniProt database (Consortium, 2015).

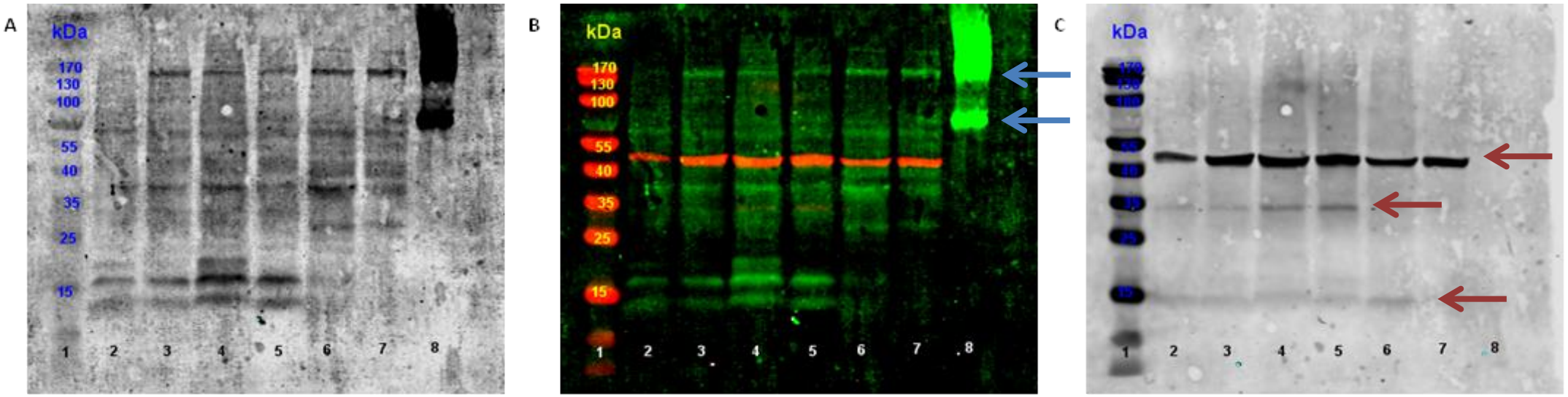

Figure 6.11: Western blot for nitrated proteins in human brain tissue from dementia and dementia free controls

This blot is representative of all the western blots performed (n=5). Lane 1 - molecular weight marker, Lanes 2 and 3 - AD samples, Lanes 4 and 5 - VaD samples, Lanes 6 and 7 - Control (no dementia) samples and Lane 8 - positive control; BSA-NO_2 (blue arrows show the monomer and an aggregate). Western blotting was performed as per the protocol described in section 6.1.2. (A) Tyr-NO_2 only staining. (B) Dual staining; red for actin binding, green for Tyr-NO_2. (C) Actin only staining (red arrows show the bands for the whole protein and cleaved products).

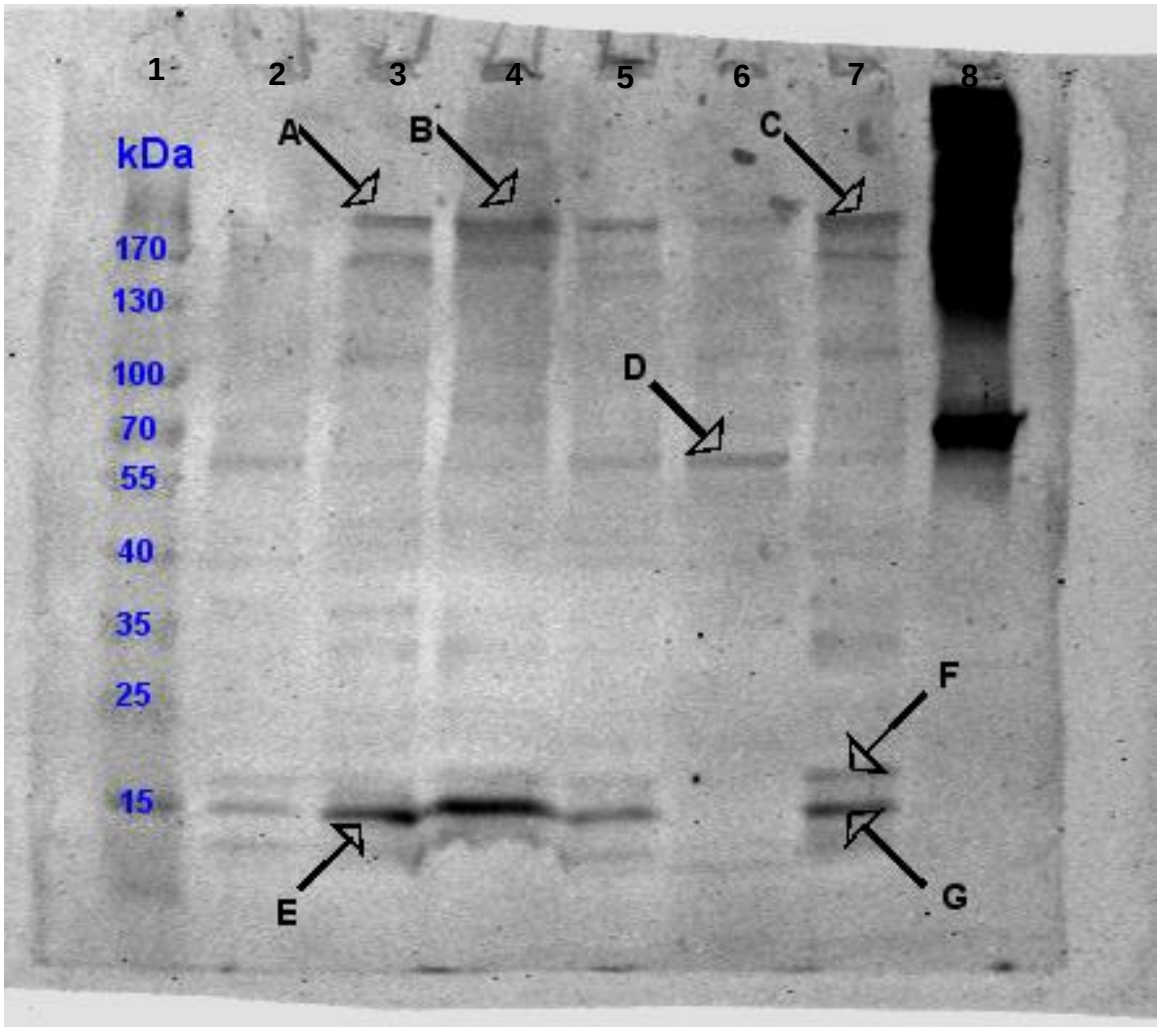

Figure 6.12: Location of nitrated bands excised for mass spectrometry

Seven Tyr-NO_2 positive bands were selected (as indicated, A-G) across the three groups, along with an actin positive band (loading control, not marked on blot), and excised from a corresponding Coomassie stained gel (protocol Chapter 2, section 2.4). These bands were then digested and underwent mass spectrometry analysis as described in section 6.1.3.

Table 6.2A: Mass spectrometry protein identification data for band A (see Figure 6.12). Proteins ordered by emPAI score. Protein information from UniProt (Consortium, 2015).

Band location	Proteins identified	N_o of Y residues	Ion Score	Protein mass (Da)	Confidence score	Protein function Information from UniProt	Affected in dementia
AD >170 kDa (resolver/stacker interface) Band A	**Spectrin-β, non-erythrocytic**	**49**	**8,240**	**274,439**	**3**	**Interacts with calmodulin in a calcium-dependent manner and is thus a candidate for the calcium-dependent movement of the cytoskeleton at the membrane.**	**(Masliah et al, 1990; Sihag and Cataldo, 1996; Fernandez-Shaw et al, 1997)**
	Pyruvate kinase	9	3,742	57,900	2	A glycolytic enzyme that catalyses the transfer of a phosphoryl group from phosphoenolpyruvate (PEP) to ADP, generating ATP. Plays a general role in caspase-independent cell death of tumour cells. The ratio between the highly active tetrameric form and nearly inactive dimeric form determines whether glucose carbons are channelled to biosynthetic processes or used for glycolytic ATP production.	(Butterfield et al, 2006b)
	Spectrin-α, non-erythrocytic	**41**	**3,654**	**284,364**	**3**	**Interacts with calmodulin in a calcium-dependent manner and is thus a candidate for the calcium-dependent movement of the cytoskeleton at the membrane.**	**(Masliah et al, 1990; Sihag and Cataldo, 1996; Fernandez-Shaw et al, 1997)**
	Serum albumin	19	20,012	69,321	2	Has a good binding capacity for water, Ca^{2+}, Na^{+}, K^{+}, fatty acids, hormones, bilirubin, and drugs. Its main function is the regulation of the colloidal osmotic pressure of blood. Major zinc transporter in plasma typically binds about 80% of all plasma zinc.	(Altunoglu et al, 2015)

Band location	Proteins identified	N_o of Y residues	Ion Score	Protein mass (Da)	Confidence score	Protein function Information from UniProt	Affected in dementia
AD >170 kDa (resolver/stacker interface) Band A	Keratin type II cytoskeletal	24	689	65,999	0	May regulate the activity of kinases such as PKC and SRC via binding to integrin beta-1 (ITB1) and the receptor of activated protein kinase C (RACK1/GNB2L1). In complex with C1QBP is a high-affinity receptor for kininogen-1/HMWK.	
	Haemoglobin-α	3	107	15,248	1	Involved in oxygen transport from the lung to the various peripheral tissues.	(Ferrer et al, 2011; Shah et al, 2011; Chuang et al, 2012)
	Creatine kinase	9	1,751	42,617	1	Reversibly catalyzes the transfer of phosphate between ATP and various phosphogens (e.g. creatine phosphate). Creatine kinase isoenzymes play a central role in energy transduction in tissues with large, fluctuating energy demands, such as skeletal muscle, heart, brain and spermatozoa.	(Bürklen et al, 2006)
	Myelin proteolipid protein	14	259	30,057	1	This is the major myelin protein from the central nervous system. It plays an important role in the formation or maintenance of the multilamellar structure of myelin.	(Roher et al, 2002; Barker et al, 2013)
	Dihydropyrimidinase-related protein	14	626	62,255	1	Plays a role in neuronal development and polarity, as well as in axon growth and guidance, neuronal growth cone collapse and cell migration. Necessary for signalling by class 3 semaphorins and subsequent remodelling of the cytoskeleton. May play a role in endocytosis.	(Castegna et al, 2002)

Band location	Proteins identified	N_o of Y residues	Ion Score	Protein mass (Da)	Confidence score	Protein function Information from UniProt	Affected in dementia
AD >170 kDa (resolver/stacker interface) Band A	V-type proton ATPase	18	544	56,465	1	Non-catalytic subunit of the peripheral V1 complex of vacuolar ATPase. V-ATPase is responsible for acidifying a variety of intracellular compartments in eukaryotic cells.	Mice (Chang et al, 2013; Fu et al, 2015)

Table 6.2B: Mass spectrometry protein identification data for band B (see Figure 6.12). Proteins ordered by emPAI score. Protein information from UniProt (Consortium, 2015).

Band location	Proteins identified	N_o of Y residues	Ion Score	Protein mass (Da)	Confidence score	Protein function Information from UniProt	Affected in dementia
VaD >170 kDa (resolver/stacker interface) Band B	**Spectrin-β, non-erythrocytic**	**49**	**7,710**	**274,439**	**3**	**Interacts with calmodulin in a calcium-dependent manner and is thus a candidate for the calcium-dependent movement of the cytoskeleton at the membrane.**	**(Masliah et al, 1990; Sihag and Cataldo, 1996; Fernandez-Shaw et al, 1997)**
	Haemoglobin-β	3	165	15,988	1	Involved in oxygen transport from the lung to the various peripheral tissues.	(Ferrer et al, 2011; Shah et al, 2011; Chuang et al, 2012)
	Myelin proteolipid protein	14	652	30,057	1	This is the major myelin protein from the central nervous system. It plays an important role in the formation or maintenance of the multilamellar structure of myelin.	(Roher et al, 2002; Barker et al, 2013)
	Tubulin-β4A	15	809	49,554	2	Tubulin is the major constituent of microtubules. It binds two moles of GTP, one at an exchangeable site on the beta chain and one at a non-exchangeable site on the alpha-chain.	(Brion et al, 2001; Boutte et al, 2005)
	Tubulin-β	16	776	49,639	2	As above	
	Tubulin-β2A	16	738	49,875	1	As above	
	Tubulin-α4A	19	497	49,892	1	As above	
	Tubulin-α1A	19	551	50,104	0	As above	
	Haemoglobin-α	3	127	15,248	1	Involved in oxygen transport from the lung to the various peripheral tissues.	(Ferrer et al, 2011; Shah et al, 2011; Chuang et al, 2012)

Band location	Proteins identified	N_o of Y residues	Ion Score	Protein mass (Da)	Confidence score	Protein function Information from UniProt	Affected in dementia
VaD >170 kDa (resolver/stacker interface) Band B	Sodium/potassium-transporting ATPase	24	1,334	112,824	2	Catalytic component of the active enzyme, which catalyzes the hydrolysis of ATP coupled with the exchange of sodium and potassium ions across the plasma membrane. This action creates the electrochemical gradient of sodium and potassium ions, providing the energy for active transport of various nutrients.	(Adav et al, 2014)

Table 6.2C: Mass spectrometry protein identification data for band C (see Figure 6.12). Proteins ordered by emPAI score. Protein information from UniProt (Consortium, 2015).

Band location	Proteins identified	N_o of Y residues	Ion Score	Protein mass (Da)	Confidence score	Protein function Information from UniProt	Affected in dementia
Control >170 kDa (resolver/stacker interface) Band C	**Spectrin-β, non-erythrocytic**	**49**	**6,271**	**274,439**	**3**	**Interacts with calmodulin in a calcium-dependent manner and is thus a candidate for the calcium-dependent movement of the cytoskeleton at the membrane.**	**(Masliah et al, 1990; Sihag and Cataldo, 1996; Fernandez-Shaw et al, 1997)**
	Haemoglobin-β	3	147	15,988	1	Involved in oxygen transport from the lung to the various peripheral tissues.	(Ferrer et al, 2011; Shah et al, 2011; Chuang et al, 2012)
	Spectrin-α, non-erythrocytic	**41**	**3,186**	**284,364**	**3**	**Interacts with calmodulin in a calcium-dependent manner and is thus a candidate for the calcium-dependent movement of the cytoskeleton at the membrane.**	**(Masliah et al, 1990; Sihag and Cataldo, 1996; Fernandez-Shaw et al, 1997)**
	Haemoglobin-α	3	156	15,248	1	Involved in oxygen transport from the lung to the various peripheral tissues.	(Ferrer et al, 2011; Shah et al, 2011; Chuang et al, 2012)
	Serum albumin	19	2,928	69,321	2	Has a good binding capacity for water, Ca^{2+}, Na^{+}, K^{+}, fatty acids, hormones, bilirubin, and drugs. Its main function is the regulation of the colloidal osmotic pressure of blood. Major zinc transporter in plasma typically binds about 80% of all plasma zinc.	(Altunoglu et al, 2015)

Band location	Proteins identified	N_o of Y residues	Ion Score	Protein mass (Da)	Confidence score	Protein function Information from UniProt	Affected in dementia
Control >170 kDa (resolver/stacker interface) Band C	Keratin type II cytoskeletal	24	433	65,999	0	May regulate the activity of kinases such as PKC and SRC via binding to integrin beta-1 (ITB1) and the receptor of activated protein kinase C (RACK1/GNB2L1). In complex with C1QBP is a high-affinity receptor for kininogen-1/HMWK.	
	Keratin type I cytoskeletal	27	339	62,027	0	Epidermal	
	Myelin proteolipid protein	14	227	30,057	1	This is the major myelin protein from the central nervous system. It plays an important role in the formation or maintenance of the multilamellar structure of myelin.	(Roher et al, 2002; Barker et al, 2013)
	Tubulin-α1B	19	83	50,120	1	Tubulin is the major constituent of microtubules. It binds two moles of GTP, one at an exchangeable site on the beta chain and one at a non-exchangeable site on the alpha-chain.	(Brion et al, 2001; Boutte et al, 2005)
	Keratin type II cytoskeletal 2	18	154	65,393	0	Epidermal	

Table 6.2D: Mass spectrometry protein identification data for band D (see Figure 6.12). Proteins ordered by emPAI score. Protein information from UniProt (Consortium, 2015).

Band location	Proteins identified	N_o of Y residues	Ion Score	Protein mass (Da)	Confidence score	Protein function Information from UniProt	Affected in dementia
Control approx. 60 kDa Band D	**Pyruvate kinase**	**9**	**16,908**	**57,900**	**3**	**A glycolytic enzyme that catalyses the transfer of a phosphoryl group from phosphoenolpyruvate (PEP) to ADP, generating ATP. Plays a general role in caspase-independent cell death of tumour cells. The ratio between the highly active tetrameric form and nearly inactive dimeric form determines whether glucose carbons are channelled to biosynthetic processes or used for glycolytic ATP production.**	**(Butterfield et al, 2006b)**
	Rab GDP dissociation inhibitor	25	6,336	50550	2	Regulates the GDP/GTP exchange reaction of most Rab proteins by inhibiting the dissociation of GDP from them, and the subsequent binding of GTP to them. Promotes the dissociation of GDP-bound Rab proteins from the membrane and inhibits their activation. Promotes the dissociation of RAB1A, RAB3A, RAB5A and RAB10 from membranes.	(Owen et al, 2009)
	Dihydropyrimidinase-related protein 2	**14**	**7,730**	**62,255**	**3**	**Plays a role in neuronal development and polarity, as well as in axon growth and guidance, neuronal growth cone collapse and cell migration. Necessary for signalling by class 3 semaphorins and subsequent remodelling of the cytoskeleton. May play a role in endocytosis.**	**(Castegna et al, 2002)**

Band location	Proteins identified	N_o of Y residues	Ion Score	Protein mass (Da)	Confidence score	Protein function Information from UniProt	Affected in dementia
Control approx. 60 kDa Band D	V-type proton ATPase	18	3,254	56,465	2	Non-catalytic subunit of the peripheral V1 complex of vacuolar ATPase. V-ATPase is responsible for acidifying a variety of intracellular compartments in eukaryotic cells.	Mice (Chang et al, 2013; Fu et al, 2015)
	Haemoglobin-β	3	235	15,988	1	Involved in oxygen transport from the lung to the various peripheral tissues.	(Ferrer et al, 2011; Shah et al, 2011; Chuang et al, 2012)
	Haemoglobin-α	3	382	15,248	1	As above	
	Syntaxin-binding protein 1	23	1,974	67,526	2	May participate in the regulation of synaptic vesicle docking and fusion, possibly through interaction with GTP-binding proteins. Essential for neurotransmission and binds syntaxin, a component of the synaptic vesicle fusion machinery probably in a 1:1 ratio. Can interact with syntaxins 1, 2, and 3 but not syntaxin 4. May play a role in determining the specificity of intracellular fusion reactions.	
	Glucose-6-phosphate isomerase	**14**	**2,461**	**63,107**	**3**	**Besides its role as a glycolytic enzyme, mammalian GPI can function as a tumour-secreted cytokine and an angiogenic factor (AMF) that stimulates endothelial cell motility. GPI is also a neurotrophic factor (Neuroleukin) for spinal and sensory neurons.**	

Band location	Proteins identified	N_o of Y residues	Ion Score	Protein mass (Da)	Confidence score	Protein function Information from UniProt	Affected in dementia
Control approx. 60 kDa Band D	**Heat shock protein (60kDa)**	**7**	**1,795**	**61,016**	**3**	**Implicated in mitochondrial protein import and macromolecular assembly. May facilitate the correct folding of imported proteins. May also prevent misfolding and promote the refolding and proper assembly of unfolded polypeptides generated under stress conditions in the mitochondrial matrix.**	
	Alpha-aminoadipic semialdehyde dehydrogenase	14	984	58,450	2	Multifunctional enzyme mediating important protective effects. Metabolizes betaine aldehyde to betaine, an important cellular osmolyte and methyl donor. Protects cells from oxidative stress by metabolizing a number of lipid peroxidation-derived aldehydes. Involved in lysine catabolism.	

Table 6.2E: Mass spectrometry protein identification data for band E (see Figure 6.12). Proteins ordered by emPAI score. Protein information from UniProt (Consortium, 2015).

Band location	Proteins identified	N_o of Y residues	Ion Score	Protein mass (Da)	Confidence score	Protein function Information from UniProt	Affected in dementia
AD approx. 15 kDa Band E	**Haemoglobin-β**	**3**	**14,423**	**15,988**	**3**	**Involved in oxygen transport from the lung to the various peripheral tissues.**	**(Ferrer et al, 2011; Shah et al, 2011; Chuang et al, 2012)**
	Haemoglobin-δ	3	9,272	16,045	2	As above (foetal subunit).	
	Haemoglobin-α	**3**	**7,804**	**15,248**	**3**	**As above**	
	Histone H4	4	1,018	11,360	2	Histones play a central role in transcription regulation, DNA repair, DNA replication and chromosomal stability.	(Narayan et al, 2015)
	Fatty acid binding protein	2	760	14,849	2	FABP are thought to play a role in the intracellular transport of long-chain fatty acids and their acyl-CoA esters.	(Desikan et al, 2013; Olsson et al, 2013)
	Cytochrome C	5	507	11,741	1	Electron carrier protein. Plays a role in apoptosis. Suppression of the anti-apoptotic members or activation of the pro-apoptotic members of the Bcl-2 family leads to altered mitochondrial membrane permeability resulting in the release of cytochrome c into the cytosol. Binding of cytochrome c to Apaf-1 triggers the activation of caspase-9, which then accelerates apoptosis by activating other caspases.	

Band location	Proteins identified	N_o of Y residues	Ion Score	Protein mass (Da)	Confidence score	Protein function Information from UniProt	Affected in dementia
AD approx. 15 kDa Band E	Profilin-1	5	406	15,045	1	Binds to actin and affects the structure of the cytoskeleton. At high concentrations, profilin prevents the polymerization of actin, whereas it enhances it at low concentrations. By binding to PIP2, it inhibits the formation of IP3 and DG. Inhibits androgen receptor (AR) and HTT aggregation and binding of G-actin is essential for its inhibition of AR.	
	Cystatin B	3	378	11,133	1	This is an intracellular thiol proteinase inhibitor. Tightly binding reversible inhibitor of cathepsins L, H, and B.	Conflicting results (Žerovnik, 2009)
	Galectin 1	2	364	14,706	2	May regulate apoptosis, cell proliferation, and cell differentiation. Binds beta-galactoside and a wide array of complex carbohydrates. Inhibits CD45 protein phosphatase activity and therefore the dephosphorylation of Lyn kinase. Strong inducer of T-cell apoptosis.	
	Profilin-2	7	654	15,036	2	Binds to actin and affects the structure of the cytoskeleton. At high concentrations, profilin prevents the polymerization of actin, whereas it enhances it at low concentrations. By binding to PIP2, it inhibits the formation of IP3 and DG.	

Table 6.2F: Mass spectrometry protein identification data for band F (see Figure 6.12). Proteins ordered by emPAI score. Protein information from UniProt (Consortium, 2015).

Band location	Proteins identified	N_o of Y residues	Ion Score	Protein mass (Da)	Confidence score	Protein function Information from UniProt	Affected in dementia
Control approx. 18 kDa Band F	**Peptidyl-prolyl cis-trans isomerase**	**2**	**4,457**	**18,001**	**3**	**PPIases accelerate the folding of proteins. It catalyses the cis-trans isomerization of proline imidic peptide bonds in oligopeptides.**	**(Thorpe et al, 2004; Blair et al, 2015)**
	Histone H2B type 1C	5	1,429	13,898	2	A core component of nucleosome. DNA accessibility is regulated via a complex set of post-translational modifications of histones, also called histone code and nucleosome remodelling. Has broad antibacterial activity. May contribute to the formation of the functional antimicrobial barrier of the colonic epithelium, and to the bactericidal activity of amniotic fluid.	(Narayan et al, 2015)
	Histone H2B type 1B	5	1,358	13,942	2	A core component of nucleosome. DNA accessibility is regulated via a complex set of post-translational modifications of histones, also called histone code and nucleosome remodelling.	
	Haemoglobin-β	3	341	15,988	1	Involved in oxygen transport from the lung to the various peripheral tissues.	(Ferrer et al, 2011; Shah et al, 2011; Chuang et al, 2012)
	Peroxiredoxin-V	2	1,443	22,073	2	Reduces hydrogen peroxide and alkyl hydroperoxides with reducing equivalents provided through the thioredoxin system. Involved in intracellular redox signalling.	

Band location	Proteins identified	N_o of Y residues	Ion Score	Protein mass (Da)	Confidence score	Protein function Information from UniProt	Affected in dementia
Control approx. 18 kDa Band F	Nucleoside diphosphate kinase	4	494	17,287	2	Major role in the synthesis of nucleoside triphosphates other than ATP. Negatively regulates Rho activity by interacting with AKAP13/LBC. Acts as a transcriptional activator of the MYC gene; binds DNA non-specifically. Exhibits histidine protein kinase activity	
	Visinin-like protein	5	355	22,128	1	Regulates (in vitro) the inhibition of rhodopsin phosphorylation in a calcium-dependent manner.	(Lee et al, 2008; Luo et al, 2013)
	Gamma-synuclein	1	291	13,323	1	Plays a role in neurofilament network integrity. May be involved in modulating axonal architecture during development and in the adult. In vitro, increases the susceptibility of neurofilament-H to calcium-dependent proteases (By similarity). May also function in modulating the keratin network in skin. Activates the MAPK and Elk-1 signal transduction pathway (By similarity).	(Mukaetova-Ladinska et al, 2008)
	Destrin	4	243	18,493	2	Actin-depolymerizing protein. Severs actin filaments (F-actin) and binds to actin monomers (G-actin). Acts in a pH-independent manner.	
	Tubulin-β2A	16	1,108	49,875	2	Tubulin is the major constituent of microtubules. It binds two moles of GTP, one at an exchangeable site on the beta chain and one at a non-exchangeable site on the alpha-chain.	(Brion et al, 2001; Boutte et al, 2005)

Table 6.2G: Mass spectrometry protein identification data for band G (see Figure 6.12). Proteins ordered by emPAI score. Protein information from UniProt (Consortium, 2015).

Band location	Proteins identified	N_o of Y residues	Ion Score	Protein mass (Da)	Confidence score	Protein function Information from UniProt	Affected in dementia
Control approx. 15 kDa Band G	**Haemoglobin-β**	**3**	**11,795**	**15,988**	**3**	**Involved in oxygen transport from the lung to the various peripheral tissues.**	**(Ferrer et al, 2011; Shah et al, 2011; Chuang et al, 2012)**
	Haemoglobin-δ	3	7,201	16,045	2	As above (foetal subunit).	
	Haemoglobin-α	**3**	**6,266**	**15,248**	**3**	**As above**	
	Histone H4	4	1,132	11,360	2	Histones play a central role in transcription regulation, DNA repair, DNA replication and chromosomal stability. DNA accessibility is regulated via a complex set of post-translational modifications of histones, also called histone code and nucleosome remodelling.	(Narayan et al, 2015)
	Cytochrome b-c1 complex	7	288	13,522	1	This is a component of the ubiquinol-cytochrome c reductase complex (complex III or cytochrome b-c1 complex), which is part of the mitochondrial respiratory chain. This component is involved in redox-linked proton pumping.	
	Cytochrome c oxidase	4	76	8,776	1	This protein is one of the nuclear-coded polypeptide chains of cytochrome c oxidase, the terminal oxidase in mitochondrial electron transport.	(Parker et al, 1990; Kish et al, 1992; Maurer et al, 2000; Cottrell et al, 2002)

Control approx. 15 kDa Band G	Cytochrome c	5	362	11,741	1	Electron carrier protein. Plays a role in apoptosis. Suppression of the anti-apoptotic members or activation of the pro-apoptotic members of the Bcl-2 family leads to altered mitochondrial membrane permeability resulting in the release of cytochrome c into the cytosol. Binding of cytochrome c to Apaf-1 triggers the activation of caspase-9, which then accelerates apoptosis by activating other caspases.	
	Haemoglobin-γ1	2	1,082	16,130	2	Sub-unit of foetal Hb. Involved in oxygen transport from the lung to the various peripheral tissues.	(Ferrer et al, 2011; Shah et al, 2011; Chuang et al, 2012)
	Haemoglobin-γ2	2	1,036	16,116	2	As above	
	Galectin 1	2	378	14,706	2	May regulate apoptosis, cell proliferation, and cell differentiation. Binds beta-galactoside and a wide array of complex carbohydrates. Inhibits CD45 protein phosphatase activity and therefore the dephosphorylation of Lyn kinase. Strong inducer of T-cell apoptosis.	

6.3. Discussion

Dementia affects 35 million people worldwide and this figure is expected to rise to 65.7 million by 2030 (Sosa-Ortiz et al, 2012). New biomarkers are needed to help identify AD pathology in the early stages and to assess drug efficacy in clinical trials (Hampel et al, 2010).

Increased oxidative stress has been observed in dementia, though its precise role in pathology is unknown. Some oxidative stress pathways thought to play a role in either initiating or maintaining the damage seen in the brain are: (a) H_2O_2 generation by amyloid-β plaques (Bush, 2003; Milton, 2004; Tabner et al, 2005), (b) reduced activity of SOD (Marcus et al, 1998; Omar et al, 1999; Esposito et al, 2006; Murakami et al, 2011), with increased $O_2^{\bullet-}$ linked with AD (Guo et al, 1999), (c) increased $^{\bullet}NO$ production (stimulated by amyloid-β (Akama et al, 1998)) and (d) Increased expression of MPO, which can lead to the generation of hypochlorous acid (Crawford et al, 2001; Green et al, 2004). Tyr-NO_2 generation has been reported in AD (Good et al, 1996; Hensley et al, 1998; Calabrese et al, 2006; Butterfield et al, 2007b), and the pathways activated above are all involved in its production, e.g. the increased $O_2^{\bullet-}$ and $^{\bullet}NO$ react to produce peroxynitrite and MPO catalyses nitration in the presence of NO_2^-.

The data collected from the 'proof of concept' mouse study suggests that a statistically significant difference in Tyr-NO_2 levels can be observed when comparing WT and Tg mice (**Figure 6.2**). This suggests that the AD pathology exhibited in these animals leads to an increase in ROS and thus nitration. Other authors have reported increased oxidative damage in the brains of animal AD models (Smith et al, 1998; Pratico et al, 2001; Sultana et al, 2009).

There was also a significant difference between the Tau35 model and the Tas-TPM model (**Figure 6.3**), with Tau35 producing a higher median nitration. As detailed previously, these models produce different pathologies associated with AD. The Tau35 model has an expression of insoluble tau and Tas-TPM has amyloid pathology. This result needs to be investigated further with a larger *n* number but, it could be hypothesised that the tau pathology is the main contributor to increased oxidative stress, rather than amyloid plaques. Given that oxidative damage is implicated in AD pathology and can affect multiple cellular pathways this would be a very important difference, with implications as

to which model is the most relevant. There is evidence that in AD amyloid-β and tau interact to increase the others toxicity (Bloom, 2014). Amyloid-β is upstream of tau which then feeds back to amyloid-β, creating a toxic loop (Castillo-Carranza et al, 2015). However, tau has a greater association with cognition and memory deficit and is increasingly being considered a more important target for AD therapy (Giacobini and Gold, 2013). Therefore, if increased oxidative/nitrative stress is associated with tau pathology, rather than amyloid-β aggregation, oxidative damage may be an important part of the neurotoxicity shown by tau and a target for treatment.

When separating the samples by all factors, e.g. different models, transgenic, wildtype and brain region the number in each group becomes very small. However, as a preliminary study, it shows that nitration is detectable within the mouse brain for both the wild type and transgenic models.

The pilot study, on human tissue, did not find a significant difference in nitration of frontal lobe brain samples when comparing AD with VaD or non-demented controls (**Figure 6.6**). This challenges the current consensus that AD patients are more prone to Tyr-NO_2 formation in the brain (Good et al, 1996; Castegna et al, 2003; Butterfield et al, 2006a; Sultana et al, 2006; Butterfield et al, 2007b; Sultana et al, 2007; Reed et al, 2009). The results reported here also show a higher concentration of NO_2^- in the AD brain tissue (**Figure 6.9**) compared to non-demented controls ($p<0.05$). This contradicts DiCiero Miranda et al (2000), who found NO_x to be decreased in the frontal cortex of the AD brain compared to non-demented age-matched controls. The NO_x levels reported by DiCiero Miranda et al (2000) are 30.66 ± 3.10 (n = 5) and 56.85 ± 8.26 (n = 7) nmol/g tissue for AD and controls respectively. If it is assumed that each of the samples measured in our study were exactly 200mg/ml tissue (see homogenization protocol, section 6.1), then the levels observed in AD brain tissue were 4 times higher than found by DiCiero Miranda et al (2000): 135 nmol/g compared to 31 nmol/g respectively. DiCiero Miranda et al (2000) used cadmium to reduce NO_3^- to NO_2^-, followed by measurement using the Griess reagent. However, the study reported here used vanadium (III) chloride (at 95°C) to reduce the NO_3^-, and ozone-based chemiluminescence for measurement. This difference in methodology could account for the vast difference in NO_3^- levels measured in brain tissue.

As both MPO and H_2O_2 have been shown to be increased in AD (Crawford et al, 2001; Bush, 2003; Green et al, 2004; Milton, 2004; Tabner et al, 2005) and MPO/H_2O_2/NO_2^- is a possible pathway for Tyr-NO_2 formation (see Chapter 1, section 1.5) the increase of NO_2^-, in AD, but not Tyr-NO_2 would seem contradictory. However, there are a few possible explanations: (a) the increased MPO expression has not translated to an increase in MPO activity and/or (b) the MPO is being inactivated by high levels of H_2O_2 (Kettle et al, 1993; Olorunniji et al, 2009; Paumann-Page et al, 2013).

Previous methods that have shown a difference in nitration between AD and controls groups (mild cognitive impairment and no dementia) have used immunoblot or immunochemistry to analyse Tyr-NO_2 in the brain (Castegna et al, 2003; Butterfield et al, 2006a; Sultana et al, 2006; Butterfield et al, 2007b; Sultana et al, 2007; Reed et al, 2009). Immunochemistry is not quantitative in terms of overall nitration but does highlight tissue localization of Tyr-NO_2, which may go some way towards explaining the differences in the literature and the results reported here.

The brain region most commonly investigated is the hippocampus, whilst this region has shown high rates of atrophy in the early (pre-symptomatic) stages of AD (Scahill et al, 2002) other hallmarks such as amyloid deposits and neurofibrillary changes are not observed here until later stages (modest in stage 3, numerous in stage 4) (Braak and Braak, 1991). The progression of AD through the brain has been shown to happen in a defined pattern, with different regions affected at different stages (Braak and Braak, 1991; Ohm et al, 1995; Scahill et al, 2002). Different levels of nitration have also been observed in different brain regions of AD patients, with the hippocampus showing very high levels (Hensley et al, 1998). Therefore, it may be that the nitrative burden was not significantly different between dementia and healthy aged brains within the frontal lobe but is within different regions, as shown in other studies.

Some of the immunoblot studies used trichloroacetic acid (TCA) protein precipitation (Sultana et al, 2006; Sultana et al, 2007; Reed et al, 2009) which, in light of the increased NO_2^- we have observed in AD, risks increased artefact formation during sample preparation in AD (due to the possibility of nitration under acidic conditions in the presence of NO_2^-) (Ohshima et al, 1990;

Shigenaga et al, 1997). A study using HPLC-electrochemical detection considered the effect this treatment may have during sample preparation and report that incubating tyrosine with NO_2^- and 6% TCA led to less than 0.01% Tyr-NO_2 formation (Hensley et al, 1998). *In vivo* levels of serum protein nitration is thought to be around 0.01% (Radi, 2004), therefore this level of artefact formation in immunoblots (where up to 15% TCA was used) could have a large impact on the relative levels of Tyr-NO_2 observed between groups. However, within this study, brain nitration levels are far higher than serum levels (Chapter 3), so 0.01% artefact nitration would have a smaller impact on the results. Artificial nitration may also affect which proteins are observed to be nitrated, as different nitration methods have shown different protein selectivity (Souza et al, 1999).

As mentioned, the mouse study (section 6.2.1) found a significant difference in brain tissue nitration levels between wildtype mice and transgenic mouse models of AD (**Figure 6.2**). There was also a statistically significant difference in median brain tissue nitration when comparing the human and mouse samples (**Figure 6.8**), with the mouse brain showing a higher median Tyr-NO_2 levels. This disagreement between the human and mouse studies may be due to species differences and/or due to the shorter delay in collecting and freezing the mouse samples. Protein degradation, for some proteins, will increase over time. Therefore, a sample with a long post-mortem interval (PMI) will have more degradation than a sample with a small PMI (Ferrer et al, 2008; ElHajj et al, 2016). However, as results are adjusted for protein content this would only affect the results if nitrated proteins were preferentially degraded post-mortem. PMI has also been found to effect post-translational modification of proteins, though Ferrer et al (2008) found that nitration levels increased after 20 hours. If this effect were seen here then the human samples would have had higher levels of Tyr-NO_2, than the mice, as the mean PMI in humans was 44 hours. Additionally, there was no correlation between Tyr-NO_2 levels and PMI in the human brain tissue.

Within the human study, western blotting revealed some bands that were consistently nitrated in brain tissue; this was also seen in the mouse western blots (**Figure 6.5**). The main Tyr-NO_2 positive bands in the human tissue were approximately 15 kDa and 18 kDa in size (**Figure 6.11**). The mouse western

blots need to be run with a biotin blocking step, prior to primary antibody incubation, due to endogenous biotin. However, the absence of the low molecular weight bands, in the blot run without the anti-Tyr-NO_2 antibody (**Figure 6.5**), suggests that they are truly nitrated in this tissue as well. When analysing the human tissue western blots the median signal ratio (Tyr-NO_2/actin) for the ~15 kDa band was slightly higher in the dementia groups but this did not reach significance (Kruskal-Wallis, p = 0.06). The ~18 kDa band had a similar median value between groups (Kruskal-Wallis, p= 0.41).

Several nitrated proteins have been identified in AD by others, such as α-enolase, triose phosphate isomerase, ATP synthase, voltage-dependent anion channel protein 1 and β-actin (Butterfield et al, 2011). Here mass spectrometry was used to identify the proteins within a selection of human Tyr-NO_2 positive bands, including the two bands discussed above (**Figure 6.12**). Due to the crude nature of the sample, numerous proteins were identified within each band. The data was therefore organised by the emPAI score (score of abundance) and the data of the top ten assessed.

As can be seen from **Table 6.2E/G** the most abundant protein for bands E and G (**Figure 6.12** ~15 kDa band, AD and control) was haemoglobin, with multiple subunits listed. The haemoglobin (Hb) subunits contain 3 Tyr residues each, are the right molecular weight for the band and had high ion scores. Hb has been shown to be nitrated by the H_2O_2/ NO_2^- pathway (Chen et al, 2008) and is thought to be a good indicator of overwhelmed anti-oxidant defences in erythrocytes (Xiang et al, 2013). α and β neuronal Hb chains have been found to be expressed in mouse, rat, and human brain tissue, the functions of this neuronal Hb are unknown but its expression is lowered in neurodegenerative diseases such as AD (Ferrer et al, 2011). Additionally, both anaemia and clinically high levels of Hb have been associated with increased risk of AD and cognitive decline in older populations (Shah et al, 2011). Hb has also been shown to bind to amyloid-β peptide (Chuang et al, 2012), a site of H_2O_2 production (Bush, 2003; Milton, 2004; Tabner et al, 2005). As altered Hb has been associated with AD, can be nitrated and is an abundant protein in the band, it would suggest that the signal in the western blot is from nitrated Hb. However, this makes the assumption that the most abundant protein is the

protein that is nitrated when it could be a low abundance protein that is highly nitrated.

If it is Hb that has been nitrated this opens up the possibility that this could be measured as a peripheral marker, i.e. in erythrocytes. This has the advantage of being a sample that is not only available prior to death but readily available through routine practice, where any differences could potentially be used as a tool for prognosis, or monitoring disease progression. There has been contradictory data regarding the oxidant/antioxidant balance in erythrocytes from AD patients, with studies reporting: decreased activity for copper containing SOD (Snaedal et al, 1998), increased activity of glutathione peroxidase (Annerén et al, 1986) and no differences in activity for copper-zinc SOD, seleno-dependent glutathione peroxidase or glutathione reductase (Ceballos-Picot et al, 1996), when comparing AD to non-demented controls. Delibas et al (2002) measured erythrocyte antioxidant enzyme levels in the same dementia patients (described as dementia of the Alzheimer type) 5 years apart and found that copper-zinc SOD levels increased and glutathione peroxidase levels decreased, they also reported a significant negative correlation between erythrocyte malondialdehyde (a measure of lipid peroxidation) and a mental state examination. Although contradictory these studies suggest that an oxidative imbalance can occur in the erythrocytes of AD patients and that therefore Tyr-NO_2 may be present, and measurable, in these cells.

Actin was used as a loading control for the western blotting, the main actin band is at 45 kDa (expected weight). However, faint staining for actin is also observed under the 35 kDa and 15 kDa markers. Cleavage of actin by caspase 1 is known to produce 31 and 15 kDa fragments, and this cleavage has been linked to apoptosis (Mashima et al, 1999). Therefore, the proportion of actin cleavage was calculated for each human sample to see if there was a difference in cleavage/apoptosis between groups. No significant difference in actin cleavage was observed between the groups (Kruskal-Wallis $p=0.74$).

A limitation to this study is the use of a single time point, rather than measuring nitrative stress over the course of the disease. This is impossible in humans due to the use of post-mortem tissue but mouse models can be studied from a time

point prior to disease manifestation right through to the advanced stages. Additionally, the measurement of other oxidative stress markers, such as carbonyls, in combination with Tyr-NO_2, nitrite and nitrate would have given a more complete picture of oxidative damage occurring in dementia.

6.4. Conclusion

Mouse models give insight into underlying pathology during disease progression and the testing of potential therapeutic strategies. Identifying a marker of oxidative stress that is increased in the transgenic mice, compared to wild-type, would allow more information of the disease process to be collected and antioxidant drug efficacy to be assessed.

Although the human study did not show any difference in nitration between the three groups (AD, VaD, and no dementia) the fact that particular proteins are responsible for the majority of the nitration seen leads us to believe that further investigation into what these proteins are, and how they are affected by nitration would be worthwhile. Mass spectrometry analysis suggests that one of these proteins is Hb. It would be of particular interest if Hb were the nitrated protein seen at ~15 kDa, as nitration of Hb in the blood could be measured at different stages of AD, in the same person, via a routine blood test. Interestingly there is a small amount of evidence that this protein is nitrated in mouse models of AD too and could therefore be a marker in animal studies as well. Currently, nitration differences in humans with AD have only be measured in brain tissue collected post-mortem and in cerebrospinal fluid, a difficult sample to obtain (Tohgi et al, 1999). Dildar et al (2010) measured plasma nitration and found no difference between AD, VaD, and no dementia. However, it could be that the protein of interest had been removed from the blood during sample preparation (i.e. the Hb in the erythrocytes). Further work could involve adaption of the sandwich ELISA so that the capture Ab binds Hb and the detection Ab binds to Tyr-NO_2 within the Hb. This would allow for the measurement of nitrated Hb only (rather than total) and show if there are any quantitative differences in nitration between sample sets, something that cannot be done accurately with a western blot.

As well as identifying the nitrated proteins, future study should determine whether, when looking at different brain regions, a difference between AD and

non-demented controls does become apparent when quantifying overall Tyr-NO_2 levels by ELISA in humans.

6.5. Acknowledgments

The mouse brain tissue samples were supplied by Professor Andrew Randall and Dr Francesco Tamagnini (University of Exeter Medical School).

The project measuring •NO metabolites and protein nitration in human brain tissue was funded by University of Exeter Research Knowledge Transfer and was in collaboration with the South West Dementia Brain Bank.

We would like to thank the South West Dementia Brain Bank (SWDBB) for providing brain tissue for this study. The SWDBB is part of the Brains for Dementia Research programme, jointly funded by Alzheimer's Research UK and Alzheimer's Society and is supported by BRACE (Bristol Research into Alzheimer's and Care of the Elderly) and the Medical Research Council.

Dr Miranda Smallwood performed the ozone-based chemiluminescence for NO_2^- and NO_3^- measurement and assisted with the western blots on human samples.

Mass spectrometry (TOF-MS/MS) was done by Professor A Pitt, Dr C Spickett and Dr K Tveen-Jensen (Aston University).

Chapter 7

General Discussion and Future Work

Oxidative/nitrative stress has been studied in many diseases and it is becoming increasingly evident that ROS/RNS mediated damage plays a role in the pathology of many, diverse conditions e.g. cardiovascular disease (Shishehbor et al, 2003; Eleuteri et al, 2009), neurodegenerative disease (Beal et al, 1997; Butterfield et al, 2007a) and dysfunctional immune responses, i.e. autoimmunity (Khan et al, 2006; Eggleton et al, 2008) and sepsis (Fukuyama et al, 1997; Ohya et al, 2002). Despite many years of research, the accurate measurement of oxidative stress is still an area in need of analytical improvement, with many markers being non-specific or requiring expensive/time-consuming techniques, such as mass spectrometry, for accurate measurement (Frijhoff et al, 2015). More clinical studies, such as randomised drug trials or prospective studies, are also needed to be able to assess the sensitivity and specificity of oxidative stress biomarkers (Frijhoff et al, 2015).

RNS such as $^{\bullet}NO$ and $ONOO^{-}$ are upregulated during inflammation and damaging levels have been associated with inflammatory diseases (e.g. sepsis), chronic diseases with an inflammatory component (e.g. Alzheimer's disease) and tissue insult (e.g. surgery). Tyr-NO_2 is becoming an increasingly popular marker of RNS production but accurate and valid measurement has faced several methodological issues (Herce-Pagliai et al, 1998; Duncan, 2003). The gold standard of measurement for Tyr-NO_2 is mass spectrometry but this is low-throughput and expensive. Commercial ELISAs are available but they have low sensitivity, limiting their usefulness when applied to diseased human plasma samples. Within this project, a new sensitive ELISA for Tyr-NO_2 measurement was developed. $^{\bullet}NO$ production is also measured as a marker of nitrative stress, this is often done by measuring its metabolites, NO_2^{-} and NO_3^{-}. Measurement of NO_2^{-} and NO_3^{-} is frequently performed using the Griess reaction. However, the more sensitive highly validated method of ozone-based chemiluminescence was utilised here.

Within in this project, the aims have been to measure nitrative stress in samples with varying inflammatory conditions and to assess the clinical utility of Tyr-NO_2. A Tyr-NO_2 ELISA was developed, based on an electrochemiluminescence

(ECL) platform, ECL uses an electrically stimulated chemical reaction to produce light and this is then measured. This platform improves the sensitivity of the assay, when compared to colorimetric platforms, due to a decreased background (**Figure 3.2**). An ELISA method offers high throughput and requires little sample preparation but is semi-quantitative. The method developed within this project provided an assay with high sensitivity (LLOQ 0.04 nM BSA-NO_2) and high reproducibility within and between runs (intra-assay CV 6.5% and inter-assay CV 14%). Additionally, the relative nitration of three BSA samples (non-modified, nitrated and dithionite treated) was measured by mass spectrometry and supported the ELISA results.

The assay was applied for the measurement of Tyr-NO_2 in serum samples from patients pre- and post-surgery. The surgery was viewed as an instigator of an acute inflammatory response, and this was confirmed by serum CRP measurements. Following the surgery/initiation of inflammation a significant increase in Tyr-NO_2 levels was observed (median (IQR): 0.59 (0 – 1.3) and 0.97 (0 – 1.7) Tyr-NO_2 fmol BSA-NO_2 equiv./mg protein for pre- and post-surgery respectively). These results are in keeping with the production of ROS during inflammation and confirm the assay's sensitivity, as many of these samples were below the LOD of commercial ELISAs for Tyr-NO_2 measurement. The assay was also successfully applied for the measurement of Tyr-NO_2 in blood cell lysates. The intracellular levels of Tyr-NO_2 were far higher than the extracellular serum levels, with the highest levels being found in the cell line U937: median Tyr-NO_2 levels – serum 0.59, erythrocytes 11.18, mononuclear cells 742.96 and U937 cells 3160 fmol BSA-NO_2 equivalents/mg protein.

Our research group has previously performed extensive studies on NO_3^- rich supplementation, due to its potential beneficial physiological effects that are thought to be a result of the reduction of NO_3^- to $^{\bullet}NO$ (Duncan et al, 1995; Gilchrist et al, 2010; Jones, 2014). Based on the fact that NO_3^- can be reduced to NO_2^- and $^{\bullet}NO$ *in vivo* (Duncan et al (1995); **Figure 4.1**) we were interested in whether increased dietary intake of NO_3^- led to nitration of proteins (i.e. Tyr-NO_2 formation), in the saliva or in plasma. This was studied with a focus on smokers, as inflammatory reactions have been shown to be stimulated by cigarette smoking, e.g. elevated serum MPO has been observed in smokers compared to non-smokers (Martins et al, 2013). Nitration of proteins can affect

their function, and oxidative post-translational modifications of proteins can create neo-epitopes that have been linked to autoimmune reactions (Ryan et al, 2014).

Both plasma and saliva, from healthy individuals, were measured for nitrated protein, NO_2^-, and NO_3^-. Following the NO_3^--rich supplementation both plasma and saliva NO_2^- and NO_3^- levels increased significantly (**Figure 4.5** and **Figure 4.8**). Plasma showed very low levels of Tyr-NO_2 (often near the LLOQ) regardless of whether the participant was a non-smoker or smoker, or taking NO_3^--rich supplementation (non-smokers and smokers after NO_3^--rich supplementation: median (IQR) 0.97 (0.57 – 1.92) and 1.13 (0.69 – 2.23) Tyr-NO_2 fmol BSA equiv./mg protein respectively, **Figure 4.3**). However, saliva showed 1000-fold higher levels of nitrated protein compared to the plasma and, interestingly, salivary Tyr-NO_2 levels were decreased with NO_3^--rich supplementation: median (IQR) before and after supplementation: 0.67 (0.31 – 1.14) and 0.42 (0.10 – 0.59) Tyr-NO_2 pmol BSA equiv./mg protein respectively, non-smokers and smokers combined. One possible explanation is $^{\bullet}NO$ production in excess of $O_2^{\bullet -}$ (so it is not all used in $ONOO^-$ formation). Salivary $^{\bullet}NO$ was previously shown to have anti-microbial activity (De Groote and Fang, 1995; Duncan et al, 1995) which would lead to less inflammation and therefore less MPO activity and $O_2^{\bullet -}$ formation, resulting in decreased Tyr-NO_2 formation.

Future work should investigate whether, following NO_3^--rich supplementation, decreased salivary Tyr-NO_2 levels did correlate with decreased salivary inflammatory markers, such as IL1-β.

Sepsis is a dysregulated immune response to infection involving pro- and anti-inflammatory components, e.g. increased levels of circulating pro-inflammatory cytokines and reduced lymphocyte numbers (Adib-Conquy and Cavaillon, 2008). Tyr-NO_2 was previously measured in septic shock (Fukuyama et al, 1997; Ohya et al, 2002), with results suggesting that Tyr-NO_2 could have a prognostic value (Ohya et al, 2002). To investigate whether increased Tyr-NO_2 levels are seen prior to diagnosis a time course of serum samples was collected, from a cohort of patients with and without postoperative sepsis, with samples being collected one day before surgery and every day subsequently

until diagnosis. At one day prior to diagnosis, the levels of Tyr-NO_2 were significantly higher in the sepsis group compared to the group which did not develop sepsis (controls); the median values were 4.5 and 1.2 fmol BSA-NO_2 equiv./mg protein respectively (**Figure 5.4**). As far as we are aware, this is the first time Tyr-NO_2 has been measured prior to a clinical diagnosis of sepsis and demonstrates that elevated oxidative/nitrative stress can already be observed at this time point when compared to non-septic controls.

The diagnostic potential of serum Tyr-NO_2 was also assessed. When compared to serum CRP concentrations, an established marker of inflammation, the Tyr-NO_2 was not as sensitive at differentiating patients who would develop sepsis from those who would not (as determined by ROC analysis). Tyr-NO_2 levels did not show a statistically significant correlation with CRP concentrations. Furthermore, when the markers were combined, there was no additive effect on specificity and sensitivity (net reclassification index –0.2).

Sepsis is a highly heterogeneous disease and future work, on a larger number of samples, would allow for stratification of samples into groups based on factors such as the type of surgery being undertaken or patient outcome. This approach has been put forward to improve sepsis definition, with the PIRO (Predisposition, Infection, Response and Organ dysfunction) staging model suggested as a means of creating more informative groupings (Vincent et al, 2009; Howell et al, 2011; Granja et al, 2013).This refined grouping would provide information on which individuals experience the highest levels of oxidative stress. The relationship, if any, between Tyr-NO_2 levels prior to diagnosis and prognosis should also be assessed.

Oxidative stress has been implicated in Alzheimer's disease (AD) pathology and Tyr-NO_2 has been observed in brain tissue (Castegna et al, 2003; Butterfield et al, 2007b; Sultana et al, 2007). We measured Tyr-NO_2 in mouse brain tissue homogenates and observed that transgenic mouse models of AD had higher median values than wildtype mice: median (IQR) 1.36 (1.07 – 1.97) and 1.04 (0.72 – 1.53) Tyr-NO_2 pmol BSA equiv./mg protein respectively.

We also investigated nitrative stress in human brain tissue homogenates, of patients with dementia, compared to age-matched control individuals without dementia. Mean NO_2^- levels in the brain tissue were significantly higher in the

AD brain compared to the controls (AD and non-demented: 0.12 ± 0.05 and 0.09 ± 0.03 nmol/mg protein respectively). This suggests an increase in $^{\bullet}NO$ formation. However, contradictory to published studies (Castegna et al, 2003; Butterfield et al, 2007b; Sultana et al, 2007), the data reported here showed no difference in total nitration between AD and controls (**Figure 6.6**). This could be due to methodological differences; here a semi-quantitative ELISA was used when many investigators have reported differences based on immunohistochemistry. The type and range of brain regions investigated could also impact on the results achieved by different groups as Hensley et al (1998) has shown oxidative damage to vary between different brain regions, for example the hippocampus has higher levels than other brain regions. In the study reported in this thesis, the levels of nitrated protein in the brain tissue were far higher than seen in serum from patients with sepsis, suggesting that nitrative modification is at its greatest in tissue rather than in circulation. Western blotting of the human brain tissue revealed that much of the nitration was in a band at approximately 15 kDa (as well as in a band at approximately 18 kDa). Mass spectrometry analysis of the bands revealed that haemoglobin subunits were abundant within the ~15kDa band (**Table 6.2**).

Future work, utilising mass spectrometry, should confirm that the haemoglobin within the western blot band is nitrated. If it is, then a further study, using the ECL ELISA, would look at red blood cell Tyr-NO_2 levels. A blood biomarker of oxidative stress in AD would be of huge benefit to the field as (a) it could allow monitoring of the disease/treatment efficacy and (b) it could aid diagnosis as, currently, a definitive diagnosis can only be obtained upon post-mortem examination.

During this project nitrative stress was measured in multiple sample types, in health and disease, using ozone-based chemiluminescence and a new ECL assay. These methods were selected for a more robust and validated approach to measuring nitrative stress as this field of study has been hindered by methodological problems. Further improvements to the Tyr-NO_2 ECL assay are envisioned. In particular, the generation of a fully quantified standard. The current standard is a commercial preparation of nitrated BSA (BSA-NO_2). The number of nitrated residues on each molecule of BSA is unknown. Therefore, results cannot be quantified in terms of the absolute Tyr-NO_2 concentration.

Instead, the results are displayed as an equivalence to the BSA-NO_2 concentration. While there are further modifications and improvements that can be made to the assay, this '*version 1.0'* has still proven to be useful in comparing sample sets and highlighting future directions of study. For example, this project has shown that Tyr-NO_2 is increased prior to a diagnosis of post-surgery sepsis. A further study, with patients staged using the PIRO model, would determine if this could be an additional marker of diagnosis/prognosis in certain patient populations. Analysis of brain tissue nitration contradicted the published literature but, when combined with the blood cell lysate analysis, highlighted that the study of intracellular (e.g. blood cells) Tyr-NO_2 levels may be an overlooked area of research.

Another important consideration is whether oxidative stress should be measured in a 'broader' way, i.e. measuring a panel of oxidative stress markers in combination rather than just one or two. This approach, whilst time consuming and more expensive, would allow for a more complete overview of what is happening in different diseases, as different oxidative stress/inflammatory pathways will be activated to varying levels and analysing just one marker may miss crucial information.

Appendix 1

No post-surgery sepsis group

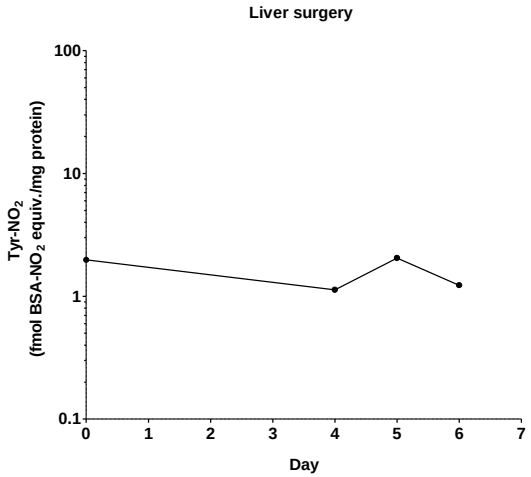

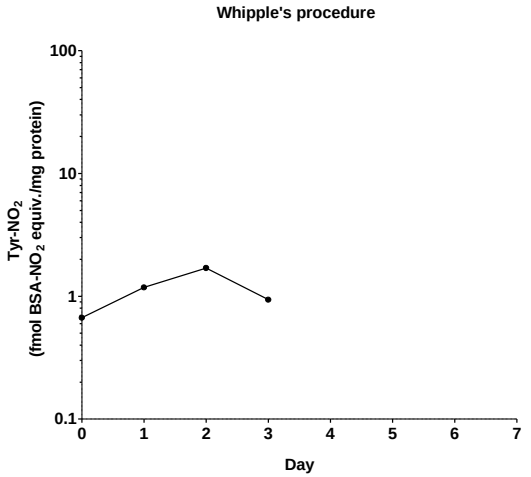

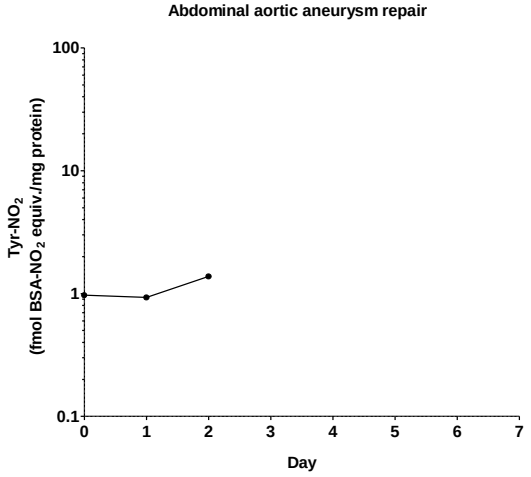

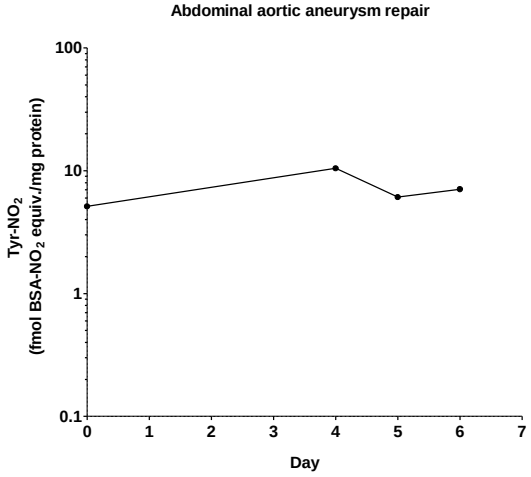

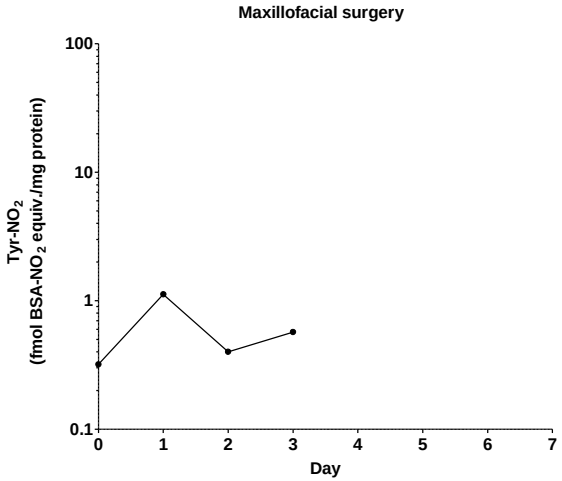
Maxillofacial surgery
Tyr-NO2
(fmol BSA-NO2 equiv./mg protein)
100
10
1
0.1
0
1
2
3
4
5
6
7
Day

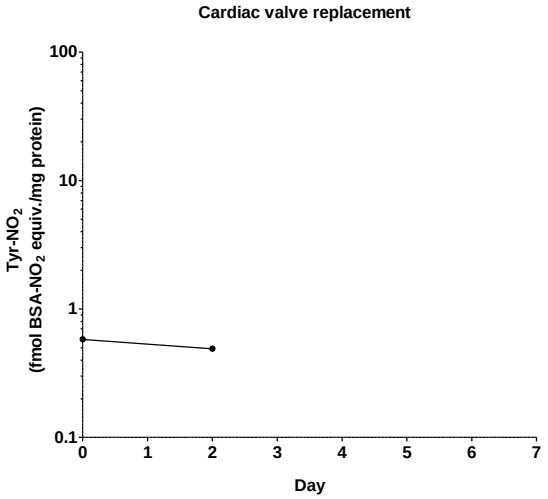
Cardiac valve replacement
Tyr-NO2
(fmol BSA-NO2 equiv./mg protein)
100
10
1
0.1
0
1
2
3
4
5
6
7
Day

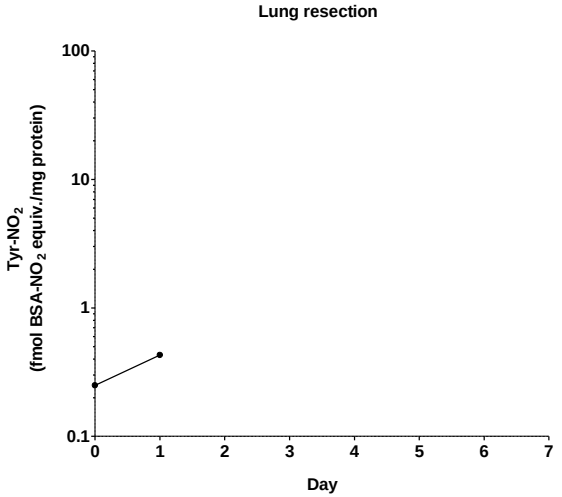
Lung resection
Tyr-NO2
(fmol BSA-NO2 equiv./mg protein)
100
10
1
0.1
0
1
2
3
4
5
6
7
Day

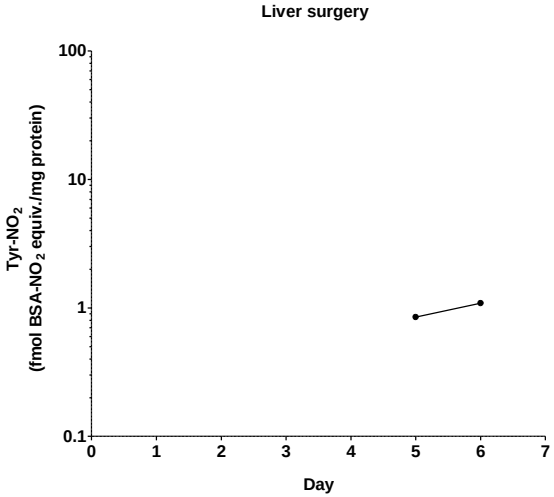
Liver surgery
Tyr-NO2
(fmol BSA-NO2 equiv./mg protein)
100
10
1
0.1
0
1
2
3
4
5
6
7
Day

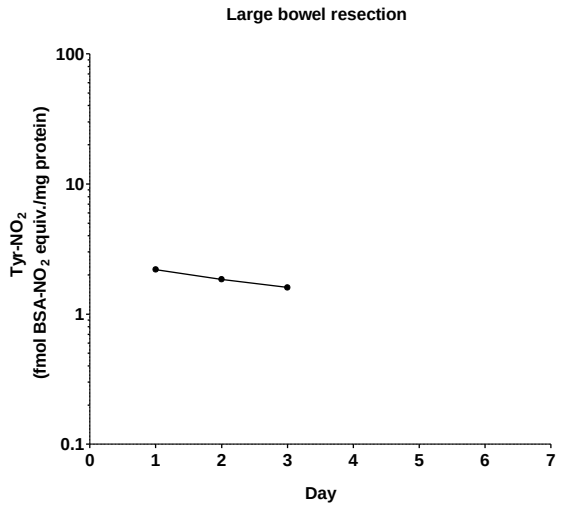
Large bowel resection
Tyr-NO2
(fmol BSA-NO2 equiv./mg protein)
100
10
1
0.1
0
1
2
3
4
5
6
7
Day

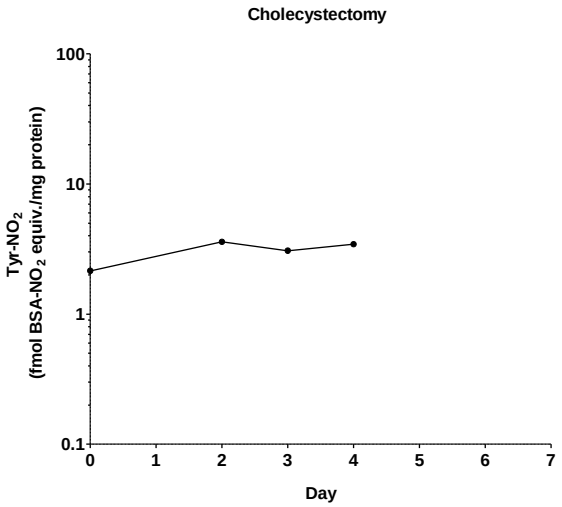
Cholecystectomy
Tyr-NO2
(fmol BSA-NO2 equiv./mg protein)
100
10
1
0.1
0
1
2
3
4
5
6
7
Day

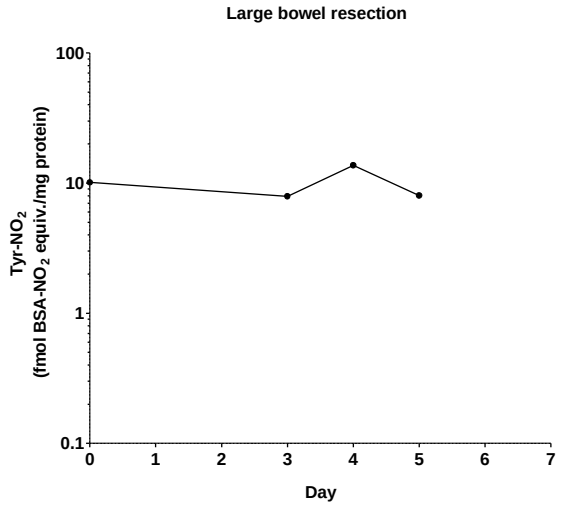
Large bowel resection
Tyr-NO2
(fmol BSA-NO2 equiv./mg protein)
100
10
1
0.1
0
1
2
3
4
5
6
7
Day

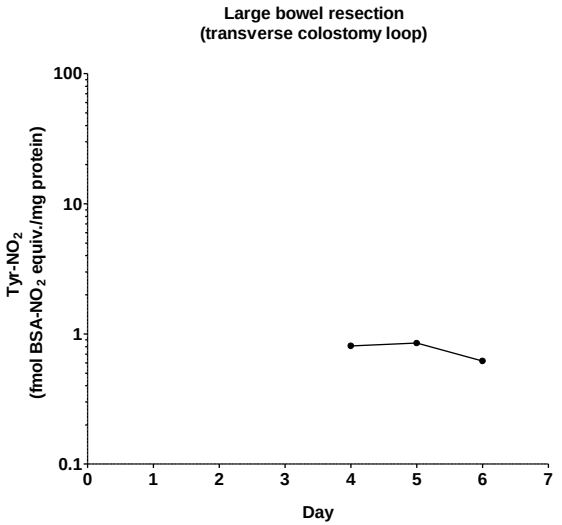
Large bowel resection
(transverse colostomy loop)
Tyr-NO2
(fmol BSA-NO2 equiv./mg protein)
100
10
1
0.1
0
1
2
3
4
5
6
7
Day

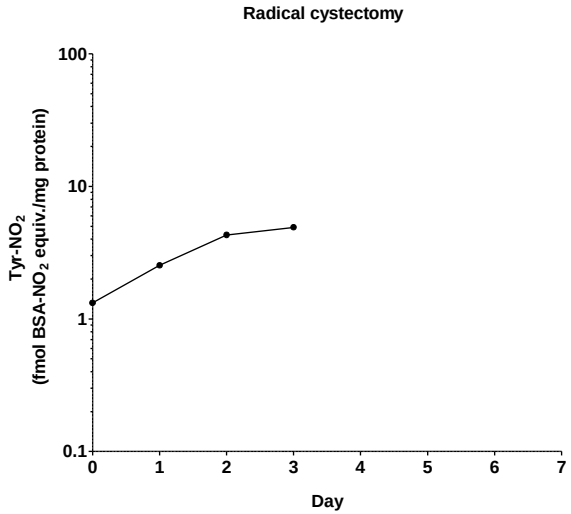
Radical cystectomy
Tyr-NO2
(fmol BSA-NO2 equiv./mg protein)
100
10
1
0.1
0
1
2
3
4
5
6
7
Day

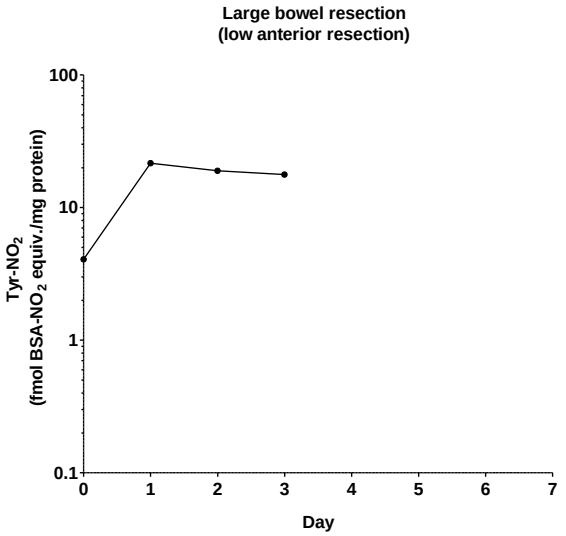
Large bowel resection
(low anterior resection)
Tyr-NO2
(fmol BSA-NO2 equiv./mg protein)
100
10
1
0.1
0
1
2
3
4
5
6
7
Day

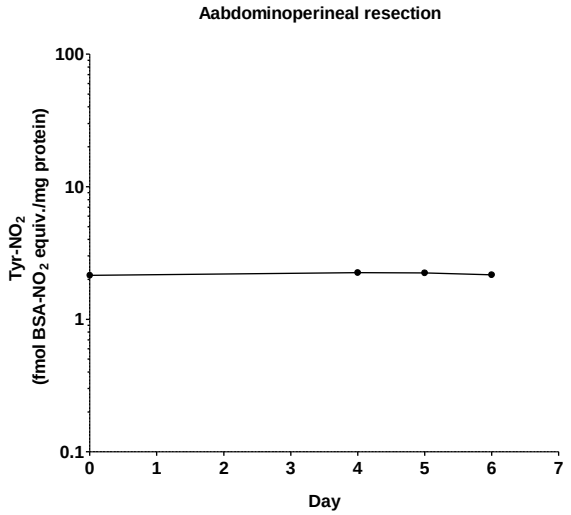
Aabdominoperineal resection
Tyr-NO2
(fmol BSA-NO2 equiv./mg protein)
100
10
1
0.1
0
1
2
3
4
5
6
7
Day

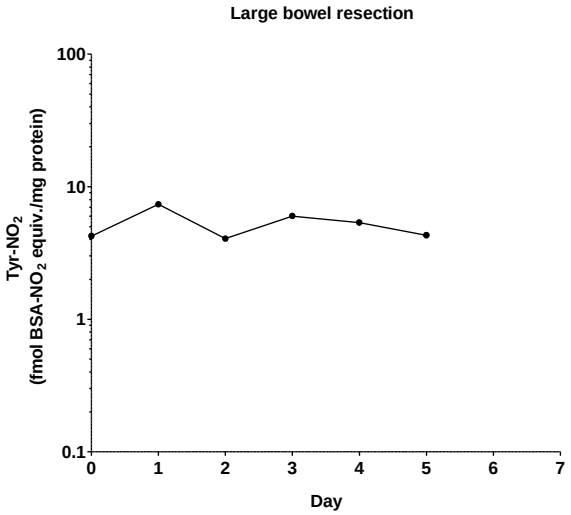
Large bowel resection
Tyr-NO2
(fmol BSA-NO2 equiv./mg protein)
100
10
1
0.1
0
1
2
3
4
5
6
7
Day

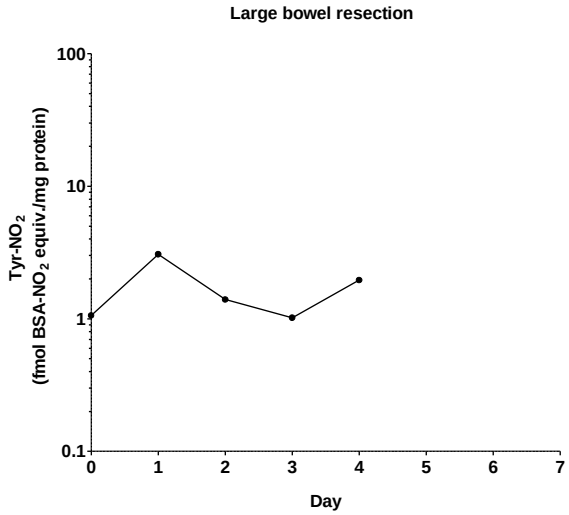
Large bowel resection
Tyr-NO2
(fmol BSA-NO2 equiv./mg protein)
100
10
1
0.1
0
1
2
3
4
5
6
7
Day

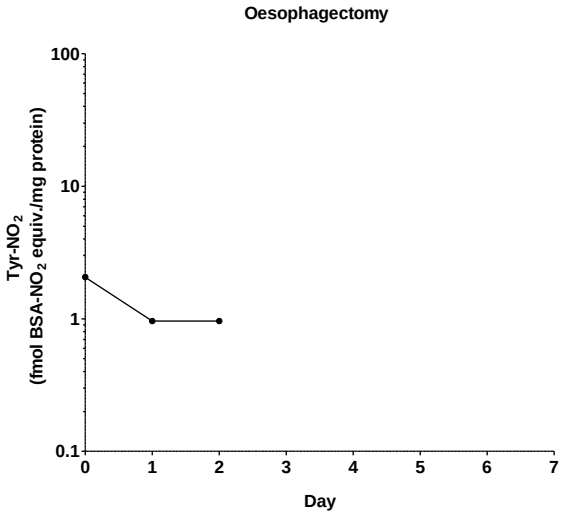
Oesophagectomy
Tyr-NO2
(fmol BSA-NO2 equiv./mg protein)
100
10
1
0.1
0
1
2
3
4
5
6
7
Day

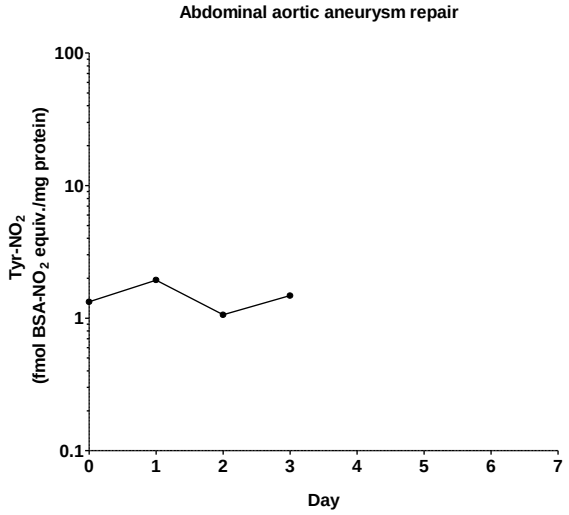
Abdominal aortic aneurysm repair
Tyr-NO2
(fmol BSA-NO2 equiv./mg protein)
100
10
1
0.1
0
1
2
3
4
5
6
7
Day

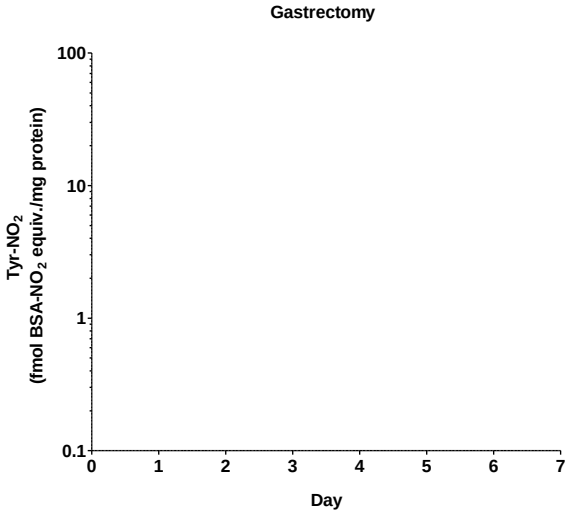
Gastrectomy
Tyr-NO2
(fmol BSA-NO2 equiv./mg protein)
100
10
1
0.1
0
1
2
3
4
5
6
7
Day

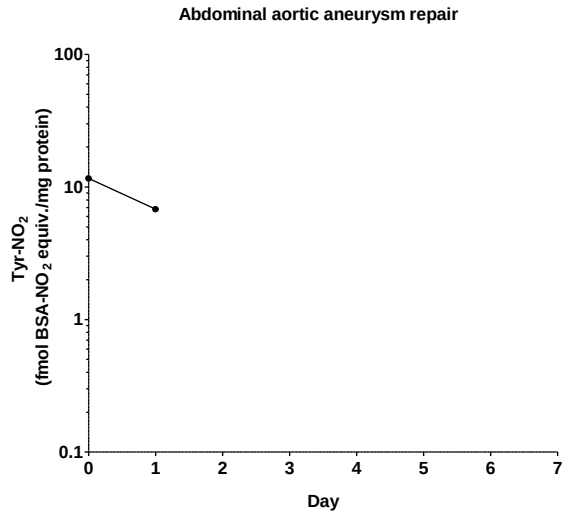
Abdominal aortic aneurysm repair
Tyr-NO2
(fmol BSA-NO2 equiv./mg protein)
100
10
1
0.1
0
1
2
3
4
5
6
7
Day

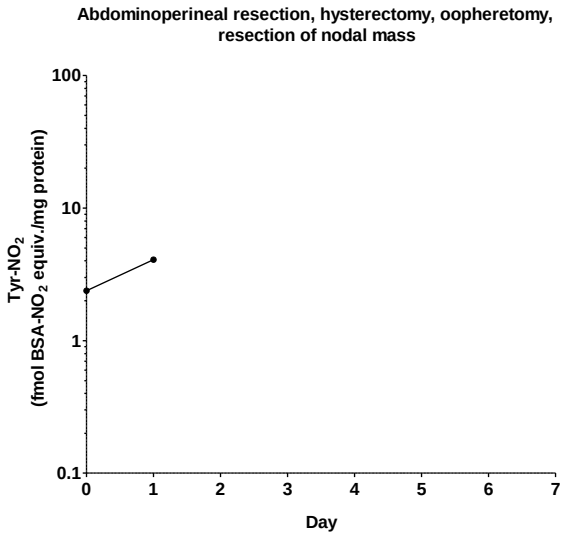
Abdominoperineal resection, hysterectomy, oopheretomy, resection of nodal mass
Tyr-NO2
(fmol BSA-NO2 equiv./mg protein)
100
10
1
0.1
0
1
2
3
4
5
6
7
Day

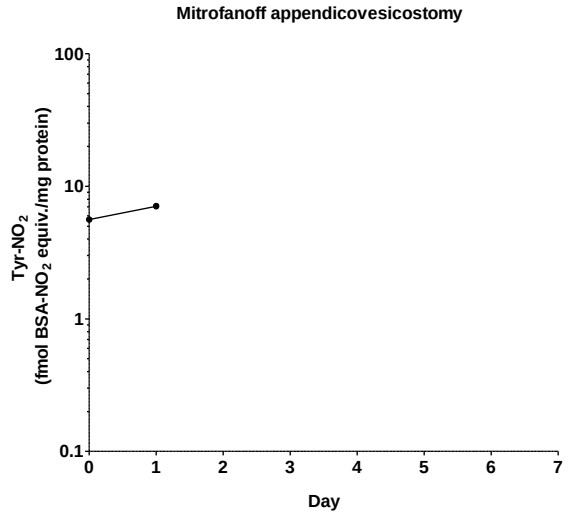
Mitrofanoff appendicovesicostomy
Tyr-NO2
(fmol BSA-NO2 equiv./mg protein)
100
10
1
0.1
0
1
2
3
4
5
6
7
Day

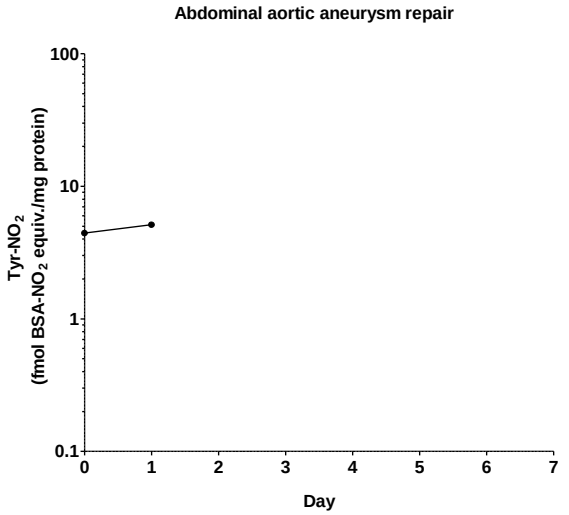
Abdominal aortic aneurysm repair
Tyr-NO2
(fmol BSA-NO2 equiv./mg protein)
100
10
1
0.1
0
1
2
3
4
5
6
7
Day

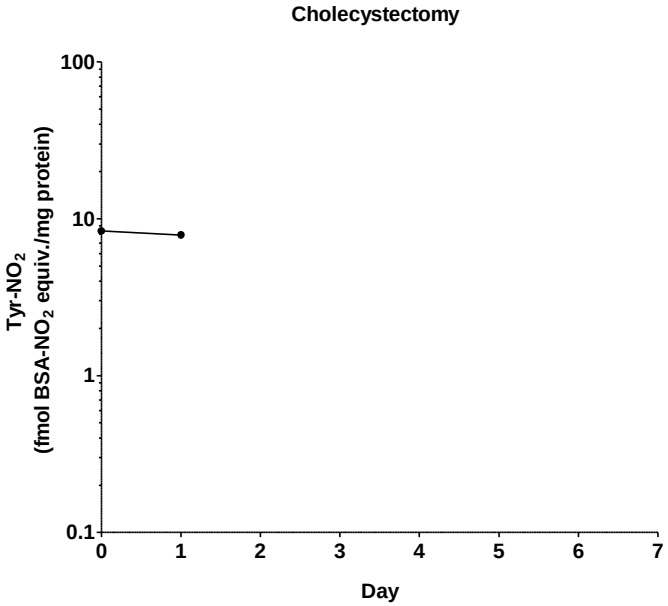
Cholecystectomy
100
10
1
0.1
Tyr-NO2
(fmol BSA-NO2 equiv./mg protein)
0
1
2
3
4
5
6
7
Day

Post-surgery sepsis

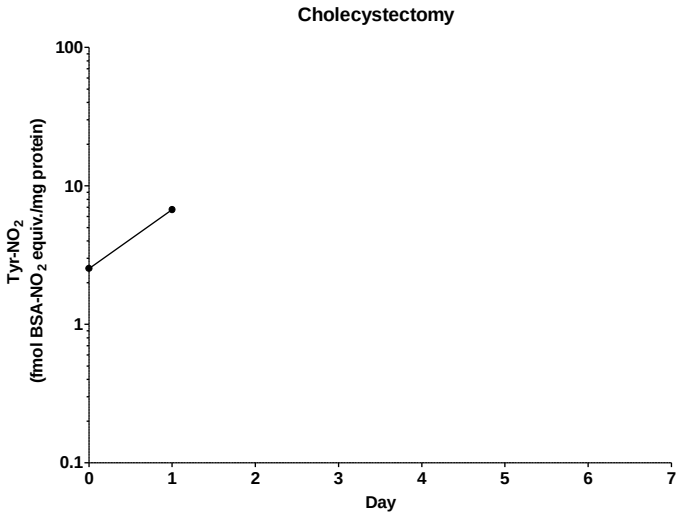

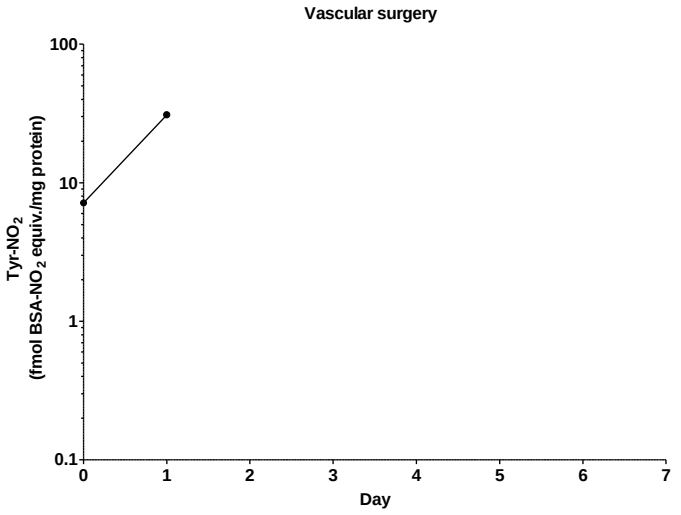

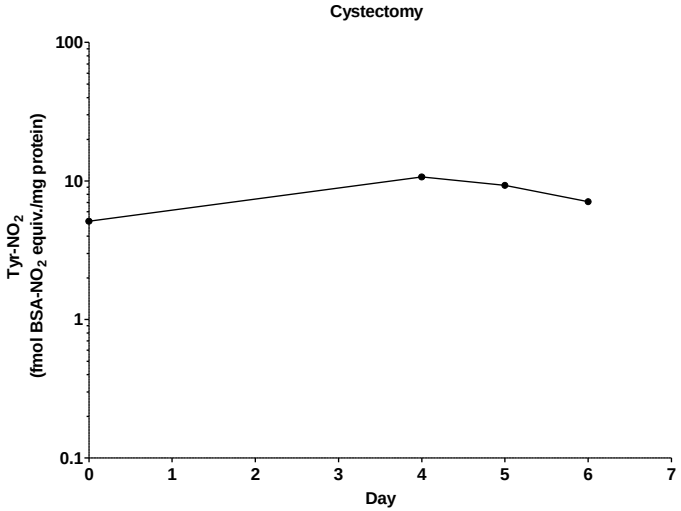

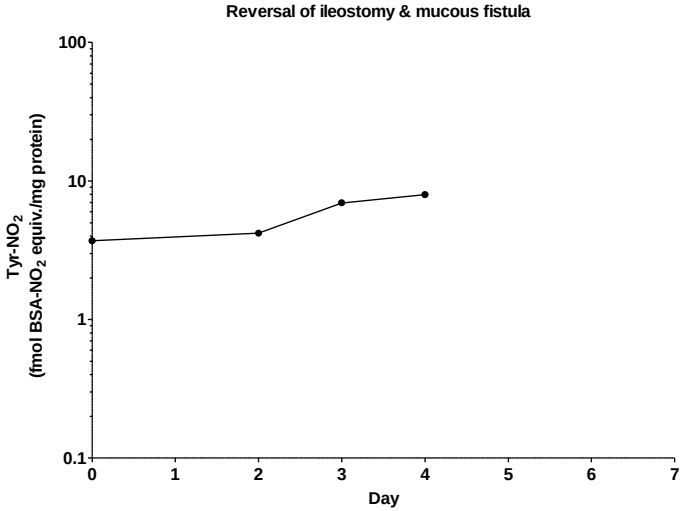

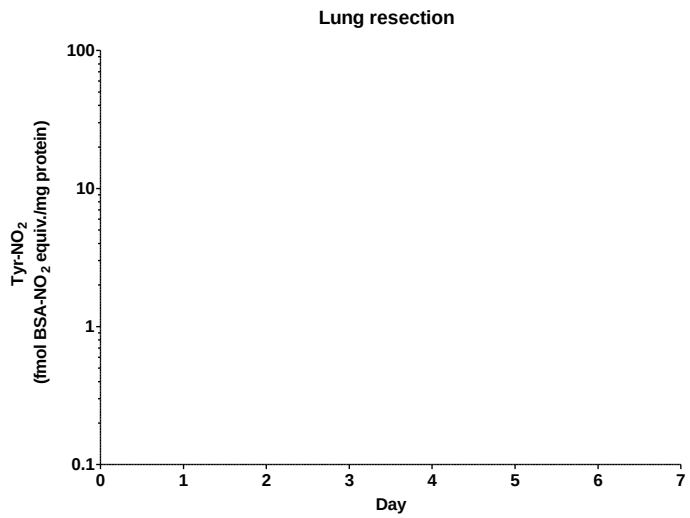
Lung resection
Tyr-NO2
(fmol BSA-NO2 equiv./mg protein)
100
10
1
0.1
0
1
2
3
4
5
6
7
Day

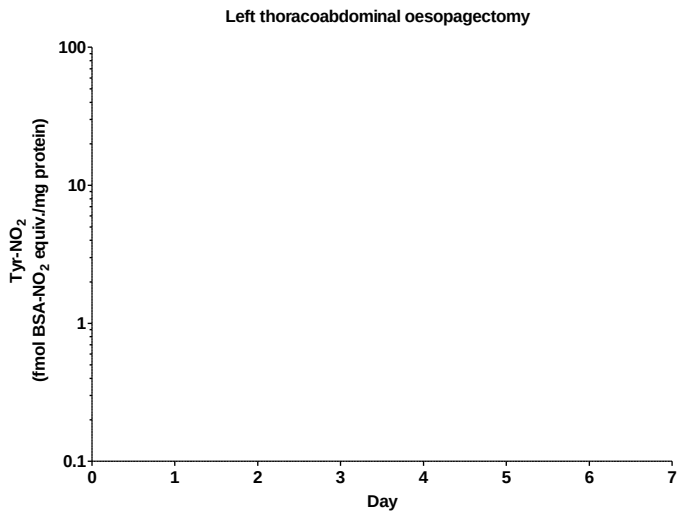
Left thoracoabdominal oesopagectomy
Tyr-NO2
(fmol BSA-NO2 equiv./mg protein)
100
10
1
0.1
0
1
2
3
4
5
6
7
Day

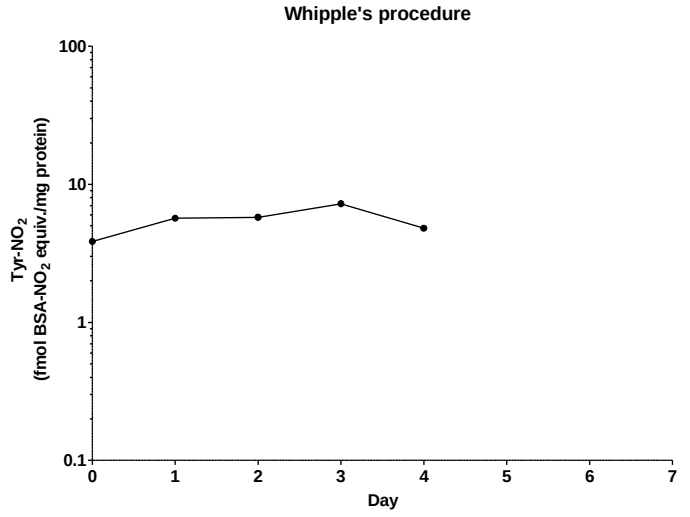
Whipple's procedure
Tyr-NO2
(fmol BSA-NO2 equiv./mg protein)
100
10
1
0.1
0
1
2
3
4
5
6
7
Day

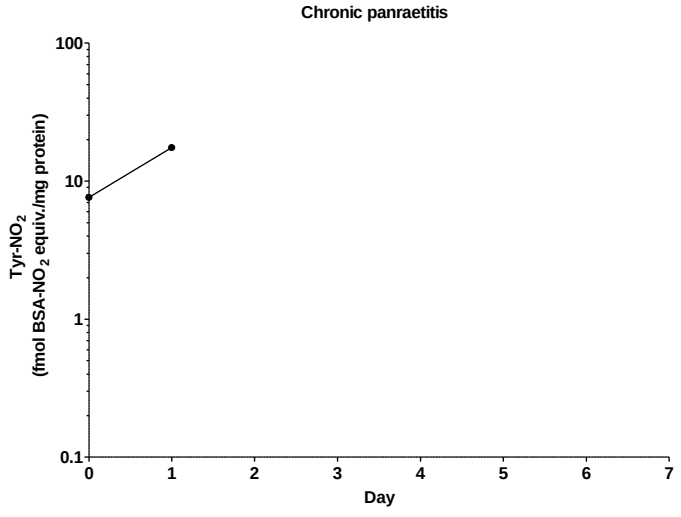
Chronic panraetitis
Tyr-NO2
(fmol BSA-NO2 equiv./mg protein)
100
10
1
0.1
0
1
2
3
4
5
6
7
Day

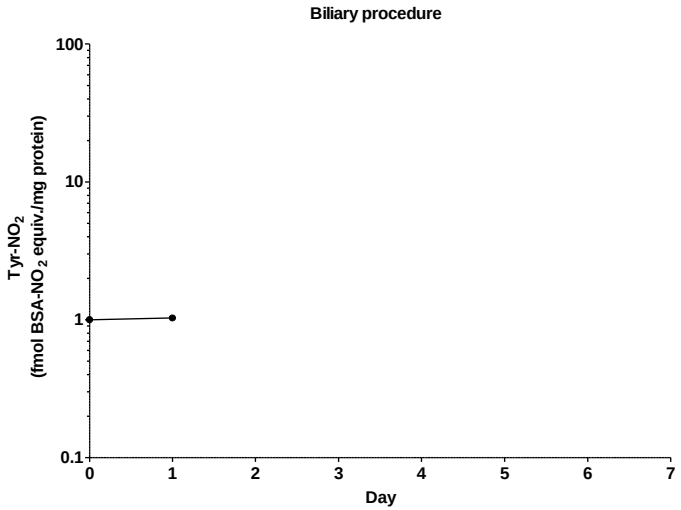
Biliary procedure
Tyr-NO2
(fmol BSA-NO2 equiv./mg protein)
100
10
1
0.1
0
1
2
3
4
5
6
7
Day

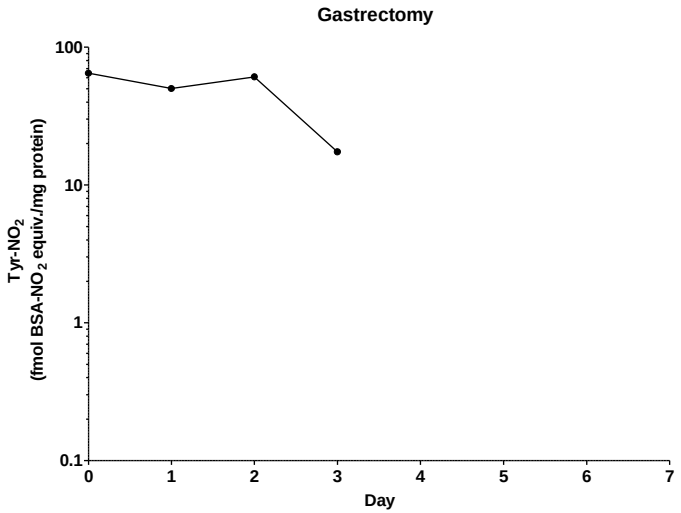
Gastrectomy
Tyr-NO2
(fmol BSA-NO2 equiv./mg protein)
100
10
1
0.1
0
1
2
3
4
5
6
7
Day

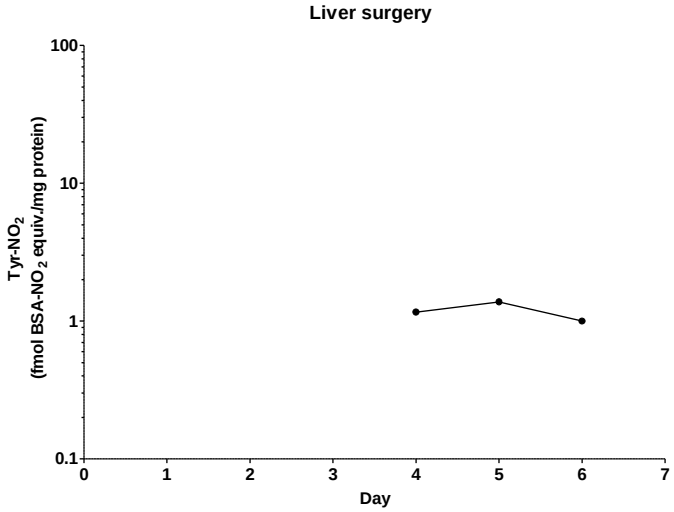
Liver surgery
Tyr-NO2
(fmol BSA-NO2 equiv./mg protein)
100
10
1
0.1
0
1
2
3
4
5
6
7
Day

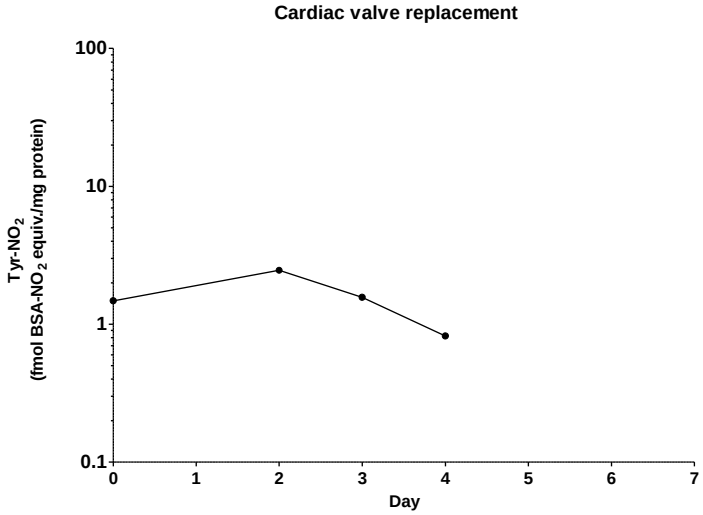
Cardiac valve replacement
Tyr-NO2
(fmol BSA-NO2 equiv./mg protein)
100
10
1
0.1
0
1
2
3
4
5
6
7
Day

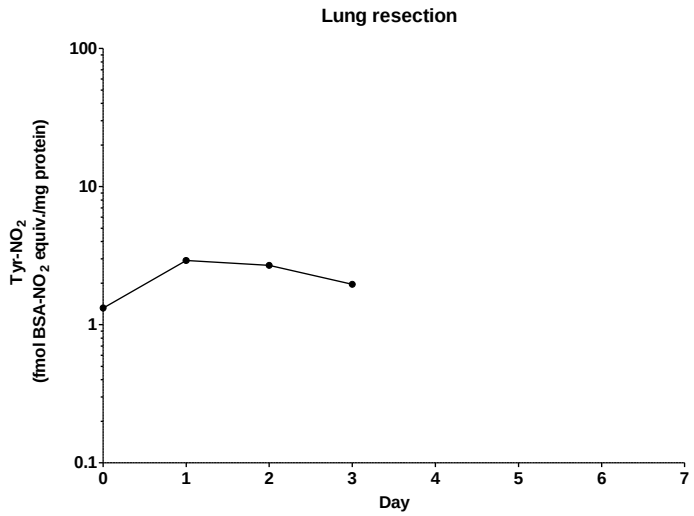
Lung resection
Tyr-NO2
(fmol BSA-NO2 equiv./mg protein)
100
10
1
0.1
0
1
2
3
4
5
6
7
Day

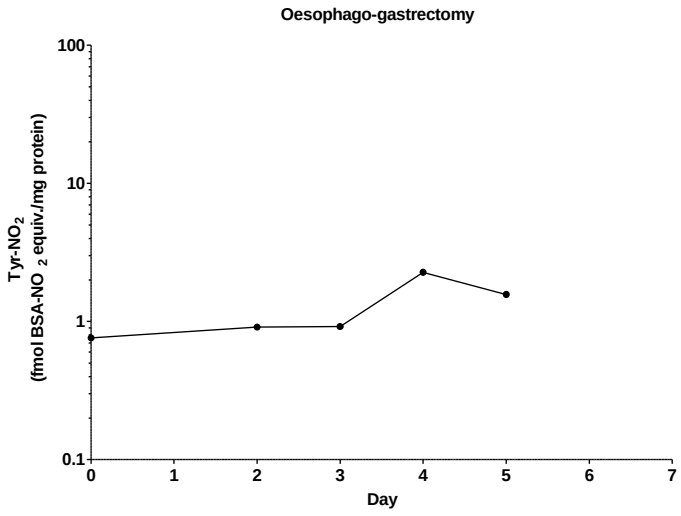
Oesophago-gastrectomy
Tyr-NO2
(fmol BSA-NO2 equiv./mg protein)
100
10
1
0.1
0
1
2
3
4
5
6
7
Day

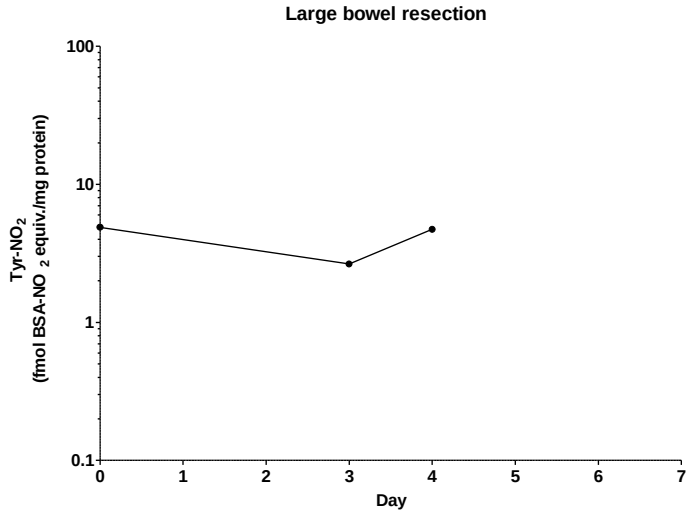
Large bowel resection
Tyr-NO2
(fmol BSA-NO2 equiv./mg protein)
100
10
1
0.1
0
1
2
3
4
5
6
7
Day

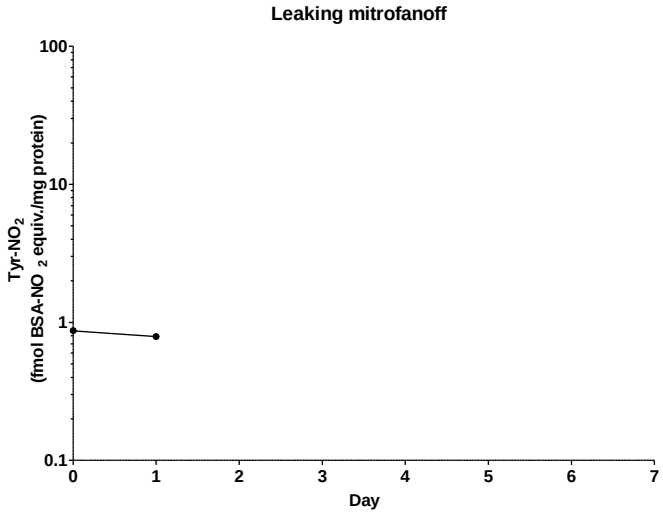
Leaking mitrofanoff
Tyr-NO2
(fmol BSA-NO2 equiv./mg protein)
100
10
1
0.1
0
1
2
3
4
5
6
7
Day

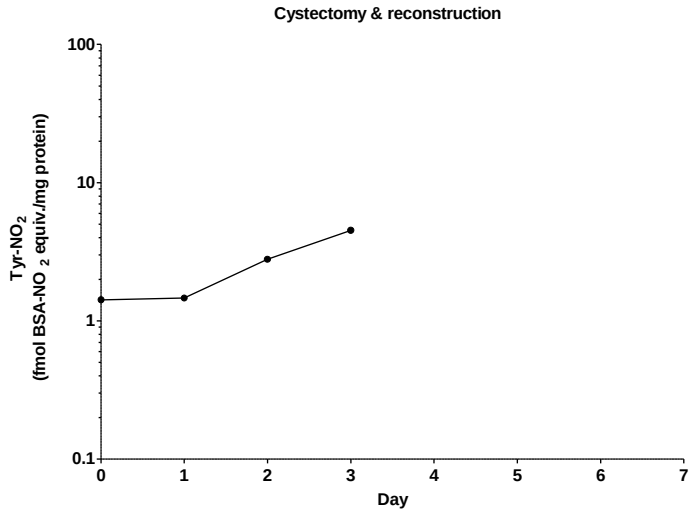
Cystectomy & reconstruction
Tyr-NO2
(fmol BSA-NO 2 equiv./mg protein)
100
10
1
0.1
0
1
2
3
4
5
6
7
Day

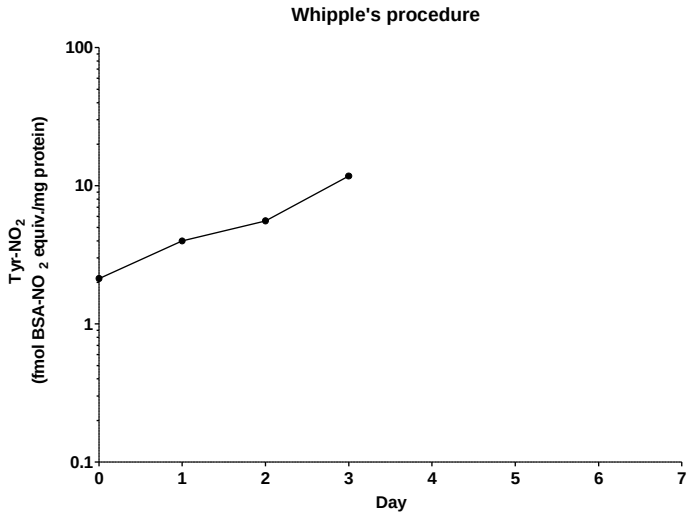
Whipple's procedure
Tyr-NO2
(fmol BSA-NO 2 equiv./mg protein)
100
10
1
0.1
0
1
2
3
4
5
6
7
Day

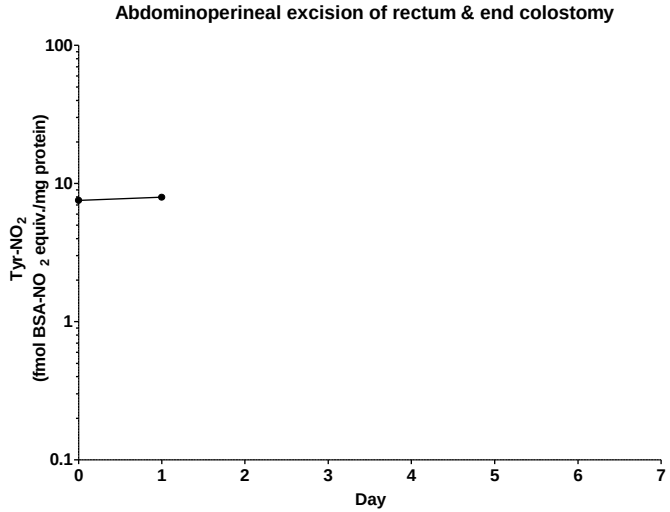
Abdominoperineal excision of rectum & end colostomy
Tyr-NO2
(fmol BSA-NO 2 equiv./mg protein)
100
10
1
0.1
0
1
2
3
4
5
6
7
Day

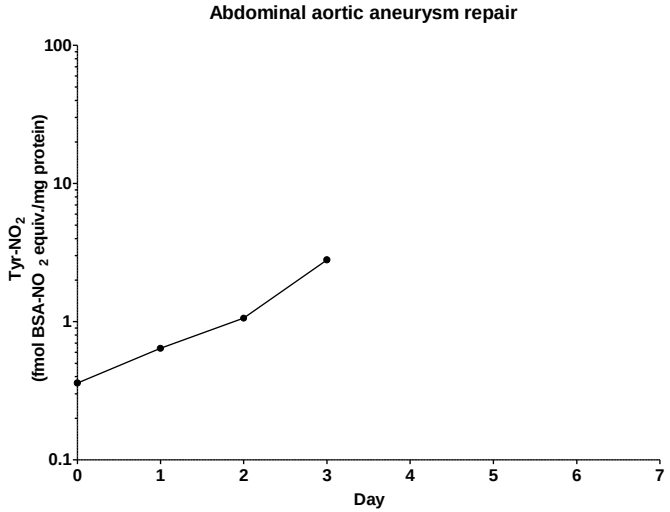
Abdominal aortic aneurysm repair
Tyr-NO2
(fmol BSA-NO 2 equiv./mg protein)
100
10
1
0.1
0
1
2
3
4
5
6
7
Day

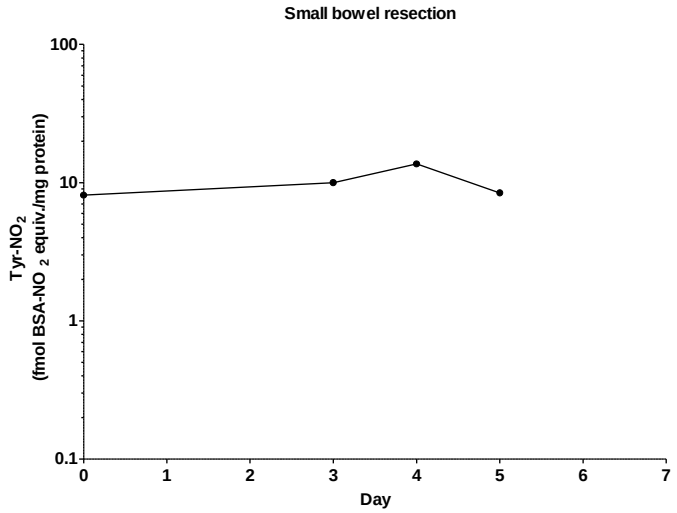
Small bowel resection
Tyr-NO2
(fmol BSA-NO 2 equiv./mg protein)
100
10
1
0.1
0
1
2
3
4
5
6
7
Day

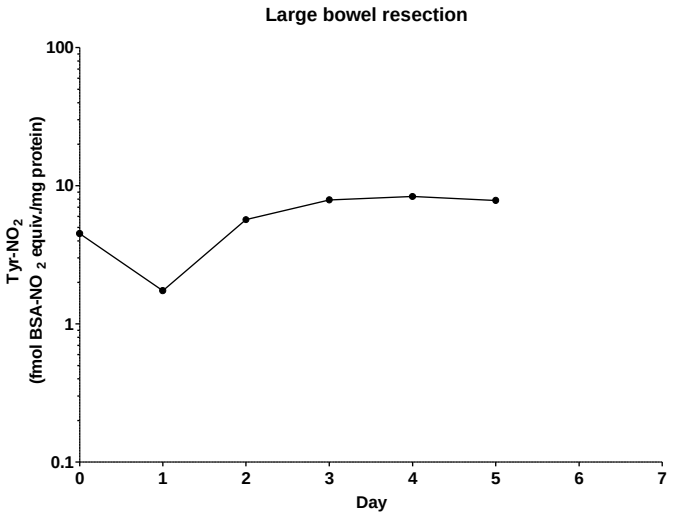
Large bowel resection
Tyr-NO2
(fmol BSA-NO 2 equiv./mg protein)
100
10
1
0.1
0
1
2
3
4
5
6
7
Day

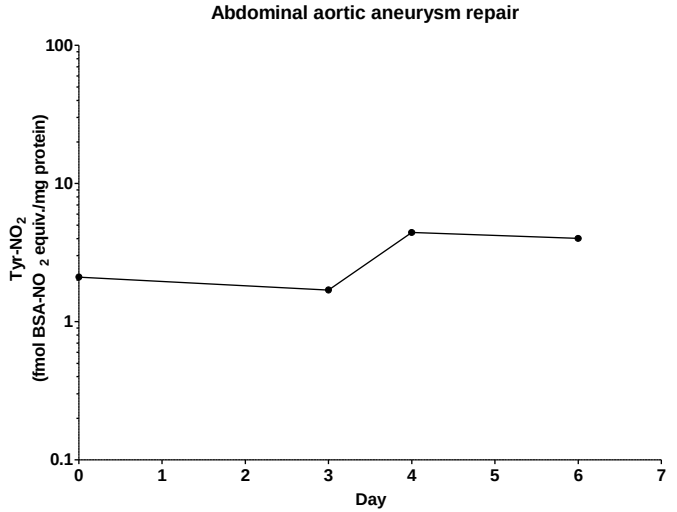
Abdominal aortic aneurysm repair
Tyr-NO2
(fmol BSA-NO 2 equiv./mg protein)
100
10
1
0.1
0
1
2
3
4
5
6
7
Day

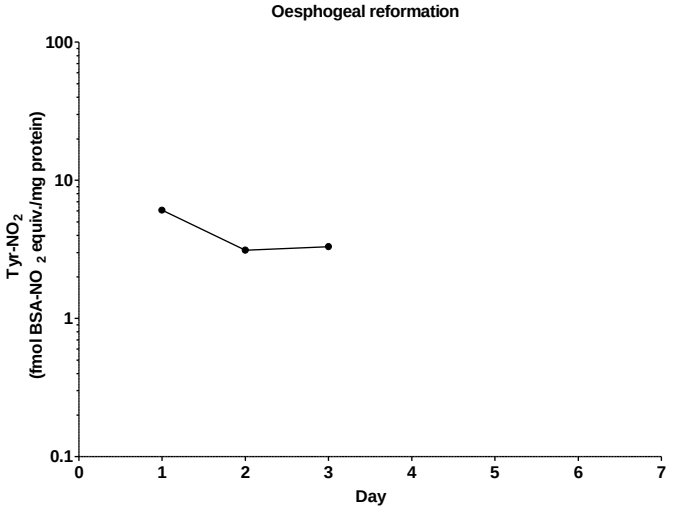
Oesphogeal reformation
Tyr-NO2
(fmol BSA-NO 2 equiv./mg protein)
100
10
1
0.1
0
1
2
3
4
5
6
7
Day

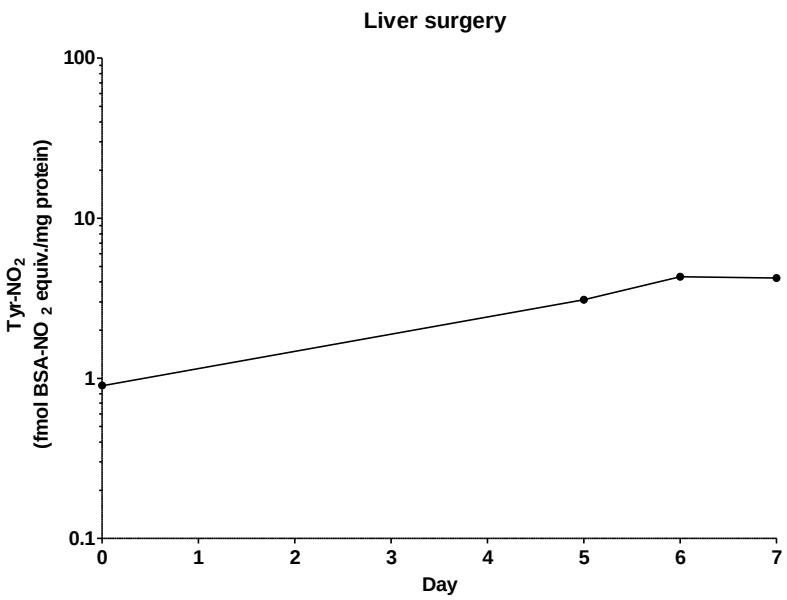
Liver surgery
100
10
1
0.1
Tyr-NO2
(fmol BSA-NO 2 equiv./mg protein)
0
1
2
3
4
5
6
7
Day

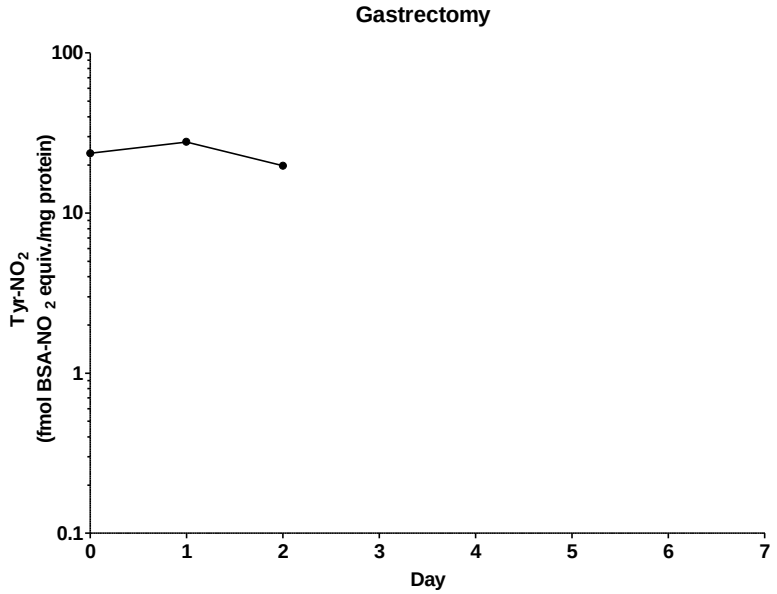
Gastrectomy
100
10
1
0.1
Tyr-NO2
(fmol BSA-NO 2 equiv./mg protein)
0
1
2
3
4
5
6
7
Day

References

ABSCIEX. *RE: PeakView® Software | Qualitative Review | AB SCIEX.*

Adav SS, Qian J, Ang YL, Kalaria RN, Lai MK, Chen CP & Sze SK 2014. iTRAQ quantitative clinical proteomics revealed role of Na(+)K(+)-ATPase and its correlation with deamidation in vascular dementia. *Journal of Proteome Research,* 13**,** 4635-4646.

Adib-Conquy M & Cavaillon J-M 2008. Compensatory anti-inflammatory response syndrome. *Thrombosis and Haemostasis,* 101**,** 36-47.

Affourtit C, Bailey SJ, Jones AM, Smallwood MJ & Winyard PG 2015. On the mechanism by which dietary nitrate improves human skeletal muscle function. *Frontiers in Physiology,* 6**,** 211.

Aggarwal A, Keluskar V, Goyal R & Dahiya P 2013. Salivary thiocyanate: a biochemical indicator of cigarette smoking in adolescents. *Oral Health & Preventive Dentistry,* 11**,** 221-227.

Agustí A, MacNee W, Donaldson K & Cosio M 2003. Hypothesis: Does COPD have an autoimmune component? *Thorax,* 58**,** 832-834.

Ahmed N, Babaei-Jadidi R, Howell SK, Beisswenger PJ & Thornalley PJ 2005. Degradation products of proteins damaged by glycation, oxidation and nitration in clinical type 1 diabetes. *Diabetologia,* 48**,** 1590-1603.

Ahmed N, Battah S, Karachalias N, Babaei-Jadidi R, Horányi M, Baróti K, Hollan S & Thornalley PJ 2003. Increased formation of methylglyoxal and protein glycation, oxidation and nitrosation in triosephosphate isomerase deficiency. *Biochimica et Biophysica Acta (BBA)-Molecular Basis of Disease,* 1639**,** 121-132.

Akama KT, Albanese C, Pestell RG & Van Eldik LJ 1998. Amyloid beta-peptide stimulates nitric oxide production in astrocytes through an NFkappaB-dependent mechanism. *Proceedings of the National Academy of Sciences of the United States of America,* 95**,** 5795-5800.

Akiyama H, Barger S, Barnum S, Bradt B, Bauer J, Cole GM, Cooper NR, Eikelenboom P, Emmerling M, Fiebich BL, Finch CE, Frautschy S, Griffin WS, Hampel H, Hull M, Landreth G, Lue L, Mrak R, Mackenzie IR, McGeer PL, O'Banion MK, Pachter J, Pasinetti G, Plata-Salaman C, Rogers J, Rydel R, Shen Y, Streit W, Strohmeyer R, Tooyoma I, Van Muiswinkel FL, Veerhuis R, Walker D, Webster S, Wegrzyniak B, Wenk G & Wyss-Coray T 2000. Inflammation and Alzheimer's disease. *Neurobiology of Aging,* 21**,** 383-421.

Altunoglu E, Guntas G, Erdenen F, Akkaya E, Topac I, Irmak H, Derici H, Yavuzer H, Gelisgen R & Uzun H 2015. Ischemia-modified albumin and advanced oxidation protein products as potential biomarkers of protein oxidation in Alzheimer's disease. *Geriatrics & Gerontology International,* 15**,** 872-880.

Alvarez B & Radi R 2003. Peroxynitrite reactivity with amino acids and proteins. *Amino Acids,* 25**,** 295-311.

AlzForum. (n.d). *Research models | TASTPM (TAS10 x TPM)* [Online]. Available: http://www.alzforum.org/research-models/tastpm-tas10-x-tpm [Accessed Feb. 22 2016].

Andelid K, Bake B, Rak S, Linden A, Rosengren A & Ekberg-Jansson A 2007. Myeloperoxidase as a marker of increasing systemic inflammation in smokers without severe airway symptoms. *Respiratory Medicine,* 101**,** 888-895.

Anderson NL & Anderson NG 2002. The Human Plasma Proteome: History, Character, and Diagnostic Prospects. *Molecular & Cellular Proteomics,* 1**,** 845-867.

Annerén G, Gardner A & Lundin T 1986. Increased glutathione peroxidase activity in erythrocytes in patients with Alzheimer's disease/senile dementia of Alzheimer's type. *Acta Neurologica Scandinavica,* 73**,** 586-589.

Anoop A, Singh PK, Jacob RS & Maji SK 2010. CSF Biomarkers for Alzheimer's Disease Diagnosis. *International Journal of Alzheimer's Disease,* 2010**,** 606802.

Arato E, Kurthy M, Sinay L, Kasza G, Menyhei G, Hardi P, Masoud S, Ripp K, Szilagyi K, Takacs I, Miklos Z, Bator A, Lantos J, Kollar L, Roth E & Jancso G 2010. Effect of vitamin E on reperfusion injuries during reconstructive vascular operations on lower limbs. *Clinical Hemorheology and Microcirculation,* 44**,** 125-136.

Ashworth A, Mitchell K, Blackwell JR, Vanhatalo A & Jones AM 2015. High-nitrate vegetable diet increases plasma nitrate and nitrite concentrations and reduces blood pressure in healthy women. *Public Health Nutrition,* 18**,** 2669-2678.

Augusto O, Bonini MG, Amanso AM, Linares E, Santos CCX & De Menezes SlL 2002. Nitrogen dioxide and carbonate radical anion: two emerging radicals in biology. *Free Radical Biology and Medicine,* 32**,** 841-859.

Avalos I, Chung CP, Oeser A, Milne GL, Morrow JD, Gebretsadik T, Shintani A, Yu C & Stein CM 2007. Oxidative stress in systemic lupus erythematosus: relationship to disease activity and symptoms. *Lupus,* 16**,** 195-200.

Azevedo LC, Janiszewski M, Soriano FG & Laurindo FR 2006. Redox mechanisms of vascular cell dysfunction in sepsis. *Endocrine, Metabolic & Immune Disorders Drug Targets,* 6**,** 159-164.

Azizova OA, Aseichev AV, Piryazev AP, Roitman EV & Shcheglovitova ON 2007. Effects of oxidized fibrinogen on the functions of blood cells, blood clotting, and rheology. *Bulletin of Experimental Biology and Medicine,* 144**,** 397-407.

Barati M, Alinejad F, Bahar MA, Tabrisi MS, Shamshiri AR, Bodouhi N-o-l & Karimi H 2008. Comparison of WBC, ESR, CRP and PCT serum levels in septic and non-septic burn cases. *Burns,* 34**,** 770-774.

Barker R, Wellington D, Esiri MM & Love S 2013. Assessing white matter ischemic damage in dementia patients by measurement of myelin proteins. *Journal of Cerebral Blood Flow and Metabolism,* 33**,** 1050-1057.

Barnes PJ 2004. Mediators of Chronic Obstructive Pulmonary Disease. *Pharmacological Reviews,* 56**,** 515-548.

Barnes PJ 2009. Role of HDAC2 in the pathophysiology of COPD. *Annual Review of Physiology,* 71**,** 451-464.

Bartels M, Biesalski HK, Engelhart K, Sendlhofer G, Rehak P & Nagel E 2004. Pilot study on the effect of parenteral vitamin E on ischemia and reperfusion induced liver injury: a double blind, randomized, placebo-controlled trial. *Clinical Nutrition,* 23**,** 1360-1370.

Bartesaghi S, Ferrer-Sueta G, Peluffo G, Valez V, Zhang H, Kalyanaraman B & Radi R 2007. Protein tyrosine nitration in hydrophilic and hydrophobic environments. *Amino Acids,* 32**,** 501-515.

Bas DF, Topcuoglu MA, Gursoy-Ozdemir Y, Saatci I, Bodur E & Dalkara T 2012. Plasma 3-nitrotyrosine estimates the reperfusion-induced cerebrovascular stress, whereas matrix metalloproteinases mainly reflect plasma activity: a study in patients treated with thrombolysis or endovascular recanalization. *Journal of Neurochemistry,* 123**,** 138-147.

Beal MF, Ferrante RJ, Browne SE, Matthews RT, Kowall NW & Brown RH 1997. Increased 3-nitrotyrosine in both sporadic and familial amyotrophic lateral sclerosis. *Annals of Neurology,* 42**,** 644-654.

Beckman JS, Chen J, Ischiropoulos H & Crow JP 1994a. Oxidative chemistry of peroxynitrite. *Methods in Enzymology,* 233**,** 229-240.

Beckman JS, Ye YZ, Anderson PG, Chen J, Accavitti MA, Tarpey MM & White CR 1994b. Extensive nitration of protein tyrosines in human atherosclerosis detected by immunohistochemistry. *Biological Chemistry Hoppe-Seyler,* 375**,** 81-88.

Bekpinar S, Kilic N, Ünlüçerçi Y, Akdag-Köse A, Azizlerli G & Özbek-Kir Z 2005. Evaluation of nitrosative and oxidative stress in Behcet disease. *Journal of the European Academy of Dermatology and Venereology,* 19**,** 167-171.

Birmingham D, Irshaid F, Nagaraja HN, Zou X, Tsao BP, Wu H, Yu CY, Hebert LA & Rovin BH 2010. The complex nature of serum C3 and C4 as biomarkers of lupus renal flare. *Lupus*.

Blair LJ, Baker JD, Sabbagh JJ & Dickey CA 2015. The emerging role of peptidyl-prolyl isomerase chaperones in tau oligomerization, amyloid processing, and Alzheimer's disease. *Journal of Neurochemistry,* 133**,** 1-13.

Bloom GS 2014. Amyloid-beta and tau: the trigger and bullet in Alzheimer disease pathogenesis. *JAMA Neurology,* 71**,** 505-508.

Bo S, Gambino R, Guidi S, Silli B, Gentile L, Cassader M & Pagano GF 2005. Plasma nitrotyrosine levels, antioxidant vitamins and hyperglycaemia. *Diabetic medicine,* 22**,** 1185-1189.

Bodini A, Peroni DG, Zardini F, Corradi M, Alinovi R, Boner AL & Piacentini GL 2006. Flunisolide decreases exhaled nitric oxide and nitrotyrosine levels in asthmatic children. *Mediators of Inflammation,* 2006**,** 31919.

Boeken U, Feindt P, Zimmermann N, Kalweit G, Petzold T & Gams E 1998. Increased preoperative C-reactive protein (CRP)-values without signs of an infection and complicated course after cardiopulmonary bypass (CPB) – operations. *European Journal of Cardio-Thoracic Surgery,* 13**,** 541-545.

Bojić DV, Bojić AL & Perović JM 2004. The effects of dietary nitrate, pH and temperature on nitrate reduction in the human oral cavity. *Facta universitatis-series: Physics, Chemistry and Technology,* 3**,** 53-60.

Bonder CS, Knight D, Hernandez-Saavedra D, McCord JM & Kubes P 2004. Chimeric SOD2/3 inhibits at the endothelial-neutrophil interface to limit vascular dysfunction in ischemia-reperfusion. *American Journal of Physiology - Gastrointestinal and Liver Physiology,* 287**,** G676-G684.

Borish LC & Steinke JW 2003. 2. Cytokines and chemokines. *Journal of Allergy and Clinical Immunology,* 111**,** S460-S475.

Boutte AM, Neely MD, Bird TD, Montine KS & Montine TJ 2005. Diminished taxol/GTP-stimulated tubulin polymerization in diseased region of brain from patients with late-onset or inherited Alzheimer's disease or frontotemporal dementia with parkinsonism linked to chromosome-17 but not individuals with mild cognitive impairment. *Journal of Alzheimers Disease,* 8**,** 1-6.

Boyland E & Walker SA 1974. Effect of thiocyanate on nitrosation of amines. *Nature,* 248**,** 601-602.
Braak H & Braak E 1991. Neuropathological stageing of Alzheimer-related changes. *Acta Neuropathologica,* 82**,** 239-259.
Brion JP, Anderton BH, Authelet M, Dayanadan R, Leroy K, Lovestone S, Octave JN, Pradier L, Touchet N & Tremp G 2001. Neurofibrillary tangles and tau phosphorylation. *In:* ONEILL, C. & ANDERTON, B. (eds.) *Neuronal Signal Transduction and Alzheimer's Disease.* London: Portland Press Ltd.
Broedbaek K, Siersma V, Henriksen T, Weimann A, Petersen M, Andersen JT, Jimenez-Solem E, Stovgaard ES, Hansen LJ, Henriksen JE, Bonnema SJ, Olivarius Nde F & Poulsen HE 2011. Urinary markers of nucleic acid oxidation and long-term mortality of newly diagnosed type 2 diabetic patients. *Diabetes Care,* 34**,** 2594-2596.
Brubaker PH 2008. Do not be statistically cenophobic: time to roc and roll! *Journal of Cardiopulmonary Rehabilitation and Prevention,* 28**,** 420-421.
Bunn HF 1981. Nonenzymatic glycosylation of protein: Relevance to diabetes. *The American Journal of Medicine,* 70**,** 325-330.
Bürklen TS, Schlattner U, Homayouni R, Gough K, Rak M, Szeghalmi A & Wallimann T 2006. The Creatine Kinase/Creatine Connection to Alzheimer's Disease: CK Inactivation, APP-CK Complexes, and Focal Creatine Deposits. *Journal of Biomedicine and Biotechnology,* 2006**,** 35936.
Burner U, Furtmuller PG, Kettle AJ, Koppenol WH & Obinger C 2000. Mechanism of reaction of myeloperoxidase with nitrite. *J Biol Chem,* 275**,** 20597-20601.
Burnette WN 1981. “Western Blotting”: Electrophoretic transfer of proteins from sodium dodecyl sulfate-polyacrylamide gels to unmodified nitrocellulose and radiographic detection with antibody and radioiodinated protein A. *Analytical Biochemistry,* 112**,** 195-203.
Bush AI 2003. The metallobiology of Alzheimer's disease. *Trends in Neurosciences,* 26**,** 207-214.
Butterfield DA, Perluigi M & Sultana R 2006a. Oxidative stress in Alzheimer's disease brain: new insights from redox proteomics. *European Journal of Pharmacology,* 545**,** 39-50.
Butterfield DA, Poon HF, St. Clair D, Keller JN, Pierce WM, Klein JB & Markesbery WR 2006b. Redox proteomics identification of oxidatively modified hippocampal proteins in mild cognitive impairment: Insights into the development of Alzheimer's disease. *Neurobiology of Disease,* 22**,** 223-232.
Butterfield DA, Reed T, Newman SF & Sultana R 2007a. Roles of amyloid beta-peptide-associated oxidative stress and brain protein modifications in the pathogenesis of Alzheimer's disease and mild cognitive impairment. *Free Radical Biology & Medicine,* 43**,** 658-677.
Butterfield DA, Reed T & Sultana R 2011. Roles of 3-nitrotyrosine- and 4-hydroxynonenal-modified brain proteins in the progression and pathogenesis of Alzheimer's disease. *Free Radical Research,* 45**,** 59-72.
Butterfield DA, Reed TT, Perluigi M, De Marco C, Coccia R, Keller JN, Markesbery WR & Sultana R 2007b. Elevated levels of 3-nitrotyrosine in brain from subjects with amnestic mild cognitive impairment: implications for the role of nitration in the progression of Alzheimer's disease. *Brain Research,* 1148**,** 243-248.

Calabrese V, Sultana R, Scapagnini G, Guagliano E, Sapienza M, Bella R, Kanski J, Pennisi G, Mancuso C, Stella AMG & Butterfield DA 2006. Nitrosative stress, cellular stress response, and thiol homeostasis in patients with Alzheimer's disease. *Antioxidants & Redox Signaling,* 8**,** 1975-1986.

Cao CF & Smith QT 1989. Crevicular fluid myeloperoxidase at healthy, gingivitis and periodontitis sites. *Journal of Clinical Periodontology,* 16**,** 17-20.

Cappelletti G, Tedeschi G, Maggioni MG, Negri A, Nonnis S & Maci R 2004. The nitration of tau protein in neurone-like PC12 cells. *FEBS Letters,* 562**,** 35-39.

Carden DL & Granger DN 2000. Pathophysiology of ischaemia–reperfusion injury. *The Journal of Pathology,* 190**,** 255-266.

Cassina AM, Hodara R, Souza JM, Thomson L, Castro L, Ischiropoulos H, Freeman BA & Radi R 2000. Cytochrome c nitration by peroxynitrite. *The Journal of Biological Chemistry,* 275**,** 21409-21415.

Castegna A, Aksenov M, Thongboonkerd V, Klein JB, Pierce WM, Booze R, Markesbery WR & Butterfield DA 2002. Proteomic identification of oxidatively modified proteins in Alzheimer's disease brain. Part II: dihydropyrimidinase-related protein 2, α-enolase and heat shock cognate 71. *Journal of Neurochemistry,* 82**,** 1524-1532.

Castegna A, Thongboonkerd V, Klein JB, Lynn B, Markesbery WR & Butterfield DA 2003. Proteomic identification of nitrated proteins in Alzheimer's disease brain. *Journal of Neurochemistry,* 85**,** 1394-1401.

Castellheim A, Brekke OL, Espevik T, Harboe M & Mollnes TE 2009. Innate immune responses to danger signals in systemic inflammatory response syndrome and sepsis. *Scandinavian Journal of Immunology,* 69**,** 479-491.

Castillo-Carranza DL, Guerrero-Muñoz MJ, Sengupta U, Hernandez C, Barrett ADT, Dineley K & Kayed R 2015. Tau Immunotherapy Modulates Both Pathological Tau and Upstream Amyloid Pathology in an Alzheimer's Disease Mouse Model. *The Journal of Neuroscience,* 35**,** 4857-4868.

Ceballos-Picot I, Merad-Boudia M, Nicole A, Thevenin M, Hellier G, Legrain S & Berr C 1996. Peripheral antioxidant enzyme activities and selenium in elderly subjects and in dementia of Alzheimer's type—Place of the extracellular glutathione peroxidase. *Free Radical Biology & Medicine,* 20**,** 579-587.

Cenini G, Sultana R, Memo M & Butterfield DA 2008. Effects of oxidative and nitrosative stress in brain on p53 proapoptotic protein in amnestic mild cognitive impairment and Alzheimer disease. *Free Radical Biology & Medicine,* 45**,** 81-85.

Ceriello A, Esposito K, Piconi L, Ihnat M, Thorpe J, Testa R, Bonfigli AR & Giugliano D 2008. Glucose "peak" and glucose "spike": Impact on endothelial function and oxidative stress. *Diabetes Research and Clinical Practice,* 82**,** 262-267.

Ceriello A, Kumar S, Piconi L, Esposito K & Giugliano D 2007. Simultaneous control of hyperglycemia and oxidative stress normalizes endothelial function in type 1 diabetes. *Diabetes Care,* 30**,** 649-654.

Ceriello A, Mercuri F, Quagliaro L, Assaloni R, Motz E, Tonutti L & Taboga C 2001. Detection of nitrotyrosine in the diabetic plasma: evidence of oxidative stress. *Diabetologia,* 44**,** 834-838.

Chang S-H, Jung I-S, Han G-Y, Kim N-H, Kim H-J & Kim C-W 2013. Proteomic profiling of brain cortex tissues in a Tau transgenic mouse model of

Alzheimer's disease. *Biochemical and Biophysical Research Communications,* 430**,** 670-675.
Chaudhry H, Zhou J, Zhong YIN, Ali MM, McGuire F, Nagarkatti PS & Nagarkatti M 2013. Role of Cytokines as a Double-edged Sword in Sepsis. *In vivo (Athens, Greece),* 27**,** 669-684.
Chen HJ, Chang CM, Lin WP, Cheng DL & Leong MI 2008. H2O2/nitrite-induced post-translational modifications of human hemoglobin determined by mass spectrometry: redox regulation of tyrosine nitration and 3-nitrotyrosine reduction by antioxidants. *ChemBioChem,* 9**,** 312-323.
Chen Y & Junger WG 2012. Measurement of Oxidative Burst in Neutrophils. *Methods in molecular biology (Clifton, N.J.),* 844**,** 115-124.
Chinetti-Gbaguidi G, Baron M, Bouhlel MA, Vanhoutte J, Copin C, Sebti Y, Derudas B, Mayi T, Bories G, Tailleux A, Haulon S, Zawadzki C, Jude B & Staels B 2011. Human Atherosclerotic Plaque Alternative Macrophages Display Low Cholesterol Handling but High Phagocytosis Because of Distinct Activities of the PPARγ and LXRα Pathways. *Circulation Research,* 108**,** 985-995.
Chu CS, Lee KT, Cheng KH, Lee MY, Kuo HF, Lin TH, Su HM, Voon WC, Sheu SH & Lai WT 2012. Postchallenge responses of nitrotyrosine and TNF-alpha during 75-g oral glucose tolerance test are associated with the presence of coronary artery diseases in patients with prediabetes. *Cardiovascular Diabetology,* 11**,** 21.
Chuang J-Y, Lee C-W, Shih Y-H, Yang T, Yu L & Kuo Y-M 2012. Interactions between Amyloid-β and Hemoglobin: Implications for Amyloid Plaque Formation in Alzheimer's Disease. *PLoS ONE,* 7**,** e33120.
Chung KF & Adcock IM 2008. Multifaceted mechanisms in COPD: inflammation, immunity, and tissue repair and destruction. *European Respiratory Journal,* 31**,** 1334-1356.
Colley CM, Fleck A, Goode AW, Muller BR & Myers MA 1983. Early time course of the acute phase protein response in man. *Journal of Clinical Pathology,* 36**,** 203-207.
Consortium TU 2015. UniProt: a hub for protein information. *Nucleic Acids Research,* 43**,** D204-D212.
Cooke MS, Evans MD, Dizdaroglu M & Lunec J 2003. Oxidative DNA damage: mechanisms, mutation, and disease. *The FASEB Journal,* 17**,** 1195-1214.
Cooke MS, Evans MD, Herbert KE & Lunec J 2000. Urinary 8-oxo-2′-deoxyguanosine — Source, significance and supplements. *Free Radical Research,* 32**,** 381-397.
Cooke MS, Mistry N, Wood C, Herbert KE & Lunec J 1997. Immunogenicity of DNA Damaged by Reactive Oxygen Species—Implications for Anti-DNA Antibodies in Lupus. *Free Radical Biology & Medicine,* 22**,** 151-159.
Cosby K, Partovi KS, Crawford JH, Patel RP, Reiter CD, Martyr S, Yang BK, Waclawiw MA, Zalos G, Xu X, Huang KT, Shields H, Kim-Shapiro DB, Schechter AN, Cannon RO, 3rd & Gladwin MT 2003. Nitrite reduction to nitric oxide by deoxyhemoglobin vasodilates the human circulation. *Nature Medicine,* 9**,** 1498-1505.
Costa D, Gomes A, Reis S, Lima JLFC & Fernandes E 2005. Hydrogen peroxide scavenging activity by non-steroidal anti-inflammatory drugs. *Life Sciences,* 76**,** 2841-2848.

Cottrell DA, Borthwick GM, Johnson MA, Ince PG & Turnbull DM 2002. The role of cytochrome c oxidase deficient hippocampal neurones in Alzheimer's disease. *Neuropathology and Applied Neurobiology,* 28**,** 390-396.
Crawford FC, Freeman MJ, Schinka JA, Morris MD, Abdullah LI, Richards D, Sevush S, Duara R & Mullan MJ 2001. Association between Alzheimer's Disease and a Functional Polymorphism in the Myeloperoxidase Gene. *Experimental Neurology,* 167**,** 456-459.
Crumley ABC, McMillan DC, McKernan M, Going JJ, Shearer CJ & Stuart RC 2006. An elevated C-reactive protein concentration, prior to surgery, predicts poor cancer-specific survival in patients undergoing resection for gastro-oesophageal cancer. *British Journal of Cancer,* 94**,** 1568-1571.
Curtis MP, Hicks AJ & Neidigh JW 2011. Kinetics of 3-Chlorotyrosine Formation and Loss due to Hypochlorous Acid and Chloramines. *Chemical Research in Toxicology,* 24**,** 418-428.
Dalle-Donne I, Aldini G, Carini M, Colombo R, Rossi R & Milzani A 2006a. Protein carbonylation, cellular dysfunction, and disease progression. *Journal of Cellular and Molecular Medicine,* 10**,** 389-406.
Dalle-Donne I, Giustarini D, Colombo R, Rossi R & Milzani A 2003a. Protein carbonylation in human diseases. *Trends in Molecular Medicine,* 9**,** 169-176.
Dalle-Donne I, Rossi R, Colombo R, Giustarini D & Milzani A 2006b. Biomarkers of Oxidative Damage in Human Disease. *Clinical Chemistry,* 52**,** 601-623.
Dalle-Donne I, Rossi R, Giustarini D, Gagliano N, Lusini L, Milzani A, Di Simplicio P & Colombo R 2001. Actin carbonylation: from a simple marker of protein oxidation to relevant signs of severe functional impairment. *Free Radical Biology & Medicine,* 31**,** 1075-1083.
Dalle-Donne I, Rossi R, Giustarini D, Milzani A & Colombo R 2003b. Protein carbonyl groups as biomarkers of oxidative stress. *Clinica Chimica Acta,* 329**,** 23-38.
Damas P, Ledoux D, Nys M, Vrindts Y, De Groote D, Franchimont P & Lamy M 1992. Cytokine serum level during severe sepsis in human IL-6 as a marker of severity. *Annals of Surgery,* 215**,** 356-362.
Davies KJA 2001. Degradation of oxidized proteins by the 20S proteasome. *Biochimie,* 83**,** 301-310.
Davies SS & Roberts LJ 2011. F2-isoprostanes as an indicator and risk factor for coronary heart disease. *Free Radical Biology & Medicine,* 50**,** 559-566.
De Filippis V, Frasson R & Fontana A 2006. 3-Nitrotyrosine as a spectroscopic probe for investigating protein protein interactions. *Protein Science : A Publication of the Protein Society,* 15**,** 976-986.
De Groote MA & Fang FC 1995. NO inhibitions: antimicrobial properties of nitric oxide. *Clinical Infectious Diseases,* 21 Suppl 2**,** S162-165.
de Jong HK, van der Poll T & Wiersinga WJ 2010. The systemic pro-inflammatory response in sepsis. *Journal of Innate Immunity,* 2**,** 422-430.
De Sanctis F, Sandri S, Ferrarini G, Pagliarello I, Sartoris S, Ugel S, Marigo I, Molon B & Bronte V 2014. The emerging immunological role of post-translational modifications by reactive nitrogen species in cancer microenvironment. *Frontiers in Immunology,* 5**,** 69.
Deeb RS, Nuriel T, Cheung C, Summers B, Lamon BD, Gross SS & Hajjar DP 2013. Characterization of a cellular denitrase activity that reverses

nitration of cyclooxygenase. *American Journal of Physiology - Heart and Circulatory Physiology,* 305**,** H687-H698.
Delévaux I, André M, Colombier M, Albuisson E, Meylheuc F, Bégue R-J, Piette J-C & Aumaître O 2003. Can procalcitonin measurement help in differentiating between bacterial infection and other kinds of inflammatory processes? *Annals of the Rheumatic Diseases,* 62**,** 337-340.
Delibas N, Ozcankaya R & Altuntas I 2002. Clinical importance of erythrocyte malondialdehyde levels as a marker for cognitive deterioration in patients with dementia of Alzheimer type: a repeated study in 5-year interval. *Clinical Biochemistry,* 35**,** 137-141.
Desikan RS, Thompson WK, Holland D, Hess CP, Brewer JB, Zetterberg H, Blennow K, Andreassen OA, McEvoy LK, Hyman BT & Dale AM 2013. Heart fatty acid binding protein and Abeta-associated Alzheimer's neurodegeneration. *Molecular Neurodegeneration,* 8**,** 39.
DiCiero Miranda M, de Bruin VM, Vale MR & Viana GS 2000. Lipid peroxidation and nitrite plus nitrate levels in brain tissue from patients with Alzheimer's disease. *Gerontology,* 46**,** 179-184.
Dijkstra G, Moshage H, van Dullemen HM, de Jager-Krikken A, Tiebosch AT, Kleibeuker JH, Jansen PL & van Goor H 1998. Expression of nitric oxide synthases and formation of nitrotyrosine and reactive oxygen species in inflammatory bowel disease. *The Journal of Pathology,* 186**,** 416-421.
Dildar K, Sinem F, Gökhan E, Orhan Y & Filiz M 2010. Serum nitrosative stress levels are increased in Alzheimer disease but not in vascular dementia. *Alzheimer Disease and Associated Disorders,* 24**,** 194-197.
Dinarello CA 2007. Historical Review of Cytokines. *European Journal of Immunology,* 37**,** S34-S45.
Doel JJ, Benjamin N, Hector MP, Rogers M & Allaker RP 2005. Evaluation of bacterial nitrate reduction in the human oral cavity. *European Journal of Oral Sciences,* 113**,** 14-19.
Doel JJ, Hector MP, Amirtham CV, Al-Anzan LA, Benjamin N & Allaker RP 2004. Protective effect of salivary nitrate and microbial nitrate reductase activity against caries. *European Journal of Oral Sciences,* 112**,** 424-428.
Domigan NM, Charlton TS, Duncan MW, Winterbourn CC & Kettle AJ 1995. Chlorination of tyrosyl residues in peptides by myeloperoxidase and human neutrophils. *J Biol Chem,* 270**,** 16542-16548.
Dorheim MA, Tracey WR, Pollock JS & Grammas P 1994. Nitric Oxide Synthase Activity Is Elevated in Brain Microvessels in Alzheimer′s Disease. *Biochemical and Biophysical Research Communications,* 205**,** 659-665.
Dorweiler B, Pruefer D, Andrasi TB, Maksan SM, Schmiedt W, Neufang A & Vahl CF 2007. Ischemia-Reperfusion Injury. *European Journal of Trauma and Emergency Surgery,* 33**,** 600-612.
Duncan C, Dougall H, Johnston P, Green S, Brogan R, Leifert C, Smith L, Golden M & Benjamin N 1995. Chemical generation of nitric oxide in the mouth from the enterosalivary circulation of dietary nitrate. *Nature Medicine,* 1**,** 546-551.
Duncan MW 2003. A review of approaches to the analysis of 3-nitrotyrosine. *Amino Acids,* 25**,** 351-361.
Dunkelberger JR & Song W-C 2009. Complement and its role in innate and adaptive immune responses. *Cell Research,* 20**,** 34-50.
Dunlop RA, Brunk UT & Rodgers KJ 2009. Oxidized proteins: Mechanisms of removal and consequences of accumulation. *IUBMB Life,* 61**,** 522-527.

Dunnill C, Patton T, Brennan J, Barrett J, Dryden M, Cooke J, Leaper D & Georgopoulos NT 2015. Reactive oxygen species (ROS) and wound healing: the functional role of ROS and emerging ROS-modulating technologies for augmentation of the healing process. *International Wound Journal***,** n/a-n/a.

Dykhuizen RS, Frazer R, Duncan C, Smith CC, Golden M, Benjamin N & Leifert C 1996. Antimicrobial effect of acidified nitrite on gut pathogens: importance of dietary nitrate in host defense. *Antimicrobial Agents and Chemotherapy,* 40**,** 1422-1425.

Edwards DAW, Fletcher K & Rowlands EN 1954. Antagonism between perchlorate, iodide, thiocyanate, and nitrate for secretion in human saliva analogy with the iodide trap of the thyroid. *The Lancet,* 263**,** 498-499.

Eggleton P, Haigh R & Winyard PG 2008. Consequence of neo-antigenicity of the 'altered self'. *Rheumatology,* 47**,** 567-571.

Eggleton P, Nissim A, Ryan BJ, Whiteman M & Winyard PG 2013. Detection and isolation of human serum autoantibodies that recognize oxidatively modified autoantigens. *Free Radical Biology & Medicine,* 57**,** 79-91.

Egner W 2000. The use of laboratory tests in the diagnosis of SLE. *Journal of Clinical Pathology,* 53**,** 424-432.

Eiserich JP, Baldus S, Brennan M-L, Ma W, Zhang C, Tousson A, Castro L, Lusis AJ, Nauseef WM, White CR & Freeman BA 2002. Myeloperoxidase, a Leukocyte-Derived Vascular NO Oxidase. *Science,* 296**,** 2391-2394.

Eiserich JP, Estévez AG, Bamberg TV, Ye YZ, Chumley PH, Beckman JS & Freeman BA 1999. Microtubule dysfunction by posttranslational nitrotyrosination of α-tubulin: A nitric oxide-dependent mechanism of cellular injury. *Proceedings of the National Academy of Sciences of the United States of America,* 96**,** 6365-6370.

Eklund KK, Niemi K & Kovanen PT 2012. Immune functions of serum amyloid A. *Critical Reviews in Immunology,* 32**,** 335-348.

Elder GA, Gama Sosa MA & De Gasperi R 2010. Transgenic mouse models of Alzheimer's disease. *Mount Sinai Journal of Medicine,* 77**,** 69-81.

Eleuteri E, Di Stefano A, Ricciardolo FLM, Magno F, Gnemmi I, Colombo M, Anzalone R, Cappello F, La Rocca G, Genta FT, Zummo G & Giannuzzi P 2009. Increased nitrotyrosine plasma levels in relation to systemic markers of inflammation and myeloperoxidase in chronic heart failure. *International Journal of Cardiology,* 135**,** 386-390.

ElHajj Z, Cachot A, Muller T, Riederer IM & Riederer BM 2016. Effects of postmortem delays on protein composition and oxidation. *Brain Research Bulletin,* 121**,** 98-104.

Engelhart MJ, Geerlings MI, Ruitenberg A & et al. 2002. Dietary intake of antioxidants and risk of alzheimer disease. *JAMA,* 287**,** 3223-3229.

Esposito L, Raber J, Kekonius L, Yan F, Yu GQ, Bien-Ly N, Puolivali J, Scearce-Levie K, Masliah E & Mucke L 2006. Reduction in mitochondrial superoxide dismutase modulates Alzheimer's disease-like pathology and accelerates the onset of behavioral changes in human amyloid precursor protein transgenic mice. *The Journal of Neuroscience,* 26**,** 5167-5179.

Fatouros IG, Jamurtas AZ, Villiotou V, Pouliopoulou S, Fotinakis P, Taxildaris K & Deliconstantinos G 2004. Oxidative stress responses in older men during endurance training and detraining. *Medicine and science in sports and exercise,* 36**,** 2065-2072.

Feldman M & Sbong S 2014. Is CRP, like ESR, Age and Gender Dependent? *Rheumatology: Current Research,* 2014.
Ferguson SK, Hirai DM, Copp SW, Holdsworth CT, Allen JD, Jones AM, Musch TI & Poole DC 2013. Impact of dietary nitrate supplementation via beetroot juice on exercising muscle vascular control in rats. *The Journal of Physiology,* 591**,** 547-557.
Fernandez-Shaw C, Marina A, Cazorla P, Valdivieso F & Vazquez J 1997. Anti-brain spectrin immunoreactivity in Alzheimer's disease: degradation of spectrin in an animal model of cholinergic degeneration. *Journal of Neuroimmunology,* 77**,** 91-98.
Ferrer I, Gomez A, Carmona M, Huesa G, Porta S, Riera-Codina M, Biagioli M, Gustincich S & Aso E 2011. Neuronal hemoglobin is reduced in Alzheimer's disease, argyrophilic grain disease, Parkinson's disease, and dementia with Lewy bodies. *The Journal of Alzheimer's Disease,* 23**,** 537-550.
Ferrer I, Martinez A, Boluda S, Parchi P & Barrachina M 2008. Brain banks: benefits, limitations and cautions concerning the use of post-mortem brain tissue for molecular studies. *Cell and Tissue Banking,* 9**,** 181-194.
Footitt J, Mallia P, Durham AL, Ho WE, Trujillo-Torralbo M-B, Telcian AG, Del Rosario A, Chang C, Peh H-Y, Kebadze T, Aniscenko J, Stanciu L, Essilfie-Quaye S, Ito K, Barnes PJ, Elkin SL, Kon OM, Wong WSF, Adcock IM & Johnston SL 2016. Oxidative and Nitrosative Stress and Histone Deacetylase-2 Activity in Exacerbations of COPD. *Chest,* 149**,** 62-73.
Fox NC, Crum WR, Scahill RI, Stevens JM, Janssen JC & Rossor MN 2001. Imaging of onset and progression of Alzheimer's disease with voxel-compression mapping of serial magnetic resonance images. *The Lancet,* 358**,** 201-205.
Foxton RH, Land JM & Heales SJ 2007. Tetrahydrobiopterin availability in Parkinson's and Alzheimer's disease; potential pathogenic mechanisms. *Neurochemical Research,* 32**,** 751-756.
Fransen EJ, Maessen JG, Elenbaas TW, van Aarnhem EE & van Dieijen-Visser MP 1999. Enhanced preoperative C-reactive protein plasma levels as a risk factor for postoperative infections after cardiac surgery. *The Annals of Thoracic Surgery,* 67**,** 134-138.
Frijhoff J, Winyard PG, Zarkovic N, Davies S, Stocker R, Cheng D, Knight A, Taylor EL, Oettrich J, Ruskovska T, Cipak Gasparovic A, Cuadrado A, Weber D, Poulsen HE, Grune T, Schmidt HH & Ghezzi P 2015. Clinical relevance of biomarkers of oxidative stress. *Antioxidants & Redox Signaling,* 23**,** 1144–1170.
Frost MT, Halliwell B & Moore KP 2000. Analysis of free and protein-bound nitrotyrosine in human plasma by a gas chromatography/mass spectrometry method that avoids nitration artifacts. *Biochemical Journal,* 345**,** 453-453.
Fu Y, Zhao D, Pan B, Wang J, Cui Y, Shi F, Wang C, Yin X, Zhou X & Yang L 2015. Proteomic Analysis of Protein Expression Throughout Disease Progression in a Mouse Model of Alzheimer’s Disease. *Journal of Alzheimer's Disease***,** 1-12.
Fujiwara N & Kobayashi K 2005. Macrophages in inflammation. *Current Drug Targets. Inflammation and Allergy,* 4**,** 281-286.

Fukai T & Ushio-Fukai M 2011. Superoxide Dismutases: Role in Redox Signaling, Vascular Function, and Diseases. *Antioxidants & Redox Signaling,* 15**,** 1583-1606.
Fukuyama N, Takebayashi Y, Hida M, Ishida H, Ichimori K & Nakazawa H 1997. Clinical Evidence of Peroxynitrite Formation in Chronic Renal Failure Patients with Septic Shock. *Free Radical Biology & Medicine,* 22**,** 771-774.
Gabay C & Kushner I 1999. Acute-Phase Proteins and Other Systemic Responses to Inflammation. *New England Journal of Medicine,* 340**,** 448-454.
Galanti LM 1997. Specificity of Salivary Thiocyanate as Marker of Cigarette Smoking Is Not Affected by Alimentary Sources. *Clinical Chemistry,* 43**,** 184-185.
Gauba V, Grünewald J, Gorney V, Deaton LM, Kang M, Bursulaya B, Ou W, Lerner RA, Schmedt C & Geierstanger BH 2011. Loss of CD4 T-cell–dependent tolerance to proteins with modified amino acids. *Proceedings of the National Academy of Sciences,* 108**,** 12821-12826.
Gaut JP, Byun J, Tran HD & Heinecke JW 2002a. Artifact-free quantification of free 3-chlorotyrosine, 3-bromotyrosine, and 3-nitrotyrosine in human plasma by electron capture-negative chemical ionization gas chromatography mass spectrometry and liquid chromatography-electrospray ionization tandem mass. *Analytical Biochemistry,* 300**,** 252-259.
Gaut JP, Byun J, Tran HD, Lauber WM, Carroll JA, Hotchkiss RS, Belaaouaj A & Heinecke JW 2002b. Myeloperoxidase produces nitrating oxidants in vivo. *The Journal of Clinical Investigation,* 109**,** 1311-1319.
Giacobini E & Gold G 2013. Alzheimer disease therapy[mdash]moving from amyloid-[beta] to tau. *Nature Reviews Neurology,* 9**,** 677-686.
Giasson BI, Duda JE, Murray IV, Chen Q, Souza JM, Hurtig HI, Ischiropoulos H, Trojanowski JQ & Lee VM 2000. Oxidative damage linked to neurodegeneration by selective alpha-synuclein nitration in synucleinopathy lesions. *Science,* 290**,** 985-989.
Gilchrist M, Winyard PG & Benjamin N 2010. Dietary nitrate – Good or bad? *Nitric Oxide,* 22**,** 104-109.
Gilchrist M, Winyard PG, Fulford J, Anning C, Shore AC & Benjamin N 2014. Dietary nitrate supplementation improves reaction time in type 2 diabetes: Development and application of a novel nitrate-depleted beetroot juice placebo. *Nitric Oxide,* 40**,** 67-74.
Goldstein DE, Little RR, Lorenz RA, Malone JI, Nathan D, Peterson CM & Sacks DB 2004. Tests of Glycemia in Diabetes. *Diabetes Care,* 27**,** 1761-1773.
Good PF, Werner P, Hsu A, Olanow CW & Perl DP 1996. Evidence of neuronal oxidative damage in Alzheimer's disease. *The American Journal of Pathology,* 149**,** 21-28.
Gow AJ, Duran D, Malcolm S & Ischiropoulos H 1996. Effects of peroxynitrite-induced protein modifications on tyrosine phosphorylation and degradation. *FEBS Letters,* 385**,** 63-66.
Granger DN & Kvietys PR 2015. Reperfusion injury and reactive oxygen species: The evolution of a concept(). *Redox Biology,* 6**,** 524-551.
Granja C, Povoa P, Lobo C, Teixeira-Pinto A, Carneiro A & Costa-Pereira A 2013. The predisposition, infection, response and organ failure (Piro)

sepsis classification system: results of hospital mortality using a novel concept and methodological approach. *PLoS One,* 8**,** e53885.
Green PS, Mendez AJ, Jacob JS, Crowley JR, Growdon W, Hyman BT & Heinecke JW 2004. Neuronal expression of myeloperoxidase is increased in Alzheimer's disease. *Journal of Neurochemistry,* 90**,** 724-733.
Griffiths HR 2000. Antioxidants and protein oxidation. *Free Radic Res,* 33 Suppl**,** S47-58.
Griffiths HR 2008. Is the generation of neo-antigenic determinants by free radicals central to the development of autoimmune rheumatoid disease? *Autoimmunity Reviews,* 7**,** 544-549.
Griffiths HR, Moller L, Bartosz G, Bast A, Bertoni-Freddari C, Collins A, Cooke M, Coolen S, Haenen G, Hoberg AM, Loft S, Lunec J, Olinski R, Parry J, Pompella A, Poulsen H, Verhagen H & Astley SB 2002. Biomarkers. *Molecular Aspects of Medicine,* 23**,** 101-208.
Grune T, Blasig IE, Sitte N, Roloff B, Haseloff R & Davies KJ 1998. Peroxynitrite increases the degradation of aconitase and other cellular proteins by proteasome. *The Journal of Biological Chemistry,* 273**,** 10857-10862.
Gruys E, Toussaint M, Niewold T & Koopmans S 2005. Review: Acute phase reaction and acute phase proteins. *Journal of Zhejiang University. Science. B,* 6**,** 1045.
Guo Q, Sebastian L, Sopher BL, Miller MW, Ware CB, Martin GM & Mattson MP 1999. Increased Vulnerability of Hippocampal Neurons from Presenilin-1 Mutant Knock-In Mice to Amyloid β-Peptide Tox. *Journal of Neurochemistry,* 72**,** 1019-1029.
Guzik TJ, Korbut R & Adamek-Guzik T 2003. Nitric Oxide and Superoxide in Inflammation and Immune Regulation. *Journal of Physiology and Pharmacology,* 54**,** 469-487.
György B, Tóth E, Tarcsa E, Falus A & Buzás EI 2006. Citrullination: A posttranslational modification in health and disease. *The International Journal of Biochemistry & Cell Biology,* 38**,** 1662-1677.
Haass C, Lemere CA, Capell A, Citron M, Seubert P, Schenk D, Lannfelt L & Selkoe DJ 1995. The Swedish mutation causes early-onset Alzheimer's disease by [beta]-secretase cleavage within the secretory pathway. *Nature Medicine,* 1**,** 1291-1296.
Halliwell B 1996. Antioxidants in Human Health and Disease. *Annual Review of Nutrition,* 16**,** 33-50.
Halliwell B 1997. What nitrates tyrosine? Is nitrotyrosine specific as a biomarker of peroxynitrite formation in vivo? *FEBS Letters,* 411**,** 157-160.
Halliwell B 2001. Free Radicals and other reactive species in Disease. *Encyclopedia of Life Sciences*.
Halliwell B 2003. Oxidative stress in cell culture: an under-appreciated problem? *FEBS Letters,* 540**,** 3-6.
Halliwell B & Whiteman M 2004. Measuring reactive species and oxidative damage in vivo and in cell culture: how should you do it and what do the results mean? *British Journal of Pharmacology,* 142**,** 231-255.
Hampel H, Frank R, Broich K, Teipel SJ, Katz RG, Hardy J, Herholz K, Bokde ALW, Jessen F, Hoessler YC, Sanhai WR, Zetterberg H, Woodcock J & Blennow K 2010. Biomarkers for Alzheimer's disease: academic, industry and regulatory perspectives. *Nature Reviews Drug Discovery,* 9**,** 560-574.

Hanazawa T, Kharitonov S & Barnes P 2000. Increased Nitrotyrosine in Exhaled Breath Condensate of Patients with Asthma. *American Journal of Respiratory and Critical Care Medicine,* 162**,** 1273-1276.
Hanger DP & Wray S 2010. Tau cleavage and tau aggregation in neurodegenerative disease. *Biochemical Society Transactions,* 38**,** 1016-1020.
Harrison D, Welch C & Eddleston J 2006. The epidemiology of severe sepsis in England, Wales and Northern Ireland, 1996 to 2004: secondary analysis of a high quality clinical database, the ICNARC Case Mix Programme Database. *Critical Care,* 10**,** R42.
Hazen SL & Heinecke JW 1997. 3-Chlorotyrosine, a specific marker of myeloperoxidase-catalyzed oxidation, is markedly elevated in low density lipoprotein isolated from human atherosclerotic intima. *The Journal of Clinical Investigation,* 99**,** 2075-2081.
Heneka MT, Carson MJ, Khoury JE, Landreth GE, Brosseron F, Feinstein DL, Jacobs AH, Wyss-Coray T, Vitorica J, Ransohoff RM, Herrup K, Frautschy SA, Finsen B, Brown GC, Verkhratsky A, Yamanaka K, Koistinaho J, Latz E, Halle A, Petzold GC, Town T, Morgan D, Shinohara ML, Perry VH, Holmes C, Bazan NG, Brooks DJ, Hunot S, Joseph B, Deigendesch N, Garaschuk O, Boddeke E, Dinarello CA, Breitner JC, Cole GM, Golenbock DT & Kummer MP 2015. Neuroinflammation in Alzheimer's disease. *The Lancet Neurology,* 14**,** 388-405.
Hensley K, Maidt ML, Yu Z, Sang H, Markesbery WR & Floyd RA 1998. Electrochemical Analysis of Protein Nitrotyrosine and Dityrosine in the Alzheimer Brain Indicates Region-Specific Accumulation. *The Journal of Neuroscience,* 18**,** 8126-8132.
Heppner FL, Ransohoff RM & Becher B 2015. Immune attack: the role of inflammation in Alzheimer disease. *Nature Reviews Neuroscience,* 16**,** 358-372.
Herce-Pagliai C, Kotecha S & Shuker DE 1998. Analytical methods for 3-nitrotyrosine as a marker of exposure to reactive nitrogen species: a review. *Nitric Oxide,* 2**,** 324-336.
Hildebrandt AG & Roots I 1975. Reduced nicotinamide adenine dinucleotide phosphate (NADPH)-dependent formation and breakdown of hydrogen peroxide during mixed function oxidation reactions in liver microsomes. *Archives of Biochemistry and Biophysics,* 171**,** 385-397.
Hill M, Hawksworth G & Tattersall G 1973. Bacteria, nitrosamines and cancer of the stomach. *British Journal of Cancer,* 28**,** 562.
Hofer N, Zacharias E, Muller W & Resch B 2012. An update on the use of C-reactive protein in early-onset neonatal sepsis: current insights and new tasks. *Neonatology,* 102**,** 25-36.
Hood JD, Meininger CJ, Ziche M & Granger HJ 1998. VEGF upregulates ecNOS message, protein, and NO production in human endothelial cells. *American Journal of Physiology - Heart and Circulatory Physiology,* 274**,** H1054-H1058.
Houdebine L-M 2007. Transgenic Animal Models in Biomedical Research. *In:* SIOUD, M. (ed.) *Target Discovery and Validation Reviews and Protocols: Volume 1, Emerging Strategies for Targets and Biomarker Discovery.* Totowa, NJ: Humana Press.
Howell MD, Talmor D, Schuetz P, Hunziker S, Jones AE & Shapiro NI 2011. Proof of principle: the predisposition, infection, response, organ failure sepsis staging system. *Critical Care Medicine,* 39**,** 322-327.

Huet O, Dupic L, Harrois A & Duranteau J 2011. Oxidative stress and endothelial dysfunction during sepsis. *Frontiers in Bioscience (Landmark Ed),* 16**,** 1986-1995.
Hughes MN & Nicklin HG 1968. The chemistry of pernitrites. Part I. Kinetics of decomposition of pernitrous acid. *Journal of the Chemical Society A: Inorganic, Physical, Theoretical***,** 450-452.
Hui Y, Wong M, Zhao SS, Love JA, Ansley DM & Chen DD 2012. A simple and robust LC-MS/MS method for quantification of free 3-nitrotyrosine in human plasma from patients receiving on-pump CABG surgery. *Electrophoresis,* 33**,** 697-704.
Ichinose M, Sugiura H, Yamagata S, Koarai A & Shirato K 2000. Increase in reactive nitrogen species production in chronic obstructive pulmonary disease airways. *American journal of respiratory and critical care medicine,* 162**,** 701-706.
Ihalin R, Loimaranta V, Lenander-Lumikari M & Tenovuo J 1998. The effects of different (pseudo)halide substrates on peroxidase-mediated killing of Actinobacillus actinomycetemcomitans. *Journal of Periodontal Research,* 33**,** 421-427.
Ihalin R, Loimaranta V & Tenovuo J 2006. Origin, structure, and biological activities of peroxidases in human saliva. *Archives of Biochemistry and Biophysics,* 445**,** 261-268.
Immundiagnostik. 2009. *ADMA ELISA* [Online]. Available: http://www.immundiagnostik.com/en/home/products/kits-assays/oxidative-stress-preventive-medicine.html?tx_mokom01immunprodukte_pi1%5Ban%5D=K%207828&tx_mokom01immunprodukte_pi1%5Bag%5D=404&cHash=c6553a00e7 .
Inoue H, Hisamatsu K, Ando K, Ajisaka R & Kumagai N 2002. Determination of nitrotyrosine and related compounds in biological specimens by competitive enzyme immunoassay. *Nitric Oxide,* 7**,** 11-11.
Irie Y, Saeki M, Kamisaki Y, Martin E & Murad F 2003. Histone H1.2 is a substrate for denitrase, an activity that reduces nitrotyrosine immunoreactivity in proteins. *Proceedings of the National Academy of Sciences of the United States of America,* 100**,** 5634-5639.
Ischiropoulos H 2003. Biological selectivity and functional aspects of protein tyrosine nitration. *Biochemical and Biophysical Research Communications,* 305**,** 776-783.
Ischiropoulos H, Zhu L & Beckman JS 1992. Peroxynitrite formation from macrophage-derived nitric oxide. *Archives of Biochemistry and Biophysics,* 298**,** 446-451.
Isik B, Ceylan A & Isik R 2007. Oxidative stress in smokers and non-smokers. *Inhalation Toxicology,* 19**,** 767-769.
Jain S, Gautam V & Naseem S 2011. Acute-phase proteins: As diagnostic tool. *Journal of Pharmacy and Bioallied Sciences,* 3**,** 118-127.
Jia M, Mateoiu C & Souchelnytskyi S 2011. Protein tyrosine nitration in the cell cycle. *Biochemical and Biophysical Research Communications,* 413**,** 270-276.
Johnson CJ & Kross BC 1990. Continuing importance of nitrate contamination of groundwater and wells in rural areas. *American Journal of Industrial Medicine,* 18**,** 449-456.

Jones AE, Fiechtl JF, Brown MD, Ballew JJ & Kline JA 2007. Procalcitonin Test in the Diagnosis of Bacteremia: A Meta-analysis. *Annals of Emergency Medicine,* 50**,** 34-41.
Jones AM 2014. Dietary Nitrate Supplementation and Exercise Performance. *Sports Medicine (Auckland, N.z.),* 44**,** 35-45.
Jung T, Höhn A & Grune T 2014. The proteasome and the degradation of oxidized proteins: Part II – protein oxidation and proteasomal degradation. *Redox Biology,* 2**,** 99-104.
Kadoi Y & Goto F 2004. Selective Inducible Nitric Oxide Inhibition Can Restore Hemodynamics, but Does Not Improve Neurological Dysfunction in Experimentally-Induced Septic Shock in Rats. *Anesthesia & Analgesia,* 99**,** 212-220.
Kalaria R 2002. Similarities between Alzheimer's disease and vascular dementia. *Journal of the Neurological Sciences,* 203–204**,** 29-34.
Kalogeris T, Baines CP, Krenz M & Korthuis RJ 2012. Cell Biology of Ischemia/Reperfusion Injury. *International review of cell and molecular biology,* 298**,** 229-317.
Kaminski KA, Bonda TA, Korecki J & Musial WJ 2002. Oxidative stress and neutrophil activation—the two keystones of ischemia/reperfusion injury. *International Journal of Cardiology,* 86**,** 41-59.
Kaminsky DA, Mitchell J, Carroll N, James A, Soultanakis R & Janssen Y 1999. Nitrotyrosine formation in the airways and lung parenchyma of patients with asthma. *The Journal of Allergy and Clinical Immunology,* 104**,** 747-754.
Kamisaki Y, Wada K, Bian K, Balabanli B, Davis K, Martin E, Behbod F, Lee Y-C & Murad F 1998. An activity in rat tissues that modifies nitrotyrosine-containing proteins. *Proceedings of the National Academy of Sciences,* 95**,** 11584-11589.
Kamisaki Y, Wada K, Nakamoto K, Kishimoto Y, Kitano M & Itoh T 1996. Sensitive determination of nitrotyrosine in human plasma by isocratic high-performance liquid chromatography. *Journal of Chromatography B: Biomedical Sciences and Applications,* 685**,** 343-347.
Kanamaru T, Kamimura N, Yokota T, Iuchi K, Nishimaki K, Takami S, Akashiba H, Shitaka Y, Katsura K-i, Kimura K & Ohta S 2015. Oxidative stress accelerates amyloid deposition and memory impairment in a double-transgenic mouse model of Alzheimer's disease. *Neuroscience Letters,* 587**,** 126-131.
Karsdal MA, Henriksen K, Leeming DJ, Woodworth T, Vassiliadis E & Bay-Jensen A-C 2010. Novel combinations of Post-Translational Modification (PTM) neo-epitopes provide tissue-specific biochemical markers--are they the cause or the consequence of the disease? *Clinical Biochemistry,* 43**,** 793-804.
Kaur H & Halliwell B 1994. Evidence for nitric oxide-mediated oxidative damage in chronic inflammation. Nitrotyrosine in serum and synovial fluid from rheumatoid patients. *FEBS letters,* 350**,** 9-9.
Kaur H, Lyras L, Jenner P & Halliwell B 1998. Artefacts in HPLC detection of 3-nitrotyrosine in human brain tissue. *Journal of neurochemistry,* 70**,** 2220-2223.
Keimer R, Stutzer FK, Tsikas D, Troost R, Gutzki F-M & Frölich JC 2003. Lack of oxidative stress during sustained therapy with isosorbide dinitrate and pentaerythrityl tetranitrate in healthy humans: a randomized, double-blind crossover study. *Journal of cardiovascular pharmacology,* 41**,** 284-292.

Kelly J, Vanhatalo A, Bailey SJ, Wylie LJ, Tucker C, List S, Winyard PG & Jones AM 2014. Dietary nitrate supplementation: effects on plasma nitrite and pulmonary O2 uptake dynamics during exercise in hypoxia and normoxia. *American Journal of Physiology - Regulatory, Integrative and Comparative Physiology,* 307**,** R920-R930.

Kettle AJ, Gedye CA & Winterbourn CC 1993. Superoxide is an antagonist of anti-inflammatory drugs that inhibit hypochlorous acid production by myeloperoxidase. *Biochemical Pharmacology,* 45**,** 2003-2010.

Khan F & Ali R 2006. Antibodies against nitric oxide damaged poly L-tyrosine and 3-nitrotyrosine levels in systemic lupus erythematosus. *Journal of Biochemistry and Molecular Biology,* 39**,** 189-196.

Khan F & Siddiqui AA 2006. Prevalence of anti-3-nitrotyrosine antibodies in the joint synovial fluid of patients with rheumatoid arthritis, osteoarthritis and systemic lupus erythematosus. *Clinica Chimica Acta,* 370**,** 100-107.

Khan F, Siddiqui AA & Ali R 2006. Measurement and Significance of 3-Nitrotyrosine in Systemic Lupus Erythematosus. *Scandinavian Journal of Immunology,* 64**,** 507-514.

Khan J, Brennand DM, Bradley N, Gao B, Bruckdorfer R, Jacobs M & Brennan DM 1998. 3-Nitrotyrosine in the proteins of human plasma determined by an ELISA method. *Biochemical Journal,* 330**,** 795-795.

Kibe S, Adams K & Barlow G 2011. Diagnostic and prognostic biomarkers of sepsis in critical care. *Journal of Antimicrobial Chemotherapy,* 66**,** ii33-ii40.

Kim-Shapiro DB, Gladwin MT, Patel RP & Hogg N 2005. The reaction between nitrite and hemoglobin: the role of nitrite in hemoglobin-mediated hypoxic vasodilation. *Journal of Inorganic Biochemistry,* 99**,** 237-246.

Kim M-H, Liu W, Borjesson DL, Curry F-RE, Miller LS, Cheung AL, Liu F-T, Isseroff RR & Simon SI 2008. Dynamics of Neutrophil Infiltration during Cutaneous Wound Healing and Infection Using Fluorescence Imaging. *The Journal of investigative dermatology,* 128**,** 1812-1820.

Kirkham PA, Caramori G, Casolari P, Papi AA, Edwards M, Shamji B, Triantaphyllopoulos K, Hussain F, Pinart M, Khan Y, Heinemann L, Stevens L, Yeadon M, Barnes PJ, Chung KF & Adcock IM 2011. Oxidative Stress–induced Antibodies to Carbonyl-modified Protein Correlate with Severity of Chronic Obstructive Pulmonary Disease. *American Journal of Respiratory and Critical Care Medicine,* 184**,** 796-802.

Kish SJ, Bergeron C, Rajput A, Dozic S, Mastrogiacomo F, Chang L-J, Wilson JM, DiStefano LM & Nobrega JN 1992. Brain Cytochrome Oxidase in Alzheimer's Disease. *Journal of Neurochemistry,* 59**,** 776-779.

Klebanoff SJ 1993. Reactive nitrogen intermediates and antimicrobial activity: role of nitrite. *Free Radical Biology & Medicine,* 14**,** 7617-7625.

Kleinbongard P, Dejam A, Lauer T, Rassaf T, Schindler A, Picker O, Scheeren T, Godecke A, Schrader J, Schulz R, Heusch G, Schaub GA, Bryan NS, Feelisch M & Kelm M 2003. Plasma nitrite reflects constitutive nitric oxide synthase activity in mammals. *Free Radical Biology & Medicine,* 35**,** 790-796.

Kolaczkowska E & Kubes P 2013. Neutrophil recruitment and function in health and inflammation. *Nature Reviews Immunology,* 13**,** 159-175.

Korolainen Ma & Pirttilä T 2009. Cerebrospinal fluid, serum and plasma protein oxidation in Alzheimer's disease. *Acta Neurologica Scandinavica,* 119**,** 32-38.

Kuhn DM, Sakowski SA, Sadidi M & Geddes TJ 2004. Nitrotyrosine as a marker for peroxynitrite-induced neurotoxicity: The beginning or the end of the end of dopamine neurons? *Journal of Neurochemistry,* 89**,** 529-536.
Kuiper MA, Visser JJ, Bergmans PLM, Scheltens P & Wolters EC 1994. Decreased cerebrospinal fluid nitrate levels in Parkinson's disease, Alzheimer's disease and multiple system atrophy patients. *Journal of the Neurological Sciences,* 121**,** 46-49.
Kumar A, Roberts D, Wood KE, Light B, Parrillo JE, Sharma S, Suppes R, Feinstein D, Zanotti S, Taiberg L, Gurka D, Kumar A & Cheang M 2006. Duration of hypotension before initiation of effective antimicrobial therapy is the critical determinant of survival in human septic shock. *Critical Care Medicine,* 34**,** 1589-1596.
Kurien BT & Scofield RH 2008. Autoimmunity and oxidatively modified autoantigens. *Autoimmunity Reviews,* 7**,** 567-573.
Kuschner W, D'Alessandro A, Wong H & Blanc P 1996. Dose-dependent cigarette smoking-related inflammatory responses in healthy adults. *European Respiratory Journal,* 9**,** 1989-1994.
Laemmli UK 1970. Cleavage of structural proteins during the assembly of the head of bacteriophage T4. *Nature,* 227**,** 680-685.
Lalkhen AG & McCluskey A 2008. Clinical tests: sensitivity and specificity. *Continuing Education in Anaesthesia, Critical Care & Pain,* 8**,** 221-223.
Larsen FJ, Weitzberg E, Lundberg JO & Ekblom B 2007. Effects of dietary nitrate on oxygen cost during exercise. *Acta Physiology (Oxf),* 191**,** 59-66.
Lauer T, Preik M, Rassaf T, Strauer BE, Deussen A, Feelisch M & Kelm M 2001. Plasma nitrite rather than nitrate reflects regional endothelial nitric oxide synthase activity but lacks intrinsic vasodilator action. *Proceedings of the National Academy of Sciences of the United States of America,* 98**,** 12814-12819.
Lavrentieva A, Kontakiotis T, Lazaridis L, Tsotsolis N, Koumis J, Kyriazis G & Bitzani M 2007. Inflammatory markers in patients with severe burn injury: What is the best indicator of sepsis? *Burns,* 33**,** 189-194.
Law A, Gauthier S & Quirion R 2001. Say NO to Alzheimer's disease: the putative links between nitric oxide and dementia of the Alzheimer's type. *Brain Research Reviews,* 35**,** 73-96.
Lee C-i, Liu X & Zweier JL 2000. Regulation of Xanthine Oxidase by Nitric Oxide and Peroxynitrite. *Journal of Biological Chemistry,* 275**,** 9369-9376.
Lee J-M, Blennow K, Andreasen N, Laterza O, Modur V, Olander J, Gao F, Ohlendorf M & Ladenson JH 2008. The Brain Injury Biomarker, VLP-1, is Increased in the CSF of Alzheimer's Disease Patients. *Clinical Chemistry,* 54**,** 1617-1623.
Leeuwenburgh C, Hardy MM, Hazen SL, Wagner P, Oh-ishi S, Steinbrecher UP & Heinecke JW 1997. Reactive nitrogen intermediates promote low density lipoprotein oxidation in human atherosclerotic intima. *Journal of Biological Chemistry,* 272**,** 1433-1436.
Leong JY, van der Merwe J, Pepe S, Bailey M, Perkins A, Lymbury R, Esmore D, Marasco S & Rosenfeldt F 2010. Perioperative metabolic therapy improves redox status and outcomes in cardiac surgery patients: a randomised trial. *Heart, Lung & Circulation,* 19**,** 584-591.
Lepoivre M, Houée-Levin C, Coeytaux K, Decottignies P, Auger G & Lemaire G 2005. Nitration of the tyrosyl radical in ribonucleotide reductase by

nitrogen dioxide: A gamma radiolysis study. *Free Radical Biology and Medicine,* 38**,** 1511-1517.
Levy MM, Fink MP, Marshall JC, Abraham E, Angus D, Cook D, Cohen J, Opal SM, Vincent JL & Ramsay G 2003. 2001 SCCM/ESICM/ACCP/ATS/SIS International Sepsis Definitions Conference. *Critical Care Medicine,* 31**,** 1250-1256.
Li J-J, Fang C-H, Jiang H, Huang C-X, Hui R-T & Chen M-Z 2004. Time course of inflammatory response after renal artery stenting in patients with atherosclerotic renal stenosis. *Clinica Chimica Acta,* 350**,** 115-121.
Lim GP, Chu T, Yang F, Beech W, Frautschy SA & Cole GM 2001. The Curry Spice Curcumin Reduces Oxidative Damage and Amyloid Pathology in an Alzheimer Transgenic Mouse. *The Journal of Neuroscience,* 21**,** 8370-8377.
Lirk P, Hoffmann G & Rieder J 2002. Inducible nitric oxide synthase--time for reappraisal. *Current Drug Targets. Inflammation and Allergy,* 1**,** 89-108.
Loft S, Olsen A, Moller P, Poulsen HE & Tjonneland A 2013. Association between 8-oxo-7,8-dihydro-2'-deoxyguanosine excretion and risk of postmenopausal breast cancer: nested case-control study. *Cancer Epidemiolology, Biomarkers & Prevention,* 22**,** 1289-1296.
Loft S, Svoboda P, Kawai K, Kasai H, Sørensen M, Tjønneland A, Vogel U, Møller P, Overvad K & Raaschou-Nielsen O 2012. Association between 8-oxo-7,8-dihydroguanine excretion and risk of lung cancer in a prospective study. *Free Radical Biology & Medicine,* 52**,** 167-172.
López A, Lorente JA, Steingrub J, Bakker J, McLuckie A, Willatts S, Brockway M, Anzueto A, Holzapfel L, Breen D, Silverman MS, Takala J, Donaldson J, Arneson C, Grove G, Grossman S & Grover R 2004. Multiple-center, randomized, placebo-controlled, double-blind study of the nitric oxide synthase inhibitor 546C88: Effect on survival in patients with septic shock. *Critical Care Medicine,* 32**,** 21-30.
Loria V, Dato I, Graziani F & Biasucci LM 2008. Myeloperoxidase: A New Biomarker of Inflammation in Ischemic Heart Disease and Acute Coronary Syndromes. *Mediators of Inflammation,* 2008**,** 135625.
Luban S & Li ZG 2010. Citrullinated peptide and its relevance to rheumatoid arthritis: an update. *International Journal of Rheumatic Diseases,* 13**,** 284-287.
Luchsinger JA, Tang M, Shea S & Mayeux R 2003. Antioxidant vitamin intake and risk of alzheimer disease. *Archives of Neurology,* 60**,** 203-208.
Lukaszewski RA, Yates AM, Jackson MC, Swingler K, Scherer JM, Simpson AJ, Sadler P, McQuillan P, Titball RW, Brooks TJG & Pearce MJ 2008. Presymptomatic Prediction of Sepsis in Intensive Care Unit Patients. *Clinical and Vaccine Immunology : CVI,* 15**,** 1089-1094.
Lundberg JO, Feelisch M, Bjorne H, Jansson EA & Weitzberg E 2006. Cardioprotective effects of vegetables: is nitrate the answer? *Nitric Oxide,* 15**,** 359-362.
Luo X, Hou L, Shi H, Zhong X, Zhang Y, Zheng D, Tan Y, Hu G, Mu N, Chan J, Chen X, Fang Y, Wu F, He H & Ning Y 2013. CSF levels of the neuronal injury biomarker visinin-like protein-1 in Alzheimer's disease and dementia with Lewy bodies. *Journal of Neurochemistry,* 127**,** 681-690.
Luzzani A, Polati E, Dorizzi R, Rungatscher A, Pavan R & Merlini A 2003. Comparison of procalcitonin and C-reactive protein as markers of sepsis. *Critical Care Medicine,* 31**,** 1737-1741.

Lymar SV & Hurst JK 1995. Rapid reaction between peroxonitrite ion and carbon dioxide: Implications for biological activity. *Journal of the American Chemical Society,* 117**,** 8867-8868.
MacArthur PH, Shiva S & Gladwin MT 2007. Measurement of circulating nitrite and S-nitrosothiols by reductive chemiluminescence. *Journal of Chromatography B,* 851**,** 93-105.
MacMillan-Crow LA, Crow JP & Thompson JA 1998. Peroxynitrite-Mediated Inactivation of Manganese Superoxide Dismutase Involves Nitration and Oxidation of Critical Tyrosine Residues. *Biochemistry,* 37**,** 1613-1622.
MacRae TH 1997. Tubulin post-translational modifications--enzymes and their mechanisms of action. *Eur J Biochem,* 244**,** 265-278.
Malinski T 2007. Nitric oxide and nitroxidative stress in Alzheimer's disease. *Journal of Alzheimers Disease,* 11**,** 207-218.
Mannino DM & Buist AS Global burden of COPD: risk factors, prevalence, and future trends. *The Lancet,* 370**,** 765-773.
Mapp PI, Klocke R, Walsh DA, Chana JK, Stevens CR, Gallagher PJ & Blake DR 2001. Localization of 3-nitrotyrosine to rheumatoid and normal synovium. *Arthritis & Rheumatism,* 44**,** 1534-1539.
Marcus DL, Thomas C, Rodriguez C, Simberkoff K, Tsai JS, Strafaci JA & Freedman ML 1998. Increased Peroxidation and Reduced Antioxidant Enzyme Activity in Alzheimer's Disease. *Experimental Neurology,* 150**,** 40-44.
Marnell L, Mold C & Du Clos TW 2005. C-reactive protein: Ligands, receptors and role in inflammation. *Clinical Immunology,* 117**,** 104-111.
Marquez LA & Dunford HB 1995. Kinetics of oxidation of tyrosine and dityrosine by myeloperoxidase compounds I and II. Implications for lipoprotein peroxidation studies. *J Biol Chem,* 270**,** 30434-30440.
Marquez LA, Huang JT & Dunford HB 1994. Spectral and Kinetic Studies on the Formation of Myeloperoxidase Compounds I and II: Roles of Hydrogen Peroxide and Superoxide. *Biochemistry,* 33**,** 1447-1454.
Martins AB, Ximenes VF & da Fonseca LM 2013. Serum myeloperoxidase level is increased in heavy smokers. *Open Journal of Clinical Diagnostics*.
Martins PS, Kallas EG, Neto MC, Dalboni MA, Blecher S & Salomao R 2003. Upregulation of reactive oxygen species generation and phagocytosis, and increased apoptosis in human neutrophils during severe sepsis and septic shock. *Shock,* 20**,** 208-212.
Masaki KH, Losonczy KG, Izmirlian G, Foley DJ, Ross GW, Petrovitch H, Havlik R & White LR 2000. Association of vitamin E and C supplement use with cognitive function and dementia in elderly men. *Neurology,* 54**,** 1265-1272.
Mashima T, Naito M & Tsuruo T 1999. Caspase-mediated cleavage of cytoskeletal actin plays a positive role in the process of morphological apoptosis. *Oncogene,* 18**,** 2423-2430.
Masliah E, Iimoto DS, Saitoh T, Hansen LA & Terry RD 1990. Increased immunoreactivity of brain spectrin in Alzheimer disease: a marker for synapse loss? *Brain Research,* 531**,** 36-44.
MatrixScience 2014. Matrix Science - Mascot - Peptide Mass Fingerprint. http://www.matrixscience.com/help/interpretation_help.html.
Matsuoka Y, Picciano M, La Francois J & Duff K 2001. Fibrillary β-amyloid evokes oxidative damage in a transgenic mouse model of Alzheimer's disease. *Neuroscience,* 104.

Maurer I, Zierz S & Möller HJ 2000. A selective defect of cytochrome c oxidase is present in brain of Alzheimer disease patients. *Neurobiology of Aging,* 21**,** 455-462.
McKhann GM, Knopman DS, Chertkow H, Hyman BT, Jack Jr CR, Kawas CH, Klunk WE, Koroshetz WJ, Manly JJ, Mayeux R, Mohs RC, Morris JC, Rossor MN, Scheltens P, Carrillo MC, Thies B, Weintraub S & Phelps CH 2011. The diagnosis of dementia due to Alzheimer's disease: Recommendations from the National Institute on Aging-Alzheimer's Association workgroups on diagnostic guidelines for Alzheimer's disease. *Alzheimer's & Dementia,* 7**,** 263-269.
McKnight GM, Duncan CW, Leifert C & Golden MH 1999. Dietary nitrate in man : friend or foe ? *British Journal of Nutrition,* 44**,** 349-358.
Mehta H, Nazzal K & Sadikot RT 2008. Cigarette smoking and innate immunity. *Inflammation Research,* 57**,** 497-503.
Mihm MJ, Jing L & Bauer JA 2000. Nitrotyrosine causes selective vascular endothelial dysfunction and DNA damage. *Journal of cardiovascular pharmacology,* 36**,** 182-187.
Miller GD, Marsh AP, Dove RW, Beavers D, Presley T, Helms C, Bechtold E, King SB & Kim-Shapiro D 2012. Plasma nitrate and nitrite are increased by a high nitrate supplement, but not by high nitrate foods in older adults. *Nutrition Research (New York, N.y.),* 32**,** 160-168.
Milton NN 2004. Role of Hydrogen Peroxide in the Aetiology of Alzheimer's Disease. *Drugs & Aging,* 21**,** 81-100.
Mirvish SS 1995. Role of N-nitroso compounds (NOC) and N-nitrosation in etiology of gastric, esophageal, nasopharyngeal and bladder cancer and contribution to cancer of known exposures to NOC. *Cancer Letters,* 93**,** 17-48.
Misko TP, Radabaugh MR, Highkin M, Abrams M, Friese O, Gallavan R, Bramson C, Hellio Le Graverand MP, Lohmander LS & Roman D 2013. Characterization of nitrotyrosine as a biomarker for arthritis and joint injury. *Osteoarthritis and Cartilage,* 21**,** 151-156.
Molon B, Ugel S, Del Pozzo F, Soldani C, Zilio S, Avella D, De Palma A, Mauri P, Monegal A, Rescigno M, Savino B, Colombo P, Jonjic N, Pecanic S, Lazzarato L, Fruttero R, Gasco A, Bronte V & Viola A 2011. Chemokine nitration prevents intratumoral infiltration of antigen-specific T cells. *The Journal of Experimental Medicine,* 208**,** 1949-1962.
Monteiro HP 2002. Signal transduction by protein tyrosine nitration: competition or cooperation with tyrosine phosphorylation-dependent signaling events?1,2. *Free Radical Biology & Medicine,* 33**,** 765-773.
Montine TJ, Neely MD, Quinn JF, Beal MF, Markesbery WR, Roberts Ii LJ & Morrow JD 2002. Lipid peroxidation in aging brain and Alzheimer's disease. *Free Radical Biology & Medicine,* 33**,** 620-626.
Montuschi P, Barnes PJ & Roberts LJ 2004. Isoprostanes: markers and mediators of oxidative stress. *The FASEB Journal,* 18**,** 1791-1800.
Moreno DM, Martí MA, De Biase PM, Estrin DA, Demicheli V, Radi R & Boechi L 2011. Exploring the molecular basis of human manganese superoxide dismutase inactivation mediated by tyrosine 34 nitration. *Archives of Biochemistry and Biophysics,* 507**,** 304-309.
Moriya A, Grant J, Mowat C, Williams C, Carswell A, Preston T, Anderson S, Iijima K & McColl KEL 2002. In vitro Studies Indicate that Acid Catalysed Generation of N-Nitrosocompounds from Dietary Nitrate Will be Maximal

at the Gastro-oesophageal Junction and Cardia. *Scandinavian Journal of Gastroenterology,* 37**,** 253-261.
Morris M, Evans DA, Bienias JL & et al. 2002. Dietary intake of antioxidant nutrients and the risk of incident alzheimer disease in a biracial community study. *JAMA,* 287**,** 3230-3237.
Morrissette DA, Parachikova A, Green KN & LaFerla FM 2009. Relevance of transgenic mouse models to human Alzheimer disease. *The Journal of Biological Chemistry,* 284**,** 6033-6037.
Mortaz E, Adcock IM, Ito K, Kraneveld AD, Nijkamp FP & Folkerts G 2010. Cigarette smoke induces CXCL8 production by human neutrophils via activation of TLR9 receptor. *European Respiratory Journal,* 36**,** 1143-1154.
Moshage H, Kok B, Huizenga JR & Jansen PL 1995. Nitrite and nitrate determinations in plasma: a critical evaluation. *Clinical Chemistry,* 41**,** 892-896.
Mukaetova-Ladinska EB, Milne J, Andras A, Abdel-All Z, Cerejeira J, Greally E, Robson J, Jaros E, Perry R, McKeith IG, Brayne C, Xuereb J, Cleghorn A, Doherty J, McIntosh G & Milton I 2008. Alpha- and gamma-synuclein proteins are present in cerebrospinal fluid and are increased in aged subjects with neurodegenerative and vascular changes. *Dementia and Geriatric Cognitive Disorders,* 26**,** 32-42.
Murakami K, Murata N, Noda Y, Tahara S, Kaneko T, Kinoshita N, Hatsuta H, Murayama S, Barnham KJ, Irie K, Shirasawa T & Shimizu T 2011. SOD1 (Copper/Zinc Superoxide Dismutase) Deficiency Drives Amyloid β Protein Oligomerization and Memory Loss in Mouse Model of Alzheimer Disease. *Journal of Biological Chemistry,* 286**,** 44557-44568.
Murakami K, Suzuki C, Fujii A & Imada T 2012. Intravenous immunoglobulin prevents release of proinflammatory cytokines in human monocytic cells stimulated with procalcitonin. *Inflammation Research,* 61**,** 617-622.
Nagababu E & Rifkind JM 2010. Measurement of Plasma Nitrite by Chemiluminescence. *Methods in molecular biology (Clifton, N.J.),* 610**,** 41-49.
Narayan PJ, Lill C, Faull R, Curtis MA & Dragunow M 2015. Increased acetyl and total histone levels in post-mortem Alzheimer's disease brain. *Neurobiology of Disease,* 74**,** 281-294.
Nathan DM, Turgeon H & Regan S 2007. Relationship between glycated haemoglobin levels and mean glucose levels over time. *Diabetologia,* 50**,** 2239-2244.
Nauseef WM 2014. Myeloperoxidase in human neutrophil host defence. *Cellular Microbiology,* 16**,** 1146-1155.
Navarro JA, Molina JA, Jiménez-Jiménez FJ, Benito-León J, Ortí-Pareja M, Gasalla T, Cabrera-Valdivia F, Vargas C, de Bustos F & Arenas J 1996. Cerebrospinal fluid nitrate levels in patients with Alzheimer's disease. *Acta Neurologica Scandinavica,* 94**,** 411-414.
Nemirovskiy OV, Radabaugh MR, Aggarwal P, Funckes-Shippy CL, Mnich SJ, Meyer DM, Sunyer T, Rodney Mathews W & Misko TP 2009. Plasma 3-nitrotyrosine is a biomarker in animal models of arthritis: Pharmacological dissection of iNOS' role in disease. *Nitric Oxide,* 20**,** 150-156.
Newton K & Dixit VM 2012. Signaling in Innate Immunity and Inflammation. *Cold Spring Harbor Perspectives in Biology,* 4.

Nikov G, Bhat V, Wishnok JS & Tannenbaum SR 2003. Analysis of nitrated proteins by nitrotyrosine-specific affinity probes and mass spectrometry. *Analytical Biochemistry,* 320**,** 214-222.

Nissim A, Winyard PG, Corrigall V, Fatah R, Perrett D, Panayi G & Chernajovsky Y 2005. Generation of neoantigenic epitopes after posttranslational modification of type II collagen by factors present within the inflamed joint. *Arthritis & Rheumatism,* 52**,** 3829-3838.

Norris PJ, Faull RLM & Emson PC 1996. Neuronal nitric oxide synthase (nNOS) mRNA expression and NADPH-diaphorase staining in the frontal cortex, visual cortex and hippocampus of control and Alzheimer's disease brains. *Molecular Brain Research,* 41**,** 36-49.

Nossuli TO, Hayward R, Jensen D, Scalia R & Lefer AM 1998. Mechanisms of cardioprotection by peroxynitrite in myocardial ischemia and reperfusion injury. *The American Journal of Physiology,* 275**,** H509-519.

Nuriel T, Hansler A & Gross SS 2011. Protein nitrotryptophan: formation, significance and identification. *Journal of Proteomics,* 74**,** 2300-2312.

O'Donnell R, Breen D, Wilson S & Djukanovic R 2006. Inflammatory cells in the airways in COPD. *Thorax,* 61**,** 448-454.

Oates JC, Christensen EF, Reilly CM, Self SE & Gilkeson GS 1999. Prospective measure of serum 3-nitrotyrosine levels in systemic lupus erythematosus: correlation with disease activity. *Proceedings of the Association of American Physicians,* 111**,** 611-621.

Ohm TG, Müller H, Braak H & Bohl J 1995. Close-meshed prevalence rates of different stages as a tool to uncover the rate of Alzheimer's disease-related neurofibrillary changes. *Neuroscience,* 64**,** 209-217.

Ohshima H, Celan I, Chazotte L, Pignatelli B & Mower HF 1999. Analysis of 3-nitrotyrosine in biological fluids and protein hydrolyzates by high-performance liquid chromatography using a postseparation, on-line reduction column and electrochemical detection: results with various nitrating agents. *Nitric Oxide,* 3**,** 132-141.

Ohshima H, Friesen M, Brouet I & Bartsch H 1990. Nitrotyrosine as a new marker for endogenous nitrosation and nitration of proteins. *Food and Chemical Toxicology,* 28**,** 647-652.

Ohya M, Marukawa S, Inoue T, Ueno N, Hosohara K, Terada N & Kosaka H 2002. Plasma nitrotyrosine concentration relates to prognosis in human septic shock. *Shock,* 18**,** 116-116.

Oldreive C, Bradley N, Bruckdorfer R & Rice-Evans C 2001. Lack of influence of dietary nitrate/nitrite on plasma nitrotyrosine levels measured using a competitive inhibition of binding ELISA assay. *Free Radical Research,* 35**,** 377-386.

Olorunniji F, Iniaghe M, Adebayo J, Malomo S & Adediran S 2009. Mechanism-Based Inhibition of Myeloperoxidase by Hydrogen Peroxide: Enhancement of Inactivation Rate by Organic Donor Substrates *The Open Enzyme Inhibition Journal,* 2**,** 28-35.

Olshaker JS & Jerrard DA 1997. The erythrocyte sedimentation rate. *The Journal of Emergency Medicine,* 15**,** 869-874.

Olsson B, Hertze J, Ohlsson M, Nagga K, Hoglund K, Basun H, Annas P, Lannfelt L, Andreasen N, Minthon L, Zetterberg H, Blennow K & Hansson O 2013. Cerebrospinal fluid levels of heart fatty acid binding protein are elevated prodromally in Alzheimer's disease and vascular dementia. *Journal of Alzheimer's Disease,* 34**,** 673-679.

Omar RA, Chyan YJ, Andorn AC, Poeggeler B, Robakis NK & Pappolla MA 1999. Increased Expression but Reduced Activity of Antioxidant Enzymes in Alzheimer's Disease. *Journal of Alzheimer's Disease,* 1**,** 139-145.

Osoata GO, Yamamura S, Ito M, Vuppusetty C, Adcock IM, Barnes PJ & Ito K 2009. Nitration of distinct tyrosine residues causes inactivation of histone deacetylase 2. *Biochemical and Biophysical Research Communications,* 384**,** 366-371.

Owen JB, Di Domenico F, Sultana R, Perluigi M, Cini C, Pierce WM & Butterfield DA 2009. Proteomics-determined differences in the concanavalin-A-fractionated proteome of hippocampus and inferior parietal lobule in subjects with Alzheimer's disease and mild cognitive impairment: implications for progression of AD. *Journal of Proteome Research,* 8**,** 471-482.

Pacher P, Beckman JS & Liaudet L 2007. Nitric oxide and peroxynitrite in health and disease. *Physiological Reviews,* 87**,** 315-424.

Pannala AS, Mani AR, Spencer JPE, Skinner V, Bruckdorfer KR, Moore KP & Rice-Evans CA 2003. The effect of dietary nitrate on salivary, plasma, and urinary nitrate metabolism in humans. *Free Radical Biology & Medicine,* 34**,** 576-584.

Parker WD, Filley CM & Parks JK 1990. Cytochrome oxidase deficiency in Alzheimer's disease. *Neurology,* 40**,** 1302.

Paumann-Page M, Furtmüller PG, Hofbauer S, Paton LN, Obinger C & Kettle AJ 2013. Inactivation of human myeloperoxidase by hydrogen peroxide. *Archives of Biochemistry and Biophysics,* 539**,** 51-62.

Peluffo G & Radi R 2007. Biochemistry of protein tyrosine nitration in cardiovascular pathology. *Cardiovascular Research,* 75**,** 291-302.

Perkins AJ, Hendrie HC, Callahan CM, Gao S, Unverzagt FW, Xu Y, Hall KS & Hui SL 1999. Association of antioxidants with memory in a multiethnic elderly sample using the Third National Health and Nutrition Examination Survey. *American Journal of Epidemiology,* 150**,** 37-44.

Perner A, Andresen L, Normark M, Fischer-Hansen B, Sorensen S, Eugen-Olsen J & Rask-Madsen J 2001. Expression of nitric oxide synthases and effects of L-arginine and L-NMMA on nitric oxide production and fluid transport in collagenous colitis. *Gut,* 49**,** 387-394.

Petros A, Lamb G, Leone A, Moncada S, Bennett D & Vallance P 1994. Effects of a nitric oxide synthase inhibitor in humans with septic shock. *Cardiovascular Research,* 28**,** 34-39.

Pfeiffer S, Lass A, Schmidt K & Mayer B 2001. Protein tyrosine nitration in cytokine-activated murine macrophages. Involvement of a peroxidase/nitrite pathway rather than peroxynitrite. *The Journal of Biological Chemistry,* 276**,** 34051-34058.

Pfeiffer S, Schmidt K & Mayer B 2000. Dityrosine formation outcompetes tyrosine nitration at low steady-state concentrations of peroxynitrite. Implications for tyrosine modification by nitric oxide/superoxide in vivo. *The Journal of Biological Chemistry,* 275**,** 6346-6352.

Pierrakos C & Vincent J-L 2010. Sepsis biomarkers: a review. *Critical Care,* 14**,** R15.

Piknova B & Schechter AN 2011. Measurement of Nitrite in Blood Samples Using the Ferricyanide-Based Hemoglobin Oxidation Assay. *Methods in molecular biology (Clifton, N.J.),* 704**,** 39-56.

Pirro M, Schillaci G, Mannarino MR, Savarese G, Vaudo G, Siepi D, Paltriccia R & Mannarino E 2007. Effects of rosuvastatin on 3-nitrotyrosine and aortic stiffness in hypercholesterolemia. *Nutrition, Metabolism and Cardiovascular Diseases,* 17**,** 436-441.

Povoa P 2002. C-reactive protein: a valuable marker of sepsis. *Intensive Care Medicine,* 28**,** 235-243.

Praticò D 2008. Evidence of Oxidative Stress in Alzheimer's Disease Brain and Antioxidant Therapy. *Annals of the New York Academy of Sciences,* 1147**,** 70-78.

Praticò D, Uryu K, Leight S, Trojanoswki JQ & Lee VM-Y 2001. Increased Lipid Peroxidation Precedes Amyloid Plaque Formation in an Animal Model of Alzheimer Amyloidosis. *The Journal of Neuroscience,* 21**,** 4183-4187.

Pratico D, Uryu K, Leight S, Trojanoswki JQ & Lee VM 2001. Increased lipid peroxidation precedes amyloid plaque formation in an animal model of Alzheimer amyloidosis. *The Journal of Neuroscience,* 21**,** 4183-4187.

Punchard NA, Whelan CJ & Adcock I 2004. The Journal of Inflammation. *Journal of Inflammation (London, England),* 1**,** 1-1.

Radák Z, Ogonovszky H, Dubecz J, Pavlik G, Sasvari M, Pucsok J, Berkes I, Csont T & Ferdinandy P 2003. Super-marathon race increases serum and urinary nitrotyrosine and carbonyl levels. *European Journal of Clinical Investigation,* 33**,** 726-730.

Radi R 2004. Nitric oxide, oxidants, and protein tyrosine nitration. *PNSA USA,* 101**,** 4003-4008.

Radi R 2012. Protein Tyrosine Nitration: Biochemical Mechanisms and Structural Basis of Functional Effects. *Accounts of Chemical Research,* 46**,** 550-559.

Radi R 2013. Peroxynitrite, a stealthy biological oxidant. *The Journal of Biological Chemistry,* 288**,** 26464-26472.

Radi R, Beckman JS, Bush KM & Freeman BA 1991. Peroxynitrite-induced membrane lipid peroxidation: the cytotoxic potential of superoxide and nitric oxide. *Archives of Biochemistry and Biophysics,* 288**,** 481-487.

Rahman I & Adcock IM 2006. Oxidative stress and redox regulation of lung inflammation in COPD. *The European Respiratory Journal,* 28**,** 219-242.

Rastrick JMD, Stevenson CS, Eltom S, Grace M, Davies M, Kilty I, Evans SM, Pasparakis M, Catley MC, Lawrence T, Adcock IM, Belvisi MG & Birrell MA 2013. Cigarette Smoke Induced Airway Inflammation Is Independent of NF-κB Signalling. *PLoS ONE,* 8**,** e54128.

Reed TT, Pierce WM, Jr., Turner DM, Markesbery WR & Butterfield DA 2009. Proteomic identification of nitrated brain proteins in early Alzheimer's disease inferior parietal lobule. *Journal of Cellular and Molecular Medicine,* 13**,** 2019-2029.

Reuter S, Gupta SC, Chaturvedi MM & Aggarwal BB 2010. Oxidative stress, inflammation, and cancer: How are they linked? *Free Radical Biology & Medicine,* 49**,** 1603-1616.

Reyes JF, Fu Y, Vana L, Kanaan NM & Binder LI 2011. Tyrosine nitration within the proline-rich region of Tau in Alzheimer's disease. *The American Journal of Pathology,* 178**,** 2275-2285.

Reynolds MR, Berry RW & Binder LI 2005. Site-Specific Nitration Differentially Influences τ Assembly in Vitro. *Biochemistry,* 44**,** 13997-14009.

Reynolds MR, Berry RW & Binder LI 2007. Current Topics Nitration in Neurodegeneration: Deciphering the “ Hows ” “ nYs ”. *Biochemistry,* 46.

Ricciardolo FLM, Caramori G, Ito K, Capelli A, Brun P, Abatangelo G, Papi A, Chung KF, Adcock I, Barnes PJ, Donner CF, Rossi A & Di Stefano A 2005. Nitrosative stress in the bronchial mucosa of severe chronic obstructive pulmonary disease. *Journal of Allergy and Clinical Immunology,* 116**,** 1028-1035.

Ridker PM 2003. C-Reactive Protein A Simple Test to Help Predict Risk of Heart Attack and Stroke. *Circulation* 108**,** e81-e85.

Rizzo AM, Berselli P, Zava S, Montorfano G, Negroni M, Corsetto P & Berra B 2010. Endogenous antioxidants and radical scavengers. *Advances in Experimental Medicine and Biology,* 698**,** 52-67.

Roher AE, Weiss N, Kokjohn TA, Kuo Y-M, Kalback W, Anthony J, Watson D, Luehrs DC, Sue L, Walker D, Emmerling M, Goux W & Beach T 2002. Increased Aβ Peptides and Reduced Cholesterol and Myelin Proteins Characterize White Matter Degeneration in Alzheimer's Disease†. *Biochemistry,* 41**,** 11080-11090.

Rokach J, Khanapure SP, Hwang SW, Adiyaman M, Lawson JA & FitzGerald GA 1997. Nomenclature of Isoprostanes: A Proposal. *Prostaglandins,* 54**,** 853-873.

Roman RM, Camargo PV, Borges FK, Rossini AP & Polanczyk CA 2010. Prognostic value of myeloperoxidase in coronary artery disease: comparison of unstable and stable angina patients. *Coronary Artery Disease,* 21**,** 129-136.

Roos D, van Bruggen R & Meischl C 2003. Oxidative killing of microbes by neutrophils. *Microbes and Infection,* 5**,** 1307-1315.

Rosenfeldt F, Wilson M, Lee G, Kure C, Ou R, Braun L & de Haan J 2013. Oxidative stress in surgery in an ageing population: Pathophysiology and therapy. *Experimental Gerontology,* 48**,** 45-54.

Rossner Jr P, Svecova V, Milcova A, Lnenickova Z, Solansky I, Santella RM & Sram RJ 2007. Oxidative and nitrosative stress markers in bus drivers. *Mutation Research/Fundamental and Molecular Mechanisms of Mutagenesis,* 617**,** 23-32.

Ryan BJ, Nissim A & Winyard PG 2014. Oxidative post-translational modifications and their involvement in the pathogenesis of autoimmune diseases. *Redox Biology,* 2**,** 715-724.

Ryberg H & Caidahl K 2007. Chromatographic and mass spectrometric methods for quantitative determination of 3-nitrotyrosine in biological samples and their application to human samples. *Journal of Chromatography B,* 851**,** 160-171.

Rytila P, Rehn T, Ilumets H, Rouhos A, Sovijarvi A, Myllarniemi M & Kinnula VL 2006. Increased oxidative stress in asymptomatic current chronic smokers and GOLD stage 0 COPD. *Respiratory Research,* 7**,** 69.

Salomao R, Brunialti MKC, Rapozo MM, Baggio-Zappia GL, Galanos C & Freudenberg M 2012. Bacterial sensing, cell signaling, and modulation of the immune response during sepsis. *Shock,* 38**,** 227-242.

Salvemini D & Cuzzocrea S 2002. Oxidative Stress In Septic Shock And Disseminated Intravascular Coagulation. *Free Radical Biology & Medicine,* 33**,** 1173-1185.

Salvemini D & Marino MH 1998. Inducible nitric oxide synthase and inflammation. *Expert Opinion on Investigational Drugs,* 7**,** 65-75.

Sandhu JK, Robertson S, Birnboim HC & Goldstein R 2003. Distribution of protein nitrotyrosine in synovial tissues of patients with rheumatoid arthritis and osteoarthritis. *The Journal of Rheumatology,* 30**,** 1173-1181.

Sano M, Ernesto C, Thomas RG, Klauber MR, Schafer K, Grundman M, Woodbury P, Growdon J, Cotman CW, Pfeiffer E, Schneider LS & Thal LJ 1997. A Controlled Trial of Selegiline, Alpha-Tocopherol, or Both as Treatment for Alzheimer's Disease. *New England Journal of Medicine,* 336**,** 1216-1222.

Santos SS, Brunialti MK, Rigato O, Machado FR, Silva E & Salomao R 2012. Generation of nitric oxide and reactive oxygen species by neutrophils and monocytes from septic patients and association with outcomes. *Shock,* 38**,** 18-23.

Scahill RI, Schott JM, Stevens JM, Rossor MN & Fox NC 2002. Mapping the evolution of regional atrophy in Alzheimer's disease: Unbiased analysis of fluid-registered serial MRI. *Proceedings of the National Academy of Sciences,* 99**,** 4703-4707.

Schellekens GA, Visser H, De Jong BAW, Van Den Hoogen FHJ, Hazes JMW, Breedveld FC & Van Venrooij WJ 2000. The diagnostic properties of rheumatoid arthritis antibodies recognizing a cyclic citrullinated peptide. *Arthritis & Rheumatism,* 43**,** 155-163.

Schulte W, Bernhagen J, #xfc, rgen & Bucala R 2013. Cytokines in Sepsis: Potent Immunoregulators and Potential Therapeutic Targets—An Updated View. *Mediators of Inflammation,* 2013**,** 16.

Schwedhelm E, Tsikas D, Gutzki FM & Frölich JC 1999. Gas chromatographic-tandem mass spectrometric quantification of free 3-nitrotyrosine in human plasma at the basal state. *Analytical biochemistry,* 276**,** 195-195.

Shah RC, Buchman AS, Wilson RS, Leurgans SE & Bennett DA 2011. Hemoglobin level in older persons and incident Alzheimer disease: prospective cohort analysis. *Neurology,* 77**,** 219-226.

Shaw CA, Taylor EL, Fox S, Megson IL & Rossi AG 2011. Differential susceptibility to nitric oxide-evoked apoptosis in human inflammatory cells. *Free Radical Biology & Medicine,* 50**,** 93-101.

Shepherd AI, Gilchrist M, Winyard PG, Jones AM, Hallmann E, Kazimierczak R, Rembialkowska E, Benjamin N, Shore AC & Wilkerson DP 2015a. Effects of dietary nitrate supplementation on the oxygen cost of exercise and walking performance in individuals with type 2 diabetes: a randomized, double-blind, placebo-controlled crossover trial. *Free Radical Biology & Medicine,* 86**,** 200-208.

Shepherd AI, Wilkerson DP, Dobson L, Kelly J, Winyard PG, Jones AM, Benjamin N, Shore AC & Gilchrist M 2015b. The effect of dietary nitrate supplementation on the oxygen cost of cycling, walking performance and resting blood pressure in individuals with chronic obstructive pulmonary disease: A double blind placebo controlled, randomised control trial. *Nitric Oxide - Biology and Chemistry,* 48**,** 31-37.

Shevchenko A, Tomas H, Havlis J, Olsen JV & Mann M 2006. In-gel digestion for mass spectrometric characterization of proteins and proteomes. *Nature Protocols,* 1**,** 2856-2860.

Shigenaga MK, Lee HH, Blount BC, Christen S, Shigeno ET, Yip H & Ames BN 1997. Inflammation and NOx-induced nitration: assay for 3-nitrotyrosine by HPLC with electrochemical detection. *Proceedings of the National Academy of Sciences,* 94**,** 3211-3216.

Shishehbor MH, Aviles RJ, Brennan ML, Fu X, Goormastic M, Pearce GL, Gokce N, Keaney JF, Jr., Penn MS, Sprecher DL, Vita JA & Hazen SL 2003. Association of nitrotyrosine levels with cardiovascular disease and modulation by statin therapy. *JAMA,* 289**,** 1675-1680.

Shiva S, Huang Z, Grubina R, Sun J, Ringwood LA, MacArthur PH, Xu X, Murphy E, Darley-Usmar VM & Gladwin MT 2007. Deoxymyoglobin is a nitrite reductase that generates nitric oxide and regulates mitochondrial respiration. *Circulation Research,* 100**,** 654-661.
Shringarpure R & Davies KJA 2002. Protein turnover by the proteasome in aging and disease. *Free Radical Biology & Medicine,* 32**,** 1084-1089.
Sierra R, Rello J, Bailen MA, Benitez E, Gordillo A, Leon C & Pedraza S 2004. C-reactive protein used as an early indicator of infection in patients with systemic inflammatory response syndrome. *Intensive Care Medicine,* 30**,** 2038-2045.
Sies H 1997. Oxidative stress: oxidants and antioxidants. *Experimental Physiology,* 82**,** 291-295.
Sihag RK & Cataldo AM 1996. Brain beta-spectrin is a component of senile plaques in Alzheimer's disease. *Brain Research,* 743**,** 249-257.
Skatchkov M, Larina L, Larin A, Fink N & Bassenge E 1997. Urinary nitrotyrosine content as a marker of peroxynitrite-induced tolerance to organic nitrates. *Journal of Cardiovascular Pharmacology and Therapeutics,* 2**,** 85-96.
Slauch JM 2011. How does the oxidative burst of macrophages kill bacteria? Still an open question. *Molecular microbiology,* 80**,** 580-583.
Smith MA, Hirai K, Hsiao K, Pappolla MA, Harris PLR, Siedlak SL, Tabaton M & Perry G 1998. Amyloid-β Deposition in Alzheimer Transgenic Mice Is Associated with Oxidative Stress. *Journal of Neurochemistry,* 70**,** 2212-2215.
Smith PK, Krohn RI, Hermanson GT, Mallia AK, Gartner FH, Provenzano MD, Fujimoto EK, Goeke NM, Olson BJ & Klenk DC 1985. Measurement of protein using bicinchoninic acid. *Analytical Biochemistry,* 150**,** 76-85.
Snaedal J, Kristinsson J, Gunnarsdottir S, Olafsdottir, Baldvinsson M & Johannesson T 1998. Copper, ceruloplasmin and superoxide dismutase in patients with Alzheimer's disease . a case-control study. *Dementia and Geriatric Cognitive Disorders,* 9**,** 239-242.
Söderling AS, Ryberg H, Gabrielsson A, Lärstad M, Torén K, Niari S & Caidahl K 2003. A derivatization assay using gaschromatography/negative chemical ionization tandem mass spectrometry to quantify 3-nitrotyrosine in human plasma. *Journal of Mass Spectrometry,* 38**,** 1187-1196.
Sosa-Ortiz AL, Acosta-Castillo I & Prince MJ 2012. Epidemiology of Dementias and Alzheimer's Disease. *Archives of Medical Research,* 43**,** 600-608.
Souza JM, Choi I, Chen Q, Weisse M, Daikhin E, Yudkoff M, Obin M, Ara J, Horwitz J & Ischiropoulos H 2000a. Proteolytic degradation of tyrosine nitrated proteins. *Arch Biochem Biophys,* 380**,** 360-366.
Souza JM, Choi I, Chen Q, Weisse M, Daikhin E, Yudkoff M, Obin M, Ara J, Horwitz J & Ischiropoulos H 2000b. Proteolytic Degradation of Tyrosine Nitrated Proteins. *Archives of Biochemistry and Biophysics,* 380**,** 360-366.
Souza JM, Daikhin E, Yudkoff M, Raman CS & Ischiropoulos H 1999. Factors determining the selectivity of protein tyrosine nitration. *Archives of Biochemistry and Biophysics,* 371**,** 169-178.
Souza JM, Peluffo G & Radi R 2008. Protein tyrosine nitration—Functional alteration or just a biomarker? *Free Radical Biology & Medicine,* 45**,** 357-366.
Stadtman ER 1992. Protein oxidation and aging. *Science,* 257**,** 1220-1224.

Stahl W, Matejovic M & Radermacher P 2010. Inhibition of nitric oxide synthase during sepsis: Revival because of isoform selectivity? *Shock,* 34**,** 321-322.
Stamp LK, Khalilova I, Tarr JM, Senthilmohan R, Turner R, Haigh RC, Winyard PG & Kettle AJ 2012. Myeloperoxidase and oxidative stress in rheumatoid arthritis. *Rheumatology (Oxford),* 51**,** 1796-1803.
Standage SW & Wong HR 2011. Biomarkers for pediatric sepsis and septic shock. *Expert review of anti-infective therapy,* 9**,** 71-79.
Steffens S, Al Ghazal A, Steinestel J, Lehmann R, Wegener G, Schnoeller TJ, Cronauer MV, Jentzmik F, Schrader M, Kuczyk MA & Schrader AJ 2013. High CRP values predict poor survival in patients with penile cancer. *BMC Cancer,* 13**,** 1-5.
Steffens S, Kohler A, Rudolph R, Eggers H, Seidel C, Janssen M, Wegener G, Schrader M, Kuczyk MA & Schrader AJ 2012. Validation of CRP as prognostic marker for renal cell carcinoma in a large series of patients. *BMC Cancer,* 12.
Stein CM 2010. Oxidative stress in systemic lupus erythematous: comment on the article by Wang et al. *Arthritis & Rheumatism,* 62**,** 3835-3836.
Su F, Huang H, Akieda K, Occhipinti G, Donadello K, Piagnerelli M, De Backer D & Vincent J-L 2010. Effects of a selective inos inhibitor versus norepinephrine in the treatment of septic shock. *Shock,* 34**,** 243-249.
Suankratay C, Mold C, Zhang Y, Potempa LA, Lint TF & Gewurz H 1998. Complement regulation in innate immunity and the acute-phase response: inhibition of mannan-binding lectin-initiated complement cytolysis by C-reactive protein (CRP). *Clinical and Experimental Immunology,* 113**,** 353-359.
Suffredini A, Fantuzzi G, Badolato R, Oppenheim J & O'Grady N 1999. New Insights into the Biology of the Acute Phase Response. *Journal of Clinical Immunology,* 19**,** 203-214.
Sugiura H, Ichinose M, Yamagata S, Koarai A, Shirato K & Hattori T 2003. Correlation between change in pulmonary function and suppression of reactive nitrogen species production following steroid treatment in COPD. *Thorax,* 58**,** 299-305.
Sukuroglu E, Güncü GN, Kilinc K & Caglayan F 2015. Using Salivary Nitrite and Nitrate Levels as a Biomarker for Drug-Induced Gingival Overgrowth. *Frontiers in Cellular and Infection Microbiology,* 5**,** 87.
Sultana R, Perluigi M & Butterfield DA 2009. Oxidatively modified proteins in Alzheimer's disease (AD), mild cognitive impairment and animal models of AD: role of Abeta in pathogenesis. *Acta neuropathologica,* 118**,** 131.
Sultana R, Perluigi M, Newman SF, Pierce WM, Cini C, Coccia R & Butterfield DA 2010. Redox proteomic analysis of carbonylated brain proteins in mild cognitive impairment and early Alzheimer's disease. *Antioxidants & Redox Signaling,* 12**,** 327-336.
Sultana R, Piroddi M, Galli F & Butterfield DA 2008. Protein Levels and Activity of Some Antioxidant Enzymes in Hippocampus of Subjects with Amnestic Mild Cognitive Impairment. *Neurochemical Research,* 33**,** 2540-2546.
Sultana R, Poon HF, Cai J, Pierce WM, Merchant M, Klein JB, Markesbery WR & Butterfield DA 2006. Identification of nitrated proteins in Alzheimer's disease brain using a redox proteomics approach. *Neurobiology of Disease,* 22**,** 76-87.

Sultana R, Reed T, Perluigi M, Coccia R, Pierce WM & Butterfield DA 2007. Proteomic identification of nitrated brain proteins in amnestic mild cognitive impairment: a regional study. *Journal of Cellular and Molecular Medicine,* 11**,** 839-851.

Sun YC, Chang PY, Tsao KC, Wu TL, Sun CF, Wu LL & Wu JT 2007. Establishment of a sandwich ELISA using commercial antibody for plasma or serum 3-nitrotyrosine (3NT). Elevation in inflammatory diseases and complementary between 3NT and myeloperoxidase. *Clinica chimica acta,* 378**,** 175-180.

Szabó-Taylor KÉ, Nagy G, Eggleton P & Winyard PG 2013. Oxidative Stress in Rheumatoid Arthritis. *In:* ALCARAZ, M. J., GUALILLO, O. & SÁNCHEZ-PERNAUTE, O. (eds.). Springer New York.

Szabo C & Ohshima H 1997. DNA damage induced by peroxynitrite: subsequent biological effects. *Nitric Oxide,* 1**,** 373-385.

Tabner BJ, El-Agnaf OMA, Turnbull S, German MJ, Paleologou KE, Hayashi Y, Cooper LJ, Fullwood NJ & Allsop D 2005. Hydrogen Peroxide Is Generated during the Very Early Stages of Aggregation of the Amyloid Peptides Implicated in Alzheimer Disease and Familial British Dementia. *Journal of Biological Chemistry,* 280**,** 35789-35792.

Takahama U, Hirota S, Nishioka T & Oniki T 2003. Human salivary peroxidase-catalyzed oxidation of nitrite and nitration of salivary components 4-hydroxyphenylacetic acid and proteins. *Archives of Oral Biology,* 48**,** 679-690.

Tang BM, Eslick GD, Craig JC & McLean AS 2007. Accuracy of procalcitonin for sepsis diagnosis in critically ill patients: systematic review and meta-analysis. *The Lancet. Infectious Diseases,* 7**,** 210-217.

Tanni SE, Correa CR, Angeleli AY, Vale SA, Coelho LS & Godoy I 2012. Increased production of hydrogen peroxide by peripheral blood monocytes associated with smoking exposure intensity in smokers. *Journal of Inflammation (London, England),* 9**,** 45-45.

Ter Steege JCA, Koster-Kamphuis L, van Straaten EA, Forget PP & Buurman WA 1998. Nitrotyrosine in plasma of celiac disease patients as detected by a new sandwich ELISA. *Free Radical Biology & Medicine,* 25**,** 953-963.

Thompson C, Wylie LJ, Fulford J, Kelly J, Black MI, McDonagh STJ, Jeukendrup AE, Vanhatalo A & Jones AM 2015. Dietary nitrate improves sprint performance and cognitive function during prolonged intermittent exercise. *European Journal of Applied Physiology,* 115**,** 1825-1834.

Thornalley PJ, Battah S, Ahmed N, Karachalias N, Agalou S, Babaei-Jadidi R & Dawnay A 2003. Quantitative screening of advanced glycation endproducts in cellular and extracellular proteins by tandem mass spectrometry. *Biochemical Journal,* 375**,** 581-581.

Thorpe JR, Mosaheb S, Hashemzadeh-Bonehi L, Cairns NJ, Kay JE, Morley SJ & Rulten SL 2004. Shortfalls in the peptidyl-prolyl cis-trans isomerase protein Pin1 in neurons are associated with frontotemporal dementias. *Neurobiology of Disease,* 17**,** 237-249.

Tohgi H, Abe T, Yamazaki K, Murata T, Ishizaki E & Isobe C 1999. Alterations of 3-nitrotyrosine concentration in the cerebrospinal fluid during aging and in patients with Alzheimer's disease. *Neuroscience Letters,* 269**,** 52-54.

Troxler M, Naseem KM & Homer-Vanniasinkam S 2004. Increased nitrotyrosine production in patients undergoing abdominal aortic aneurysm repair. *The British Journal of Surgery,* 91**,** 1146-1151.
Tsikas D 2004. Measurement of nitric oxide synthase activity in vivo and in vitro by gas chromatography-mass spectrometry. *Methods in Molecular Biology* 279**,** 81-103.
Tsikas D 2007. Analysis of nitrite and nitrate in biological fluids by assays based on the Griess reaction: appraisal of the Griess reaction in the L-arginine/nitric oxide area of research. *Journal of Chromatography. B, Analytical technologies in the biomedical and life sciences,* 851**,** 51-70.
Tsikas D & Caidahl K 2005. Recent methodological advances in the mass spectrometric analysis of free and protein-associated 3-nitrotyrosine in human plasma. *Journal of Chromatography. B, Analytical technologies in the biomedical and life sciences,* 814**,** 1-9.
Tsikas D & Duncan MW 2014. Mass spectrometry and 3-nitrotyrosine: Strategies, controversies, and our current perspective. *Mass Spectrometry Reviews,* 33**,** 237-276.
Tsikas D, Mitschke A & Gutzki FM 2012. Measurement of 3-nitro-tyrosine in human plasma and urine by gas chromatography-tandem mass spectrometry. *Methods in Molecular Biology,* 828**,** 255-270.
Tsikas D, Schwedhelm E, Stutzer FK, Gutzki F-M, Rode I, Mehls C & Frölich JC 2003. Accurate quantification of basal plasma levels of 3-nitrotyrosine and 3-nitrotyrosinoalbumin by gas chromatography-tandem mass spectrometry. *Journal of Chromatography. B, Analytical Technologies in the Biomedical and Life Sciences,* 784**,** 77-77.
Tsuge K, Kataoka M & Seto Y 2000. Cyanide and Thiocyanate Levels in Blood and Saliva of Healthy Adult Volunteers. *Journal of Health Science,* 46**,** 343-350.
Ueshima K, Minakata Y, Sugiura H, Yanagisawa S, Ichikawa T, Akamatsu K, Hirano T, Nakanishi M, Matsunaga K, Yamagata T & Ichinose M 2007. The influence of free 3-nitrotyrosine and saliva on the quantitative analysis of protein-bound 3-nitrotyrosine in sputum. *Analytical Chemistry Insights,* 2**,** 1-7.
Uzzan B, Cohen R, Nicolas P, Cucherat M & Perret GY 2006. Procalcitonin as a diagnostic test for sepsis in critically ill adults and after surgery or trauma: A systematic review and meta-analysis. *Critical Care Medicine,* 34**,** 1996-2003.
Vadseth C, Souza JM, Thomson L, Seagraves A, Nagaswami C, Scheiner T, Torbet J, Vilaire G, Bennett JS, Murciano JC, Muzykantov V, Penn MS, Hazen SL, Weisel JW & Ischiropoulos H 2004. Pro-thrombotic state induced by post-translational modification of fibrinogen by reactive nitrogen species. *The Journal of Biological Chemistry,* 279**,** 8820-8826.
van der Vaart H, Postma DS, Timens W & Ten Hacken NHT 2004. Acute effects of cigarette smoke on inflammation and oxidative stress: a review. *Thorax,* 59**,** 713-721.
van der Vliet A, Eiserich JP, Halliwell B & Cross CE 1997. Formation of Reactive Nitrogen Species during Peroxidase-catalyzed Oxidation of Nitrite. A Potential additional Mechanism of Nitric Oxide-Dependent Toxicity. *Journal of Biological Chemistry,* 272**,** 7617-7625.
van der Zee R, Duisterwinkel FJ & Welling GW 1977. Antigenicity of bovine ribonuclease modified at tyrosine or arginine residues. *European Journal of Biochemistry,* 77**,** 125-131.

Venardos KM, Perkins A, Headrick J & Kaye DM 2007. Myocardial ischemia-reperfusion injury, antioxidant enzyme systems, and selenium: a review. *Current Medicinal Chemistry,* 14**,** 1539-1549.
Victor VM, Rocha M & De la Fuente M 2004. Immune cells: free radicals and antioxidants in sepsis. *International Immunopharmacology,* 4**,** 327-347.
Vincent J-L & Abraham E 2006. The last 100 years of sepsis. *American Journal of Respiratory and Critical Care Medicine,* 173**,** 256-263.
Vincent J-L & Beumier M 2013. Diagnostic and prognostic markers in sepsis. *Expert Review of Anti-infective Therapy,* 11**,** 265-275.
Vincent J-L, Donadello K & Schmit X 2011. Biomarkers in the critically ill patient: C-reactive protein. *Critical Care Clinics,* 27**,** 241-251.
Vincent J-L, Martinez EO & Silva E 2009. Evolving concepts in sepsis definitions. *Critical Care Clinics,* 25**,** 665-675, vii.
Vincent JL, Habib AM, Verdant C & Bruhn A 2006. Sepsis diagnosis and management: work in progress. *Minerva Anestesiologica,* 72**,** 87-96.
Vogel TR, Dombrovskiy VY & Lowry SF 2009. Trends in postoperative sepsis: are we improving outcomes? *Surgical Infections* 10**,** 71-78.
Volanakis JE 2001. Human C-reactive protein: expression, structure, and function. *Molecular Immunology,* 38**,** 189-197.
Vossenaar ER & van Venrooij WJ 2004. Citrullinated proteins: sparks that may ignite the fire in rheumatoid arthritis. *Arthritis Research & Therapy,* 6**,** 107-111.
Wang G, Pierangeli SS, Papalardo E, Ansari G & Khan MF 2010. Markers of oxidative and nitrosative stress in systemic lupus erythematosus: correlation with disease activity. *Arthritis & Rheumatism,* 62**,** 2064-2072.
Ward NS, Casserly B & Ayala A 2008. The Compensatory Anti-inflammatory Response syndrome (CARS) in Critically ill patients. *Clinics in Chest Medicine,* 29**,** 617-viii.
Waseem S, Mobarak M, Islam N & Ahmad Z 2012. Comparative study of pulmonary functions and oxidative stress in smokers and non-smokers. *Indian Journal of Physiology and Pharmacology,* 56**,** 345-352.
Watson D, Grover R, Anzueto A, Lorente J, Smithies M, Bellomo R, Guntupalli K, Grossman S, Donaldson J & Le Gall JR 2004. Cardiovascular effects of the nitric oxide synthase inhibitor NG-methyl-L-arginine hydrochloride (546C88) in patients with septic shock: results of a randomized, double-blind, placebo-controlled multicenter study (study no. 144-002). *Critical Care Medicine,* 32**,** 13-20.
Wayenberg JL, Cavedon C, Ghaddhab C, Lefevre N & Bottari SP 2011. Early transient hypoglycemia is associated with increased albumin nitration in the preterm infant. *Neonatology,* 100**,** 387-397.
Wayenberg JL, Ransy V, Vermeylen D, Damis E & Bottari SP 2009. Nitrated plasma albumin as a marker of nitrative stress and neonatal encephalopathy in perinatal asphyxia. *Free Radical Biology & Medicine,* 47**,** 975-982.
Weber D, Kneschke N, Grimm S, Bergheim I, Breusing N & Grune T 2012. Rapid and sensitive determination of protein-nitrotyrosine by ELISA: Application to human plasma. *Free Radical Research,* 46**,** 276-285.
Weiss SL, Fitzgerald JC, Balamuth F, Alpern ER, Lavelle J, Chilutti M, Grundmeier R, Nadkarni VM & Thomas NJ 2014. Delayed antimicrobial therapy increases mortality and organ dysfunction duration in pediatric sepsis. *Critical Care Medicine* 42**,** 2409-2417.

Whiteman M & Halliwell B 1999. Loss of 3-Nitrotyrosine on Exposure to Hypochlorous Acid: Implications for the Use of 3-Nitrotyrosine as a Biomarkerin Vivo. *Biochemical and Biophysical Research Communications,* 258**,** 168-172.

WHO. 2001. *Biomarkers In Risk Assessment: Validity And Validation* [Online]. International Programme on Chemical Safety (IPCS). Available: http://www.inchem.org/documents/ehc/ehc/ehc222.htm [Accessed Accessed Jan. 16th 2015.

Wiegman CH, Michaeloudes C, Haji G, Narang P, Clarke CJ, Russell KE, Bao W, Pavlidis S, Barnes PJ, Kanerva J, Bittner A, Rao N, Murphy MP, Kirkham PA, Chung KF & Adcock IM 2015. Oxidative stress-induced mitochondrial dysfunction drives inflammation and airway smooth muscle remodeling in patients with chronic obstructive pulmonary disease. *The Journal of Allergy and Clinical Immunology,* 136**,** 769-780.

Willerson JT & Ridker PM 2004. Inflammation as a Cardiovascular Risk Factor. *Circulation,* 109**,** II-2-II-10.

Williams DR 2006. Tauopathies: classification and clinical update on neurodegenerative diseases associated with microtubule-associated protein tau. *Internal Medicine Journal,* 36**,** 652-660.

Winrow VR, Winyard PG, Morris CJ & Blake DR 1993. Free radicals in inflammation: second messengers and mediators of tissue destruction. *British Medical Bulletin,* 49**,** 506-522.

Winterbourn CC, Buss IH, Chan TP, Plank LD, Clark MA & Windsor JA 2000. Protein carbonyl measurements show evidence of early oxidative stress in critically ill patients. *Critical Care Medicine,* 28**,** 143-149.

Wray S, Saxton M, Anderton BH & Hanger DP 2008. Direct analysis of tau from PSP brain identifies new phosphorylation sites and a major fragment of N-terminally cleaved tau containing four microtubule-binding repeats. *Journal of Neurochemistry,* 105**,** 2343-2352.

Wylie LJ, Bailey SJ, Kelly J, Blackwell JR, Vanhatalo A & Jones AM 2016a. Influence of beetroot juice supplementation on intermittent exercise performance. *European Journal Of Applied Physiology,* 116**,** 415-425.

Wylie LJ, Ortiz de Zevallos J, Isidore T, Nyman L, Vanhatalo A, Bailey SJ & Jones AM 2016b. Dose-dependent effects of dietary nitrate on the oxygen cost of moderate-intensity exercise: Acute vs. chronic supplementation. *Nitric Oxide,* 57**,** 30-39.

Xiang W, Weisbach V, Sticht H, Seebahn A, Bussmann J, Zimmermann R & Becker C-M 2013. Oxidative stress-induced posttranslational modifications of human hemoglobin in erythrocytes. *Archives of Biochemistry and Biophysics,* 529**,** 34-44.

Yakovlev VA & Mikkelsen RB 2010. Protein tyrosine nitration in cellular signal transduction pathways. *Journal of Receptors and Signal Transduction,* 30**,** 420-429.

Yang C-Y, Xu P, Yang Y-J, Li B-Y, Sun S-Z, Yang Q-Z & Wang L-X 2014. Systemic capillary leak syndrome due to systemic inflammatory response syndrome in infants: a report on 31 patients. *Central European Journal of Medicine,* 9**,** 477-480.

Yang H, Zhang Y & Pöschl U 2010. Quantification of nitrotyrosine in nitrated proteins. *Analytical and Bioanalytical Chemistry,* 397**,** 879-886.

Yeh CC, Hou MF, Wu SH, Tsai SM, Lin SK, Hou LA, Ma H & Tsai LY 2006. A study of glutathione status in the blood and tissues of patients with breast cancer. *Cell biochemistry and function,* 24**,** 555-559.

Yew DT, Wong HW, Li WP, Lai HWL & Yu W-hA 1999. Nitric oxide synthase neurons in different areas of normal aged and Alzheimer's brains. *Neuroscience,* 89**,** 675-686.
Yi D, Ingelse BA, Duncan MW & Smythe GA 2000. Quantification of 3-nitrotyrosine in biological tissues and fluids: generating valid results by eliminating artifactual formation. *Journal of the American Society for Mass Spectrometry,* 11**,** 578-586.
Zahlten-Hinguranage A, Goldschmidt H, Cremer FW, Egerer G, Moehler T, Witte D, Bernd L, Sabo D & Zeifang F 2006. Preoperative elevation of serum C - reactive protein is predictive for prognosis in myeloma bone disease after surgery. *British Journal of Cancer,* 95**,** 782-787.
Žerovnik E 2009. The emerging role of cystatins in Alzheimer's disease. *BioEssays,* 31**,** 597-599.
Zetterquist W, Pedroletti C, Lundberg JO & Alving K 1999. Salivary contribution to exhaled nitric oxide. *The European Respiratory Journal,* 13**,** 327-333.
Zhang Z, Naughton D, Winyard PG, Benjamin N, Blake DR & Symons MC 1998. Generation of nitric oxide by a nitrite reductase activity of xanthine oxidase: a potential pathway for nitric oxide formation in the absence of nitric oxide synthase activity. *Biochemical and Biophysical Research Communications,* 249**,** 767-772.
Zhao X, He G, Chen YR, Pandian RP, Kuppusamy P & Zweier JL 2005. Endothelium-derived nitric oxide regulates postischemic myocardial oxygenation and oxygen consumption by modulation of mitochondrial electron transport. *Circulation,* 111**,** 2966-2972.
Zhao Y & Jensen ON 2009. Modification-specific proteomics: Strategies for characterization of post-translational modifications using enrichment techniques. *PROTEOMICS,* 9**,** 4632-4641.
Zhou X, Fragala MS, McElhaney JE & Kuchel GA 2010. Conceptual and methodological issues relevant to cytokine and inflammatory marker measurements in clinical research. *Current opinion in clinical nutrition and metabolic care,* 13**,** 541-547.
Zhu A, Ge D, Zhang J, Teng Y, Yuan C, Huang M, Adcock IM, Barnes PJ & Yao X 2014. Sputum myeloperoxidase in chronic obstructive pulmonary disease. *European Journal of Medical Research,* 19**,** 12-12.
Zhu CW & Sano M 2006. Economic considerations in the management of Alzheimer's disease. *Clinical Interventions in Aging,* 1**,** 143-154.
Zhu L, Gunn C & Beckman JS 1992. Bactericidal activity of peroxynitrite. *Archives of Biochemistry and Biophysics,* 298**,** 452-457.
Zitka O, Skalickova S, Gumulec J, Masarik M, Adam V, Hubalek J, Trnkova L, Kruseova J, Eckschlager T & Kizek R 2012. Redox status expressed as GSH:GSSG ratio as a marker for oxidative stress in paediatric tumour patients. *Oncology Letters,* 4**,** 1247-1253.
Zweier JL & Talukder MAH 2006. The role of oxidants and free radicals in reperfusion injury. *Cardiovascular Research,* 70**,** 181-190.